The Entanglement Structure of Topological Quantum Phases

Michaël Mariën

Supervisors: prof. dr. F. Verstraete
Dissertation submitted in fulfillment of the requirements for the degree of
Doctor (Ph.D.) in Science: Physics

Department of Physics and Astronomy
Faculty of Sciences
Ghent University
Academic year 2016-2017

UNIVERSITEIT GENT

Members of the examination committee

Chair

Jan Ryckebusch (Universiteit Gent)

Promotor

Frank Verstraete (Universiteit Gent and Universität Wien)

Other members

J. Ignacio Cirac (Max-Planck-Institut für Quantenoptik)
Jutho Haegeman (Universiteit Gent)
David Pérez-García (Universidad Complutense de Madrid)
Jos Van Doorsselaere (Universiteit Gent)
Henri Verschelde (Universiteit Gent)

A Word of Thanks

First and foremost, I wish to express my gratitude to the free people of the Kingdom of Belgium, who, in their generosity have made it possible for me to, for four rewarding years, focus solely on learning, thinking and improving myself.

Second, my thanks and appreciation go to my supervisor, professor Frank Verstraete, for (un)consciously creating an environment where people like myself can luxuriate, develop and employ their talents to the best of their capacities. Moreover, without his ceaseless encouragements to make mistakes, I would not have learned or achieved remotely as much as I have now.

My examination committee, for their extraordinary patience when reading this dissertation as well as their supportive and helpful comments and questions.

Four years would have been utterly unpleasant without the company of great colleagues, Boye, Dominic, Frank, James, Jutho, Jos, Karel, Laurens, Matthias (both), Nick, Paul, Vid, Volkher. I thank all of them for making a PhD fellowship feel less of a job than it already is. Especially, I am grateful for the numerous discussions throughout the years. Although the subjects and levels of seriousness varied wildly, all of them were interesting, delightful and stimulating. The same is true for the members of the quantum group in Vienna and Madrid, whose hospitality I enjoyed on several occasions.

I also thank Inge, Gerbrand and Guy, they ensure that the administrative, technical, infrastructural and administrative aspects of the depart-

ment run as smoothly as possible, which has freed me to focus on the things I like as much as possible.

Sometimes, it is those incidents in a human life that seem irrelevant or unimportant at first sight that turn out to be the most important ones. It is a pleasure to thank my friends, although I do not know specifically for what yet. So to the Springsteen-Squad, the Ronnie O' Sullivan and Red Devils fanboys, those that do futile attempts to go running with me, the London society, Gingertube, the members of Mariën's Martini-avond or other groups of people brought together by alcohol, I promise that your contribution will be appreciated in the future.

Even more, sometimes overlooked, help and support did I get from my parents, grandparents and two sisters. Although we do not always share the same interests, I do hope my existence is as enriching to their lives as they are to mine.

Finally, Sofie, for sticking with me, accepting the chaos as something good and being the eye in the midst of the hurricane called Life.

Preface

This dissertation contributes to the mutually enriching cross-fertilization between information theory and many-body physics. The central concept from quantum information theory is entanglement and the understanding thereof in a many-body context leads to the introduction of tensor network states for the understanding of low-energy physics in strongly correlated systems. This work contributes to both these central aspects of the field.

First, we study the dynamics of entanglement and prove how fast it can be created by a local Hamiltonian. With this result in hand we show that the celebrated area law is a characteristic of a quantum phase, meaning it is a property of all states in such a phase or of none of them. This can be seen as a justification of the belief in the validity of the area law, which is the main motivation behind tensor network states, and a first step towards a proof thereof. Second, we continue our understanding of entanglement by clarifying its meaning in the context of gauge theories. We achieve this by taking an operational point of view. Third, we study tensor network states in more detail and focus on how they can describe topologically ordered states. We clarify which conditions on the local tensors imply such order. We furthermore provide an equally local characterization of the possible anyon excitations in the system, as well as their properties. We use these results to simulate a non-Abelian phase transition. Last, under the guidance of perturbation theory, we introduce a variational class of tensor network states that only depends on a handful of parameters to clarify how tensor network states can encode physical properties and to overcome numerical issues in optimization algorithms.

Dutch Summary - Nederlandstalige Samenvatting

Inleiding en Achtergrond

Deze thesis behandelt kwantum veeldeeltjessystemen op het rooster. Voor zulke niet-relativistische systemen zijn de fundamentele wetten reeds lange tijd gekend. Toch zijn er nog veel onopgehelderde mysteries te vinden in zelfs de eenvoudigste modellen. De reden hiervoor is dat om grote systemen te kunnen simuleren, het beschikbare computationele vermogen van zo'n omvangrijke aard dient te zijn dat het met de huidige technologie volledig ondenkbaar is er binnen afzienbare tijd over te beschikken. Met de huidige supercomputers kan men slechts ontzettend kleine roosters van niet meer dan om en bij de vijftig deeltjes behandelen.

Reeds sinds het begin van de twintigste eeuw heeft de creativiteit van de menselijke geest verscheidene methoden voortgebracht om toch grote systemen te kunnen bestuderen. De drie meest succesvolle uit het oog springende hiervan zijn de perturbatietheorie, gemiddelde veldbenaderingen en Monte Carlo methoden. De laatste omvat een uitgebreide waaier aan technieken en zijn uitermate succesvol gebleken voor de studie van veeldeeltjessystemen. Toch hebben ze vaak te kampen met hun eigen karakteristieke problemen, zoals het beruchte tekenprobleem, en schalen ze niet altijd even goed voor erg grote systemen. De per-

turbatieve methoden daarentegen kunnen enkel gebruikt worden in de nabijheid van systemen die men analytisch exact kan oplossen. Tot slot missen de gemiddeldeveldmethoden typisch net de interessante fysische fenomenen waarvan de oorzaak in sterke correlaties en verstrengeling te vinden is.

Een alternatieve manier, die reeds lange tijd gekend is, is de variationele methode. Hierbij is het echter cruciaal om over een goede klasse toestanden te beschikken, zodat deze complex genoeg is om de fysica te vatten maar tegelijkertijd eenvoudig genoeg om mee te werken. Inzichten vanuit de kwantuminformatietheorie hebben de laatste twee decennia een erg succesvolle klasse geïntroduceerd in de veeldeeltjesfysica, de zogenaamde tensornetwerktoestanden. Zij vormen de rode draad doorheen deze thesis.

Achtergrond: Nieuwe Inzichten in Veeldeeltjessystemen

In het eerste deel van deze thesis introduceren we enkele recente ideeën en concepten die, ondanks het feit dat ze relatief nieuw zijn, hun plaats in de studie van sterk gecorreleerde kwantumveeldeeltjessystemen reeds glansrijk verworven hebben.

Het eerste idee zijn de reeds vermelde tensornetwerktoestanden. Een van de meest verbazingwekkende concepten in de kwantummechanica is zonder twijfel het bestaan van verstrengelde toestanden. Dit is meteen echter ook de oorzaak van de moeilijkheden in het beschrijven van veeldeeltjessystemen omdat verstrengelde toestanden erg complex zijn. Gelukkig biedt de fysica ons een weg uit deze wiskundige moeilijkheid. De meeste interacties zijn in de praktijk erg lokaal, het blijkt nu dat de toestanden die ons interesseren, met name de lage energietoestanden, typisch weinig verstrengeling hebben. De lokaliteit van interacties weerspiegelt zich in het feit dat in deze toestanden, deeltjes enkel met hun buren verstrengeld en gecorreleerd zijn. Als men nu dus toestanden modelleert die dit gewenste gedrag vertonen, verkrijgt men precies de tensornetwerktoestanden.

Het tweede concept, de zogenaamde quasi-adiabatische evolutie, is van een wat technischere aard. Het kan bewezen worden dat toestanden in

dezelfde fase aan elkaar gerelateerd kunnen worden door een evolutie met een lokale interactie. Net zoals hiervoor, biedt de lokaliteit van deze interactie ons een uitweg uit vervelende wiskundige problemen. Het blijkt dat dit inzicht een grote waaier aan mogelijkheden doet ontstaan om verschillende eigenschappen van deze toestanden in dezelfde fase aan elkaar te relateren. Op deze manier kan men eigenschappen van complexe systemen bewijzen door ze te verbinden aan eenvoudige systemen, waarvan we alle kenmerken goed begrijpen.

Tot slot is er de topologische orde. Een van de belangrijkste inzichten in de statistische fysica is dat van fases, faseovergangen en ordeparameters. Door experimenten met fractionele kwantum Hall toestanden werd echter duidelijk dat dit verhaal niet compleet is. Er zijn toestanden die men niet met een ordeparameter kan onderscheiden, maar die toch niet tot dezelfde fase behoren. Zulke toestanden verkrijgen dan het label topologisch geordend omdat hun speciale eigenschappen, die hen van gebruikelijke fasen onderscheiden, het duidelijkst tot uiting komen wanneer we ze op een topologisch niet-triviaal rooster plaatsen zoals een torus. Het meest tot de verbeelding sprekende rekwisiet van een topologisch geordende toestand is het bestaan van atypische deeltjes, zogenaamde anyonen, die men kan beschouwen als een veralgemening van alledaagse bosonen en fermionen.

Verstrengeling doorheen een Kwantumfase

Het eerste hoofdstuk uit het tweede deel van deze thesis, behandelt meteen een vraagstuk dat zijn origine heeft in de uitdagende combinatie van informatietheorie en veeldeeltjesfysica. Er staan in dit hoofdstuk twee, op het eerste zicht ongerelateerde, vragen centraal. De eerste bevindt zich in het domein van de dynamica, met name vragen we ons af hoe snel twee systemen verstrengeld kunnen worden wanneer we ze laten evolueren met een lokale Hamiltoniaan. De tweede vraag daarentegen betreft een statische eigenschap. We onderzoeken of de verstrengeling van kwantumtoestanden in dezelfde fasen gelijkaardige eigenschappen vertoont. Meer bepaald tonen we aan dat toestanden in dezelfde fase ofwel allemaal een hoeveelheid verstrengeling hebben die slechts schaalt als de omtrek van een gebied in plaats van de inhoud,

ofwel geen enkele van hen deze eigenschap heeft. Het verband tussen beide problemen wordt gelegd door de quasi-adiabatische evolutie die toestanden in dezelfde fase met elkaar verbindt.

Verstrengeling in IJktheorieën

In het tweede hoofdstuk richten we onze blik op ijktheorieën. Door de speciale structuur van de fysische, ijkinvariante Hilbertruimte is het niet meteen duidelijk hoe we verstrengeling in een ijktheorie moeten definiëren. Normaal vertrekken we hiervoor van een opdeling van het systeem in twee delen, elk met een onafhankelijke Hilbertruimte, dit laatste is niet langer mogelijk in een ijktheorie.

We nemen dus een operationeel standpunt in. Gegeven een toestand, zelfs een ijkinvariante, kunnen we ons altijd afvragen hoeveel kwantuminformatie taken en protocollen we kunnen vervullen met behulp van deze toestand. Dit brengt ons heel natuurlijk bij de notie van distilleerbare verstrengeling en we tonen dan ook wat deze notie is voor ijkinvariante toestanden. We illustreren vervolgens onze resultaten in een eenvoudige, zwak interagerende ijktheorie.

Topologische Orde in Tensornetwerktoestanden

In het derde hoofdstuk nemen de tensornetwerktoestanden hun plaats op de voorgrond van het toneel uiteindelijk helemaal in, waar ze zich in de eerste hoofdstukken nog aan de zijlijn bevonden. We bestuderen hoe tensornetwerken gebruikt kunnen worden om de exotische, topologisch geordende toestanden te bestuderen.

We beredeneren hoe alle globale, topologische eigenschappen verklaard kunnen worden door lokale restricties op de individuele tensoren. Meer bepaald verduidelijken we de oorzaak van de topologische degeneratie van de grondtoestand en de origine van de topologische correctie tot de verstrengelingsentropie.

Uiteindelijk kijken we ook naar het meest opvallende aspect van topologische orde, de zogenaamde anyonen. Opnieuw kunnen we, enkel met behulp van de eigenschappen van de lokale tensoren, bepalen welke

anyonen er mogelijk zijn in het systeem. Dit geeft ons nieuwe tensoren die alle topologische eigenschappen van de anyonen bevatten, zoals hun spin en windingsgedrag. We illustreren onze methoden uitvoerig met behulp van verschillende standaardvoorbeelden, zowel analytisch als numeriek.

Een Variationele Klasse Toestanden

Het laatste hoofdstuk behandelt een numeriek aspect van tensornetwerktoestanden. We laten ons inspireren door perturbatietheorie om een klasse tensornetwerktoestanden op te schrijven die, ondanks het feit dat ze slechts van een handvol parameters afhangen, toch in staat zijn op een goede manier de interessante fysische fenomenen te beschrijven. We illustreren dit aan de hand van de fasetransities in twee modellen, het kwantum Ising model en Kitaev's topologisch geordende toestand, beide in een magnetisch veld.

Onze motivatie voor het gebruik van deze toestanden is enerzijds theoretisch, we willen namelijk inzicht verkrijgen in hoe precies een tensornetwerk de fysica codeert en topologische orde bestuderen, anderzijds praktisch, om problemen met numerieke optimalisatie over een erg grote hoeveelheid parameters te omzeilen.

Contents

Part I

Preliminaries

Chapter 1

Introduction

1.1 General Introduction

This dissertation deals with extended quantum many-body spin systems. We thus assume that there are finite degrees of freedom located in fixed positions on a lattice. Such systems arise as a simplification of the true systems in Nature. In theory, the fundamental laws and equations that govern the behavior of non-relativistic quantum mechanical systems are known, and have been known for a long time already. However, it is by no means clear how these equations can be solved, even after the advent of powerful computing resources.

For instance, in condensed matter physics, our main area of interest, the Hamiltonian is the crucial object of study and the goal is to understand the low energy and low temperature physics. This amounts to the determination of the ground state and low-lying excitations of the Hamiltonian. Although present day resources allow us to solve systems of order fifty spin-$1/2$ particles exactly, these are still incredibly small systems compared to the number of degrees of freedom that appear in typical physical systems, even when these are treated with a simplified effective description.

Approaches such as mean field theory can provide insightful and often remarkably accurate predictions for the behavior of many-body systems.

However, many of the most fascinating phenomena in condensed matter physics cannot be described with such an overly simplified model. Some of the experimentally most remarkable examples are High-Temperature Superconductivity and the Fractional Quantum Hall Effect. Especially for the latter, an example of a topologically ordered system, the mean field assumptions of non-interacting particles fail to capture the most essential physical properties of the system.

Some systems can be dealt with analytically, the most famous non-trivial examples are the so-called integrable systems. In the vicinity of systems that we can solve analytically, perturbation theory can be used to gain insight. Other methods exist, such as density functional theory and Monte Carlo methods, arguably the most widely used and successful methods in the study of many-body system. However, despite its accomplishments, the application of quantum Monte Carlo methods is limited due to the notorious sign problem and the fact that such methods don't always scale favorable in the system size.

In one spatial dimension, the celebrated Density Matrix Renormalization Group (DMRG) is a very accurate method that can be used for the computation of low energy properties of quantum spin chains. This is just one of the algorithms that belongs to the fairly recently developed realm of tensor network states. The success of DMRG, and more generally all tensor network methods, can be explained with the following non-trivial observation. It turns out that the ground states of gapped, local Hamiltonians are not random states in the exponentially large Hilbert space but have a very specific form.

To understand what singles out these states as special, we need to turn to quantum information theory and the concept of entanglement, but suffice it to say for now that the states of interest are exactly described by the class of tensor network states because they capture their essential entanglement properties. This is all the more remarkable as tensor network states comprise only a very small part of the full Hilbert space.

In Part I we introduce the concepts introduced here in more detail. We provide our new results in Part II, which deal both with the understanding of entanglement in quantum many-body systems and with the

description of strongly-correlated systems with tensor network states. We now give a quick overview of these results.

1.2 Overview

Chapter 1 starts our study of entanglement in quantum many-body spin systems. We first introduce the notion of a gapped quantum phase, which is similar as a classical phase but defined at zero temperature. Our goal is to find the relation between the entanglement entropies of different ground states in the same phase. The main technical tool is of interest of its own. We show a maximal upper bound on the rate at which entanglement can grow in spin systems under the evolution with a local Hamiltonian. This finally allows us to show that the entropy properties of ground states in the same quantum phase are more similar than one would expect at first sight, which translates to a proof of the stability of the famous area law of the entanglement entropy.

Chapter 2 continues the study of entanglement. However, we change the setting from the familiar spins systems to lattice gauge theories. In gauge systems the Hilbert space is not a tensor product of local spaces. Consequently, the usual definition of entanglement entropy is no longer applicable. We take an operational point of view and identify the distillable entanglement that is present in gauge theories, this is the entanglement that can be used for quantum information protocols. Moreover, we calculate the entanglement entropy of a simple discrete gauge theory in perturbation theory and discuss what happens to the universal constant correction of the entanglement entropy of large systems.

Chapter 3 deals with topologically ordered systems. We explain how topological properties are encoded and reveal themselves in the structure of the local tensors of a tensor network state. We start by describing the ground states of topologically ordered systems. Next, we identify how the topological excitations, called anyons, in these systems can be described and we give algorithms to determine and classify them. We also illustrate how the topological spin, fusion and braiding information can be extracted in a straightforward manner from the tensors. We

illustrate the abstract results by looking at perturbed string-net wave functions and compute the dispersion relation of the excitations in such systems. This way we clarify and numerically illustrate the condensation and confinement phenomena in tensor network states.

Chapter 4 focuses on a numerical approach to tensor networks. Inspired by perturbation theory, we introduce a class of states that only depends on a few parameters, but does still capture a lot of the essential physics. We use this class of states to study the quantum Ising model in a transverse magnetic field and the Toric Code in a magnetic field. The ansatz gives decent approximations of the critical points, which is non-trivial in the case of topologically ordered systems.

Chapter 2

New Concepts in Many-Body Theory

2.1 Tensor Network States

One of the main important realizations of the last decade in the study of quantum spin systems is that the locality of interactions has an important consequence for the structure of correlations and entanglement in the ground state and low-lying excitations of the local Hamiltonian that describes the system. Moreover, to capture the exotic behavior of models where entanglement is indeed a very important phenomenon, the correct modeling of quantum correlations is vital for a proper understanding.

This insight led to the introduction of concepts and methods of quantum information theory into the realm of many-body physics. The central concept of this trademark blend of information theory and many-body physics are the so-called Tensor Network States (TNS). From our perspective, we can look at these states as the fundamental variational class capturing the essential locality properties of low energy physics, although a variety of different viewpoints and motivations can be found throughout the literature.

We focus on Matrix Product States (MPS) [1] and Projected Entangled Pairs States (PEPS) [2], ignoring very important classes of tensor network states such as the Multiscale Entanglement Renormalization Ansatz (MERA) [3]. Good overviews of tensor networks states and the relation with and applications in quantum information theory and condensed matter physics can be found in [4–9].

For an overview of the most important algorithms we refer to Refs. [10, 11], although for state of the art methods and algorithms the reader is advised to consult the latest research papers as this is an area where a lot of progress is still made at a fast speed, especially for systems in two or more spatial dimensions. At the moment of writing, we refer the reader to Refs. [12, 13] for the most advanced methods. These all deal with algorithms for approximating the low-energy properties of many-body Hamiltonians.

In this section we quickly list some of the most important properties and features of tensor network states without giving proofs of the statements and claims. We assume the reader is already familiar with the concepts and provide the upcoming section only as a reminder. For readers new to the subject we recommend the aforementioned references.

2.1.1 Matrix Product States

The first and still most widely used and successful class of tensor network states are the so-called **Matrix Product States (MPS)**. These are based on Quantum Markov States and were introduced in Ref. [1] as finitely correlated states. The same paper already established their most important properties. In the same year an amazing numerical breakthrough happened with the introduction of the DMRG algorithm [14] which has fundamentally changed our understanding of 1D quantum spin chains. Only later was it understood that this algorithm can be seen as a variational method over the class of MPS [15].

2.1.1.1 Definition of MPS

The definition of an MPS $|\psi[A]\rangle$ on a periodic, finite ring of sites is given in Eq. (2.1). The state is generated by a set of d fixed $D \times D$ matrices $\{A^i \mid i = 1, \ldots, d\}$. The number d is the dimension of the local Hilbert space on each site, i.e. for qubits $d = 2$. The number D is the bond dimension of the MPS and the degrees of freedom corresponding with this dimension are referred to as the virtual space or the virtual degrees of freedom.

For open boundary conditions the trace in Eq. (2.1) is replaced by left and right (fixed) boundary vectors that are used to project the product of matrices to a complex number. For such systems d and D can be site dependent. The limit $N \to \infty$ in Eq. (2.1) gives a uniform MPS in the thermodynamic limit.

$$|\psi[A]\rangle = \sum_{i_1,\ldots,i_N} \mathrm{Tr}\left(A^{i_1} A^{i_2} \ldots A^{i_N}\right) |i_1, i_2, \ldots, i_N\rangle \,. \tag{2.1}$$

An MPS description of a state on a finite system can be obtained as follows. Take the tensor of coefficients of a state and perform sequential singular value decompositions between every possible bipartition of the lattice in two connected parts. Clearly every state can be written in such a way, but the states of interest are these that have a maximal Schmidt rank that is much lower, for instance D bounded or $D \sim \mathrm{poly}(N)$, than expected, which is $D \sim \exp(N)$. We reserve the term MPS for such states. If we refer to theoretical results about the states that can be approximated efficiently as MPS, we typically mean with a bond dimension D and error ε polynomial in the system size N.

The MPS are the states first used in the DMRG algorithm in the context of finite systems with open boundary conditions. As mentioned, extending the definition of MPS to periodic systems is straightforward. Our main interest lies in translation-invariant systems in the thermodynamic limit, which is one of the area where tensor networks really shine, as alternative methods such as Monte Carlo cannot directly be used here. In the thermodynamic limit we demand that the Schmidt rank across a certain bond is finite and we refer to this number as the bond dimension of the MPS. Similarly, we can represent certain operators in such

an efficient way, we call these Matrix Product Operators (MPO) [16, 17]. They are key to the understanding of thermal Gibbs states as tensor networks [18–20] and for dealing with topologically ordered models [21–26].

2.1.1.2 Entanglement in MPS

Let us now focus on the translation-invariant MPS. From our perspective, these MPS are the idealization of 1D quantum states that have an area law for their entanglement. They are exactly those states that have a finite Schmidt number for every bipartition of the chain, which implies that every possible sensible entanglement measure between a connected subchain and the rest of the chain converges to a constant if the size of the subsystem is increased. Consequently an MPS obeys the so-called area law for every entanglement measure such as the von Neumann entanglement entropy and all possible Rényi entropies. An upper bound for the value of such measures only depends on the bond dimension D, for instance for the widely used von Neumann entropy an upper bound is given by $\log(D)$.

There is a folk wisdom in the tensor network community that every state that satisfies an area law can be represented efficiently as a matrix product state. This is indeed true, as long as we demand an area law to hold for all Rényi entropies. However, at least in practice, the equivalence between translation-invariant states with a constant von Neumann entropy and states that can be represented efficiently by an MPS indeed holds [27–30].

2.1.1.3 MPS as Projected Entangled Qudits

A different view on MPS clarifies the connection with quantum information theory. Let us consider a 1D chain of maximally entangled pairs of qudits. We now perform a measurement on every pair of neighboring qudits that belong to different pairs and project the outcome on a chosen subspace. The resulting state is exactly an MPS. Moreover every MPS can easily be obtained using such a procedure.

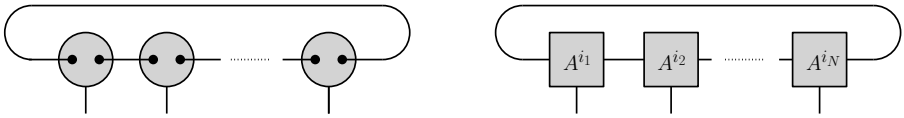

(a) The virtual EPR pairs (black lines and dots) are mapped to physical indices with an arbitrary chosen map.

(b) The same MPS, from the maps we can extract the set of matrices A^i. The EPR pairs account for the matrix multiplication.

Figure 2.1

This construction also clarifies immediately why an MPS has finite entanglement across ever cut as the projections and measurements are stochastic local operations assisted by classical communication (SLOCC) and therefore they cannot increase the number of non-zero Schmidt values across every cut. Thus, the maximal number of non-zero Schmidt values is that of the entangled qudit pair we started from, which is exactly the bond dimension D. This gives immediately an upper bound for every sensible measure of entanglement. Another importance of this construction lies in the fact that it can be generalized naturally to higher dimensions as we shall discuss shortly.

2.1.1.4 Correlations in MPS

The fundamental building blocks of any translation-invariant MPS are the injective MPS. These are exactly the MPS whose set of matrices $\{A^i\}$ generate the full matrix algebra $\mathbb{C}^{D\times D}$, possibly after a finite number of blockings. One can think of the injectivity property as the fact that we can implement any operation on the virtual level of the MPS by acting on the physical degrees of freedom.

To these states, we can naturally associate a transfer matrix which governs the behavior of correlation functions. This transfer matrix is a quantum channel, and for injective MPS the contiguous application of this channel converges to the fixed point subspace exponentially fast, hence connected correlation functions in MPS decay likewise. Just like in the case of the entanglement, MPS indeed have the desired properties we know that the ground states of local, gapped Hamiltonians obey [31, 32]. Again a converse result holds in the sense that a state on

a quantum spin chain with an exponential decay of correlations can be approximated efficiently by an MPS [33].

2.1.1.5 MPS as Ground States

As already discussed MPS have several properties we expect from the ground state of local gapped Hamiltonians such as exponential decay of correlations [31, 32] and an area law for the entanglement entropy [29, 30]. It can indeed be proven that every ground state of a local, gapped Hamiltonian can be represented efficiently by an MPS [29, 30]. Conversely, every injective MPS is the unique ground state of a local, gapped Hamiltonian called a parent Hamiltonian [1]. Similarly, non-injective MPS can often naturally be seen as the symmetry breaking ground state subspace of a Hamiltonian [34]. Hence, at least in 1D, we end up with a neat equivalence between ground states, states with an area law and states with exponential decay of correlations. Unfortunately, as we shall see, the situation is less understood in higher dimensions.

2.1.1.6 Example: The AKLT State

The prime example of an MPS was introduced by Affleck, Kennedy, Lieb and Tasaki and is commonly known as the AKLT state after its inventors [35]. It is a state believed to be in the same phase as the anti-ferromagnetic spin-1 Heisenberg model and can be seen as a perturbation of the latter. A natural way to obtain the AKLT state, is to write down a globally $\mathrm{SO}(3)$ invariant state. We start from a state consisting of all spin-$\frac{1}{2}$ singlets, such that each site contains exactly one qubit from two different singlet pairs. This state is clearly globally $\mathrm{SU}(2)$ invariant. Let us now act with the projector onto the spin-1 subspace on every site. This can be done with the following operator,

$$P = |1'\rangle\langle 00| + |0'\rangle \frac{\langle 01| + \langle 10|}{\sqrt{2}} + |-1'\rangle\langle 11|\,.$$

Clearly this projector commutes with the representations in the sense that $J_x P = P\frac{X_1+X_2}{2}$ and similarly for J_y, J_z with the J_a the generators of the spin-1 vector representation. We now have an $\mathrm{SO}(3)$ invariant

state which is clearly an MPS with bond dimension $D = 2$. This MPS is constructed as explained in Section 2.1.1.3. The following, not uniquely defined, set of matrices generate this MPS,

$$A^1 = \begin{pmatrix} 0 & \sqrt{2/3} \\ 0 & 0 \end{pmatrix}, \quad A^0 = \begin{pmatrix} -1/\sqrt{3} & 0 \\ 0 & 1/\sqrt{3} \end{pmatrix}, \quad A^{-1} = \begin{pmatrix} 0 & 0 \\ -\sqrt{2/3} & 0 \end{pmatrix}.$$

Moreover, this state is clearly the ground state of a local Hamiltonian. Indeed, if we denote by

$$C_1 = \mathbf{S}_1^2 = J_x^2 + J_y^2 + J_z^2 = 2\mathbb{1}$$

the Casimir operator for a spin-1 representation and by $C_{1,1}$ the same operator for the reducible representation on two of such spins, we find that the the projector onto the spin-2 subspace is given by

$$\begin{aligned} \frac{1}{24} C_{1,1}^2 (C_{1,1}^2 - 2) &= \frac{1}{24} (C_1 + C_2 + 2\mathbf{S}_1\mathbf{S}_2 - 2)(C_1 + C_2 + 2\mathbf{S}_1\mathbf{S}_2) \\ &= \frac{1}{3}\mathbb{1} + \frac{1}{2}\mathbf{S}_1\mathbf{S}_2 + \frac{1}{6}(\mathbf{S}_1\mathbf{S}_2)^2. \end{aligned}$$

Clearly this projector annihilates the AKLT state. The projector onto the spin-2 subspace commutes with the operator P as explained above. However, of the four spin-$\frac{1}{2}$ on which it then acts, the middle two are in a spin-0 singlet. Hence the four together can never be in the spin-2 representation, which implies that the AKLT state is annihilated by the projector onto the spin-2 subspace. We can now make a local, positive Hamiltonian by taking the sum of all the translates of such a two-body spin-1 operator. The AKLT state is then a ground state of this, by consequence, frustration free Hamiltonian.

2.1.2 Projected Entangled Pair States

The perspective on MPS explained in Section 2.1.1.3 provides an insight from quantum information theory that immediately allows for an extension to higher dimensions although we restrict ourselves to two spatial dimensions. The name of such state shows the idea behind their introduction and is **Projected Entangled Pair States (PEPS)** [2]. We illustrate the construction of a PEPS in Fig. 2.2a.

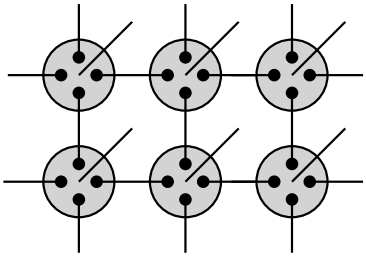

(a) The virtual EPR pairs (black lines and dots) are mapped to physical indices with an arbitrary chosen map (not necessarily a projector).

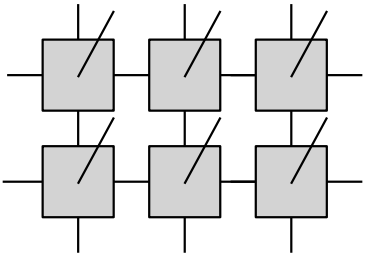

(b) The same PEPS, from the maps, we can extract the set of tensors A^i. The EPR pairs account for the tensor contraction.

Figure 2.2

Clearly, a PEPS still satisfies the area law because of similar reasons as the MPS. Indeed, the Schmidt rank scales at most as the number of maximally entangled pairs that cross the boundary of the bipartition. Other properties an MPS possesses are not as nicely inherited by PEPS in general, for instance even injective PEPS can be critical and exhibit polynomially decaying correlation functions [36]. Also, there exist states with a strict area law for their Schmidt spectrum that are not PEPS [37]. However, as a wrong, but practically useful, rule of thump we can treat them as higher-dimensional MPS with similar properties. We give an example of a PEPS in Section 2.4.1 when discussing the Toric Code.

2.2 Quantum Phases and Quasi-Adiabatic Continuation

2.2.1 Quantum Spin Systems and Locality

In this section we introduce quantum spin systems in a more mathematically well defined manner. This will be crucial for proving the main results in Chapter II.1. Let us first introduce these systems in more detail. A quantum spin system is defined on an underlying set of vertices $\mathcal{L}$, commonly referred to as sites. The set of vertices $\mathcal{L}$ is referred to as lattice. For simplicity we restrict ourselves mainly to finite subsets

$\mathcal{L} = \mathbb{Z}_L^\nu = [1, L]^\nu$ of the ν-dimensional integer lattice $\mathbb{Z}^\nu$, $\nu \in \mathbb{N}$. The sites v can be denoted by their coordinates $v = (v_1, \ldots, v_\nu)$. As the notation $\mathbb{Z}_L^\nu$ suggests, we assume periodic boundary conditions, hence $\mathcal{L}$ has the structure of a ν-dimensional torus.

Given such a subset, we obtain a quantum spin system by attaching to every vertex $v \in \mathcal{L}$ a d-dimensional Hilbert space $\mathcal{H}_v \cong \mathbb{C}^d$. The restriction to isomorphic Hilbert spaces can be removed, although a uniform upper bound on the local dimension is required for some of the arguments. The Hilbert space $\mathcal{H}_\mathcal{L}$ of the lattice $\mathcal{L}$ is defined as

$$\mathcal{H}_\mathcal{L} = \bigotimes_{v \in \mathcal{L}} \mathcal{H}_v.$$

We need a metric on the set $\mathcal{L}$. There are a few natural and equivalent metrics one can equip $\mathcal{L} \subset \mathbb{Z}^\nu$ with, like the Manhattan metric or the shortest path metric. In this paper, we use the shortest path metric. We denote the shortest path distance between two points $x, y \in \mathcal{L}$ as $\mathbf{d}(x, y)$. Other metrics are denoted by $d(x, y)$.

Definition 1. *Let $x, y \in \mathcal{L}$ and denote the coordinates of x by $(x_1, \ldots, x_\nu)$ and of y by $(y_1, \ldots, y_\nu)$. Then, the **shortest path distance** $\mathbf{d}(x, y)$ is defined as*

$$\mathbf{d}(x, y) = \sum_{i=1}^{\nu} \min_{n \in \mathbb{N}} |x_i - y_i + nL| .$$

The distance between two subsets $X, Y \subset \mathcal{L}$ is defined as

$$\mathbf{d}(X, Y) = \min_{x \in X, y \in Y} \mathbf{d}(x, y).$$

*The **diameter** of a subset $X \subset \mathcal{L}$ is defined as*

$$\mathit{diam}(X) = \max_{x_1, x_2 \in X} \mathbf{d}(x_1, x_2).$$

*The **ball** centered at $v_0 \in \mathcal{L}$ with radius r is defined as*

$$B_r(v_0) = \{w \in \mathcal{L} \mid \mathbf{d}(v_0, w) \leq r\}.$$

Given a metric, we can define the boundary of a given subset $\mathcal{V} \subset \mathcal{L}$ and the area of the boundary between two subsets.

Definition 2. *The **neighborhood** $N(v)$ of a site $v \in \mathcal{L}$ is defined as*

$$N(v) = \{w \in \mathcal{L} \mid \mathbf{d}(v, w) = 1\}.$$

*The **boundary** $\partial\mathcal{V}$ of a subset $\mathcal{V} \subset \mathcal{L}$ is defined as the points of $\mathcal{V}$ that have a neighbor not in $\mathcal{V}$,*

$$\partial\mathcal{V} = \{v \in \mathcal{V} \mid N(v) \cap (\mathcal{L} \setminus \mathcal{V}) \neq \emptyset\}.$$

*Let $\mathcal{B}_1, \mathcal{B}_2$ be a bipartition of $\mathcal{L}$, $\mathcal{L} = \mathcal{B}_1 \bigsqcup \mathcal{B}_2$. The size A of the **area** of the boundary of this bipartition is defined as $A = \max(|\partial\mathcal{B}_1|, |\partial\mathcal{B}_2|)$.*

Remark 1. We can consider more general lattices and different metrics. The most important property we need for the lattice and the metric is that the volume of a ball with radius r does not increase too fast as r increases. More precisely, we require the existence of a polynomial $P(r)$ such that

$$\max_{v \in \mathcal{L}} |B_r(v)| \leq P(r). \tag{2.2}$$

Clearly, $\mathcal{L} = \mathbb{Z}_L^\nu$ equipped with the metric of Definition 1 satisfies the requirement in Eq. (2.2) with $P(r) = (2r)^\nu$.

Although we only consider finite sets, quantum spin systems can be rigorously defined and used in the thermodynamic limit. For infinite systems non-trivial conditions on the lattice and the metric are needed to use a similar formalism as in finite Hilbert spaces, see [38] for more details. These conditions are all satisfied for $\mathbb{Z}^\nu$ equipped with the metric d. To work in the thermodynamic limit, one considers the relevant algebra of observables. For finite lattices the approach based on Hilbert spaces and on the algebra of observables are equivalent. The algebra of observables associated to a given site $v \in \mathcal{L}$ is given by

$$\mathcal{A}_v = B(\mathcal{H}_v) \cong M_d(\mathcal{C}).$$

The algebra of observables of the entire lattice $\mathcal{L}$ is given by

$$\mathcal{A}_\mathcal{L} = \bigotimes_{v \in \mathcal{L}} \mathcal{A}_v.$$

The **support** $\text{supp}(A)$ of an operator $A \in \mathcal{A}_\mathcal{L}$ is defined as the smallest set of sites on which A acts non-trivially. If $\text{supp}(A) = \mathcal{V} \subset \mathcal{L}$, then $A \in \mathcal{A}_\mathcal{V} = \bigotimes_{v\in\mathcal{V}} \mathcal{A}_v$.

It is often useful to define an **potential** Φ that generates the Hamiltonian H of a quantum spin system. This is especially convenient if we want to consider the same type of interaction on lattices $\mathcal{L}$ of different sizes, or to rigorously study quantum spin systems in the thermodynamic limit [38]. Given a lattice, a potential is a map Φ from the finite subsets $\mathcal{V}$ of this lattice to the operator algebra, $\Phi : \mathcal{V} \mapsto \Phi(\mathcal{V}) \in \mathcal{A}_\mathcal{V}$ such that $\Phi(\mathcal{V})$ is Hermitian for all finite $\mathcal{V}$. The Hamiltonian of H on $\mathcal{L}$ is then defined as

$$H = \sum_{\mathcal{V}\subset\mathcal{L}} \Phi(\mathcal{V}).$$

If we define a potential Φ on $\mathbb{Z}^\nu$, we can use it to generate Hamiltonians $H_\mathcal{L}$ for all lattices $\mathcal{L} \subset \mathbb{Z}^\nu$.

Since $\mathcal{L}$ has periodic boundary conditions, there exist well defined shift operators T_k that map $\mathcal{A}_{(v_1,\ldots,v_k,\ldots,v_\nu)}$ to $\mathcal{A}_{(v_1,\ldots,v_k+1,\ldots,v_\nu)}$ for every direction $k \in \{1,\ldots,\nu\}$. We use these elementary shift operators to define the operator $T_{\vec{e}}$ for every direction $\vec{e} \in \mathbb{Z}^\nu$.

We now turn our attention to the interactions on quantum spin systems. We need several restrictions on the type of interactions we consider. Most importantly, we require interactions to be local. For several applications a gap between the lowest eigenvalues and the rest of the spectrum is also required. We now define these notions rigorously.

Definition 3. *Suppose we have a quantum spin system defined on a lattice $\mathcal{L}$. A **strictly local**, bounded Hamiltonian H with range R is a Hamiltonian that can be written as a sum of terms h_v with $v \in \mathcal{L}$, where each term h_v only acts non-trivially on sites $w \in B_R(v)$ for a fixed, finite $R \geq 0$. Moreover, we require that the norm of the local terms h_v is uniformly bounded by a constant C,*

$$H = \sum_{v\in\mathcal{L}} h_v, \quad \textit{supp}(h_v) \subset B_R(v), \quad \|h_v\| \leq C.$$

*A Hamiltonian is **quasi-local** with decay function f if it can be written as*

$$H = \sum_{v\in\mathcal{L}} \sum_{r\in\mathbb{N}} h_v(r), \quad \textit{supp}(h_v(r)) \subset B_r(v), \quad \|h_v(r)\| \leq f(r).$$

If we do not specify the decay function f, we assume that f decreases super-polynomially in r. We call a unitary local or quasi-local if it is generated by a local or quasi-local Hamiltonian respectively. A local or quasi-local potential is one that generates local or quasi-local Hamiltonians. A potential Φ is called ***translation-invariant*** *if $T_{\vec{e}}\Phi(\mathcal{V})T_{\vec{e}}^\dagger = \Phi(\mathcal{V}+\vec{e})$ for all subsets $\mathcal{V} \subset \mathcal{L}$ and all directions $\vec{e} \in \mathbb{Z}^\nu$. Here we use the notation $\mathcal{V}+\vec{e} = \{v \in \mathcal{L} \mid v - \vec{e} \in \mathcal{V}\}$.*

Given a translation-invariant potential Φ on the lattice $\mathbb{Z}^\nu$, we can use it to obtain Hamiltonians H_L for all lattices $\mathcal{L} = \mathbb{Z}_L^\nu$ for all values of L. These Hamiltonians are themselves translation-invariant and can be decomposed as $H_L = \sum_{v\in\mathcal{L}} h_v$ with $T_{\vec{e}} h_v T_{\vec{e}}^\dagger = h_{v+\vec{e}}$ for all sites $v \in \mathcal{L}$ and all directions $\vec{e} \in \mathbb{Z}^\nu$.

Next, we define the notion of a gapped Hamiltonian. Thereto, we need to consider the same interaction on lattices $\mathcal{L}$ of increasing size. Hence, it is natural to consider translation-invariant Hamiltonians. Indeed, translation-invariant Hamiltonians can naturally be defined on lattices $\mathcal{L} = \mathbb{Z}_L^\nu$ for all sizes L, because we can define a translation-invariant potential Φ on the infinite lattice $\mathbb{Z}^\nu$. We can now look at the behavior of the sequence of Hamiltonians $H_L = \sum_{\mathcal{V}\subset\mathcal{L}} \Phi(\mathcal{V})$ defined on lattices $\mathcal{L} = \mathbb{Z}_L^\nu$ of increasing size L.

Definition 4. *Let Φ be a potential on $\mathbb{Z}^\nu$ and denote by H_L the translation-invariant Hamiltonians generated by Φ defined on the Hilbert space associated with the lattice $\mathbb{Z}_L^\nu$ for all values of L. Then we call the Hamiltonians H_L and the interaction Φ* ***gapped*** *with ground state degeneracy q if the following two conditions are satisfied. First, the ground state of H_L is q-fold degenerate, i.e. there is a constant $q \in \mathbb{N}$ such that the q lowest eigenvalues $E_{0,1}(L), \ldots, E_{0,q}(L)$ of H_L satisfy*

$$\delta E = \max_{k,k'} |E_{0,k}(L) - E_{0,k'}(L)| \to 0 \text{ as } L \to \infty.$$

Second, the distance between the ground state sector $E_{0,1}, \ldots, E_{0,q}$ and the rest of the spectrum is larger than a positive constant Δ which is independent of L. The constant Δ is called the ***spectral gap****.*

Given the lattice $\mathcal{L}$ equipped with the metric $\mathbf{d}$ and a strictly local Hamiltonian H, one can prove that the time evolution of a strictly local ob-

servable A under the evolution generated by H is still approximately local after a finite time t. We need this property in Section 2.2.2. The property is reminiscent of the concept of strict light cones in relativistic theories. The precise statement is given below in Theorem 1. We discuss it in a general setting since this allows us to apply our results to other quantum spin systems than $\mathcal{L}$ equipped with the metric $\mathbf{d}$.

For local or quasi-local interactions with exponential decay function on graphs $\mathcal{L} \subset \mathbb{Z}^\nu$ the following important theorem holds [39].

Theorem 1 (Lieb-Robinson)**.** *Let $\mathcal{L}$ be a lattice equipped with a metric d and a potential Φ. Suppose that for all sites $v \in \mathcal{L}$, the following holds,*

$$\sum_{\mathcal{V} \ni v} \|\Phi(\mathcal{V})\| |\mathcal{V}| \exp(\mu \operatorname{diam}(\mathcal{V})) \leq s < \infty.$$

for some positive constant μ, s. Take a finite subset $\mathcal{W} \subset \mathcal{L}$ and let H be the Hamiltonian generated by Φ on $\mathcal{W}$. Let A_X, B_Y be local operators supported on disjoint finite sets $X, Y \subset \mathcal{W}$, respectively. Denote the time evolution of A by $\tau_t^H(A) = e^{-iHt} A e^{iHt}$. Then,

$$\|[\tau_t^H(A_X), B_Y]\| \leq 2\|A_X\| \|B_Y\| |X| \exp(2s|t| - \mu d(X, Y)).$$

This theorem quantifies the speed at which information can propagate through the system [40]. The effective speed is given by $2s/\mu$. Clearly, the quantum spin system defined by $\mathcal{L} = \mathbb{Z}_L^\nu$ equipped with the metric $\mathbf{d}$ and a strictly local Hamiltonian satisfies the conditions in Theorem 1. It can also be used to prove the existence of dynamics associated with a potential Φ in the thermodynamic limit [38, 41–43].

It turns out that Theorem 1 also holds for more general quasi-local interactions H on more general lattices [31, 32, 39]. We state the extended theorem since we need it to generalize our results to a broader family of quantum spin systems.

Theorem 2. *Let $\mathcal{L}$ be a lattice equipped with a metric d and Φ a potential. Suppose there exists a positive real function Q such that for all $v, w \in \mathcal{L}$ we have*

$$\sum_{x \in \mathcal{L}} Q(d(v, x)) Q(d(x, w)) \leq \lambda Q(d(v, w)) \tag{2.3}$$

for some constant λ. Furthermore, suppose that for all $v, w \in \mathcal{L}$,

$$\sum_{\mathcal{V} \ni v,w} \|\Phi(\mathcal{V})\| \leq Q(d(v,w))$$

for $\mathcal{V}$ a finite subset of $\mathcal{L}$. Take a finite subset $\mathcal{W} \subset \mathcal{L}$ and let H be the Hamiltonian generated by Φ on $\mathcal{W}$. Let A_X, B_Y be local operators supported on disjoint finite sets $X, Y \subset \mathcal{W}$, respectively. Then,

$$\|[\tau_t^H(A_X), B_Y]\| \leq 2\|A_X\|\|B_Y\||X||Y|Q(d(X,Y))\frac{\exp(2\lambda|t|)}{\lambda}. \quad (2.4)$$

Functions Q that satisfy inequality (2.3) are called **reproducing** [44]. For $\mathcal{L} = \mathbb{Z}_L^\nu$ equipped with the shortest distance metric d, $Q(r) = r^{-a}$ is reproducing for sufficiently large a. The exponential function $Q(r) = e^{-r}$ is not reproducing, but $Q(r) = e^{-r}r^{-a}$ is reproducing for a large enough. In the literature [32, 41, 45, 46], small adaptations of Theorem 2 appear. Most notably, with slightly different conditions on the functions K, the upper bound can depend on $\min(|X|, |Y|)$ instead of on the product $|X||Y|$. These differences are not important for our purposes.

Definition 5. *Suppose we have a quantum spin system on a lattice $\mathcal{L}$ equipped with a metric d and let Φ be a potential on $\mathcal{L}$. We call such a system **LR-local** with decay function Q if Q satisfies the conditions in Theorem 2, which implies that inequality* (2.4) *holds for all Hamiltonians $H_\mathcal{W}$ generated by Φ on finite subsets $\mathcal{W} \subset \mathcal{L}$. We only consider the case where Q decreases at least super-polynomially in r and we refer to such systems simply as LR-local.*

There is a close connection between the notions of quasi-locality and LR-locality. Indeed, suppose we have a lattice $\mathcal{L}$ equipped with a metric d such that the volume of balls with radius r only increases polynomially in r. This requirement was discussed in Remark 1. Suppose that Φ is a potential such that the system is LR-local with a super-polynomial decay function Q. Let $H = \sum_v \sum_r h_v(r)$ be the Hamiltonian generated by Φ on some finite subset $\mathcal{W} \subset \mathcal{L}$. Then we have for a fixed $v \in \mathcal{W}$ that

$$\left\| \sum_{r>R} h_v(r) \right\| \leq \sum_{w:d(w,v)>R} \sum_{\mathcal{V} \ni w,v} \|\Phi(\mathcal{V})\| \leq \sum_{r>R} |B_v(r)|Q(r).$$

Here, the summations are restricted to sites $w \in \mathcal{W}$ and $\mathcal{V} \subset \mathcal{W}$. Since Q decays super-polynomially and $|B_v(r)|$ only increases polynomially in r, this last summation still decays super-polynomially in r with decay function $\tilde{Q}$. We see that the LR-locality of this system implies that the Hamiltonian itself is quasi-local. In many applications the decay functions $Q, \tilde{Q}$ will be very similar [44]. Without loss of generality we will assume that they are equal and use the notation Q. This can be achieved by using a decay function that dominates both $Q, \tilde{Q}$. Clearly, strictly local Hamiltonians are always LR-local.

2.2.2 Exact Quasi-Adiabatic Continuation

In this section we discuss the formalism of quasi-adiabatic continuation[1], first introduced by Hastings and Wen [47, 48] and further developed and used by Hastings and collaborators [45, 50, 51] as well as other authors [49, 52].

2.2.2.1 Quasi-Adiabatic Continuation: Results

The aim of this section is to present the results that were obtained in the literature and that are needed in this dissertation. Since these results are scattered throughout the literature and the conventions and notations of different authors vary, we present a self contained introduction to the subject of quasi-adiabatic continuation in this section. For the convenience of the reader, we discuss the results first, while a more elaborate discussion and proofs of the statements are provided in Section 2.2.2.2.

The setting we consider is as follows. We have a quantum spin system defined on a lattice. Consider a path of Hamiltonians $H(s)$ smoothly depending on a parameter $s \in [0, 1]$ such that there is a uniform lower bound for the gap Δ above the ground state energy of these Hamiltonians. We call such an interpolation a quasi-adiabatic path. The rigorous definition is as follows.

1. The term *quasi-adiabatic* is somewhat of a misnomer since we work with exact filter functions. The original authors [47, 48] worked with approximate Gaussian filter functions. Some authors [49] prefer the terminology *spectral flow*.

Definition 6. *Consider a quantum spin system defined on a lattice $\mathcal{L}$ and let Φ_s be LR-local and gapped potentials for all $s \in [0,1]$. We call Φ_s a **quasi-adiabatic path** between Φ_0 and Φ_1 if the following conditions are satisfied. The potentials Φ_s are differentiable with respect to s. More specific, we require that $\partial_s \Phi_s(\mathcal{V}) \in \mathcal{A}_\mathcal{V}$ for all finite $\mathcal{V} \subset \mathcal{L}$ and that there exists a constant C_N such that for all s, $\|\partial_s \Phi_s(\mathcal{V})\| \leq C_N \|\Phi_s(\mathcal{V})\|$. Moreover, we demand that the LR-locality is uniform in the sense that there exists a super-polynomial decay function Q that dominates the decay functions of all $\Phi(s), \partial_s \Phi_s$. We denote by $\Delta > 0$ a uniform lower bound on the gap of the interactions $\Phi(s)$.*

We immediately limit ourselves to translation-invariant systems although all calculations can be done similarly for spatially varying interactions. Let us note that the formalism applies to every eigenstate whose corresponding eigenvalue is separated from the rest of the spectrum by a gap, or even every subspace of eigenstates whose eigenvalues are separated from the rest of the spectrum. We restrict our discussion here to gapped unique ground states only. Moreover, although we only apply the formalism to Hamiltonians on finite lattices, the formalism of quasi-adiabatic continuation can be rigorously used in the thermodynamic limit [49].

Definition 6 induces an equivalence relation on the gapped, LR-local potentials. Indeed, it is clear that this relation is transitive. Let Φ_s be a path connecting Φ_0, Φ_1 and $\tilde{\Phi}_s$ a path connecting Φ_1, Φ_2. Then,

$$\Psi(s) = \begin{cases} \Phi_{2s} & \text{if } 0 \leq s \leq 1/2 \\ \tilde{\Phi}_{2s-1} & \text{if } 1/2 \leq s \leq 1 \end{cases}$$

is a quasi-adiabatic path connecting Φ_0 and Φ_2.

This equivalence relation on the set of gapped, bounded, LR-local interactions also defines an equivalence relation on the set of ground states of these Hamiltonians. We refer to the equivalence classes as gapped quantum phases.

Definition 7. *Let $\mathcal{L}$ be a lattice and Φ_s a quasi-adiabatic path. Take a finite $\mathcal{V} \subset \mathcal{L}$ and denote the Hamiltonians induced by the potentials Φ_s on $\mathcal{A}_\mathcal{V}$ simply by $H(s)$. Then the unique ground states $|\psi(0)\rangle, |\psi(1)\rangle$ of $H(0)$ and $H(1)$ respectively are in the same **gapped quantum phase**.*

Clearly, the property that the ground states of $H(0), H(1) \in \mathcal{A}_\mathcal{V}$ are in the same phase is independent of the set $\mathcal{V}$. Hence, the above definition can also be applied to the sets of ground states $\{|\psi(0)_\mathcal{V}\rangle\}, \{|\psi(1)_\mathcal{V}\rangle\}$ for all finite $\mathcal{V} \subset \mathcal{L}$.

Let us now fix a finite $\mathcal{V} \subset \mathcal{L}$ and denote the Hamiltonians induced by the potentials $\Phi(s)$ simply by $H(s)$ and their unique and gapped ground states by $|\psi_0(s)\rangle$. The results we obtain are independent of the finite subset $\mathcal{V}$. The evolution of the ground states $|\psi_0(s)\rangle$ can, under general conditions [53], be expressed exactly as $|\psi_0(s)\rangle = U(s)\,|\psi_0(0)\rangle$. The unitaries $U(s)$ are the solutions of a differential equation with generator $K(s)$,

$$\frac{dU(s)}{ds} = iK(s)U(s).$$

We are interested in the structure of the generator $K(s)$ of these unitaries. Hastings has shown that these generators are quasi-local Hamiltonians [47, 48]. This last statement is highly non-trivial and very powerful and is the main result and idea behind the use of quasi-adiabatic continuation to solve a variety of problems [31, 32, 44, 45, 48–52, 54–59].

To construct the operator $K(s)$, we need a so-called filter function $F(t)$ which is an odd function that decays rapidly in time (faster than any polynomial) and such that its Fourier transform satisfies $\hat{F}(\omega) = -1/\omega$ for $|\omega| \geq \Delta$. The fact that such function exists is not trivial, but can be proven [60–63].

We now use such a filter function to construct the quasi-adiabatic continuation operator. Notice that we immediately drop the dependence of K on the filter function F in the notation. The generator of the quasi-adiabatic evolution is given by

$$K(s) = -i \int_\mathbb{R} F(\Delta t) e^{iH_s t}\,(\partial_s H_s)\, e^{-iH_s t} dt.$$

Using perturbation theory we can show that, indeed,

$$iK(s)\,|\psi_0(s)\rangle = \partial_s\,|\psi_0(s)\rangle$$

which justifies the definition of $K(s)$. Furthermore, the generator $K(s)$ is a quasi-local Hamiltonian. More precisely, $K(s)$ can be written as a sum of quasi-local terms that decay super-polynomially in r,

$$K(s) = \sum_{v \in \mathcal{V}} \sum_{r \geq 0} k_v(r), \quad \text{supp}(k_v(r)) \subset B_r(v), \quad \|k_v(r)\| \leq f(r)$$

with $\lim_{r \to \infty} f(r)P(r) = 0$ for every polynomial $P(r)$.

2.2.2.2 Quasi-Adiabatic Continuation: Derivations

In this technical section we review the derivations and proofs of the results given in Section 2.2.2.1. The material in this section is based on several the good overviews [46, 49, 52].

We again consider the situation discussed before and in Definition 6. For notational convenience we restrict ourselves to strictly local, translation-invariant Hamiltonians $H(s)$. We can modify Definition 6 to obtain the following definition that applies to these restricted interactions. We emphasize that the restriction in Definition 8 is only used for notational convenience and that all relevant results are also valid for the quasi-adiabatic paths defined in Definition 6.

Definition 8. *Consider a quantum spin system defined on a lattice $\mathcal{L}$ and let Φ_s be local, bounded and gapped potentials for all $s \in [0, 1]$. We call Φ_s a **quasi-adiabatic path** between Φ_0 and Φ_1 if the following conditions are satisfied. The potentials Φ_s are differentiable with respect to s. More specific, we require that $\partial_s \Phi_s(\mathcal{V}) \subset \mathcal{A}_\mathcal{V}$ for all finite $\mathcal{V} \subset \mathcal{L}$. Moreover, we require the existence of constant R and C_N such that,*

$$\Phi_s(\mathcal{V}), \partial_s \Phi_s(\mathcal{V}) = 0 \text{ if } diam(\mathcal{V}) > R$$
$$\sup_s \sup_\mathcal{V} \{\|\Phi_s(\mathcal{V})\|, \|\partial_s \Phi(\mathcal{V})\|\} \leq C_N.$$

We denote by $\Delta > 0$ a uniform lower bound on the gap of the interactions $\Phi(s)$.

Let us now fix a finite $\mathcal{V} \subset \mathcal{L}$ and denote the Hamiltonians induced by the potentials $\Phi(s)$ simply by $H(s)$ and their unique and gapped ground

states by $|\psi_0(s)\rangle$. The results we obtain are independent of the finite subset $\mathcal{V}$. As mentioned before, the evolution of the ground state $|\psi_0(s)\rangle$ can be expressed as $|\psi_0(s)\rangle = U(s)\,|\psi_0(0)\rangle$ and the unitaries $U(s)$ are the solutions of a differential equation with generator $K(s)$,

$$\frac{dU(s)}{ds} = iK(s)U(s).$$

Our main goal is to show that the generators $K(s)$ are quasi-local Hamiltonians. We first show the existence of the filter functions that we used in Section 2.2.2.1. We start with the following result from Fourier analysis.

Lemma 1. *Let $\Delta > 0$. There exists an odd function F such that $F(t)$ decays super-polynomially and such that $\hat{F}(\omega) = -1/\omega$ for $|\omega| \geq \Delta$. Here $\hat{F}$ is the Fourier transform of the function F.*

Proof. We follow the argument given in Refs. [44, 46]. An explicit example of such a function was given in Ref. [49]. From now on, we assume that $\Delta = 1$. We start with a function g such that its Fourier transform $\hat{g}$ has compact support $[-1, 1]$, $\hat{g}(0) = 1$ and g itself vanishes rapidly. It is a well-known result in Fourier theory that such functions exist, several different arguments are used in the literature [60–63]. In Ref. [62], functions are constructed such that g decays faster than $\exp(-|t|\epsilon(|t|))$ for large t. Here, ϵ can be any monotonically decreasing positive function with

$$\int_1^\infty \frac{\epsilon(y)}{y} dy \leq \infty.$$

Take such a g even. We can now define $f(t) = \delta(t) - g(t)$, which is also an even function. Moreover, $\hat{f}(0) = 0$ and $\hat{f}(\omega) = 1$ for $|\omega| \geq 1$. Finally, we can build the desired function by a convolution with the sign function,

$$F(t) = \frac{i}{2} \int_{\mathbb{R}} du f(u) \text{sign}(t - u).$$

Since $|F(t)| \leq \left| \int_{|t|}^\infty f(u)du \right|$, the super-polynomial decay of f implies a similar large t behavior of F. Furthermore, we have that

$$\hat{F}(\omega) = \frac{i}{2} \int_{\mathbb{R}} dt \exp(i\omega t) \int_{\mathbb{R}} du f(u) \text{sign}(t - u).$$

This last expression can be integrated by parts in t to yield

$$\begin{aligned}\hat{F}(\omega) &= \text{boundary terms} - \frac{1}{\omega}\frac{1}{2}\int_{\mathbb{R}} d\left(\int_{\mathbb{R}} du f(u)\text{sign}(t-u)\right)e^{i\omega t} \\ &= -\frac{1}{\omega}\int_{\mathbb{R}} du f(u)\delta(t-u)\exp(i\omega t) \\ &= -\frac{1}{\omega}\hat{f}(\omega)\end{aligned}$$

as the boundary terms cancel. □

We now use such functions to define the quasi-adiabatic continuation operator. Notice that we immediately drop the dependence of K on F.

Definition 9. *The generator of the quasi-adiabatic evolution is defined as*

$$K(s) = -i\int_{\mathbb{R}} F(\Delta t)e^{iH_s t}\left(\partial_s H_s\right)e^{-iH_s t}dt.$$

To show that this is a good definition we proceed with the following calculation. We have that

$$\begin{aligned}iK(s)\left|\psi_0(s)\right\rangle &= \int_{\mathbb{R}} F(\Delta t)e^{iH_s t}\partial_s H_s e^{-iH_s t}\left|\psi_0(s)\right\rangle dt \\ &= \left(\mathbb{1} - P_0(s)\right)\int_{\mathbb{R}} F(\Delta t)e^{iH_s t}\partial_s H_s e^{-iH_s t}\left|\psi_0(s)\right\rangle dt \\ &= \sum_{i\neq 0}\left|\psi_i(s)\right\rangle\left\langle\psi_i(s), \partial_s H_s\psi_0(s)\right\rangle\int_{\mathbb{R}} F(\Delta t)e^{i(E_i(s)-E_0(s))t}dt \\ &= \sum_{i\neq 0}\frac{1}{E_0(s)-E_i(s)}\left|\psi_i(s)\right\rangle\left\langle\psi_i(s), \partial_s H_s\psi_0(s)\right\rangle \\ &= \partial_s\left|\psi_0(s)\right\rangle.\end{aligned}$$

We now study the generator $K(s)$. We decompose the local Hamiltonians $H(s)$ as

$$H(s) = \sum_{v\in\mathcal{V}} h_{\mathbf{j}}(s).$$

We now show that $K(s)$ is a quasi-local operator. To lighten the notation we write the quasi-adiabatic evolution of every operator X as

$$\mathcal{F}_s(X) = -i \int_{\mathbb{R}} F(\Delta t) e^{iH(s)t} X e^{-iH(s)} dt.$$

We also need a local approximation of the operator $\mathcal{F}_s(X)$, only supported on a subset $\Lambda \cup \text{supp}(X)$,

$$\mathcal{F}_s^{\Lambda}(X) = -i \int_{\mathbb{R}} F(\Delta t) e^{iH_{\Lambda}(s)t} X e^{-iH_{\Lambda}(s)} dt. \tag{2.5}$$

It is now clear that the ground state $|\psi_0(s)\rangle$ evolves according to the unitary dynamics generated by the Hamiltonian

$$K(s) = \sum_{v \in \mathcal{V}} \mathcal{F}_s(\partial_s h_v) = \sum_{v \in \mathcal{V}} k_v(s),$$

with $k_v(s) = \mathcal{F}_s(\partial_s h_v)$. We now take an arbitrary origin and for convenience we drop the index referring to the origin both for the interaction $h(s)$ and for $k(s) = \mathcal{F}_s(\partial_s h)$. Given that we consider a translation-invariant system, we can just focus on these terms in the subsequent arguments.

Our goal is to show that $k(s)$ is a quasi-local operator. By definition this means we can decompose

$$k(s) = \sum_{r=0}^{\infty} k_r(s)$$

such that the interaction $k_r(s)$ has growing support but its norm decays super-polynomially in r. To obtain such a decomposition we first define the sets

$$\Lambda_r = \{v \mid d(\mathbf{0}, v) \leq r\} \bigcup_{s \in [0,1]} \text{supp}(h(s)).$$

We will show that $k(s)$ decomposes in local terms $k_r(s)$ such that

$$\text{supp}(k_r(s)) \subset \Lambda_r.$$

The main idea is to write $k(s)$ as a telescoping sum of strictly local terms using the approximate evolution defined in Eq. (2.5). We first define

$$k_0(s) = \mathcal{F}_s^{\Lambda_0}(\partial_s h(s))$$

and

$$k_r(s) = \mathcal{F}^{\Lambda_r}(\partial_s h(s)) - \mathcal{F}^{\Lambda_{r-1}}(\partial_s h(s)), \quad r > 0. \tag{2.6}$$

With this definition it is also clear that $\text{supp}(k_r(s)) = \Lambda_r$ and that $k(s) = \sum_{r=0}^{\infty} k_r(s)$. Hence we only need to show that the norm of these terms decays sufficiently rapid in r.

To show the decay of the operators $k_r(s)$, we use the Lieb-Robinson bounds [31, 32, 39] of the original, physical Hamiltonians $H(s)$, see Theorem 1. The calculations generalize to quasi-local interactions h which satisfy a Lieb-Robinson bound, see Theorem 2.

We use the Lieb-Robinson bound to show a statement that is very similar is spirit. For large r the evolution of a local operator A by H_{Λ_r} or $H_{\Lambda_{r-1}}$ is almost the same. This is exactly what we need to bound the integrand of the terms (2.6). The argument is similar to existing ones in the literature [38, 52]. Indeed let A be an operator acting on the ball centered at the origin with radius a. We have that,

$$\begin{aligned}
\|\tau_t^{\Lambda_r}(A) - \tau_t^{\Lambda_{r-1}}(A)\| &= \left\| \int_0^t dt' \frac{d}{dt'} \left(\tau_{t'}^{\Lambda_{r-1}} \left(\tau_{t-t'}^{\Lambda_r}(A) \right) \right) \right\| \\
&= \left\| \int_0^t dt' \tau_{t'}^{\Lambda_{r-1}} \left(\left[H_{\Lambda_r} - H_{\Lambda_{r-1}}, \tau_{t-t'}^{\Lambda_r}(A) \right] \right) \right\| \\
&\leq \int_0^{|t|} dt' \left\| \left[H_{\Lambda_r} - H_{\Lambda_{r-1}}, \tau_{t'}^{\Lambda_r}(A) \right] \right\| \\
&\leq 2\|A\| \|H_{\Lambda_r} - H_{\Lambda_{r-1}}\| |\text{supp}(A)| \int_0^{|t|} dt' e^{2s|t'| - \mu(r-a)} \\
&\leq \|A\| P(r) |\text{supp}(A)| \frac{1}{s} e^{-\mu(r-a)+2s|t|} \\
&= C_{LB} P(r) \|A\| |\operatorname{supp}(A)| e^{-\mu(r-a)+2s|t|}
\end{aligned}$$

Here C_{LB} is a constant and $P(r)$ is a polynomial which is depend on the number of lattice points that are contained in the set $\Lambda_r \setminus \Lambda_{r-1}$. We can now use the last estimate to show the quasi-locality of the operator $k(s)$.

Proposition 1. *The generator $K(s)$ of the quasi adiabatic evolution can be written as a sum of quasi-local terms.*

Proof. After the previous discussion it suffices to show that the norm of the operators $k_r(s)$ defined in Eq. (2.6) decays quickly in r. We have that

$$\begin{aligned}
\|k_r(s)\| &= \left\| \int_{\mathbb{R}} dt F(\Delta t) \left(\tau_t^{\Lambda_r}(\partial_s h(s)) - \tau_t^{\Lambda_{r-1}}(\partial_s h(s)) \right) \right\| \\
&\leq 2 \int_0^\infty dt |F(\Delta t)| \left\| \tau_t^{\Lambda_r}(\partial_s h(s)) - \tau_t^{\Lambda_{r-1}}(\partial_s h(s)) \right\| \\
&\leq 2 C_N C_S C_{LB} P(r) \int_0^{cr} dt |F(\Delta t)| e^{-\mu(r - C_S/2) + 2s|t|} \\
&\quad + 4 \int_{cr}^\infty dt |F(\Delta t)| \|\partial_s h(s)\| \\
&\leq \tilde{C} P(r) \|F\|_{\sup} \frac{1}{s} e^{-r(\mu - 2sc)} + 4 C_N \int_{cr}^\infty dt |F(\Delta t)|.
\end{aligned}$$

This last expression clearly vanishes super-polynomially in r. Indeed, for the right choice of the constant c, say $c \leq \mu/(2s)$ the first term decays exponentially. For a super-polynomially decaying filter function F, the last term also decays super-polynomially, although this decay typically only starts for quiet large values of r. Notice that this result implies a Lieb-Robinson bound for the interaction $K(s)$ similar to Theorem 2. □

This result remains valid if we start with quasi-local Hamiltonians $H(s)$ as long as the decay function f of $H(s)$ is super-polynomially, $\tilde{f}(R) = \sum_{r>R} f(r)$ decays super-polynomially and the volume of balls of radius r only grows polynomially in r. Then, the decay of the generator $K(s)$ is still super-polynomial. Hence, Proposition 1 remains valid for the situation described in Definition 6.

2.3 Topological Order

For a long time, physicists where convinced that the Landau-Ginzburg theory [64] of symmetry breaking, with its central concepts of order parameters and long-range correlations, described more or less all phases

and phase transitions both in classical and quantum many-body theory. One of the prime examples is the classical Ising model in two spatial dimensions which undergoes a phase transition from an ordered to a disordered phase at a non-zero temperature. This transition is understood to be caused by fluctuations due to temperature. In quantum systems, phase transitions can already happen at zero temperature due to intrinsic quantum mechanical fluctuations. For such transitions, the model example is the Ising model in a transverse magnetic field in just one spatial dimension. Here again, as the magnetic field increases the ground state subspace goes from a symmetry breaking state, where the ground state subspace is degenerate, to a symmetric, unique ground state.

Perhaps surprisingly, not all phases of matter can be described within this paradigm. Historically, the first phase transitions that fall beyond Landau-Ginzburg theory are Wegner's generalized Ising models [65]. We now understand these models in the context of lattice gauge theories with local symmetries. Around the same time the phenomenon of Kosterlitz-Thouless phase transitions was also introduced [66]. For our purposes, the prime example of a physically realized state of matter that does not fall into the Landau-Ginzburg framework is the Fractional Quantum Hall Effect (FQHE). These states are gapped ground states of a cooled 2D gas of electrons that is placed in a perpendicular strong magnetic field [67]. Just as in the classical Hall effect an electric field in the transverse direction is induced by a current density. Field and density are proportional with a constant called the Hall coefficient. Amazingly, this quantity is quantized and different values of this constant correspond to different phases that cannot be distinguished by a symmetry breaking argument. The fractional quantum Hall states and the different quantum phases of matter they correspond to can be understood in the framework of topological order [68–70].

2.3.1 Topologically Ordered Hamiltonians

Several different definitions of topological order can be found in the literature [71]. Below, we shall provide our own. However, there are at least two concepts that are key to topological order, both historically and

conceptually, which every reasonable definition should encompass. At this point, we shall focus on Hamiltonians, and take the viewpoint that topological order is a property of a Hamiltonian and its ground state subspace. Later, we explain the concept on the level of the individual ground states and excitations themselves, an approach which is often more natural.

The first concept is that of topological ground state degeneracy. That ground state degeneracy shows up as a criterion for discriminating quantum phases comes as no surprise. Indeed, it is also present in the case of symmetry breaking. The crucial difference is that in the latter case the degeneracy is not stable against a generic, symmetry breaking, perturbation. In contrast, topological degeneracy is stable against any perturbation of the Hamiltonian [47, 51], hence not detectable with local order parameters. Naturally, we only ask for exact degeneracy in the thermodynamic limit and allow for (exponentially small) splitting in finite systems. Above the (finite) ground state subspace we demand for a stable gap that does not close in the thermodynamic limit.

The second property is the non-Abelian geometric phase [72–74] of the topologically degenerate ground states. This geometric phase is in general a unitary matrix U associated to a closed path of Hamiltonians. Let us put the model on a torus. Two paths are obtained by shearing and squeezing the torus. The unitary that describes how the ground state subspace transforms is given by matrices S and T that form a projective representation of the modular group on the torus. These unitaries now serve as quantum numbers for the phase. The idea behind the S- and T-matrices is presented here very vaguely as they come from the language of abstract conformal field theories and tensor categories [75, 76], which is not our viewpoint. We believe that for lattice systems these quantities can be introduced more clearly using the anyon excitations on top of the ground state subspace. We provide such an explanation in Section 2.3.2.

2.3.2 Anyons in Topological Phases

Another way to understand topological phases, is to look at the possible types of excitations in a system. This is especially useful in two

spatial dimensions on which we now focus. We first review the classic argument for the existence of only bosons and fermions in three spatial dimensions.

One can ask what the possible phase is when two particles are exchanged. Doing this operation twice is topologically trivial in three dimensions because a point (one of the particles) is never an obstruction to deforming and shrinking a circle (the path of the other particle) arbitrary. Hence the exchange operations squares to the identity. This gives as a possible phase for just one exchange only -1 (fermions) and $+1$ (bosons).

Now in two spatial dimensions this argument clearly doesn't work anymore as world lines become braided and cannot be untangled with smooth deformations. Hence in two dimensions there can be arbitrary phases, or even unitary operations associated with exchanging two particles. Such particles are then called anyons [77].

There is one important remark we make before we continue. In the upcoming sections anyons will be algebraically represented by a label a. Such a label is to be interpreted from the viewpoint of quantum many-body systems as an equivalence class of excitations that can be mapped to each other using local operations only. The labels thus correspond to a classification of excitations up to all microscopic degrees of freedom.

2.3.2.1 Labels and Fusion Rules

We now discuss the theory of anyons from the abstract algebraic viewpoint of (unitary modular) fusion categories. We only scratch the surface of this complicated subject and refer the reader to the literature [78, 79] for more information. In the fusion category language we start with a finite set of N labels $\{a\}$ or anyons, with a unique identity label 1, and a fusion map

$$a \times b = \sum_c N_{ab}^c c$$

where the tensor N_{ab}^c only contains non negative integers. If there are several fusion possibilities for two anyons, we call the theory non-Abelian. The tensor N satisfies some extra symmetry constraints due

to commutativity, the existence of an identity element and duals etc. which we do not discuss in detail. We denote the fusion map graphically as in Fig. 2.3a. To every fusion process, there is an associated Hilbert space V_{ab}^{c}, denoted in the figures by Greek letters μ, ν that describes the degrees of freedom corresponding to the process. The dimension of this space corresponds to the number of different ways two particles can fuse to a third, which is precisely N_{ab}^{c}.

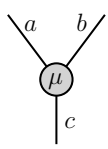

(a) The fusion tree for the process $a \times b$.

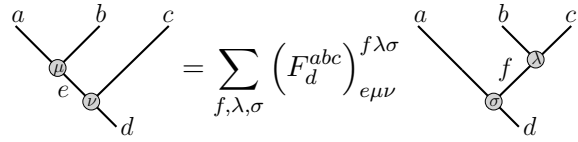

(b) The F-matrix gives the unitary transformation on the fusion spaces.

Figure 2.3

Fusing several particles is associative,

$$(a \times b) \times c = a \times (b \times c).$$

This requirement tells us that although there are several ways to fuse three particles to a fourth, there is an equivalence between them. This means that one way of fusing the three particles, given by a certain fusion tree in the left hand side of Fig. 2.3b can be written as a linear combination of different fusion trees, as is done in the right hand side of Fig. 2.3b. The coefficients of such linear combinations are combined in an important tensor, the F-symbol. This tensor can be chosen such that the matrices between the different fusion trees are unitaries, which gives a nice equivalence between both trees. It should then be thought of as a unitary transformation on the fusion spaces,

$$F_d^{abc} : \bigoplus_e V_{ab}^e \otimes V_{ec}^d \to V_{af}^d \otimes V_{bc}^f.$$

The associativity condition imposes stringent constraints on the F-symbol. It turns out that it is equivalent to the notorious Pentagon equation [80,

81]. We can equate the F-moves along both paths in Fig. 2.4 to obtain Eq. (2.7).

$$\sum_{h,\sigma\lambda\omega} \left(F_g^{abc}\right)_{h\sigma\lambda}^{f\mu\nu} \left(F_e^{ahd}\right)_{i\omega\kappa}^{g\lambda\rho} \left(F_i^{bcd}\right)_{j\gamma\delta}^{h\sigma\omega} = \sum_{\sigma} \left(F_e^{fcd}\right)_{j\gamma\sigma}^{g\nu\rho} \left(F_e^{abj}\right)_{i\delta\kappa}^{f\mu\sigma} \tag{2.7}$$

Finally we mention that every label has a number associated to it, the quantum dimension d_a, which can be derived from the F-symbols.

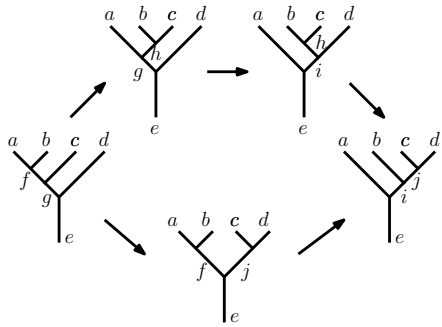

Figure 2.4: The two paths, upper and lower, used to obtain the fundamental pentagon equation.

2.3.2.2 Braiding Rules

Apart from fusion, which is a procedure that can also be carried out in one dimension, we are interested in the exchanging and braiding of anyons. These are the processes that make the non-trivial topological properties of the excitations very clear.

The exchange of two particles is represented by the R-matrix and graphically as in Fig. 2.5a. As it is a bit unclear how to compare states with different anyons a, b before and after an exchange, we often look at the double exchange for different anyons, see Fig. 2.5b. It is therefore often also convenient to only apply exchanges to fusion results as in Fig. 2.5c. All these R-symbols contain the same information.

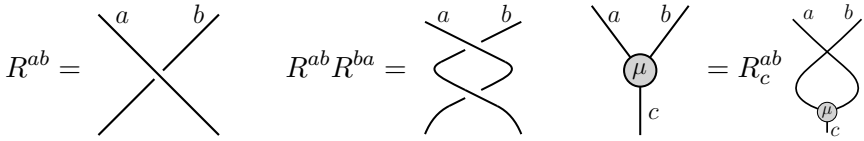

(a) Braiding anyons represented with world-lines.

(b) The full exchange, or double braiding.

(c) Braiding induces a unitary action on the fusion space (μ).

Figure 2.5

There is also a compatibility condition between fusion and braiding which is given by the hexagon equation, a stringent condition involving both F- and R-symbols [82]. Of course the R-matrices also have to satisfy the famous Yang-Baxter equation. We do not pursue this further.

2.3.2.3 The S- and T-matrices

Just as with bosons and fermions, the topological character of particle excitations is also reflected in the spins θ_a of particles a as given in Fig. 2.6a. It can be proven that if there is a finite number of labels the spins are always rational numbers [83]. Again there is a spin-statistic theorem [84]. The spins are gathered in a (diagonal) matrix T. There is also an S-matrix which represents the creation of a particle anti-particle pair of type a, braiding it around b and annihilating it again as in Fig. 2.6b.

(a) Graphical representation of the topological spin or twist of an anyon.

(b) The S-matrix contains the results of transporting an anyon a around an anyon b.

Figure 2.6

The relation between these S- and T-matrices, which are properties of the anyons and the matrices that were introduced in Section 2.3.1 is as follows. Ground states on the torus can be seen as having a definite anyon flux through one of the directions of the torus. These are special ground states as they have a minimal amount of entanglement [85]. Another set of ground states is given by states with anyon fluxes through the other direction. The unitary matrix to go from one basis to the other is given by the S-matrix as defined here but was exactly how we introduced this matrix before as the relation between ground states after transforming the torus (rotating by 90 degrees). The same is true for the T-matrix. The transformation of the torus is given by cutting it open, twisting it and gluing it back together. If one tracks what happens to an anyon flux during these procedures, one finds it is exactly implemented by the braiding and twist operations in Fig. 2.6. Both matrices generate a representation of the modular group, the mapping class group of the torus, hence all topologically allowed transformations can be achieved by products of those two. In our opinion, the interpretation of the S- and T-matrix as describing properties of the excitations is the most natural for lattice systems. As we shall see the equivalence between both definitions is something that is clear in the PEPS picture, which is one of the many benefits of this language.

2.3.3 Long-range Entanglement in Topological Phases

We now refer to the equivalence relation in Definition 7, to relate the notion of topological order and long-range entanglement. The intuition is based on the following fact. Starting from a product state and applying a finite depth quantum circuit, or equivalently evolving for a finite time with a local Hamiltonian, can never create long-range entanglement. Hence, the definition of a quantum phase in Definition 7 gives rise to a picture where the ground states of systems in the same quantum phase all have the same long-range entanglement pattern, the local unitaries only allowing for short range differences. We thus expect our definition of a quantum phase to already encompass the notion of topological order.

2.3.3.1 Topological Properties in a Quantum Phase

It is clear that all Hamiltonians in the same phase according to our definition have the same ground state degeneracy, as unitaries do not change the spectrum. Furthermore the braiding and spin properties of anyons cannot be changed by local unitaries. Indeed, all known anyons are created by a string operator. The algebra of such operators, most importantly the commutation relations, determine the S- and T-matrix. If we apply some local unitaries, we end up with a Hamiltonian and ground state subspace that still allow for anyons, created by fattened operators that are conjugated with the unitaries, hence these are still string operators, whose algebraic relations have not changed. This implies that also the S- and T-matrix remain the same [47].

Clearly then, the definition based on quasi-adiabatic paths captures the vital elements of topological order. At least it makes clear which systems are in the same phase, the trivial phase just one among them, although a completely general invariant to distinguish them is still missing. Symmetries are readily added to this definition by demanding that the interpolating Hamiltonians, hence the associated unitaries, respect them. This gives rise to a finer classification [22, 86–89].

2.3.3.2 Topologically Ordered States

We can use the fact that local unitaries leave all topological and other relevant properties invariant to define a notion of topological order independent of the Hamiltonian. Although our interest is definitely not in random states but in low energy eigenstates of local Hamiltonians, we state the idea behind this definition because it can give more insight especially for readers familiar with error correction.

In Ref. [40], topological order is defined as a property of states instead of Hamiltonians. A quantum state $|\psi_1\rangle$ is said to be topologically ordered if and only if there is a different state $|\psi_2\rangle$ such that for every local observable A we have that $\langle\psi_1|A|\psi_2\rangle = 0$ and $\langle\psi_1|A|\psi_1\rangle = \langle\psi_2|A|\psi_2\rangle$. This definition is reminiscent of the definition of error correction and explains the interest in topologically ordered systems for protecting and storing quantum information as well as doing robust computations [90].

Instead of this strict definition one can of course introduce small quantities ε and demand the properties to be fulfilled up to an error ε. Using this definition one can show stability of the relevant properties under local unitary evolutions.

In conclusion, topologically ordered systems have very interesting and useful properties and exhibit a new playground for theoretical condensed matter physics as well as a challenge for experimentalists. The understanding of these systems is still not completed although in two dimensions a lot is known. One main missing feature is a complete topological invariant to classify a certain phase. Candidates such as degeneracy, topological entropy [91, 92] and importantly, the S- and T-matrices themselves [93, 94], have proven to be very useful. As we shall see, our framework naturally puts forward the F-symbol itself as a candidate. This is expected to be equivalent to a classification based on the S- and T-matrices.

2.4 Case Study: The Toric Code

In this section we focus our attention on a particular model, the famous Toric Code, to illustrate the previously introduced notions of tensor network states, topological order and anyons. Throughout this dissertation we often refer back to this model as a clarifying illustration of the concepts we introduce. Most of the results in Part II are formulated in a general way, such that they are applicable to as large a class of systems as possible. However, this has the disadvantage of obscuring the presentation with technical details. Therefore we shall often return to the Toric Code model to illustrate the results in the simplest non-trivial setting.

2.4.1 The Toric Code

We first introduce the Hamiltonian and the ground states of the Toric Code, before turning our attention on the anyons and looking at their topological properties in more detail.

2.4.1.1 The Toric Code Hamiltonian

The Toric Code was introduced by Kitaev [95] and can be seen as a Hamiltonian version of a discrete Ising gauge theory. It is the simplest toy-model available for understanding the phenomenon of topological order. The name Toric Code derives from its natural topological habitat, a torus, as its topological properties are most clearly visible on such a lattice. The Toric Code is a Hamiltonian defined on a lattice of qubits and it has properties which make it the dream of every quantum-many body theorist, it is simply a sum of commuting projectors. Hence, we immediately know all eigenstates of the Hamiltonian. Still, as we shall see, the model contains more interesting physics than one would first expect. Let us consider a square lattice of qubits on a toroidal topology. The qubits live on the edges of the lattice. The Hamiltonian of the Toric Code consists of a sum of two type of projectors, star projectors A_v, centered around a vertex v and plaquette projectors B_p,

$$H_{\text{TC}} = \sum_{\text{stars } s} \left(\prod_{j \in s} \mathbb{1}_j - A_v \right) + \sum_{\text{plaquettes } p} \left(\prod_{j \in p} \mathbb{1}_j - B_p \right).$$

Here, the star projectors are given by

$$A_s = \prod_{j \in s} X_j$$

and the plaquette operators are given by

$$B_p = \prod_{j \in p} Z_j.$$

As two operators A_v and B_p always share an even number of qubits they act on, either 0 or 2, they clearly commute. See Figure 2.7 for a clarifying illustration of the Toric Code Hamiltonian.

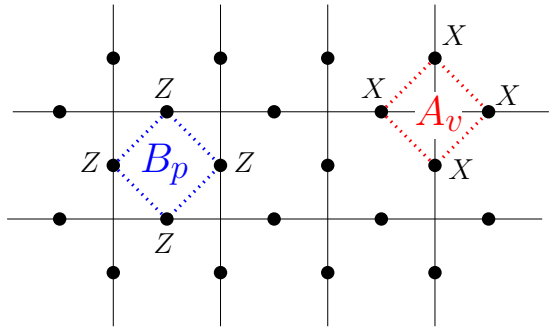

Figure 2.7: The plaquette term B_p and vertex term A_v that appear in the Toric Code Hamiltonian.

2.4.1.2 Ground States of the Toric Code

As the Hamiltonian of the Toric Code consists of commuting projectors, a ground state is given by a state that is in the kernel of all these projectors if such a state exists. One can easily see that such a state exists in the following way. The product state $\prod_j |+\rangle$ is clearly in the $+1$ eigenspace of all the star projectors A_v. In the computational basis that consists of the eigenstates $|0\rangle, |1\rangle$ of Z, the state $\prod_j |+\rangle$ is just the superposition of all product states, of which clearly some, such as $\prod_j |0\rangle$, are also in $+1$ eigenspace of all the B_p. These states are thus in the kernel of all the star and plaquette terms. The question remains now how many ground states exist. The answer to this question will clearly illustrate the topological character of the Toric Code.

The A_v operators make sure that around every vertex there is an even number of $|+\rangle$ states present. This condition implies that the configurations present in a ground state of the Toric Code Hamiltonian consist only of closed loops of $|+\rangle$ states in the X basis. The action of a B_p operator is simply the deformation of such loops. On a plane, every configuration of closed loops can be reached from a given configuration by applying such B_p operators. Hence, the ground state is unique and can be seen as the equal superposition of all closed loops in the computational basis.

However on a topologically non-trivial manifold, one with a non-trivial homotopy group, this is no longer true. On the torus for instance, there are conserved numbers measured by the following operators that commute with H_{TC}, reminiscent of Wilson operators in gauge theories,

$$W_\ell = \prod_{i \in \ell} X_i$$

where ℓ is one of the two loops illustrated in Fig. 2.8 or a topologically equivalent one, i.e. one that can be reached with B_p operators from these basic non-trivial loops. There is now one ground state for every combination of quantum numbers of the operators W_ℓ. On a torus this clearly gives four ground states. More general, the ground state degeneracy only depends on the genus g of the manifold and is given by 2^{2g}.

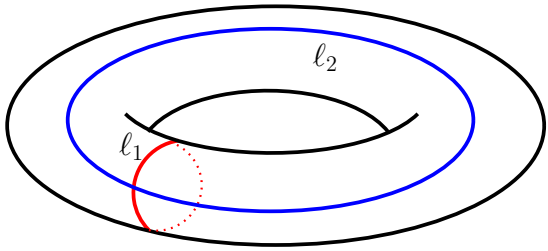

Figure 2.8: On a torus, there a two non-trivial topological loops, ℓ_1, ℓ_2. Strings of Z operators around these loops give rise to the four different ground states.

2.4.1.3 The Toric Code as PEPS

We now illustrate how the Toric Code ground states can be written as a PEPS with bond dimension $D = 2$. Surprisingly, the global, topological, properties of these states can be encoded locally in the PEPS tensors. This, once again, illustrates the power of tensor network methods.

We work on a square lattice and block all four spins around alternating, non-neighboring vertices, which is well defined as the dual lattice is also square, hence bipartite. We initialize all spins in the product state $\prod_j |+\rangle$. As mentioned before, this state satisfies all the vertex constraints in H_{TC}.

We now only need to make sure the plaquette terms are satisfied. These terms demand that the sum of the four spins around every plaquette has even parity in the Z basis. We can satisfy this requirement as follows. Consider first the operator in Fig. 2.9a. It acts as the identity on two physical qubits or as $Z \otimes Z$, conditioned upon the value of an extra virtual index. We now apply this operator on every of the four pairs of neighboring qubits in a super-site as illustrated in Fig. 2.9b. As they all commute, the order of the sequential application is not important. This gives a PEPS tensor with physical dimension $2^4 = 16$ and bond dimensions $D = 2$. In the final state, all virtual indices are to be contracted and the operators in Fig. 2.9a then implement all plaquette constraint projectors. This PEPS is thus a ground state of the Toric Code Hamiltonian H_{TC}.

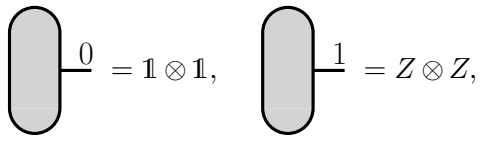

(a) The tensor that is used to implement the plaquette constraints. The combination of two such tensors contracted along the horizontal, virtual index gives the desired operator.

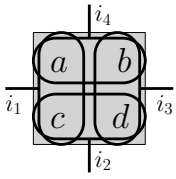

(b) Application of the four operators to a super-site. The qubits a, b, c, d are initially in the $|+\rangle$ state.

Figure 2.9

Let us now identify how the topological properties are encoded in this tensor. We first give an explicit formula for the PEPS tensor A_{TC},

$$A_{\text{TC}} = \sum_{i_1,i_2,i_3,i_4} |i_1 + i_4\rangle\, |i_3 + i_4\rangle\, |i_2 + i_3\rangle\, |i_1 + i_2\rangle\, \langle i_1|\, \langle i_2|\, \langle i_3|\, \langle i_4|\,.$$

Note that the first four kets refer to the degrees of freedom a, b, c, d in Fig. 2.9. The crucial fact is that this tensor only has support in the sector of its four virtual degrees of freedom that is invariant under the application of $X^{\otimes 4}$. We see thus that this tensor has a virtual $\mathbb{Z}_2$ symmetry implemented by the identity and a string of X operators. Moreover, this immediately implies that a string of X operators can

move freely around in the lattice, a property referred to as the pulling through condition.

This behavior lies at the heart of the framework of G-injectivity [21] and MPO-injectivity[23] for the description of topologically ordered PEPS. In this framework the easiest PEPS one can write down in the same phase as the Toric Code, and easily obtained from it by some local manipulations, is a local projector on the even parity subspace. This projector is illustrated in Fig. 2.10 and we refer to the PEPS it defines as the the $\mathbb{Z}_2$-isometric PEPS. We also introduce a graphical notation in Fig. 2.10 and Fig. 2.11 that is used throughout this dissertation.

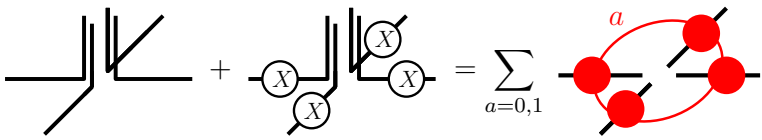

Figure 2.10: The easiest $\mathbb{Z}_2$ topologically ordered PEPS, a local projector on the even parity subspace or the trivial representation. The notation on the right hand side is used throughout this work. The label a gives us a sum over the two MPOs, a loop of $\mathbb{1}$ and a loop of X operators.

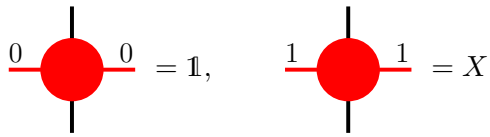

Figure 2.11: The tensor used to construct the PEPS in Fig. 2.10

It is clear that the PEPS built from the tensor in Fig. 2.10 is invariant under the action of closed loops of X tensors on the virtual level and that strings of X operators can be moved freely as illustrated in Fig. 2.12. For all information on G-injective PEPS we refer to the original paper [21]. An introduction to the advanced topic of MPO-injective PEPS [24] is provided in Section II.3.1.

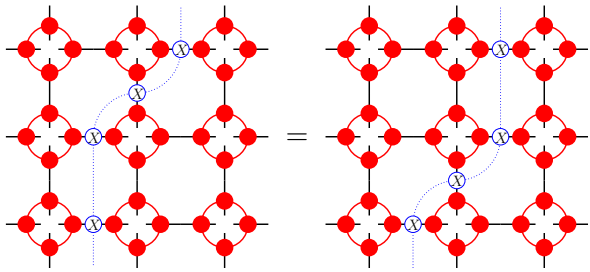

Figure 2.12: The MPO strings can be moved freely through a PEPS network built from the tensors in Figure 2.10, as can be easily checked from their explicit form.

2.4.2 Anyons in the Toric Code

We now discuss the different types of anyons that are present in the Toric Code and study their topological properties, which were introduced in general in Section 2.3.2.

2.4.2.1 Electric and Magnetic Excitations

There are two fundamental topological excitations in the Toric Code model. They correspond to electric charges and magnetic vortices if we think about the theory as a real $\mathbb{Z}_2$ gauge theory. The electric charges correspond to violations of the A_v operators. Indeed, such a violation occurs if a loop (in the X basis) ends at a certain point in the lattice. In the gauge theory this is possible if an electric charge lives on the vertex v whose term is violated, hence the name.

To violate a term A_{v_1}, we can act with a Z operator on one of the qubits on a link around the vertex v. Notice that this immediately violates two different terms A_{v_1}, A_{v_2}, which are those neighboring the link we acted on. Clearly we can only make pairs of excitations this way. The electric path operator

$$W_\ell^E = \prod_{i \in \ell} Z_i$$

with ℓ a path going from A_{v_1} to A_{v_2} can similarly be used to create a pair of excitations, one located at v_1, the other, arbitrary far away, at v_2. One can check that indeed the operator W_ℓ^E commutes with all terms B_p and all A_v, except A_{v_1} and A_{v_2} with whom it anti-commutes. Hence, indeed for every (open) path ℓ the state $W_\ell^E |\psi_0\rangle$ is an eigenstate of the Toric Code Hamiltonian H_{TC} with energy $E = 2$.

Because of the duality between the electric and magnetic parts of the theory, we expect a similar procedure to describe magnetic vortices. Indeed, one can check that the operator

$$W_{\ell^*}^M = \prod_{i \in \ell^*} X_i$$

creates a pair of violations of the two B_p terms at the open ends p_1, p_2 of the path. Here, importantly, ℓ^* is a path in the dual lattice from p_1 to p_2. One again readily checks that $W_{\ell^*}^M$ commutes with all A_v and B_p except B_{p_1} and B_{p_2}, with whom it anti-commutes. It is now clear that $W_{\ell^*}^M |\psi_0\rangle$ is also an eigenstate of the Toric Code Hamiltonian H_{TC} with energy $E = 2$ for every open path ℓ^*.

We denote the topological label associated with electric excitations by e and with magnetic excitations by m. It is clear that in the framework from Section 2.3.2, two electric excitations are in the trivial sector as are two magnetic excitations,

$$e \times e = 1, \qquad m \times m = 1.$$

The combination of one of each type however constitutes a different sector denoted by em,

$$e \times m = em.$$

This gives us a total of four superselection sectors, or anyon excitations, in the Toric Code phase. We have the regular, topologically trivial excitations, we have electric and magnetic excitations and their composite which is often called a dyonic excitation. We now turn our attention to what makes these excitations special and distinguishes them.

2.4.2.2 Anyon Properties of the Excitations

To illustrate the anyon properties of the excitations discussed previously, we calculate the mutual statistics of an e and m excitation. This is the fundamental relation to understand the anyons in the Toric Code as they are the fundamental building blocks, hence other relations, with for instance an em anyon can be deduced from it. Note that clearly e and m excitations behave as bosons among themselves.

We now take an electric charge and drag it around a plaquette containing a vortex. We hence act with a closed loop of Z operators around an excited plaquette p'. Let us denote the state with just the vortex excitations as $|\psi_m\rangle$. The dragging gives

$$\prod_{i\in\ell} Z_i \,|\psi_m\rangle = \prod_{p \text{ in } \ell} B_p \,|\psi_m\rangle \,.$$

Notice that ℓ is here a closed loop and we used a property reminiscent from Stokes' theorem. This is easily seen to be valid here as the action of all plaquette operators cancels on the bulk qubits, since $Z^2 = \mathbb{1}$ and therefor only the boundary remains. Now $|\psi_m\rangle$ is invariant under all operators B_p except $B_{p'}$, which gives $B_{p'}\,|\psi_m\rangle = -\,|\psi_m\rangle$. Hence the mutual statistic of the e and m particles is non-trivial and gives a minus sign.

As claimed, from this fundamental relation we can derive more information such as the self-statistics of the composite em particles, or dyons. To do this, let us go back to the diagrammatic notation of Section 2.3.2 to illustrate its power. With the help of the relations in Fig. 2.13 we illustrate in Fig. 2.14 how we can conclude that the em excitations are fermions.

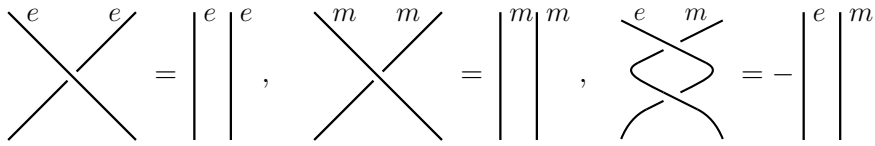

Figure 2.13: The graphical representation of the expression that the e and m excitations are bosons (a,b) and that braiding an e around an m excitations gives a minus sign (c).

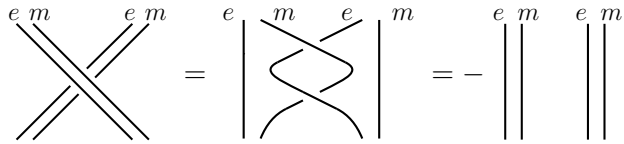

Figure 2.14: The graphical derivation of the claim that the em excitations are fermions.

2.4.2.3 The Anyons in the $\mathbb{Z}_2$-injective PEPS Picture

One of the main benefits of the use of the PEPS in Fig. 2.10 is that the basic types of anyons, the electric and magnetic excitations, can be identified very easily. Recall that this PEPS is not exactly the Toric Code but the $\mathbb{Z}_2$-injective PEPS in the same phase.

A pair of magnetic, or flux, excitations is created by an open string of X operators as in Fig. 2.15a. Due to the way we wrote down this PEPS, the corresponding plaquette operator that is violated now acts on eight spins, but the idea remains identical.

The electric, or charge, excitation is obtained by changing a local tensor from the projector $\mathbb{1}^{\otimes 4} + Z^{\otimes 4}$ to $\mathbb{1}^{\otimes 4} - Z^{\otimes 4}$. Subtly, a single charge can be described in the PEPS, but not created[2]. As local operations cannot change the topological sector, which is the vacuum, they indeed only come in charge, anti-charge pairs. To describe this excitation in the

2. However, notice that a PEPS state that contains only one charge is zero on a sphere, appropriate boundary conditions are required to make this a well-defined state.

MPO picture, we can think about acting with a Z on the inner MPO label as in Fig. 2.10. This indeed changes the projector exactly as mentioned before as it gives an extra minus sign to the X MPO, see Fig. 2.15b.

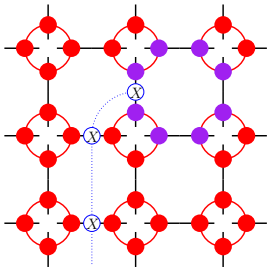

(a) A single flux excitation. It violates the $Z^{\otimes 8}$ plaquette constraint on the eight purple qubits.

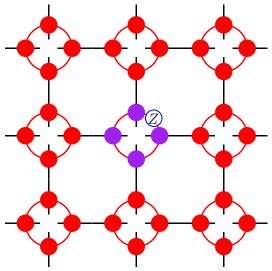

(b) A single charge excitation. It violates the $X^{\otimes 4}$ vertex constraint on the four purple qubits.

Figure 2.15

The difference in the description between electric and magnetic excitations is due to the way we construct the PEPS representation, on the physical level, both still correspond to a string of X or Z operators although only one of them appears on the virtual level.

2.4.3 The Toric Code in a Magnetic Field

Topological phases in two dimensions are not expected to be stable against thermal fluctuations and our example, the Toric Code, is definitely unstable [96–98]. Luckily, the topological phase is stable against (small enough) arbitrary Hamiltonian perturbations [51, 99–102]. Notice that the situation is exactly the reverse situation compared to the two-dimensional classical Ising model, where the symmetry breaking phase is stable against thermal fluctuations but not Hamiltonian perturbations. Let us now focus on a specific Hamiltonian perturbation of the

Toric Code and apply extra magnetic fields. We then get the Hamiltonian

$$H_{\text{TC}}^{h_x,h_z} = \sum_{\text{stars } s} \left(\prod_{j \in s} \mathbb{1}_j - A_s \right) + \sum_{\text{plaquettes } p} \prod_{j \in p} (\mathbb{1}_j - B_p) - h_x \sum_i X_i - h_z \sum_i Z_i.$$

This model has been studied extensively in the literature. The main question to be solved is at which value of the magnetic field the model is no longer topologically ordered. For only one of the fields present, the model can be mapped to the three-dimensional classical Ising model [99] whereas the full model can be mapped to a three dimensional classical $\mathbb{Z}_2$ gauge Higgs model [100]. Both these models can be tackled with standard Monte Carlo methods. Other methods that can be used are high order perturbation expansions [101] or PEPS methods [103]. We shall focus on the easiest case to illustrate our results, i.e. $h_z = 0$ and thus only an X field is applied.

The X field can cause violations of the B_p terms, hence the closed loop condition (in the Z basis) can be violated and magnetic vortices created. We use such a perturbation to illustrate the results in Part II. In Section II.2.2 we calculate, up to lowest order, the quasi-adiabatic generator that gives us the evolution of the ground state along the parameter h_x. Using this generator we calculate the lowest order correction to the entanglement entropy. One can look at the dispersion relation of this model and classify the sectors using the methods explained in Section II.3.6. This was illustrated extensively in [104], we repeat this procedure for the Fibonacci model. Furthermore, this model is ideal to test the variational class introduced in Chapter II.4. We obtain a decent approximation of the critical field in Section II.4.2.2.

Part II

Results

Chapter 1

Stability of the Area Law

In this first chapter of Part II we discuss two different results. One deals with the dynamic properties of quantum many-body systems. We prove a general upper bound on the rate at which entanglement in a system can be generated by evolving a system in time with a local Hamiltonian. Second, we use this result to show that ground states in the same gapped quantum phase have similar entanglement properties in the sense that they all satisfy the area law or none of them does. These results were reported in:

- K. Van Acoleyen, M. Mariën, and F. Verstraete
  Entanglement Rates and Area Laws
  Phys. Rev. Lett. 111, 170501 (2013)

- M. Mariën, K. Audenaert, K. Van Acoleyen and F. Verstraete
  Entanglement Rates and the Stability of the Area Law for the Entanglement Entropy
  Commun. Math. Phys. (2016) 346: 35.

1.1 Entanglement Rate

1.1.1 Introduction

Since its first appearance in a series of ground breaking papers, entanglement has become one of the defining trademarks of quantum mechanics, appearing ubiquitously, both at the theoretical and experimental level. The main goal of these first efforts to describe and understand this phenomenon was to show the incompleteness of the theory of quantum mechanics. However, entanglement has been experimentally verified and is nowadays considered an important feature of the theory and a valuable resource in quantum information and computation protocols.

Because of its importance, it is not surprising that the dynamical properties of entanglement are also of great interest. A very important aspect of a physical system is the rate at which entanglement is, or can be created. The first step in many applications, notably in quantum optics, nuclear magnetic resonance and condensed matter physics, is the creation of entanglement, and much experimental effort has been devoted to optimize this process.

The entanglement rate is very important from a theoretical viewpoint as well and can be used in a wide variety of problems, since it is the dynamical version of one of the most fundamental concepts in quantum information theory, the von Neumann entropy. Some applications are straightforward [105–109] while other applications are more surprising. For example in quantum computing one is interested in establishing bounds on the running time and quantum complexity of algorithms. Since these quantum algorithms are based on the phenomenon entanglement, they often generate it themselves as a by-product. Hence bounding how fast this generation can occur can also establish lower bounds on the running times of these algorithms [110].

On the other hand, the entanglement generated in a system can also have deleterious effects. Decoherence [111] is a result of the entanglement between a system and its environment. This effect is very undesirable in quantum computing, since it destroys the information

stored in a coherent superposition of several qubits. It severely shortens the time a quantum computer can use to do reliable calculations and makes it hard to construct robust quantum memories [112]. Bounds on the entanglement generation therefore also yield bounds on the decoherence time.

In this section we answer the following fundamental question about entanglement dynamics. Given a Hamiltonian interaction between two subsystems A and B, what is the maximal rate at which the corresponding unitary evolution can generate entanglement between these subsystems [105, 106, 113]? We provide a tight upper bound on the maximal entanglement rate in the most general setting.

As a very important application we show that surprisingly, these dynamic properties also have important consequences for the static entanglement properties of quantum many-body systems. Indeed, as an application we prove a stability result for the area law of entanglement entropy. Over the last two decades it has been realized that ground states of gapped local Hamiltonians have very specific properties. One finds that the entanglement entropy of the reduced density matrix of such a ground state of a certain subregion scales with the size of the boundary of this region, instead of the volume law scaling of a typical quantum many-body state [114–116]. It is exactly this boundary scaling that is referred to as the area law [117]. This feature of the entanglement of ground states provides a new window on these systems that allows for a better understanding. Indeed, guided by the area law, efficient tensor network representations of the ground states of quantum many-body systems have been proposed. The link between the area law and an efficient representation of the ground state was proven rigorously for one-dimensional systems [28, 29, 118]. These insights led to the development of several efficient numerical tensor network methods [11]. Moreover, important theoretical advances, for instance the classification of different quantum phases of matter [87, 119], were made through the use of these methods.

However, despite its importance, the area law has only been proven for gapped one-dimensional systems. Our results provide a step in the direction of a general proof for higher dimensions. The formalism of

quasi-adiabatic continuation induces an equivalence relation on the set of ground states of gapped Hamiltonians, these equivalence classes are commonly referred to as gapped quantum phases. Our bound on the entanglement rate allows us to show that for states in the same gapped quantum phase, a subsystem's entropy obeys the same scaling law in both states. Hence, the area law is a property of an entire quantum phase and it suffices to consider one single representative of a phase and show that it satisfies the area law. A related, but weaker, result was obtained in Ref. [120] under additional assumptions.

Moreover, the stability of the area law of the entanglement entropy validates the use of this entropy as a good measure for quantum many-body systems. Indeed, the strongest continuity bound on the entropy is given by the Fannes-Audenaert inequality [121, 122], which has a volume law scaling in the dimensions of the underlying Hilbert space. Unfortunately, we seldom know the exact ground state of a quantum many-body system, but instead we have to rely on an approximation, often in the form of a tensor network state. As the Fannes-Audenaert inequality suggests that the entropy of quantum many-body states is fragile against perturbations, this inequality is too weak to infer features of the entanglement of the true ground state from the approximation. In contrast, our result implies that such an inference is possible, the scaling of two states in the same phase differs at most by the area instead of the volume, hence giving a quantitative notion of the robustness of the entanglement entropy.

1.1.2 Mixing and Entanglement Rates

We start our discussion with a property of ensembles of quantum states known as *small incremental mixing* (SIM). This property was first conjectured by Bravyi [113]. Part of the physical relevance of this property lies in its relation to the *small entangling rate property* (SIE), which we introduce in Section 1.1.2.3. We discuss the connection between SIE and SIM in more detail in Section 1.1.2.4.

1.1.2.1 Small Incremental Mixing

The situation we consider is the following. Suppose we have a probabilistic ensemble of states $\mathcal{E}$. We immediately restrict ourselves for now to the case with only two different states, $\mathcal{E} = \{(p, \rho_1), (1-p, \rho_2)\}$. The expected state of the system is the convex combination of both, $\rho = p\rho_1 + (1-p)\rho_2$. Let each state of this system evolve according to a different Hamiltonian, H_0 and H_1. Without loss of generality we can assume that $H_1 = 0$ and write $H_0 = H$. The evolved expected density operator is then given by

$$\rho(t) = p\rho_1 + (1-p)e^{-iHt}\rho_2 e^{iHt}.$$

We are interested in the von Neumann entropy of this mixture. It is well known that the entropy of this state remains bounded from below and from above for any time t. The precise result is as follows.

Proposition 2. *Let $\mathcal{E} = \{\rho_i, p_i\}$ be a probabilistic ensemble of states and let each state evolve according to a different Hamiltonian H_i. Then the entropy of the expected state satisfies*

$$\overline{S} \leq S(\rho(t)) \leq \overline{S} + \mathsf{h}(\{p_i\}).$$

*Here, $\overline{S} = \sum_i p_i S(\rho_i)$ is the average entropy of the ensemble, which is constant in time, and $\mathsf{h}(\{p_i\})$ is the Shannon entropy of the distribution $\{p_i\}_i$. This property is called **small total mixing**.*

The proof of this proposition relies on well-known properties of the von Neumann entropy. Observe that for two states, this proposition implies that the variation of the entropy goes to zero if p_1 or p_2 goes to zero, as one expects.

Proof. To prove the lower bound we use the following inequalities,

$$\begin{aligned}\overline{S} &= \sum_i p_i S(\rho_i) \\ &= \sum_i p_i S(\rho_i(t)) \\ &\leq S\left(\sum_i p_i \rho_i(t)\right) \\ &= S(\rho(t))\end{aligned}$$

where we first used the unitary invariance of the von Neumann entropy and then the concavity.

To prove the upper bound we introduce a classical system C and the joint state

$$\rho_{CQ}(t) = \sum_i p_i \left|i\right\rangle \left\langle i\right| \otimes \rho_i(t).$$

This state is a density operator on the tensor product of a classical system C and the original Hilbert space. The entropy of this state is given by

$$S(\rho_{CQ}(t)) = \mathsf{h}(\{p_i\}) + \overline{S}.$$

We now define the following matrix

$$R(t) = \begin{pmatrix} \sqrt{p_1\rho_1(t)} \\ \sqrt{p_2\rho_2(t)} \\ \vdots \end{pmatrix}.$$

Both density matrices $\rho_{CQ}(t)$ and $\rho(t)$ are related to the matrix $R(t)$. First, we note that $\rho_{CQ}(t)$ is a pinching of

$$R(t)R(t)^\dagger = \sum_{ij} \sqrt{p_i p_i}\left|i\right\rangle \left\langle j\right| \otimes \sqrt{\rho_i(t)}\sqrt{\rho_j(t)}.$$

From the concavity of the von Neumann entropy it follows that

$$S(R(t)R^\dagger(t)) \leq S(\rho_{CQ}(t)).$$

Second, we have that $\rho(t) = R(t)^\dagger R(t)$. Moreover, the non zero part of the spectrum of $R(t)R^\dagger(t)$ and $R(t)^\dagger R(t)$ are equal. This implies that also the von Neumann entropy of both operators is equal,

$$S(R(t)R^\dagger(t)) = S(R(t)^\dagger R(t)) = S(\rho(t)). \tag{1.1}$$

Combining the relations Eq. (1.1.2.1) and Eq. (1.1), we obtain the desired upper bound. □

Given Proposition 2 it is natural to consider the immediate change of the entropy instead of the total change. Bravyi conjectured the following upper bound on this quantity [113].

Theorem 3 (SIM)**.** *Let $\mathcal{E}$ be a probabilistic ensemble of two states, let $\rho(t) = p_1\rho_1 + p_2 e^{-iHt}\rho_2 e^{iHt}$ be the expected state through time. Then there exists a constant c such that*

$$\Lambda(\mathcal{E}, H) = \left.\frac{dS(\rho(t))}{dt}\right|_{t=0} \leq c\|H\|\mathsf{h}(\{p_1, p_2\})$$

*independent of the ensemble $\mathcal{E}$ and of the details of the Hamiltonian H. This property is called **small incremental mixing (SIM)**.*

In Ref. [113] this conjecture was proven under certain restrictions. The first full proof for finite Hilbert spaces was given in Ref. [123], obtaining $c = 9$. A better constant, $c = 2$ was proven in Ref. [124], by a completely different method. Numerical analysis suggests that $c = 1$ might be the sharpest constant possible. In this chapter we prove Theorem 3 in the more general scenario of infinite-dimensional separable Hilbert spaces. We employ the same method as in Ref. [123], with small adaptations that result in an increase of the constant to $c = 11$.

1.1.2.2 SIM for Larger Ensembles

Until now we have focused on ensembles consisting of only two states. There are two reasons for this restriction. First of all, our primary interest is not the mixing rate but the entangling rate. The latter typically deals with a bipartition of the system, which corresponds to the

mixing rate of just two states. We refer to Section 1.1.2.4 for a detailed explanation of the relation between SIM and SIE. Second, the general case can easily be deduced from the case with only two states, and the arguments are much clearer presented for a small ensemble. For completeness, we discuss the case of general ensembles in this section. We use some results we obtain further on in this chapter. This section may be skipped on first reading.

In Ref. [125] the following was conjectured with a constant $c = 1$ for general probabilistic ensembles that consist of more than two states.

Theorem 4. *For any probabilistic ensemble $\{(p_i, \rho_i)\}$, let*

$$\Lambda(\mathcal{E}) = \max\{|\Lambda(\mathcal{E}, H)| : -\mathbb{1} \leq H_i \leq \mathbb{1}, \forall i\}$$

be the maximally possible mixing rate. Then, an upper bound for this quantity is given by a constant times the Shannon entropy of the distribution $\{p_i\}$,

$$\Lambda(\mathcal{E}) \leq c\mathsf{h}(\{p_i\}) = -c\sum_i p_i \log p_i. \tag{1.2}$$

Here c is a constant independent of the ensemble.

Lieb and Vershynina provided an upper bound

$$\Lambda(\mathcal{E}) \leq 2\sum_i \sum_{j\neq i} \sqrt{p_i p_j}$$

that is rather sharp for large values of the p_i but unfortunately fails to capture the behavior of the conjectured bound Eq. (1.2) for small values of p_i. We give a proof of this bound with a larger constant that nevertheless does capture the small p_i behavior.

Proof. We can obtain an explicit expression of the mixing rate by calculating the derivative. We find that

$$\Lambda(\mathcal{E}, H) = -i\sum_i p_i \operatorname{Tr}\left(H_i[\rho_i, \log\rho]\right).$$

Assuming that SIM for an ensemble of two states holds, which we prove later on, we can apply the upper bound given in equation Eq. (1.2.2)

to each term separately. We restate the bound Eq. (1.2.2) here for convenience of the reader,

$$|\mathrm{Tr}(\log(B)[A,H])| \leq 11p\log(1/p).$$

The conditions on the operators A, B can be found in the statement of Theorem 6. We now have that

$$\Lambda(\mathcal{E},H) \leq 11\sum_i p_i \log\frac{1}{p_i} = 11\mathsf{h}(\{p_i\}).$$

Using the tighter bound obtained in Ref. [124], we obtain a constant 4 instead of 11. The constant $c = 4$ is only valid for finite-dimensional Hilbert spaces. □

1.1.2.3 Small Incremental Entangling

In this section we discuss another property, also first conjectured in Ref. [113], and attributed by its author to Kitaev. This property is called *small incremental entangling* (SIE) and is physically more relevant than SIM. We consider two parties, Alice and Bob who both have a Hilbert space, A respectively B, at their disposal. Clearly, an interaction Hamiltonian H_{AB} can create or destroy entanglement between the two parties. We are interested in the maximal rate at which an interaction can change the bipartite entanglement through time.

Without ancillae, a tight upper bound can easily be proven as was done in Ref. [113], or using different methods in Ref. [126]. We consider the more general and interesting case of ancilla assisted entangling. Apart from the systems A, B, Alice and Bob each have an ancilla a, b respectively, but the interaction Hamiltonian H_{AB} only acts on the systems A, B. The initial state $|\psi_0\rangle$ of the system $aABb$ is assumed to be pure, hence it stays pure throughout its evolution. The state $|\psi_0\rangle$ can have initial entanglement that can dramatically change the rate at which entanglement can be created [105]. Given that we are interested in an upper bound on this rate, independently of the initial state and its entanglement, we only assume that the initial state is pure. Mathematically,

the quantity we study is given by

$$\Gamma(H,\psi) = \left.\frac{dS(\rho_{aA}(t))}{dt}\right|_{t=0}$$

where ρ_{aA} is the reduced density matrix of the total state on subsystem aA and

$$\rho_{aA}(t) = \mathrm{Tr}_{Bb}\left(e^{-iHt}\left|\psi_0\right\rangle\left\langle\psi_0\right|e^{iHt}\right)$$

with

$$H = \mathbb{1}_a \otimes H_{AB} \otimes \mathbb{1}_b.$$

In the absence of ancillae, Bravyi proved that

$$\Gamma(H) \leq c\|H\|\log(d) \tag{1.3}$$

with c a constant and d the smallest of the dimensions of systems A, B. Moreover, he conjectured that this bound also holds in the presence of ancillae but could not prove it.

Since this problem has significant importance in the optimal creation of entanglement, it has been studied by several authors. In Ref. [105] the optimal initial state to create entanglement in the absence of ancillae was identified. Moreover, the authors found that in general, ancillae can increase the entanglement rate, showing the relevance of the presence of ancillae. In Ref. [109], the asymptotic entanglement rate of interaction Hamiltonians between two qubit systems was studied in detail. In Ref. [127], arbitrary dimensions and ancillae were considered with the interaction given by a self-inverse product Hamiltonian. Under these restrictions, the bound $\Gamma(H) \leq \beta$, with $\beta \approx 1.9123$, was obtained. This result was generalized to arbitrary bipartite product Hamiltonians in Ref. [108]. The first general bound independent of the dimension of the ancillae was proven in Ref. [106, bound 4]. For a general Hamiltonian H_{AB} the authors argued that $\Gamma(H) \leq cd^4\|H\|$ with $d = \min(A, B)$ and c a constant, independent of the ancillae a, b. The work of Bravyi [113] implies a refinement, of the form $\Gamma(H) \leq 2\|H\|d^2$. Finally, the results obtained in Ref. [125] imply a bound of the form $\Gamma(H) \leq 4/\ln(2)\|H\|d$, which is still exponentially weaker than the conjectured bound Eq. (1.3) for large values of d. In this work we prove the logarithmic bound

Eq. (1.3), see Theorem 5, which is known to be tight.

To motivate the conjectured bound we first prove a simple upper bound on the total change of the entropy. As in the case of SIM, we can bound the total change of entanglement throughout time.

Proposition 3. *For the system described above, the total change of entanglement through time is bounded from above by*

$$\Delta S(\rho_{aA}(t)) \leq 2 \log d \tag{1.4}$$

with $d = \min\{\dim A, \dim B\}$. *This property is called* ***small total entangling****.*

Proof. The proof is based on the following observation [106]. Every non-local unitary gate U_{AB} can be simulated by first teleporting system A to system B, perform the gate and teleport A back. The amount of entanglement consumed in such a double teleportation is exactly $2 \log A$.

Alternatively, we can give a proof based on the following inequalities. Suppose $d = \dim(B) \leq \dim(A)$. Denote by ρ_{aA} and $\tilde{\rho}_{aA}$ the reduced density matrix of the system before and after applying the unitary U_{AB} respectively. We have that

$$\begin{aligned} |S(\rho_{aA}) - S(\tilde{\rho}_{aA})| &= |S(\rho_{aA}) - S(\rho_{aAB}) + S(\tilde{\rho}_{aAB}) - S(\tilde{\rho}_{aA})| \\ &\leq |S(\rho_{aA}) - S(\rho_{aAB})| + |S(\tilde{\rho}_{aAB}) - S(\tilde{\rho}_{aA})| \\ &\leq S(\rho_B) + S(\tilde{\rho}_B) \\ &\leq 2 \log(d). \end{aligned}$$

In the second line we used the fact that $S(\rho_{aAB}) = S(\tilde{\rho}_{aAB})$ since U_{AB} does not act on system b. The last inequality follows from the subadditivity of the von Neumann entropy. The bound Eq (1.4) is tight, as setting U_{AB} equal to the swap gate shows. □

Kitaev proposed a related upper bound on the maximal rate at which the entanglement can change.

Theorem 5 (SIE)**.** *Denote $d = \min\{\dim A, \dim B\}$, then there is a constant c such that*

$$\Gamma(H, \psi) \leq c\|H\| \log d \tag{1.5}$$

independently of the dimensions of the ancillae a, b, the initial state $|\psi\rangle$ of $aABb$ and the details of the interaction Hamiltonian H. We call this property ***small incremental entangling (SIE)****.*

As it is implied that H is an interaction Hamiltonian only acting on A, B, we dropped the explicit subscript for clarity. Bravyi proved this upper bound under certain restrictions. Using his method, a proof for this conjecture was first obtained in Ref. [123]. As we explain in Section 1.1.2.4, our method gives a constant c that is twice the constant obtained in Theorem 3. Here, we obtain a constant $c = 22$. Based on numerical evidence, we expect $c = 2$ to be the optimal value.

Bravyi already showed that the logarithmic scaling in the bound (1.5) is tight. Surprisingly, this is already true for systems without ancillae [113]. One can wonder about the importance of using ancillae. As already noted, examples are known where the use of ancillae allows for a larger entangling rate. Furthermore, several phenomena have been studied in the literature where local ancillae and some initial entanglement between a part of the system and an ancillae can have unexpected results. The well known example of the swap operator illustrates this for the entanglement rate [106]. If no ancillae are present this operator cannot change the entanglement between A and B. However, if both A, B have an identical copy as ancillae and we start from the state $|M_{aA}\rangle \otimes |M_{Bb}\rangle$ with $|M\rangle$ a maximally entangled state, it is clear that the swap operator creates the maximal amount of entanglement as given in Proposition 3.

There are other manifestations of the importance of ancillae. For example in Ref. [128] it was shown that the mutual information can violate a property called incremental proportionality. In the presence of ancillae it is possible to increase the classical mutual information between two parties by an arbitrary amount just by sending a single qubit. In contrast, the mutual information does satisfy a property called total proportionality, which can be considered the analogue of Proposition 2 and 3. At first sight, there is no reason to believe the same cannot happen for the

von Neumann entropy. Is it possible to lock entanglement in a state, such that in a short time an interaction can free this entanglement and hence allow for an arbitrary change in the entropy? As we shall prove, this is not the case.

1.1.2.4 Relating SIM and SIE

At first sight, SIM and SIE look like two rather unrelated dynamical properties of the entanglement entropy. In this section we show that SIM is actually a stronger version of SIE. This connection was made by Bravyi [113], but for completeness we repeat his argument here in detail. To make the connection between the quantities Λ and Γ, we first give explicit expressions for both. An easy calculation shows that the mixing rate is given by

$$\Lambda(\mathcal{E}, H) = -ip_2 \operatorname{Tr}\left(H[\rho_2, \log(\rho)]\right) \text{ with } \rho = p_1\rho_1 + p_2\rho_2. \tag{1.6}$$

Similarly we can work out the derivative and obtain an expression for the entangling rate,

$$\Gamma(H, \psi) = -i \operatorname{Tr}\left(\mathbb{1}_a \otimes H_{AB}[\rho_{AaB}, \log(\rho_{Aa}) \otimes \mathbb{1}_B]\right). \tag{1.7}$$

Without loss of generality we assume that $d = \dim B \leq \dim A$. Since the bound in Theorem 5 only depends on the smallest dimension, we can extend A to $a \otimes A$, hence we can assume that $\dim a = 1$ and reduce the total system to ABb. We now define the state

$$\tau_{AB} = \rho_A \otimes \frac{\mathbb{1}_B}{d}$$

and rewrite

$$\Gamma(H, \psi) = -i \operatorname{Tr}\left(H[\rho_{AB}, \log \tau_{AB}]\right). \tag{1.8}$$

This last expression already starts to look like the mixing rate (1.6). We continue by defining a well suited probabilistic ensemble $\mathcal{E}$ to complete the reduction of SIE to SIM. By comparing the equations (1.6) and (1.8) it is clear that we want τ_{AB} to be the expected state of an ensemble of which ρ_{AB} is one of the constituents. The following simple lemma, again taken from Ref. [113], shows that such an ensemble exists.

Lemma 2 ([113])**.** *Let ρ_{AB} be a mixed state. Then there exists another mixed state μ_{AB} such that*

$$\rho_A \otimes \frac{\mathbb{1}_B}{d} = \frac{1}{d^2}\rho_{AB} + \left(1 - \frac{1}{d^2}\right)\mu_{AB}.$$

Proof. Clearly the existence of the state μ_{AB} is equivalent to the condition

$$\rho_{AB} \leq d(\rho_A \otimes \mathbb{1}_B).$$

Furthermore, since the partial trace is a linear operation, it suffices to consider the case that $\rho_{AB} = |\psi\rangle\langle\psi|$, a pure state. Define the maximally entangled unnormalized state

$$|I\rangle = \sum_{j=1}^{d} |j\rangle_A |j\rangle_B$$

with $\{|j\rangle_A\}$ a basis of the Hilbert space A and $\{|j_B\rangle\}$ of the Hilbert space B. By the Schmidt decomposition there exist an operator X and a unitary U such that

$$|\psi\rangle = X \otimes U |I\rangle .$$

Since $\langle I, I\rangle = d$, we have that $|I\rangle\langle I| \leq d\mathbb{1}_{AB}$. Conjugating this inequality with $X \otimes U$ we immediately get

$$|\psi\rangle\langle\psi| \leq d(X^\dagger X \otimes \mathbb{1}_B) = d(\rho_A \otimes \mathbb{1}_B)$$

which finishes the proof. □

We can now continue our strategy to show that SIM implies SIE. We define the ensemble

$$\mathcal{E} = \left\{ \left(1 - \frac{1}{d^2}, \mu_{AB}\right), \left(\frac{1}{d^2}, \rho_{AB}\right) \right\}$$

whose existence is assured by Lemma 2. Indeed, μ_{AB} is precisely the state appearing in that lemma. Moreover, the average state of this ensemble is exactly $\rho_A \otimes \mathbb{1}_B/d$.

Proposition 4. *The small incremental mixing theorem implies the small incremental entangling theorem.*

Proof. Let us assume that SIM is true. We are clearly only interested in the case where $p \leq 1/2$. To sharpen the constant we assume the conjecture in the following slightly adapted form,

$$\Lambda(\{p, 1-p\}, H) \leq -cp \log(p) \|H\|. \tag{1.9}$$

This inequality is clearly equivalent with the SIM conjecture, apart from a possible modification of the constant. We use inequality (1.9) because it allows for the smallest constant prefactor.

Inequality (1.9) gives for the ensemble $\mathcal{E}$ that

$$\Lambda(\mathcal{E}, H) \leq \frac{2c}{d^2} \log(d) \|H\| \tag{1.10}$$

with $H = H_{AB}$ the Hamiltonian from Eq. (1.8). Using Eq. (1.6) we can write the expression for Λ as

$$\Lambda(\mathcal{E}, H) = -i \frac{1}{d^2} \operatorname{Tr}\left(H[\rho_{AB}, \log \tau_{AB}]\right). \tag{1.11}$$

We combine equation (1.10) and (1.11) and find that

$$-i \operatorname{Tr}\left(H[\rho_{AB}, \log \tau_{AB}]\right) \leq 2c \log(d) \|H\|.$$

Comparing the expression on the left hand side with Eq. (1.8) we find that

$$\Gamma(H, \psi) \leq 2c \log(d) \|H\|.$$

Hence, we can conclude that SIM with a constant c implies SIE with a constant $2c$. □

It remains to show the validity of the SIM conjecture, in the form of the inequality (1.6) or (1.9).

1.2 A Trace Norm Inequality for Commutators

In this section we discuss Theorem 6, which was first conjectured in Ref. [113]. From expression (1.6) it is clear that the statement of this theorem is equivalent with the small incremental mixing property, Theorem 3. For the sake of clarity, we state it as an independent result that may be of interest in matrix analysis. Therefore, we prove this result in the more general case of separable Hilbert spaces, although for the physically relevant spin systems, it suffices to deal with finite-dimensional Hilbert spaces.

Theorem 6. *Let A, B be positive trace class operators on a separable Hilbert space $\mathcal{H}$, such that $A \leq B$, $\mathrm{Tr}(A) = p \in [0, 1]$, $\mathrm{Tr}(B) = 1$. Then there is a constant c such that*

$$\|[A, \log B]\|_1 \leq c\, \mathsf{h}(p). \tag{1.12}$$

As noted in Ref. [129], the more general case without extra restrictions on $\mathrm{Tr}(A), \mathrm{Tr}(B)$ can easily be reduced to the inequality (1.12). A proof yielding $c = 9$ was obtained in Ref. [123] for $\mathcal{H}$ finite-dimensional and a completely different proof, based on the continuity properties of the quantum skew divergence, was given in Ref. [124]. The latter proof gives a constant $c = 2$. The proof given here is a generalization of the method in Ref. [123] and gives a constant $c = 11$. The increase of the constant from 9 to 11 is entirely due to the use of infinite-dimensional Hilbert spaces. We remark that numerical evidence suggests that $c = 1$ is in fact the best possible constant.

To be complete we mention the following conjecture, which is a natural generalization of Theorem 6.

Conjecture 1 ([129])**.** *Let A and B be positive semidefinite $d \times d$ matrices with $\mathrm{Tr}\, A = a$ and $\mathrm{Tr}\, B = b$. For certain functions $f : \mathbb{R} \to \mathbb{R}$ (still to be determined), there exists a constant c, independent of d such that*

$$\|[B, f(A + B)]\|_1 \leq c\, (F(a + b) - F(a) - F(b))\,,$$

with $F(x) = \int_0^x f(y)dy$.

Theorem 6 concludes the proof of Theorem 3 (SIM). It also finishes the argument given in Section 1.1.2.4, hence the proof of Theorem 5 (SIE).

We now give the proof of Theorem 6 in the next two sections. Both can be skipped entirely by readers only interested in the result and the applications. For clarity, we start with some minor lemmas that allow us to deal with a very simplified version of the problem. The idea of the full proof is to reduce the problem to this simplified case.

1.2.1 Some Technical Lemmas

We start with some lemmas that can be used to treat the case $\mathrm{Tr}(A) \leq \lambda_{min}(B)$. This makes the extra constraint $A \leq B$ redundant.

Lemma 3. *Suppose A is a positive trace class operator and B is a positive operator such that* $\operatorname{spec} B \subset [b_L, b_U]$. *We have that*

$$\|[A, \log B]\|_1 \leq 2 \operatorname{Tr} A \log \left(\frac{b_U}{b_L} \right).$$

Proof. We have that

$$\begin{aligned} \|[A, \log B]\|_1 &= \|[A, \log B - \log b_L \mathbb{1}]\|_1 \\ &\leq 2\|A(\log B - \log b_L \mathbb{1})\|_1 \\ &\leq 2\|A\|_1 \|\log B - \log b_L \mathbb{1}\|_{\mathrm{op}} \\ &\leq 2 \operatorname{Tr}(A)(\log b_U - \log b_L). \end{aligned}$$

In the first line we use the invariance of a commutator under adding a scalar operator to one of the arguments. The second and third line follow from the triangle and Hölder's inequality. In the last line we use the positivity of A and the restriction on $\operatorname{spec}(B)$. □

Since we want to obtain a proof for a constant c as small as possible, we give a stronger statement that removes the factor 2. The proof is analogous but uses a commutator inequality for positive operators by Kittaneh [130] instead of the triangle inequality.

Lemma 4. *Suppose A is a positive trace class operator and B is a positive operator such that* $\operatorname{spec} B \subset [b_L, b_U]$. *We have that*

$$\|[A, \log B]\|_1 \leq \log\left(\frac{b_U}{b_L}\right) \operatorname{Tr} A.$$

Our general strategy is to reduce the general case to the case where we can use Lemma 4 and bound the remaining cases with a Cauchy-Schwarz inequality. We use similar ideas as in Ref. [123]. The main difference with the finite-dimensional case is that we need the following theorem by Kittaneh [131].

Lemma 5 ([131])**.** *Let A, B be bounded self-adjoint operators such that* $\operatorname{spec}(A) \subset [a_L, a_U]$ *and* $\operatorname{spec}(B) \subset [b_L, b_U]$. *Then, for every operator X and every unitarily invariant norm $|||.|||$ we have that*

$$|||AX - XB||| \leq \max(a_U - b_L, b_U - a_L)|||X|||.$$

For completeness we reproduce the short proof.

Proof. We introduce the notation

$$a_M = \frac{a_L + a_U}{2} \text{ and } b_M = \frac{b_L + b_U}{2}.$$

Then we have that

$$\begin{aligned}
|||AX - XB||| &= |||(A - a_M)X - X(B - b_M) + (a_M - b_M)X||| \\
&\leq (\|A - a_M\| + \|B - b_M\| + |a_M - b_M|)\,|||X||| \\
&= ((a_U - a_M) + (b_U - b_M) + |a_M - b_M|)\,|||X||| \\
&= \max(a_U - b_L, b_U - a_L)|||X|||.
\end{aligned}$$

□

We need a last technical lemma that is a matrix version of the Cauchy-Schwarz inequality.

Lemma 6. *Let $\bigoplus_k S_k, \bigoplus_k T_k$ be block diagonal Hilbert Schmidt operators. Then, the following holds,*

$$\sum_k |\mathrm{Tr}(S_k T_k)| \leq \left(\sum_k \|S_k\|_2^2\right)^{1/2} \left(\sum_k \|T_k\|_2^2\right)^{1/2}.$$

Proof. The proof is immediate,

$$\begin{aligned}\sum_k |\mathrm{Tr}(S_k T_k)| &= \left|\mathrm{Tr} \bigoplus_k S_k \bigoplus_k T_k\right| \\ &\leq \left\|\bigoplus_k S_k\right\|_2 \left\|\bigoplus_k T_k\right\|_2 \\ &= \left(\sum_k \|S_k\|_2^2\right)^{1/2} \left(\sum_k \|T_k\|_2^2\right)^{1/2}.\end{aligned}$$

□

We use Lemma 6 to replace the Cauchy-Schwarz argument used on the matrix elements in the finite-dimensional case [123].

1.2.2 Proof of Theorem 6

After the previous technical intermission, we return to the main subject of this section, the proof of the matrix inequality (1.12).

Proof. To prove Theorem 6 we first fix $\mathrm{Tr}(A) = p \in (0,1)$ and partition the spectrum of B in countably many subsets related to this value p. To be specific, consider the intervals $I_k = [p^{k+1}, p^k)$ for all $k \in \mathbb{N}$. Notice that we can always restrict the Hilbert space to the support of B. Furthermore, since B is positive and has trace equal to 1, 1 itself cannot be in the spectrum of B. Hence the union of these intervals I_k ultimately contains the entire spectrum of B. Of course, some I_k may be empty, let $K \subset \mathbb{N}$ be the set of integers k for which $\mathrm{spec}(B) \cap I_k \neq \emptyset$.

We now use the orthonormal basis consisting of eigenvectors of B and the spectral partitioning $\{I_k\}_{k\in K}$ to decompose the Hilbert space $\mathcal{H}$. Let $\mathcal{H}_k$ be the subspace of $\mathcal{H}$ spanned by the eigenvectors of B that correspond to eigenvalues in I_k. This induces a direct sum decomposition

$$\mathcal{H} = \bigoplus_{k\in K} \mathcal{H}_k.$$

By definition of the direct summands, the operator B also decomposes as a block diagonal operator

$$B = \bigoplus_{k\in K} B_k$$

where each of the operators B_k only acts on $\mathcal{H}_k$. We now introduce the resolution of the identity related to this decomposition. Let $\{P_k\}_{k\in K}$ be the complete set of mutually orthogonal projectors such that $P_k : \mathcal{H} \to \mathcal{H}_k$ is the projector onto $\mathcal{H}_k$ and $\sum_{k\in K} P_k = \mathbb{1}$ with $\mathbb{1}$ the identity operator on the full Hilbert space $\mathcal{H}$. By definition of these projectors we have that $P_k B P_l = B_k \delta_{kl}$. The reason for this decomposition is that the spectrum of the restricted operators B_k is bounded from below and above as $\mathrm{spec}\,(B_k) \subset I_k$.

We now use the following variational characterization of the trace norm for a self-adjoint trace class operator O,

$$\|O\|_1 = \max_{-\mathbb{1}\leq H\leq \mathbb{1}} \mathrm{Tr}(HO).$$

We have that

$$\begin{aligned}
\|[A, \log B]\|_1 &= \|i[A, \log B]\|_1 \\
&= \max_{-\mathbb{1}\leq H\leq \mathbb{1}} i\,\mathrm{Tr}([A, \log B]H) \\
&= \max_{-\mathbb{1}\leq H\leq \mathbb{1}} i\,\mathrm{Tr}(\log B[A, H]).
\end{aligned}$$

Take a random H, it suffices to prove that

$$W = i\,\mathrm{Tr}\,(\log(B)[A, H]) \leq c\mathsf{h}(p).$$

We now write W as a sum of several terms, where each term has contributions based on the partitioning of $\mathcal{H}$ introduced above. Let us define

$$A_{kl} = P_k A P_l, \quad H_{lk} = P_l H P_k$$

and

$$W_{kl} = i \operatorname{Tr} \left(\log(B_k) A_{kl} H_{lk} - H_{lk} A_{kl} \log(B_l) \right).$$

It is clear from this definition that $W_{kl} = \overline{W_{lk}}$. This notation allows us to write

$$\begin{aligned} W &= i \operatorname{Tr} \left[\log B \left(\sum_k P_k \right) A \left(\sum_l P_l \right) H \right. \\ &\qquad \left. - \log B \left(\sum_l P_l \right) H \left(\sum_k P_k \right) A \right] \\ &= \sum_{k,l \in K} W_{kl}. \end{aligned}$$

We continue the strategy of expressing everything in the basis of B. Since $0 \leq A \leq B$ there exists an $0 \leq X \leq \mathbb{1}$ such that

$$A = B^{1/2} X B^{1/2}.$$

This implies that $A_{kl} = B_k^{1/2} X_{kl} B_l^{1/2}$ with $X_{kl} = P_k X P_l$.

We now introduce the central idea to bound W. We make a distinction between couples of parts of the spectrum k, l which are close together, i.e. in the same or neighboring intervals I_k, I_l, and those which are far from each other. More specifically, we split the sum as

$$W = \underbrace{\sum_{k,l \in K, |k-l|<2} W_{kl}}_{W'} + \underbrace{\sum_{k,l \in K, |k-l| \geq 2} W_{kl}}_{W''}. \tag{1.13}$$

The first sum contains the contributions of pairs of eigenvalues close to each other, while the second contains those of further separated pairs. The logic behind the particular rearrangement (1.13) is that the terms in the first sum are the terms that can be bounded using Lemma 4. The

terms in the second sum, W'', are precisely those that can be bounded using the Cauchy-Schwarz inequality. We proceed by bounding the latter terms, W''. The general case considered here requires a bit more care than the finite-dimensional case [123]. This causes an increase of the constant c from 9 to 11.

We introduce some extra operators to lighten the notation. Let

$$Z_{kl} = B_k^{1/2} X_{kl}, \quad Y_{kl} = X_{kl} B_l^{1/2} = B_k^{-1/2} Z_{kl} B_l^{1/2}.$$

We only consider the indices (k,l) such that $l > k+1$, call this set I. We now have that

$$W'' = \sum_{(k,l)\in I} (W_{kl} + W_{lk}).$$

From Lemma 6 it follows that

$$\begin{aligned}
|W''| &\leq 2 \sum_{(k,l)\in I} |W_{kl}| \\
&= 2 \sum_{(k,l)\in I} \left| \operatorname{Tr}\left(\log(B_k) B_k^{1/2} X_{kl} B_l^{1/2} H_{lk} - H_{lk} B_k^{1/2} X_{kl} B_l^{1/2} \log(B_l) \right) \right| \\
&= 2 \sum_{(k,l)\in I} \left| \operatorname{Tr}\left[(\log(B_k) Y_{kl} - Y_{kl} \log(B_l)) \left(H_{lk} B_k^{1/2} \right) \right] \right| \\
&\leq 2 \left(\sum_{(k,l)\in I} \| \log(B_k) Y_{kl} - Y_{kl} \log(B_l) \|_2^2 \right)^{1/2} \left(\sum_{(k,l)\in I} \left\| H_{lk} B_k^{1/2} \right\|_2^2 \right)^{1/2}.
\end{aligned}$$

Recall that by definition, $p^{k+1} \leq B_k \leq p^k$ for all $k \in K$. We find the following inequality

$$\|Y_{kl}\|_2 \leq \|B_k^{-1/2}\| \|Z_{kl}\|_2 \|B_l^{1/2}\| \leq \sqrt{p^l / p^{k+1}} \|Z_{kl}\|_2.$$

By Lemma 5 we have that,

$$\begin{aligned}
\| \log(B_k) Y_{kl} - Y_{kl} \log(B_l) \|_2 &\leq \max\left(\log(p^k/p^{l+1}), \log(p^l/p^{k+1}) \right) \|Y_{kl}\|_2 \\
&\leq \max\left(\log(1/p^{l-k+1}), \log(p^{l-k-1}) \right) \\
&\qquad \times \sqrt{p^{l-k-1}} \|Z_{kl}\|_2.
\end{aligned}$$

Since we only sum over indices $(k,l) \in I$ for which $l > k+1$, we have that $p^l < p^{k+1}, 1 \leq 1/p^{l-k+1}$ and $p^{l-k-1} \leq 1$. Thus, we can bound the prefactor in the previous inequality as

$$\begin{aligned}\max\left(\log\left(p^{-l+k-1}\right), \log(p^{l-k-1})\right) p^{\frac{l-k-1}{2}} &= \log\left(p^{-l+k-1}\right) p^{\frac{l-k-1}{2}} \\ &= \frac{l-k+1}{l-k-1} \log\left(p^{-l+k-1}\right) p^{\frac{l-k-1}{2}} \\ &\leq 3 \log\left(p^{-l+k-1}\right) p^{\frac{l-k-1}{2}}.\end{aligned}$$

Due to the slightly different Cauchy-Schwarz argument, here a factor 3 appears, which differs from the finite-dimensional case and results in a bigger constant $c = 11$. To bound the contributions of the form $\log(1/x)\sqrt{x}$ we consider the function

$$x \mapsto \log(1/x)\sqrt{x},$$

which is monotonously increasing on the interval $[0, e^{-2}]$ and attains its maximum value, $2e^{-1}$, at $x_{\max} = e^{-2}$. Since $l-k-1 \geq 1$, we have that

$$\log(1/p^{l-k-1})\sqrt{p^{l-k-1}} \leq f(p)$$

with the function f defined as

$$f(p) = \begin{cases} \log(1/p)\sqrt(p) & \text{if } 0 < p \leq e^{-2} \\ 2e^{-1} & \text{otherwise.} \end{cases}$$

For applications, we are mainly interested in the regime $p \ll 1$, since $1/p$ corresponds to $\dim(B)^2$, the dimension of the Hilbert space. Moreover for large p, better bounds can be established [125] that do not suffer from a relatively large constant prefactor. Clearly, it is the first case in the definition of f that is important.

We now bound the contribution of W''. By the previous observations, we have that

$$|W''| \leq 6 f(p) \left(\sum_{(k,l)\in I} \|Z_{kl}\|_2^2\right)^{1/2} \left(\sum_{(k,l)\in I} \|H_{lk} B_k^{1/2}\|_2^2\right)^{1/2}.$$

Now the initial condition $0 \leq A \leq B$ gives that $0 \leq X \leq \mathbb{1}$, which immediately implies that $0 \leq X^2 \leq X$. Therefore, we have that

$$\sum_{l \in L} X_{kl} (X_{kl})^\dagger \leq X_{kk}$$

for any possible index set $L \subset K$. We now have that

$$\begin{aligned} \sum_{(k,l) \in I} \|Z_{kl}\|_2^2 &= \sum_{(k,l) \in I} \operatorname{Tr}\left(X_{kl}^\dagger B_k X_{kl} \right) \\ &\leq \sum_{k \in K} \operatorname{Tr}(B_k X_{kk}) \\ &= \sum_{k \in K} \operatorname{Tr} A_{kk} = \operatorname{Tr} A = p. \end{aligned}$$

We continue in the same fashion to bound the final factor. As we considered normalized interactions, we have that $\|H\| = 1$ and $0 \leq H^2 \leq \mathbb{1}$. Therefore,

$$\sum_{l \in L} H_{lk}^\dagger H_{lk} \leq \mathbb{1}$$

for every set $L \subset K$. Hence we find that

$$\begin{aligned} \sum_{(k,l) \in I} \|H_{lk} B_k^{1/2}\|_2^2 &= \sum_{(k,l) \in I} \operatorname{Tr}\left(H_{lk}^\dagger H_{lk} B_k \right) \\ &\leq \sum_{k \in K} \operatorname{Tr} B_k = \operatorname{Tr} B = 1. \end{aligned}$$

Combining these estimates, we find that

$$|W''| \leq 6 f(p) \sqrt{p}. \tag{1.14}$$

We now bound the first part of the sum in Eq. (1.13), W'. These are actually the easy terms that can be treated as the case in Lemma 3 and Lemma 4. We first need to split up the first term W' even more. Define the set

$$K' = \{k \mid k, k+1 \in K\}$$

and

$$V_k = \begin{cases} W_{k,k} + W_{k,k+1} + W_{k+1,k} + W_{k+1,k+1} & \text{if } k \in K' \\ W_{k,k} & \text{if } k \in K \setminus K'. \end{cases}$$

We can now rewrite the first term as

$$W' = V - V' = \sum_{k \in K} V_k - \sum_{k \in K'} W_{k+1,k+1}.$$

Here we introduce an extra term $V' = \sum_{k \in K'} W_{k+1,k+1}$ to compensate the double counting of some of the diagonal elements $W_{k,k}$. We have obtained the finale decomposition of $W = V - V' + W''$. By the triangle inequality,

$$|W| \leq |V| + |V'| + |W''| \tag{1.15}$$

and since we already obtained a bound on W'', it suffices to bound the first two terms separately.

We first deal with the term $|V|$. Once again, we first introduce some notation. Let us define the projector

$$Q_k = \begin{cases} P_k \oplus P_{k+1} & \text{if } k \in K' \\ P_k & \text{if } k \in K \setminus K'. \end{cases}$$

Now we define

$$\tilde{B}_k = Q_k B Q_k, \quad \tilde{A}_{kl} = Q_k A Q_l, \quad \tilde{H}_{kl} = Q_k H Q_l.$$

Since $p^{k+2} \leq \tilde{B}_k \leq p^k$, we still have good bounds on the spectrum of $\tilde{B}_k$, although slightly weaker than in the case of the operator B_k. We now write the contribution of V_k as

$$V_k = i \operatorname{Tr} \left(\log \tilde{B}_k \tilde{A}_{k,k} \tilde{H}_{k,k} - \tilde{H}_{k,k} \tilde{A}_{k,k} \log \tilde{B}_k \right)$$

independently of $k \in K'$ or not, which was the motivation behind the introduction of the projectors Q_k. Since $\|H\| \leq 1$, we have for all k that $\|\tilde{H}_{k,k}\| \leq 1$. Hence,

$$|V_k| \leq \|[\log \tilde{B}_k, \tilde{A}_{k,k}]\|_1.$$

We now apply Lemma 4 and use that $p^{k+2} \leq \tilde{B}_k \leq p^k$ to conclude that

$$|V_k| \leq \operatorname{Tr}\left(\tilde{A}_{k,k}\right) \log\left(\frac{1}{p^2}\right).$$

To bound the contribution of $|V|$ we sum over all k and since all terms are positive, we find that

$$|V| \leq \log\left(\frac{1}{p^2}\right) \sum_{k\in K} \operatorname{Tr} \tilde{A}_{k,k} \tag{1.16}$$

$$\leq \log\left(\frac{1}{p^2}\right) 2 \sum_{k\in K} \operatorname{Tr} A_{k,k} \tag{1.17}$$

$$= 4p \log\left(\frac{1}{p}\right). \tag{1.18}$$

The extra factor 2 in the second line appears because of the double counting of some of the diagonal elements, i.e. when $k \in K'$.

With a similar reasoning we can bound the contribution of $|V'|$. We have that

$$|W_{k,k}| \leq \|[\log B_k, A_{k,k}]\|_1 \leq \operatorname{Tr}\left(A_{k,k}\right) \log\left(\frac{1}{p}\right).$$

We can now sum over $k \in K'$ and obtain

$$|V'| \leq \log\left(\frac{1}{p}\right) \sum_{k\in K'} \operatorname{Tr} A_{k+1,k+1} \tag{1.19}$$

$$\leq \log\left(\frac{1}{p}\right) \sum_{k\in K} \operatorname{Tr} A_{k,k} \tag{1.20}$$

$$= \log\left(\frac{1}{p}\right) \operatorname{Tr} A \tag{1.21}$$

$$= p \log\left(\frac{1}{p}\right). \tag{1.22}$$

We obtained the final upper bound on $|W|$. Indeed, putting all obtained upper bounds (1.15), (1.14), (1.18), (1.22) together, we find that

$$|W| \leq 6\sqrt{p} f(p) + 5p \log(1/p). \tag{1.23}$$

As claimed, for $p \leq e^{-2}$, which is the regime of interest, we find that

$$|W| \leq 11p\log(1/p). \tag{1.24}$$

More generally, for $p \leq 1/2$ one can easily show that the bound (1.23) is itself smaller than $11\mathsf{h}(p)$ which proves Theorem 6 for $p \leq 1/2$ and with $c = 11$.

We can transform the case $1/2 \leq p < 1$ to the discussed case $0 < p \leq 1/2$ by using the substitution $A \mapsto B - A$ and using the fact that $\mathrm{Tr}(B-A) = 1 - p$ and $[A, \log(B)] = -[B - A, \log(B)]$. Hence, the claim holds for all $p \in [0, 1]$. □

1.3 Entanglement Generation in Spin Systems

We first give a very simple application of the SIE bound (1.5) as an introduction to the main application and as a demonstration of the importance of the logarithmic dependence of this upper bound. We consider the lattice $\mathcal{L} = \mathbb{Z}^\nu$ equipped with the metric $\mathbf{d}$ and a quasi-local, translation-invariant Hamiltonian H. For this application we only need the property discussed in Remark 1 and the quasi-local properties of H, the LR-locality of this system is not needed. The restriction to translation-invariant interactions can be removed, especially when considering more general lattices.

Recall the notions discussed in Definition 2. We now define the following additional quantities. Let $m(v) = \mathbf{d}(v, \partial\mathcal{B}_1)$ for $v \in \mathcal{B}_2$ and $m(v) = \mathbf{d}(v, \partial\mathcal{B}_2)$ for $v \in \mathcal{B}_1$ and let $M(r) = \{v \in \mathcal{L} \mid m(v) \leq r\}$. This last set contains exactly the sites of the lattice whose distance to the boundary between $\mathcal{B}_1$ and $\mathcal{B}_2$ is at most r. It is clear that

$$|M(r)| \leq \sum_{v \in \partial\mathcal{B}_1} |B_r(v)| + \sum_{v \in \partial\mathcal{B}_2} |B_r(v)|.$$

Hence for $\mathbb{Z}^\nu$ equipped with the metric $\mathbf{d}$, it holds that $M(r) \leq 2A(2r)^\nu$. More generally, we can prove the following proposition if $M(r) \leq cAr^\mu$ for constants $c > 0$ and $\mu \geq 0$. The existence of such constants is clear for all lattices that satisfy the condition in Remark 1.

Proposition 5. *Consider the lattice $\mathbb{Z}^\nu$ equipped with the metric $\mathbf{d}$ and let each site support a Hilbert space of dimension d. Let Φ be a translation-invariant potential that generates a quasi-local Hamiltonian H_L on the lattice $\mathcal{L} = \mathbb{Z}_L^\nu$ for all L with decay function f that decreases faster than $r^{-(2\nu+1+\delta)}$ for a $\delta > 0$. Let the system be in the initial state $|\psi\rangle$ and denote by $|\psi(s)\rangle$ the time evolution of this state and by $\rho_{\mathcal{B}_1} = \mathrm{Tr}_{\mathcal{B}_2} |\psi\rangle\langle\psi|$ the reduced density matrix at $\mathcal{B}_1$. We denote the entanglement entropy at time s by by*

$$S_{B_1}(s) = -\operatorname{Tr}(\rho_{\mathcal{B}_1}(s)\log(\rho_{\mathcal{B}_1}(s))).$$

Then the entanglement rate of H relative to this bipartition satisfies an area law,

$$\left|\frac{dS_{\mathcal{B}_1}(s)}{ds}\right| \leq CA$$

with C a constant that depends on the details of the lattice, the metric and the Hamiltonian, but, importantly, not on the lattice size L.

Proof. By definition H can be decomposed as

$$H = \sum_{v\in\mathcal{L}}\sum_{r\in\mathbb{N}} h_v(r) \quad \text{with} \quad \|h_v(r)\| \leq f(r).$$

By definition, the rate at which the Hamiltonian H creates entanglement between $\mathcal{B}_1$ and $\mathcal{B}_2$ is given by

$$\frac{dS_{\mathcal{B}_1}(s)}{ds} = i\sum_{v\in\mathcal{L}}\sum_{r\in\mathbb{N}} \operatorname{Tr}\left(h_v(r)[|\psi\rangle\langle\psi|, \log\rho_{\mathcal{B}_1}\otimes\mathbb{1}_{\mathcal{B}_2}]\right). \tag{1.25}$$

It is clear that operators $h_v(r)$ that only act within $\mathcal{B}_1$ or $\mathcal{B}_2$ do not contribute to this rate. Indeed, suppose h only acts within $\mathcal{B}_2$, then $[\rho_{\mathcal{B}_1}, h] = 0$. It follows immediately that

$$\operatorname{Tr}\left(h[|\psi\rangle\langle\psi|, \log\rho_{\mathcal{B}_1}\otimes\mathbb{1}_{\mathcal{B}_2}]\right) = 0$$

using the cyclicity of the trace. If h only acts on $\mathcal{B}_1$, similar arguments allow us to conclude the contribution of h to the sum in Eq. (1.25) vanishes. Indeed, if h is only supported on $\mathcal{B}_1$ we have that

$$\operatorname{Tr}\left(h[|\psi\rangle\langle\psi|, \log\rho_{\mathcal{B}_1}\otimes\mathbb{1}_{\mathcal{B}_2}]\right) = \operatorname{Tr}_R\left(h[\rho_{\mathcal{B}_1}, \log\rho_{\mathcal{B}_1}]\right) = 0.$$

Therefore we can restrict the summation over v. We are interested in interaction terms $h_v(r)$ whose range r is larger than the distance of the site v to the boundary of the bipartition. We have that

$$\left|\frac{dS_{\mathcal{B}_1}(s)}{ds}\right| \leq \sum_{v\in\mathcal{L}} \sum_{r\geq m(v)} |\mathrm{Tr}\left(h_v(r)[|\psi\rangle\langle\psi|, \log\rho_{\mathcal{B}_1}\otimes \mathbb{1}_{\mathcal{B}_2}]\right)| \tag{1.26}$$

$$\leq \sum_{r\in\mathbb{N}} \sum_{v\in\mathcal{L}:m(v)\leq r} |\mathrm{Tr}\left(h_v(r)[|\psi\rangle\langle\psi|, \log\rho_{\mathcal{B}_1}\otimes \mathbb{1}_{\mathcal{B}_2}]\right)| \tag{1.27}$$

$$\leq \sum_{r\in\mathbb{N}} |M(r)| \left(\log\left(d^{(2r)^\nu}\right)\|h(r)\|\right) \tag{1.28}$$

$$\leq 2^{\nu+1} c\log(d) A \sum_r r^{2\nu}\|h(r)\|. \tag{1.29}$$

In the first step we use the triangle inequality and restrict the summation to terms that contribute a non-zero value. In the second step, we change the order of the summations. In the third step we use Theorem 5 and the fact that the support of $h(r)$ only grows like a polynomial in r as stated in Remark 1. We use the polynomial $P(r) = (2r)^\nu$, but clearly the specific choice of the polynomial will only influence the constant prefactor. In the last step, we use the assumption on the increase of $M(r)$. Clearly the condition on the decay of $\|h(r)\|$ assures that the last summation over r converges. □

Remark that the proposition remains valid for time dependent potentials $\Phi(s)$ and Hamiltonians $H_L(s)$ as every step in the proof can be repeated and is still valid for time dependent systems.

This proposition is most interesting when the geometry of the bipartition of $\mathcal{L}$ in subsets $\mathcal{B}_1, \mathcal{B}_2$ is not too complicated. Indeed, for complicated bipartitions, the size of the area might be of the same order as the volume, L^ν. For more regular bipartitions, like a rectangular subset, the size of the boundary is typically only of the order $L^{\nu-1}$.

For strictly local Hamiltonians, or interactions with rapid exponential decay, the previously obtained bounds on the entanglement rate with a polynomial dependence on the dimension of the Hilbert spaces were good enough to obtain a similar result [40] and prove that the entanglement rate scales like the area of the boundary of a bipartition. In

contrast, it is clear that for general quasi-local Hamiltonians, only the logarithmic dependence of Theorem 5 is strong enough to make the summation over r in expression (1.29) converge.

1.4 The Area Law in a Gapped Phase

1.4.1 The Stability of the Area Law

Recall Definition 7 that introduces the concept of a gapped quantum phase. In this section we prove that the entanglement entropy relative to a fixed bipartition of a quantum spin system is the same for all states in a given quantum phase, up to a term that scales like the boundary area of the bipartition. Hence, we prove that an area law for one specific ground state automatically carries over to all other ground states that are in the same quantum phase. To apply the formalism of quasi-adiabatic continuation, we need that the Hamiltonians $H(s)$ are LR-local. Indeed, this is a crucial requirement to prove that the generator of the quasi-adiabatic evolution is quasi-local.

Let us first define what it means for a quantum spin system to satisfy an area law for the von Neumann entropy.

Definition 10. *Let Φ be a gapped, translation-invariant potential on $\mathbb{Z}^\nu$ that generates Hamiltonians H_L on $\mathcal{L} = \mathbb{Z}_L^\nu$ for all L. We say that this quantum spin system satisfies an area law if the following holds. Let $S(\mathcal{B})$ be the entanglement entropy of the unique ground state of H_L relative to a bipartition $\mathcal{B}_1, \mathcal{B}_2$ of $\mathcal{L}$, then*

$$S(\mathcal{B}) \leq CA(\mathcal{B})$$

with C a constant independent of L and the bipartition and $A(\mathcal{B})$ the area of the boundary between $\mathcal{B}_1, \mathcal{B}_2$.

The non-trivial part of this definition is the statement that C is independent of L. Indeed, for a fixed L we can always take $C = \log(\dim(\mathcal{H}_\mathcal{L}))$. Hence, both the definition of a gapped quantum phase and the area law property are best formulated for sequences of states defined on

lattices of increasing size. The formulation in terms of a potential of Definitions 7 and 10 allows us to look at the sequence of ground states of the Hamiltonians H_L generated by this potential.

A similar definition holds for ground state subspaces with a finite degeneracy q. Moreover, we are not restricted to lattices $\mathcal{L} = \mathbb{Z}_L^\nu$ or translation-invariant Hamiltonians, but we should be able to define the system on lattices of increasing size, hence some spatial homogeneity seems necessary.

If we can bound the rate at which entanglement is generated along a quasi-adiabatic path, we can prove an upper bound on the total change of entanglement along the entire path. Recall that $m(v) = \mathbf{d}(v, \partial\mathcal{B}_1)$ for $v \in \mathcal{B}_2$, $m(v) = \mathbf{d}(v, \partial\mathcal{B}_2)$ for $v \in \mathcal{B}_1$ and $M(r) = \{v \in \mathcal{L} \mid m(v) \leq r\}$. Moreover, we have that $M(r) \leq 2A(2r)^\nu$ for $\mathbb{Z}^\nu$ equipped with $\mathbf{d}$.

Theorem 7. *Consider the lattice $\mathbb{Z}^\nu$ equipped with the metric $\mathbf{d}$ and let each site support a Hilbert space of dimension d. Let Φ_s be a quasi-adiabatic path on the quantum spin system. Consider the finite lattice $\mathcal{L} = \mathbb{Z}_L^\nu$ and denote the Hamiltonians induced by the potentials $\Phi(s)$ simply by $H(s)$. Denote by $|\psi(0)\rangle, |\psi(1)\rangle \in \mathcal{H}_\mathcal{L}$ the unique ground states of $H(0)$ and $H(1)$ respectively. Let $\mathcal{B}_1, \mathcal{B}_2$ be a fixed bipartition of the lattice. Denote the size of the area of the boundary between $\mathcal{B}_1$ and $\mathcal{B}_2$ by A. Then, the entanglement entropy of $|\psi(0)\rangle$ and $|\psi(1)\rangle$ differ at most by a constant times the area of the boundary between $\mathcal{B}_1, \mathcal{B}_2$. Therefore, if $|\psi(0)\rangle$ satisfies an area law, so does $|\psi(1)\rangle$ and vice versa.*

Proof. We are interested in the entanglement entropy of the ground states $|\psi(s)\rangle$ of $H(s)$ and more precisely in the rate of change of this quantity as s changes. We can use Proposition 5 to bound the entanglement rate along s,

$$\left|\frac{dS_{\mathcal{B}_1}(s)}{ds}\right| \leq cA2^{\nu+1} \log d \sum_{r\in\mathbb{N}} r^{2\nu} \|k_r(s)\|.$$

Since $\|k_r(s)\|$ decays super-polynomially, it is clear that this last sum is bounded by a constant. Hence we find that the rate of change is bounded by a constant C times the area A of the boundary between

$\mathcal{B}_1, \mathcal{B}_2$,

$$\left| \frac{dS_{\mathcal{B}_1}(s)}{ds} \right| \leq CA. \tag{1.30}$$

Now consider two Hamiltonians $H(0), H(1)$ which are in the same quantum phase. By Definition 7, there exists a quasi-adiabatic path connecting them. We can bound the entanglement rate along this path and upon integration of inequality (1.30) we find that

$$\Delta S_{\mathcal{B}_1} = S_{\mathcal{B}_1}(1) - S_{\mathcal{B}_1}(0) \leq CA$$

for a constant C independent of the system size L or boundary area A. Hence, we have shown that all ground states within the same gapped quantum phase have the same area law behavior. Either they all satisfy the area law for the entanglement entropy or they all violate it. □

The proof can be generalized to quantum spin systems defined on different lattices that satisfy the condition in Remark 1, which implies that $M(r)$ is bounded by a polynomial in r.

1.4.2 Degenerate Ground States

The stability of the area law readily generalizes to the case of a finitely degenerate ground state subspace. The formalism of quasi-adiabatic continuation still applies to these systems. Let us take two Hamiltonians $H(0), H(1)$ that are in the same phase. Necessarily, the ground state degeneracy of $H(0)$ and $H(1)$ is the same. Let us assume that there is a basis of the ground state subspace of $H(0)$ such that all basis vectors satisfy an area law. Under quasi adiabatic evolution, this basis is mapped to a basis of the ground state subspace of $H(1)$. By Theorem 7, these basis states all satisfy the area law.

Moreover, given a basis of the ground state subspace of a Hamiltonian such that all basis vectors satisfy the area law, we can bound the entanglement of a general state in the ground state subspace. Indeed, a finite superposition of states that satisfies the area law, still satisfies the area law itself [132]. Given a two orthogonal ground states $|\psi_1\rangle, |\psi_2\rangle$, we

find that

$$S(\alpha\,|\psi_1\rangle + \beta\,|\psi_2\rangle) \leq 2\left(|\alpha|^2 S(|\psi_1\rangle) + |\beta|^2 S(|\psi_2\rangle) + \mathsf{h}(|\alpha|^2, |\beta^2|)\right)$$

For a general basis or for larger superpositions, the entanglement can still be bounded and the area laws continue to hold. However, the expression for the increase of the prefactors is more complicated [132] than the previous expression.

For a degeneracy that grows with the system size, the existence of linearly independent ground states of H_0 that satisfy the area law still implies the existence of an equal number of linearly independent ground states of H_1 with the same property. However, one can draw no conclusions about the entanglement of a general ground state in the huge ground state subspace of such a Hamiltonian.

1.4.3 Fermionic Lattice Systems

We can extend Theorem 7 to systems consisting of fermions living on a lattice and with the fermionic Hamiltonian H_f local in the sense of fermionic modes. An example of such a fermionic Hamiltonian is given by the famous Fermi-Hubbard model,

$$H_{FH} = -t \sum_{\langle ij\rangle\sigma} c^\dagger_{i\sigma} c_{j\sigma} + U \sum_i n_{i\uparrow} n_{i\downarrow} - \mu \sum_i n_i.$$

The modes correspond to the lattice points where the fermions live and possibly extra labels such as the spin of the fermions. For simplicity we only consider the lattice labels and ignore these extra degrees of freedom. Fix an ordering of the fermions and apply the Jordan-Wigner transformation [133]. This transformation turns the fermionic Hamiltonian into a spin Hamiltonian of the following form,

$$H_{JW} = \sum_{v\in\mathcal{L}} h_v \otimes Z_{G_v}.$$

Here, h_v is a local interaction term centered around site v and Z_{G_v} is a non-local string of Pauli Z operators working on a certain region G_v. This region depends on the chosen ordering.

We first note the following simple fact.

Proposition 6. *The maximal entanglement rate of a Hamiltonian H relative to a bipartition $\mathcal{B}_1, \mathcal{B}_2$ does not change under unitary transformations of the form $U = U_{\mathcal{B}_1} \otimes U_{\mathcal{B}_2}$,*

$$\Gamma(H) = \Gamma(UHU^\dagger).$$

Proof. It is straightforward to check the following relation for every state $|\psi\rangle$,

$$\Gamma(H, \psi) = \Gamma(UHU^\dagger, U\psi).$$

Indeed, due to the factorized form of U all unitaries in equation (1.7) cancel. This implies that the entanglement rate Γ, which is a maximum over all possible states $|\psi\rangle$ is equal for both Hamiltonians. □

Several possible ways to quantify the entanglement of a fermionic system have been studied in the literature [134]. Here we define the entanglement rate of H_f as that of H_{JW}. It now suffices to bound the entanglement rate of a term $h_v \otimes Z_{G_v}$ similarly as we bounded h_v.

We write $Z_{G_v} = Z_{G_v}^{\mathcal{B}_1} \otimes Z_{G_v}^{\mathcal{B}_2}$ with both operators supported strictly on one side of the bipartition. Since $Z_{G_v}^{\mathcal{B}_1}$ has a spectrum containing an equal number of ± 1, there exists a unitary operator $U_{\mathcal{B}_1}$ such that

$$U_{\mathcal{B}_1} Z_{G_v}^{\mathcal{B}_1} U_{\mathcal{B}_1}^\dagger = Z_{v^*} \otimes \mathbb{1}_{G_v \setminus \{v^*\}}.$$

Here, $v^* \in G_v$ is a vertex site neighboring the support of h_v. A similar unitary $U_{\mathcal{B}_2}$ can be found for $Z_{G_v}^{\mathcal{B}_2}$. Both these unitaries map the entire string of Z operators to a Z on a single site. We now use Proposition 6 to obtain that

$$\begin{aligned}\Gamma(h_v \otimes Z_{G_v}) &= \Gamma\left(U_{\mathcal{B}_1} \otimes U_{\mathcal{B}_2}(h_v \otimes Z_{G_v})U_{\mathcal{B}_1}^\dagger \otimes U_{\mathcal{B}_2}^\dagger\right) \\ &= \Gamma\left(Z_{v_1^*} \otimes h_v \otimes Z_{v_2^*}\right) \leq c\|h_v\| \log(D+2).\end{aligned}$$

Corollary 1. *The entanglement rate of a fermionic Hamiltonian H_f that is local in the sense of modes, obeys an area law.*

Proof. The result follows from the previous discussion and the results on spin lattices and local spin Hamiltonians given in Proposition 5. □

1.5 Outlook and Conclusion

1.5.1 Outlook: The Area Law under Adiabatic Growing

In the previous sections we have given a rigorous proof of the stability of the area law in a gapped quantum phase. One of the main motivations to obtain the stability of the area law was to find a new method to prove the area law itself. This section is of a more speculative character and we do not claim that all our arguments can be made rigorous.

First we give some intuition as to why the stability of the area law can be used to infer properties about the validity of the area law. We give some conditions under which this intuition can be turned into a rigorous proof. Second, we discuss some related work by other authors and some directions to improve on these results.

1.5.1.1 Intuition and Obstructions

Consider a two-dimensional square lattice $\mathcal{L} \subset \mathbb{Z}^2$ of arbitrary, but finite, size $L \times L$. Here, we do not assume periodic boundary conditions. Each vertex v has a local Hilbert space of dimension d. We consider a uniformly bounded, local potential Φ on $\mathbb{Z}^2$ on this lattice such that the Hamiltonians H_L have a gap and a unique ground state. We are interested in the entanglement entropy of the reduced density matrix of the ground state of a square region $\mathcal{V}$ of size $\ell \times \ell$, with $1 \ll \ell \ll L$. Consider the ground state of the Hamiltonian $H_\mathcal{V}$ on this $\ell \times \ell$ subset $\mathcal{V}$ and think of it as consisting of the ground state $|\psi_\mathcal{V}\rangle$ on the $\ell \times \ell$ lattice and a product state of all $|0\rangle$ on all other sites. Now consider the same model, but on a slightly bigger subset $\mathcal{W} = \mathcal{V} \cup \{v\}$. Here $v \in \mathcal{L} \setminus \mathcal{V}$ is just a single lattice site neighboring $\mathcal{V}$. We denote the ground state of $H_\mathcal{W}$ by $|\psi_\mathcal{W}\rangle$.

Intuitively, it should be possible to go from $|\psi_\mathcal{V}\rangle \otimes |0\rangle_w$ to $|\psi_\mathcal{W}\rangle$ by acting with a unitary that acts only on the state $|0\rangle$ of the extra added site v and the sites close to it, within a ball of radius ξ, the correlation length. This formalizes the idea that both ground states should be in the same gapped quantum phase once the system is big enough. We

keep repeating this procedure until we end up with the ground state of the model on a lattice of size $L \times L$. This procedure is illustrated in Fig.1.1.

We can now look at the entanglement of this state, relative to a bipartition of the system into the subset $\mathcal{V}$ and the rest. Since we started with a product state between both systems, we started without entanglement. Every step involved a unitary which created an amount of entanglement $\sim \xi^2 \log d$. After going from the $\ell \times \ell$ subsystem to an $(\ell + \xi) \times (\ell + \xi)$ subsystem, we applied $\sim 4\ell\xi$ of these unitaries. Hence the state now has no more entanglement than a constant times ℓ, it has an area law. We can now grow the system until we obtain the ground state on the entire lattice. The unitaries we now apply do not act on the subset A, hence they create no additional entanglement. See again Fig. 1.1 for an illustration of this argument. We conclude that the ground state of our model obeys the area law,

$$S(\rho_A) \leq C\xi^3 \log d\ell.$$

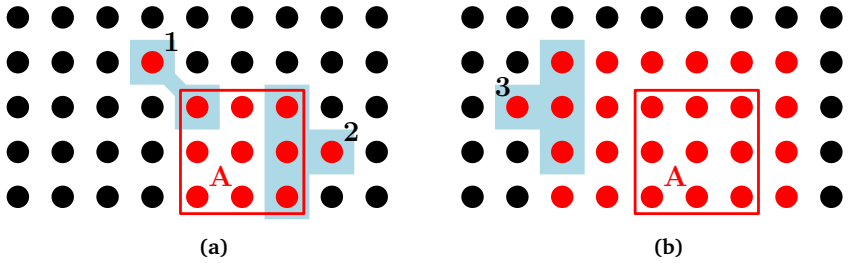

Figure 1.1: We are interested in the entropy of region A. The red dots are in the ground state, the black dots are ancillae in a product state. In Fig 1.1a we act with two unitaries, blue colored, to create the ground state on region A and qubits 1,2. After acting with a number of these unitaries proportional to the boundary we are in the situation of Fig. 1.1b. Adding more qubits does not change the entropy of region A since the unitary needed to create the ground state on the extra qubit 3 only acts within the complement of A.

There are three obstacles that need to be overcome to turn this argument into a proof. First, the unitaries that are used to grow the ground state can never be expected to act strictly on a number of sites $\sim \xi^2$. In general they are generated by a quasi-local Hamiltonian which is more or less supported around these sites. This situation is of course exactly the kind of problem that Theorem 5 was designed to solve.

There are two more serious issues that we cannot solve without extra assumptions. First, we ignored the fact that typically Hamiltonians have edge modes. A model that has a unique ground state on a closed lattice, like a sphere, or in the thermodynamic limit, can have a degenerate ground state subspace on a lattice with open boundary conditions. It will have a, possibly exponentially large, degenerate ground state subspace, with exponentially small splitting, separated from the rest of the spectrum by a gap Δ. This problem can be dealt with if we can make the ground state unique by introducing some local boundary Hamiltonian. It is known that this is possible for several interesting models like the Toric Code or more general string-net models [135–137], but there are certainly counterexamples like the fractional quantum Hall effect [78, 138].

The last problem concerns the existence of a quasi-local unitary that maps the ground state of a model on $\ell \times \ell$ sites to the ground state on a slightly bigger lattice. This assumption expresses the fact that if ℓ is large enough and the model has a well defined thermodynamic limit, adding a single particle shouldn't change anything concerning the phase of the ground state. Hence, there should be a gapped adiabatic path between both states, which ensures the existence of such a unitary. Unfortunately, counterexamples to this condition exist, for instance Haah's cubic code [139] does not satisfy this requirement, although it obeys the area law trivially since it is a PEPS.

If both conditions hold, a proof for the area law follows immediately as discussed in the following corollary.

Corollary 2. *Consider the lattice $\mathbb{Z}^\nu$ with the metric $\mathbf{d}$ and let every site support a Hilbert space of dimension d. Let $\{|\psi_\mathcal{V}\rangle \mid \mathcal{V} \subset \mathbb{Z}^\nu\}$ be a collection of states, with $|\psi_\mathcal{V}\rangle \in \mathcal{H}_\mathcal{V}$ for every finite $\mathcal{V} \subset \mathbb{Z}^\nu$. Take such a finite set $\mathcal{V}$ and let $v \in \mathbb{Z}^\nu \setminus \mathcal{V}$ be a site neighboring but not in $\mathcal{V}$. Suppose that for all such $\mathcal{V}, v$ the state $|\psi_{\mathcal{V}\cup\{v\}}\rangle$ can be obtained from $|\psi_\mathcal{V}\rangle\otimes|0\rangle$ by evolving with a quasi-local Hamiltonian centered around v for finite time T. Moreover, we require an uniform upper bounds T on the time and the existence of a super-polynomial decay function Q that can be used for all Hamiltonians. Then, this collection of states satisfies an area law in the sense that there is*

C independent of $\mathcal{V}$ such that for every bipartition $\mathcal{B}_1, \mathcal{B}_2$ of $\mathcal{V}$,

$$S(\mathrm{Tr}_{\mathcal{B}_1}(|\psi_{\mathcal{V}}\rangle\langle\psi_{\mathcal{V}}|)) \leq CA$$

with A the size of the boundary between $\mathcal{B}_1$ and $\mathcal{B}_2$.

Proof. Take a finite $\mathcal{V}$ and a bipartition $\mathcal{B}_1, \mathcal{B}_2$. Consider the state $|\psi_{\mathcal{B}_1}\rangle$. We then go to the state $|\psi_{\mathcal{V}}\rangle$ by adding more and more ancillae sites and evolving with quasi-local Hamiltonians. We can sum all the contributions to the entanglement when we evolve $|\psi_{\mathcal{B}_1}\rangle \otimes |0\rangle^{|\mathcal{B}_2|}$ to $|\psi_{\mathcal{V}}\rangle$ with these Hamiltonians. This gives us expressions very similar to the one used in the proof of Theorem 7. These expressions can be bounded analogously as inequalities (1.26)-(1.29) and the claim follows. Moreover, it is clear that there exists a constant C that only depends on the uniform quantities T, K. □

Remark 2. Corollary 2 can be used in the following situation. Consider again the lattice $\mathbb{Z}^\nu$ and suppose we have a potential Φ such that the Hamiltonians H_L on $[0, L]^\nu$ have edge modes, such that the degeneracy of the ground state subspace potentially depends on L. If we can obtain a ground state of H_L from a ground state on a smaller lattice by evolving with a quasi-local Hamiltonian centered around the boundary, we can still prove that this collection of ground states satisfies the area law.

One way to obtain a collection of states as described in Corollary 2 is by using boundary terms. Fix an $R > 0$, we call an operator B a boundary term if it acts only on sites $v \in \mathcal{L}$ whose distance to the boundary between $\mathcal{V}$ and $\mathbb{Z}^\nu \setminus \mathcal{V}$ is smaller than R. Now suppose that for all finite subsets $\mathcal{V} \subset \mathbb{Z}^\nu$,

(a) There exists local boundary terms B that can be added to $H_{\mathcal{V}}$ such that the Hamiltonian $\tilde{H}_{\mathcal{V}} = H_{\mathcal{V}} + B$ is gapped and has a unique ground state.

(b) One can go from the ground state of $\tilde{H}_{\mathcal{V}}$ to that of $\tilde{H}_{\mathcal{V}\cup v}$ by evolving with a quasi-local Hamiltonian centered around v. Here $v \in \mathbb{Z}^\nu \setminus \mathcal{L}$ is a site neighboring $\mathcal{V}$.

Then the collection of unique ground states of $\tilde{H}_{[0,L]^\nu}$ for all L satisfies the area law by Corollary 2.

Similarly as Theorem 7, we can generalize this corollary to different lattices. By now, it is clear which conditions we need to obtain the result.

Remark 3. We would like to comment on a subtle point. Since the procedure we described above consists of the application of several quasi-local unitaries, one could naively think that the state we start with and the state we end up with are in the same phase. However, this is not necessarily true, since the length of the adiabatic path we need scales with the system size, in contrast to Definition 7. Indeed it is well known that non-trivial topologically ordered models such as the Toric Code and other string-net models can be obtained by a very similar procedure as the one we described [96, 140]. We only assume that the ground states on lattices of size N or $N+1$ are in the same phase and this does not necessarily imply that ground states on for instance N and N^2 sites are in the same phase.

1.5.1.2 Related Work

Independently, very similar ideas were reported and further elaborated on by other authors. For completeness and to illustrate the general idea of turning the stability of the area law in a proof of the area law itself, we summarize the work of these authors.

In Ref. [141] an area law was proven for systems obeying the following two conditions. First, there exists a sequence of Hamiltonians

$$\{H_1, H_2, \ldots, H_N\}$$

acting on N qubits, such that the next Hamiltonian is constructed from its predecessor by adding a term only at the boundary close to the added point. Furthermore all Hamiltonians have a gap at least Δ. This requirement takes care of the problem concerning edge modes that was mentioned before.

Second, it is assumed that the ground states $|\psi_0^k\rangle, |\psi_0^{k+1}\rangle$ of two consecutive Hamiltonians have a finite, non zero overlap. Using this condition

the author can prove the existence of a gapped Hamiltonian path between consecutive Hamiltonians. Hence the formalism of quasi-adiabatic continuation assures the existence of a quasi-local unitary that maps one ground state to its successor. This takes care of the second problem we mentioned. Importantly, it gives a clear condition under which such a path can be rigorously proven.

Under these conditions, the following result can be proven with the SIE theorem, since the entropy created by such quasi-local unitaries can be bounded.

Theorem 8. *[141] Consider a D-dimensional spin system satisfying the above conditions. The entanglement entropy of a ball of radius R_0 is bounded by*

$$S(\rho_{ball}) \leq c_{D-1}R_0^{D-1} + c_{D-2}R_0^{D-2} + \ldots + c_1 R_0 + c_0.$$

The constants c_i are system dependent constants.

Related ideas were also reported in Ref. [142]. Inspired by renormalization group ideas, the authors proposed the following definition which is conjectured to capture physically relevant gapped quantum phases.

Definition 11. *[142] A D-dimensional s* ***source RG fixed point*** *is a system whose ground state on $(2L)^D$ sites can be constructed from s copies of the ground state on L^D sites plus some unentangled degrees of freedom by acting with a quasi-local unitary on these spins.*

This definition can be modified to include the use of models on L^D sites, different than the original model, in the construction of the model on $(2L)^D$ sites. This is for instance the case in Haah's cubic code [143]. The entropy generated by the quasi-local unitaries can be bounded by the SIE theorem. If s is not too big, $s < 2^{D-1}$, repeating this procedure gives an area law. The calculation of the scaling of the entanglement entropy of such systems is similar to the one for branching MERA [144]. In this calculation, only strictly local unitaries are considered. Hence, the main difference here is the presence of quasi-local unitaries. This additional issue is solved by the SIE theorem.

Remark 4. A very similar definition was given in [145]. The authors called the systems they studied *gapped quantum liquids*. They corresponds intuitively to the $s = 1$ source RG fixed points. In Ref. [142] these systems were called *topological quantum liquids*. For all these systems, the growing procedure and the SIE theorem imply the validity of the area law.

1.5.2 Conclusion

In this chapter we addressed two main subjects. First, we discussed the entanglement that can be created by a local Hamiltonian in a quantum spin system. We gave a comprehensive overview of the motivation and previous work. The original contribution is the solution of the dynamical part of this question. We proved a sharp upper bound on the maximal instantaneous rate at which a local Hamiltonian can create entanglement in a spin system even in the presence of arbitrary ancillae.

Second, the upper bound on the entanglement rate allowed us to prove the stability of the area law for the entanglement entropy in gapped quantum phases. An area law for a ground state of a local gapped Hamiltonian automatically carries over to all systems to which it is connected via a gapped path of Hamiltonians. The formalism of quasi-adiabatic continuation provides the existence of quasi-local Hamiltonians which governs the evolution of a ground state to the ones connected with it by such a gapped path of Hamiltonians. The entanglement created by this evolution can be controlled and shown to be proportional to the area of the boundary of the bipartition and not to the volume of the constituents of the bipartition. This result carries over to systems with a finitely degenerate ground state subspace and fermionic lattice systems. We also discussed how under certain assumptions a similar argument can be used to prove the area law itself.

Several open questions remain. First, it would be interesting to see if a similar bound can be obtained for the mutual information. Given a local Lindblad generator, can we prove a non-trivial upper bound on the speed at which the mutual information can change? This question was studied in Ref. [146] where it was shown that starting from a pure

initial state and evolving with a local Lindblad operator, a result similar to Theorem 5 holds.

Another open problem concerns the area law itself. As we discussed, several authors have already shown that under certain restriction our results can be used to prove the area law. A natural question is how far these results can be generalized. Moreover, due to the stability result it suffices to show the area law for a single system in every phase. For a very large class of physical systems, we conjecture that there is a commuting, frustration free Hamiltonian in the same phase, this system corresponds to the renormalization fixed point. Such a system trivially fulfills the area law. Alternatively, one could show that certain phases have at least one representative ground state that can be written as a PEPS. Such a state satisfies the area law by construction.

Third, a natural generalization of this work concerns the Rényi entropies. Counterexamples to a straightforward generalization can easily be given. It thus would be interesting to better understand this very different behavior of the entanglement rate as measured by the Rényi entropies or the von Neumann entropy. Moreover, under extra restrictions, for instance on the initial state, it might be possible to obtain similar bounds. One can also consider other measures of entropy apart from the von Neumann and Rényi entropies [146].

Chapter 2

Entropy in Gauge Theories

In this chapter, we discuss the notion of entanglement in gauge theories, where the usual notions of local Hilbert spaces, tensor products and bipartitions cannot be used directly to define entanglement. The results in this chapter are based on:

- K. Van Acoleyen, N. Bultinck, J. Haegeman, M. Mariën, V.B. Scholz and F. Verstraete
  The Entanglement of Distillation for Gauge Theories
  Accepted for publication in PRL
  arXiv preprint arXiv:1511.04369 (2015).

2.1 Distillable Entanglement in Gauge Theories

Given the central place entanglement is taking in recent years in the study of quantum information and quantum many-body systems it is very natural to study this quantity in the context of gauge theories. However, one immediately runs into troubles at the start. Even defining entanglement in a gauge theory is not straightforward. Indeed, entanglement is intrinsically a quantity between two systems, A, B, whose combined Hilbert space is given by the tensor product $A \otimes B$ of the separate Hilbert spaces [147]. This fundamental property is no longer

true in gauge theories as an action on A that is not gauge invariant is only allowed combined with a restricted action in B such that the combination is gauge invariant.

It is natural to take an operational point of view to overcome this problem. We shall look at states on spin systems with a discrete gauge group and ask ourselves how many quantum information tasks the parties that have this common state can perform. In other words, we ask how many maximally entangled states they can extract using only local operations and classical communication (LOCC). Similar ideas where reported in Ref. [148], and different approaches in Refs. [147, 149–156]. Our goal is to show that the usual entanglement entropy can be written as the sum of a distillable and undistillable part and give explicit formulas for both. We do so in Theorem 9. The main tool of the approach is replacing the state with one that is polarized in the different gauge superselection sectors, as this state is equivalent to the original one for all possible allowed operations.

2.1.1 Hamiltonian Lattice Gauge Theory

Lattice gauge theories are usually studied using Lagrangians and the path integral formalism. For our purposes, the Hamiltonian formalism, although less widely known, is more suited. It was introduced by Kogut and Susskind [157–159].

2.1.1.1 Gauge and Matter Degrees of Freedom

We start with a compact (for our purposes finite suffices) gauge group and a lattice (V, L) with vertices $v \in V$ that contain matter degrees of freedom and edges $e \in L$ that support gauge degrees of freedom.

Every vertex has a Hilbert space $\mathcal{H}_m$ associated to it, which can be of arbitrary (finite) dimension. Each matter space $\mathcal{H}_m$ supports an (arbitrary) action of the gauge group, denoted by $V(g)$. The Hilbert spaces on the edges, that describe the gauge degrees of freedom, are taken to be the space of square integrable functions over G, which we denote by $\mathcal{H}_e = L^2(G)$. For finite groups this space is isomorphic to $\mathbb{C}^{|G|}$.

The gauge group has a natural action on this Hilbert space by the regular left (L_e) and right (R_e) multiplication. Without a gauge constraint, the total Hilbert space would be given by the tensor product of all matter and gauge Hilbert spaces and entanglement could be defined in the usual way.

2.1.1.2 Local Gauge Constraints

We now introduce the local gauge constraints. In the Kogut-Susskind Hamiltonian formulation of lattice gauge theory these symmetries are implemented by time-independent local gauge transformations. To define the gauge actions consistently we first need to assign an orientation to every edge in the lattice. The local gauge transformation $U_v(g)$ at a vertex v is then defined as

$$U_v(g) = V_v(g) \otimes_{e \in E_v^+} R_e(g) \otimes_{e \in E_v^-} L_e(g),$$

where the sets E_v^+ and E_v^- consist respectively of all incoming and outgoing edges of the vertex v. For the simple case of a square lattice that we consider in the figure, E_v^+ contains the edges at the left hand side and at the top, while E_v^- consists of the edges at right hand side and the bottom, as illustrated in Figure 2.1a. An important observation is that gauge operations on different vertices always commute, $[U_{v_1}(g_1), U_{v_2}(g_2)] = 0$. This follows from the trivial observation that if they act on the same edge, one acts with the right regular representation and the other with the left regular.

A gauge theory is one in which only gauge invariant states and operators are allowed. The physical Hilbert space of the gauge theory is then the subspace of the total Hilbert space of states that are invariant under all local actions of the gauge group,

$$U_v(g) \, |\psi\rangle = |\psi\rangle \tag{2.1}$$

for all vertices v and all group elements g. Correspondingly, the algebra $\mathcal{B}(\mathcal{H}_{phys})$ of physically allowed operations O, consist of all gauge invariant operators on $\mathcal{H}$, i.e. operators obeying $U_v^+(g) O U_v(g) = O$, for all v and g.

It is now crucial to notice that the local gauge operations $U_v(g)$ on a certain vertex are not strictly local, as they act on a matter degree and the surrounding gauge degrees of freedom. This feature prohibits the decomposition of the physical Hilbert space in a tensor product of local Hilbert spaces. The tensor product structure of the Hilbert space $\mathcal{H}$ is nothing but a convenient illusion that is used to define the true Hilbert space $\mathcal{H}_{\text{phys}}$.

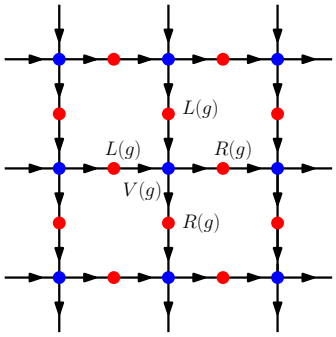

(a) The setting of K-S gauge theory. The edges support gauge field (red) and the vertices matter (red). A local gauge transformation around the central vertex is shown.

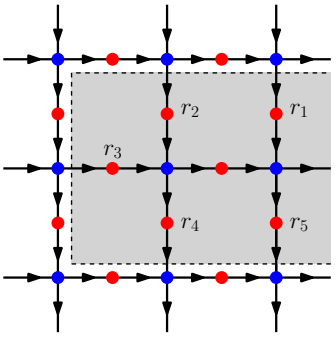

(b) A bipartition of the lattice in a white and gray area. If we fix the irreps on the edges that are on the boundary to specific values r_i, we recover a tensor product structure.

Figure 2.1

2.1.1.3 The Toric Code as a Gauge Theory

We now illustrate and clarify the previous definitions with the help of our favorite toy model, the Toric Code. This spin model is very closely related to $\mathbb{Z}_2$ gauge theories. At first, we discuss the Toric Code as a pure gauge theory, without matter degrees of freedom on the vertices and only gauge degrees of freedom on the links. This is indeed the situation familiar from Section 2.4. The local Hilbert space on the edges is then $\mathbb{C}^2$ and on the vertices $\mathbb{C}$. The gauge group $\mathbb{Z}_2$ then has the trivial action on the matter degrees of freedom, this is why we can discard them. The left and right multiplication on the gauge degrees of freedom is implemented both by operators $\mathbb{1}, X$. The X operator is often referred to as an electric field operator, due to its analogue in QED. As here

the matter degrees transform trivially, the gauge constraint is given by $A_v = \prod_{\ell \in v} X_v$, an operator familiar from the Toric Code Hamiltonian, but here used as a true constraint.

Important gauge invariant operators can be constructed from the other operators in the Toric Code Hamiltonian, the plaquette operators B_p. As discussed earlier they commute with the A_v, hence are indeed gauge invariant. They are called Wilson loop operators in QED. To get all the allowed physical states on the plane, we can now start from a product state of $|+\rangle$ and apply all products of B_p operators to it. On a torus, one also needs to start from states with non-trivial fluxes, one for each different topological sector. Such fluxes can be implemented by a closed loop of $|-\rangle$ states around some of the topologically non-trivial paths. We see that all states are given by superpositions of closed loops on $|-\rangle$ states on a background of $|+\rangle$ states.

We can also include matter by including a matter space $\mathbb{C}^2$ to every vertex and giving it the representation $\mathbb{1}, X$. The gauge constraint then becomes $A_v \otimes X_v$. The introduction of the matter degrees of freedom thus allows for the existence of gauge invariant states that have loop patterns on the edge degrees of freedoms with open strings. This has to be accompanied with a corresponding $|-\rangle$ state on the vertex where the string ends, such a vertex is said to contain a charge.

2.1.2 Bipartitions in Gauge Theories

We take a lattice which supports a Hamiltonian gauge theory and consider a bipartition of the lattice into a connected spatial region A and its complement B, connected by n boundary edges. We define the boundary vertices v_b as those vertices for which the gauge transformations have non-trivial support on both A and B, these are exactly the vertices one would intuitively consider to be on the boundary. An example of such a bipartition is shown in Fig. 2.1b.

2.1.2.1 The Dual Basis

We defined the Hilbert spaces locally, using as basis the group elements. However, with respect to the bipartition it is convenient to work in a different basis. The local gauge transformations that cross the boundary induce an action of $G^{\oplus n}$ on A and on B since they all commute. The action on A is given by the action of the part of the gauge operators that act in A, whereas the action on B is given by the remaining part that acts in B. These parts can have different forms,

$$L_{e_1}(g), L_{e_1}(g) \otimes R_{e_2}(g), L_{e_1}(g) \otimes R_{e_2}(g) \otimes V_b(g), \ldots .$$

Remark that the irreps of a direct product of finite groups are given by the direct product of the irreps of the groups.

We now use the Peter-Weyl theorem. As a basis for the Hilbert space $\mathcal{H}_A$ on A we can take the orthonormal irreducible representation basis that corresponds to this action. We denote the elements of this basis by $\{|\vec{r}, \vec{i}, \alpha\rangle_A\}$. As usual in such a decomposition, there are three different labels. First, there is the label that runs over the irreducible representations. The irreps of $G^{\oplus n}$ are just the possible direct products of n irreps of G. It is thus natural to label them with $\vec{r} = (r_1, r_2, \ldots, r_n) \in \Lambda^n$ and $\vec{i} = (i_1, i_2, \ldots, i_n)$. First, Λ is the set of equivalence classes of irreducible representations of G and the subindex runs over the n different boundary lattice vertices v_b. Second, there is a Hilbert space associated with every irrep of G, the tensor product of all these spaces is the representation space for the irrep $\vec{r}$ of $G^{\oplus n}$. The label $\vec{i}$ runs over a basis of this space. Third, every irrep can appear multiple times. This multiplicity is taken into account by the label α , which can be zero if a certain combination of irreps $\vec{r}$ of G does not appear.

The group action is implemented on these basis vectors as

$$U_1^A(g_1) \ldots U_n^A(g_n) \, |\vec{r}, (i_1, \ldots, i_n), \alpha\rangle_A = \sum_{(j_1, \ldots, j_n)} \Gamma^{r_1}_{j_1 i_1}(g_1) \ldots \Gamma^{r_n}_{j_n i_n}(g_n) \, |\vec{r}, (j_1, \ldots, j_n), \alpha\rangle_A \, .$$

In a similar way we can take for $\mathcal{H}_B$ the irreducible representation basis of $G^{\oplus n}$ on B, $\{|\vec{r}, \vec{i}, \beta\rangle_B\}$. The only subtlety is that we now label the

states according to their transformation under the complex conjugate irreps $\Gamma^{r*}_{ij}(g)$. This is purely a matter of convenience.

2.1.2.2 Gauge Invariant States in the Dual Basis

The representations and the corresponding bases we discussed give us a decomposition of the Hilbert spaces for A and B,

$$\mathcal{H}_A = \oplus_{\vec{r}} \mathcal{H}^{\vec{r}}_{Ag} \otimes \mathcal{H}^{\vec{r}}_{Am}\,, \qquad \mathcal{H}_B = \oplus_{\vec{r}} \mathcal{H}^{\vec{r}}_{Bg} \otimes \mathcal{H}^{\vec{r}}_{Bm}. \tag{2.2}$$

In this expression $\mathcal{H}^{\vec{r}}_{Ag}$ denotes the representation space for $\vec{r}$ and $\mathcal{H}^{\vec{r}}_{Am}$ the multiplicity space of the irrep $\vec{r}$ in A. Similarly we use $\mathcal{H}^{\vec{r}}_{Bg}$ and $\mathcal{H}^{\vec{r}}_{Bm}$ for these spaces in B.

We are of course not immediately interested in bases for A and B but rather in a basis for the gauge invariant physical space on both A, B together. Remember that we cannot use the direct product of a basis state in A and one in B as basis. Indeed, only those combinations of vectors in A and B that satisfy

$$U^A_{v_b}(g) \otimes U^B_{v_b}(g) \left|\psi\right\rangle = \left|\psi\right\rangle$$

for all boundary vertices v_b and all group elements g are allowed. The decomposition in Eq. (2.2) and the associated bases allow us to identify precisely the gauge invariant states.

We can use the implications of the Peter-Weyl theorem, in particular the relation

$$\frac{1}{|G|} \sum_g \sqrt{d_r d'_r} \Gamma^{r*}_{ij}(g) \Gamma^{r'}_{lk}(g) = \delta_{rr'} \delta_{il} \delta_{jk}\,, \tag{2.3}$$

with $d_r, d_{r'}$ the dimension of the irreps r, r' of G, to show that the only gauge invariant states are of the form

$$\mathcal{H}_{\text{phys}} = \bigoplus_{\vec{r} \in \Lambda^n} \left(\left|\phi^{\vec{r}}\right\rangle_{gAB} \otimes \mathcal{H}^{\vec{r}}_{Am} \otimes \mathcal{H}^{\vec{r}}_{Bm} \right). \tag{2.4}$$

Here we denote by $\left|\phi^{\vec{r}}\right\rangle_{gAB} = \sum_{\vec{i}} \left|\vec{i}\right\rangle_A \left|\vec{i}\right\rangle_B / \sqrt{d_{\vec{r}}}$ the maximally entangled state in the representation space $\mathcal{H}^{\vec{r}}_{Ag} \otimes \mathcal{H}^{\vec{r}}_{Bg}$.

One clarifying remark is in order. We only focused on those gauge operations that act on both parts of the bipartition to find the physical states and Hilbert space. Notice that for the A, B partition the other gauge transformation, which only act either on A or B, can be considered local. The effect of these constraints is taken into account implicitly by restricting the multiplicity spaces accordingly. This does not effect the space in equation (2.4).

2.1.2.3 Conditioning on the Boundary Representation

The crucial issue for gauge theories is now evident,

$$\mathcal{H}_{\text{phys}} \neq \mathcal{H}_A \otimes \mathcal{H}_B.$$

To recover a tensor product structure between A, B we can proceed as follows. We can fix the representation label $\vec{r}$ along the boundary between A, B by a suited projection on the subspaces of A, B compatible with this label. The result is a nice tensor product space $\mathcal{H}^{\vec{r}}_{Am} \otimes \mathcal{H}^{\vec{r}}_{Bm}$. We see that such a projection on a label $\vec{r}$ brings us back to the familiar realm of quantum information theory.

From the definition of the physical Hilbert space in equation 2.4 it is moreover clear that by acting locally only in A or B with an allowed operation can never change the superselection sector associated with the label $\vec{r}$ on the boundary. To change the label, we need to do a coordinated operation in A and B together, which is not an allowed LOCC operation. Thus, all allowed LOCC actions have to commute with the projection

$$P_{\vec{r}} = |\phi^{\vec{r}}\rangle_{gAB} \langle\phi^{\vec{r}}|_{gAB} \otimes P_{\mathcal{H}^{\vec{r}}_{Am}} \otimes P_{\mathcal{H}^{\vec{r}}_{Bm}}$$

on a superselection sector $\vec{r}$.

As pointed out in Ref. [150], we recognize the non-trivial gauge constraints also in the operator algebra $\mathcal{A}_{\text{phys}}$ which has a non-trivial center spanned by the operators $P_{\vec{r}}$. Let us now consider the operators that are allowed in a LOCC protocol for the parties A, B. This algebra is given

by

$$\mathcal{A}^{AB}_{\text{phys}} = \bigoplus_{\vec{r}\in\Lambda^n} \mathcal{A}_A(\vec{r}) \otimes \mathcal{A}_A(\vec{r})' \subset \mathcal{A}_{\text{phys}}.$$

In this expression we use $\mathcal{A}_A(\vec{r}) = P_{\vec{r}}\mathcal{A}_A P_{\vec{r}}$ and $\mathcal{A}_A(\vec{r})'$ is the commutant of $\mathcal{A}_A(\vec{r})$ in $\mathcal{B}(P_{\vec{r}}\,\mathcal{H}_{\text{phys}})$. This algebra consists of all operators in $\mathcal{B}(P_{\vec{r}}\,\mathcal{H}_{\text{phys}})$ that commute with all operators in $\mathcal{A}_A(\vec{r})$. The choice of the commutant ensures the locality demanded by the LOCC formalism. It contains exactly those physically allowed operations, as it is calculated in $\mathcal{B}(P_{\vec{r}}\,\mathcal{H}_{\text{phys}})$, that can be performed by only acting in B, since they commute with operations in A.

2.1.3 Equivalence of Pure and Mixed States

The operations that are allowed within the LOCC formalism are thus not only constrained by geometric locality but also by the gauge constraints in the theory. If we take a state $|\psi\rangle$ in the physical Hilbert space and calculate the expectation value of an operator $O \in \mathcal{A}^{AB}_{\text{phys}}$ in this state, we have that

$$\begin{aligned}\langle\psi|O|\psi\rangle &= \sum_{\vec{r},\vec{r}'} \langle\psi|P_{\vec{r}'}OP_{\vec{r}}|\psi\rangle \\ &= \sum_{\vec{r}} \mathrm{Tr}\left(P_{\vec{r}}\,|\psi\rangle\,\langle\psi|\,P_{\vec{r}}O\right) \\ &= \mathrm{Tr}\left(\sigma^{\psi}O\right).\end{aligned}$$

In the first line we use that $\sum_{\vec{r}} P_{\vec{r}}\,|\psi\rangle = |\psi\rangle$, in the second line that the allowed operation O commutes with $P_{\vec{r}}$ and that $P_{\vec{r}}P_{\vec{r}'} = \delta_{r,r'}$. Finally in the last line we define the state

$$\sigma^{\psi} = \sum_{\vec{r}\in\Lambda^n} P_{\vec{r}}\,|\psi\rangle\,\langle\psi|\,P_{\vec{r}}.$$

From the viewpoint of local operations, the states $|\psi\rangle$ and σ^{ψ} are thus indistinguishable [160]. The same then holds for any operational definition of entanglement. To obtain the distillable entanglement of $|\psi\rangle$ it thus suffices to look at the distillable entanglement of σ^{ψ}.

2.1.4 The Distillable Entanglement

One common approach to introduce entanglement in gauge theories is through the use of the so-called extended Hilbert space. In a nutshell, one just ignores the gauge constraints and treats a state $|\psi\rangle$ as a state in the tensor product Hilbert space $\mathcal{H}_A \otimes \mathcal{H}_B$ and proceeds as usual by tracing out one of the systems. The usage of the extended Hilbert space picture allows one to at least formally define a bipartite entanglement measure although the physical interpretation is not clear.

Due to the structure of gauge invariant states as discussed in the previous section, the reduced density matrix is block diagonal in the different superselection sectors. The corresponding von Neumann entropy can then be decomposed as follows [149],

$$\begin{aligned} S_A &= -\operatorname{Tr}_A(\rho_A \ln \rho_A) \\ &= -\sum_{\vec{r}} \operatorname{Tr}_A\left(\rho_A^{\vec{r}} \ln \rho_A^{\vec{r}}\right) \end{aligned}$$

We can decompose this even further. Recall that gauge invariant states have their representation basis degrees of freedom in the maximally entangled state. Hence we can write

$$\rho_A^{\vec{r}} = \frac{\mathbb{1}_{\mathcal{H}_{Ag}^{\vec{r}}}}{d_{\vec{r}}} \otimes \tilde{\rho}_{Am}^{\vec{r}} = \frac{\mathbb{1}_{\mathcal{H}_{Ag}^{\vec{r}}}}{d_{\vec{r}}} \otimes \frac{p_{\vec{r}}}{p_{\vec{r}}} \tilde{\rho}_{Am}^{\vec{r}}$$

Here $p_{\vec{r}} = \operatorname{Tr}_A(\rho_A^{\vec{r}}) = \operatorname{Tr}_A(\rho_{Am}^{\vec{r}})$ such that $\rho_{Am}^{\vec{r}} = \frac{1}{p_{\vec{r}}} \tilde{\rho}_{Am}^{\vec{r}}$ is now normalized. The state $\rho_{Am}^{\vec{r}}$ is the reduced density matrix of the multiplicity space of the irrep superselection sector $\vec{r}$.

We then have

$$S_A = -\sum_{\vec{r}} \operatorname{Tr}_A\left(\frac{p_{\vec{r}}}{d_{\vec{r}}}(\mathbb{1} \otimes \rho_{Am}^{\vec{r}}) \ln\left(\frac{p_{\vec{r}}}{d_{\vec{r}}}(\mathbb{1} \otimes \rho_{Am}^{\vec{r}})\right)\right) \tag{2.5}$$

$$= -\sum_{\vec{r}} p_{\vec{r}} \ln \frac{p_{\vec{r}}}{d_{\vec{r}}} + \sum_{\vec{r}} p_{\vec{r}} S_A^{\vec{r}} \tag{2.6}$$

with $S_A^{\vec{r}} = -\operatorname{Tr}\rho_{Am}^{\vec{r}} \ln \rho_{Am}^{\vec{r}}$ the von Neumann entropy of the density matrix on the multiplicity space of the irrep sector $\vec{r}$. This is the approach most common in literature, but the operational meaning of the calculated entanglement is not clear. Our goal now is to clarify exactly the operationally accessible part of the the entropy in equation (2.6). We do so in the next Theorem.

Theorem 9. *The distillable entanglement of a state $|\psi\rangle \in \mathcal{H}_{phys}$ in a gauge invariant spin system with discrete gauge group G is given by the mean of entanglement entropies of the states on the multiplicity spaces in every superposition sector $\vec{r}$,*

$$E_D^{gauge}(|\psi\rangle) = \sum_{\vec{r}} p_{\vec{r}} S_{Am}^{\vec{r}}.$$

This is the entanglement that possesses a clear operational meaning and should be considered the physical part of the entanglement expression in equation (2.6)*, the other parts are artifacts of the extended Hilbert space formalism.*

Proof. As discussed in Section 2.1.3, the pure state $|\psi\rangle$ and depolarized mixed state σ^{ψ} are equivalent from the point of view of gauge invariant LOCC protocols. We divide the proof of the Theorem in two parts.

First we prove that we can extract asymptotically at least a ratio of $\sum_{\vec{r}} p_{\vec{r}} S_{Am}^{\vec{r}}$ maximally entangled states, i.e.

$$E_D^{\text{gauge}}(|\psi\rangle) \geq \sum_{\vec{r}} p_{\vec{r}} S_{Am}^{\vec{r}}.$$

We start with the state $|\psi\rangle$ and first let A perform a measurement with respect to the projectors $\{P_{\vec{r}}\}$. Notice that both parties can perform this measurement locally and gauge invariant. This brings the state on average in the state σ^{ψ} and for one measurement we get a pure state $\frac{1}{\sqrt{p_{\vec{r}}}} P_{\vec{r}} |\psi\rangle$ with probability $p_{\vec{r}}$. Once this measurement is performed, we are in the usual realm of quantum information theory as the Hilbert space projected onto the superselection sector $\vec{r}$ does factorize as a familiar tensor product. For a state $\frac{1}{\sqrt{p_{\vec{r}}}} P_{\vec{r}} |\psi\rangle$ we can use the standard

entanglement distillation protocol [161, 162], which is well known to give an asymptotic rate of $S^{\vec{r}}_{Am}$ maximally entangled pairs.

Conversely, we now show that $E_D^{\text{gauge}}(|\psi\rangle) \leq \sum_{\vec{r}} p_{\vec{r}} S^{\vec{r}}_{Am}$. We use the entanglement cost E_C^{gauge}, the asymptotic rate of ebits needed to successfully create many copies of the state by LOCC, a task called entanglement dilution [161–163]. It trivially holds that $E_C \geq E_D$, otherwise we could keep running both protocols and generate entanglement using only LOCC. Hence, to show the desired inequality

$$E_D^{\text{gauge}}(|\psi\rangle) \leq \sum_{\vec{r}} p_{\vec{r}} S^{\vec{r}}_{Am}$$

it suffices to show that $E_C^{\text{gauge}}(|\psi\rangle) \leq \sum_{\vec{r}} p_{\vec{r}} S^{\vec{r}}_{Am}$ Let party A first create the desired state $|\psi\rangle$ locally using ancillae. Then, A performs the measurement $\{P_{\vec{r}}\}$ after which she possesses the state $\frac{1}{\sqrt{p_{\vec{r}}}} P_{\vec{r}} |\psi\rangle$ with probability $p_{\vec{r}}$. She now uses the usual entanglement dilation protocol for this state. Asymptotically the standard protocol creates the state σ^{ψ} between A and B at a cost of a rate of $\sum_{\vec{r} \in \Lambda^n} p_{\vec{r}} S^{\vec{r}}_{A}$ maximally entangled states.

This finishes the proof since the operational entanglement of $|\psi\rangle$ and σ^{ψ} is equal and we can conclude that indeed

$$E_D^{\text{gauge}}(|\psi\rangle) = E_C(\sigma^{\psi}) = \sum_{\vec{r}} p_{\vec{r}} S^{\vec{r}}_{Am}.$$

□

2.1.4.1 Distillable Entanglement in a Pure $\mathbb{Z}_2$ Gauge Theory

We consider again the $\mathbb{Z}_2$ gauge theory nephew of the Toric Code. We consider no matter degrees, the gauge constraint is then given by the operator A_v for every vertex v. The zero coupling Hamiltonian in the Kogut-Susskind formulation is just the plaquette term $\left(\mathbb{1}^{\otimes 4} - Z^{\otimes 4}\right)$ familiar from the Toric Code Hamiltonian. The only difference between this theory and the Toric Code is that in the gauge theory the vertex constraint cannot be violated, while in the Toric Code this is allowed

but gives an energy penalty. Of course this makes no difference for the ground state which is thus given by the equal superposition of all closed loop configurations of $|-\rangle$ on top of a background of $|+\rangle$ states.

The group $\mathbb{Z}_2$ has just two irreps, both one-dimensional, these are the trivial representation, corresponding to the $|+\rangle$ states and the non-trivial, corresponding to the $|-\rangle$ states. Consider a bipartition A, B, every operator $P_{\vec{r}}$ thus projects the gauge degrees of freedom crossing the boundary in a product state of $|+\rangle$ and $|-\rangle$ states. One can convince oneself that the ground state after projection is in a product state in the multiplicity spaces in A and B. Hence, there is no useful, distillable entanglement present in the ground state. This argument generalizes to all finite Abelian groups and twisted versions thereof.

The situation is different for non-Abelian theories at zero coupling, one can show that the distillable entanglement for the ground state is non-zero. If we denote by $N^1_{\vec{r}}$ the number of inequivalent ways the representations $\vec{r}$ can fuse to the trivial representation 1 of G we can prove that the distillable entanglement is given by

$$E_D^{\text{gauge}}(|\psi_0\rangle) = \frac{1}{|G|^{n-1}} \sum_{\vec{r}\in\Lambda^n} d_{\vec{r}} N^1_{\vec{r}} \log N^1_{\vec{r}}.$$

For a proof of this statement we refer the reader to Ref. [164].

2.2 A $\mathbb{Z}_2$ Gauge Theory in a Magnetic Field

In the previous section we briefly discussed the distillable entanglement present in pure gauge theories. Now, we add matter and interactions between the matter and gauge degrees of freedom to the picture and again look at the distillable entanglement in such a model. We focus on the $\mathbb{Z}_2$ theory and calculate the lowest order contribution to the entanglement when hopping terms between the matter degrees of freedom are turned on. Our main tools are the quasi-adiabatic continuation discussed in Section I.2.2.2 and the entanglement rate bound from Section II.1.3.

2.2.1 Lowest Order Perturbation Theory

In this section we calculate the lowest order corrections to the entropy of the $\mathbb{Z}_2$ gauge theory with matter if an interaction between the matter degrees of freedom is turned on. A similar calculation can be done for all Abelian gauge theories. We calculate the full entanglement entropy of the zero-coupling gauge theory state in lowest order, and decompose this into a distillable and non-distillable part, recovering the appropriate forms.

2.2.1.1 The Pure Gauge Theory

The Hamiltonian for the pure gauge theory is given by

$$H = \sum_{\text{plaquettes } p} \left(\prod_{j \in p} \mathbb{1}_j - B_p \right) + \sum_{\text{vertices}} X_v$$

where the first term is the projector onto the even subspace of the four gauge qubits around a plaquette. The ground state of this Hamiltonian is given by the equal superposition of all closed loop configurations on the gauge fields and all matter in the product state $|+\rangle$, as enforced by the X_v terms. The local gauge condition is given by the operators $X_g^{\otimes 4} \otimes X_m$ which act on a matter degree and all neighboring gauge fields.

We now consider a bipartition A, B of the lattice corresponding to a topologically trivial cut, we are interested in the entanglement entropy between A and B. Let there be n_A edges in A, n_B in B and n on the boundary. For the Toric Code, or any Abelian gauge theory, the different superselection sectors can be obtained by fixing the elements on every edge on the boundary in one of the eigenvectors $|+\rangle, |-\rangle$ of the electric field operator X. We can decompose the ground state $|gs\rangle$ as

$$|gs\rangle = \frac{1}{\sqrt{2^{n-1}}} \bigoplus_{|\vec{r}| \text{ even}} |A, \vec{r}\rangle \, |\vec{r}\rangle \, |B, \vec{r}\rangle \, .$$

Here, $|\vec{r}\rangle$ is the product state of the edges of the boundary and $|\vec{r}|$ refers to the product of all the signs, i.e. the label of the combined representation of the boundary. The vectors $|A, \vec{r}\rangle, |B, \vec{r}\rangle$ are given by the

equal superpositions of all string configurations in A and B respectively that are compatible with the boundary values. All matter is still in the product state $|+\rangle$.

2.2.1.2 The Gauge Invariant Perturbation

We now perturb the Hamiltonian with a gauge invariant term V_ℓ on every edge ℓ with $V_\ell = Z_m \otimes Z_g \otimes Z_m$. Here the Z_m operators work on the two vertices connected to the edge ℓ and Z_g acts on the gauge field on this particular edge. The operators V_ℓ create excitations of the X fields on neighboring vertices. This operator also couples and entangles different gauge and matter degrees of freedom, hence the latter are no longer in a product state.

Unfortunately, we do not know the exact ground state of this perturbed model. Luckily, we can still obtain the relevant scaling of the entanglement of the ground state in lowest order perturbation with the use of the tools explored in this dissertation. Let us now approximate the entanglement of the ground state $|gs(\varepsilon)\rangle$ of $H + \varepsilon \sum_\ell V_\ell$. The results from Section I.2.2.2 imply that the exact ground state $|gs(\varepsilon)\rangle$ of the Hamiltonian $H + \varepsilon \sum_\ell V_\ell$ can be obtained by evolving $|gs\rangle$ in time,

$$|gs(\varepsilon)\rangle = \mathcal{P} \exp\left(-i \int_0^\varepsilon D(x) dx\right) |gs\rangle$$

with $D(x)$ quasi-local in the sense that the strength of the interactions of $D(x)$ decay super-polynomially as a function of the size of their support. Here, we assume that all Hamiltonians have a finite mass gap larger than a fixed constant Δ and this gives the scale on which the interactions decay. The existence of such a Δ for a finite range of ε follows from the stability of topological order [**BravyiHastingsMichalakis**].

2.2.1.3 An Approximate Ground State

We now argue that instead of focusing on the entanglement of $|gs(\varepsilon)\rangle$ we can calculate the entanglement of a simpler state, called $|\tilde{gs}'(\varepsilon)\rangle$ in

the remainder of this section. The argument goes as follows. Denote by $A^{tB} = e^{itB} A e^{-itB}$ the Heisenberg evolution. We first rewrite

$$\begin{aligned} |gs(\varepsilon)\rangle &= \mathcal{P} \exp\left(-i \int_0^\varepsilon D(x) dx\right) |gs\rangle \\ &= \mathcal{P} \exp\left(-i \int_0^\varepsilon (D(x) - D(0))^{(\varepsilon - x) D(0)} dx\right) \exp(-i\varepsilon D(0)) \, |gs\rangle \end{aligned}$$

and define the state

$$|\tilde{gs}(\varepsilon)\rangle = \exp\left(-i\varepsilon D(0)\right) |gs\rangle \, .$$

Clearly $D(x) - D(0)$ is a local operator. Moreover, for every quasi-local term $d(x)$ in $D(x)$ we have

$$\begin{aligned} \left|(d(x) - d(0))^{D(x)}\right| &= \|d(x) - d(0)\| \\ &\leq \int_0^x \|d'(x)\| dx \\ &\leq Cx \|d(0)\| \end{aligned}$$

with C an unimportant constant, hence $D(x) - D(0)$ is also bounded, with local terms of order $x \leq \varepsilon$. Using the formula for the entanglement from Section 1.3, we see that the difference in the entropy of the two states is,

$$|S(|gs(\varepsilon)\rangle) - S(|\tilde{gs}(\varepsilon)\rangle)| \leq C\varepsilon^2 n$$

with C again some unimportant constant.

2.2.1.4 The Quasi-Adiabatic Generator

The operator $D(0)$ can easily be calculated using the formulas obtained in Section I.2.2.2. We have that

$$K(s) = -i \int F(\Delta t) e^{i(H+sV)t} V e^{-i(H+sV)t} dt,$$

hence

$$\begin{aligned} K(0) &= -i \int F(\Delta t) e^{i(H)t} V e^{-i(H)t} dt \\ &= -i \int F(\Delta t) e^{it \sum X} V e^{-it \sum X} dt. \end{aligned}$$

We now use that $e^{itX}Ze^{-itX} = \cos(2t)Z + \sin(2t)Y$ to obtain that

$$\begin{aligned} K(0) &= -i\int F(\Delta t)\sum_{v,\ell,v'}\left(\cos^2(2t)Z_vZ_\ell Z_{v'} + \sin^2(2t)Y_vZ_\ell Y_{v'}\right. \\ &\quad \left. + \cos(2t)\sin(2t)\left(Z_vZ_\ell Y_{v'} + Y_vZ_\ell Z_{v'}\right)\right)dt \\ &= -i\int F(\Delta t)\sum_{v,\ell,v'}\frac{1}{2}\left(\sin(4t)Y_vZ_\ell Z_{v'} + \sin(4t)Z_vZ_\ell Y_{v'}\right)dt \\ &= \frac{1}{8}\sum_{v,\ell,v'}\left(Y_vZ_\ell Z_{v'} + Z_vZ_\ell Y_{v'}\right). \end{aligned}$$

We used that F is odd to make the first simplification and that $\hat{F}(\omega) = -\frac{1}{\omega}$ for $|\omega| > \Delta$ to get the final result. With v, ℓ, v' we denote pairs of neighboring vertices v, v' and the edge ℓ in between, which is oriented form v to v'. If we now denote by W_ℓ the operator $Z_v \otimes Z_\ell \otimes Y_{v'} + Y_v \otimes Z_\ell \otimes Z_{v'}$, very similar to the operator V_ℓ, then $D(0) = \sum_\ell W_\ell$. We drop the factor $\frac{1}{8}$ because it can be absorbed in ε.

Let us make a decomposition of

$$D(0) = \sum_{\ell\in\partial AB} W_\ell + \sum_{\ell\notin\partial AB} W_\ell = W_{\partial AB} + W_{AB}.$$

Notice that $W_{\partial AB}$ is a sum of commuting terms, one for each link crossing the boundary. We now have

$$\begin{aligned} |\tilde{gs}(\varepsilon)\rangle &= \exp\left(-i\varepsilon(W_{\partial AB} + W_{AB})\right)|gs\rangle \\ &= \exp\left(-i\varepsilon\int_0^1 W_{AB}^{(\varepsilon-x)W_{\partial AB}}dx\right)\exp\left(-i\varepsilon(W_{\partial AB})\right)|gs\rangle. \end{aligned}$$

Recall that W_{AB} is a sum of local terms[1], most of which commute with $W_{\partial AB}$, except for those at the boundary. However, even those terms commute with most terms in $W_{\partial AB}$ and the time evolution of such a

1. This fails whenever W_ℓ for two different $\ell = \ell'$ share a vertex degree of freedom, i.e. at a corner. This would give rise to corner corrections to the entanglement which we henceforth ignore. Alternatively, for a state on a sphere, with A one half of the sphere, or for A a suitably chosen region on a hexagonal lattice, this problem does not occur.

term with $W_{\partial AB}$ is still strictly local. For such a term w it is clear that $w^{i\varepsilon x W_{\partial AB}} = w + \varepsilon R_w$ with R_w a local, bounded term. The fact that $W_{\partial AB}$ commutes is not strictly necessary here, a slightly more involved argument can be used to deal with the general scenario. We now have that

$$\begin{aligned}|\tilde{gs}(\varepsilon)\rangle &= \exp\left(-i\varepsilon\int_0^1 W_{AB} + \varepsilon\sum_w R_w dx\right)\exp\left(-i\varepsilon(W_{\partial AB})\right)|gs\rangle \\ &= \exp\left(-i\varepsilon^2\int_0^1\sum_w R_w^{W_{AB}\varepsilon x}dx\right) \\ &\qquad \times \exp\left(-i\varepsilon(W_{AB})\right)\exp\left(-i\varepsilon(W_{\partial AB})\right)|gs\rangle\,.\end{aligned}$$

Clearly, due to standard arguments based on Lieb-Robinson bounds, $\sum_w R_w^{W_{AB}\varepsilon x}$ is still a quasi-local Hamiltonian. The main result in Section 1.3 shows that evolving a state with such a Hamiltonian for a time ε^2 can only create as much as $n\varepsilon^2$ entanglement. Moreover the unitary $\exp\left(-i\varepsilon(W_{AB})\right)$ does not create any entanglement at all.

Hence we can now approximate the state $|\tilde{gs}\rangle$ with

$$|\tilde{gs}'(\varepsilon)\rangle = \exp\left(i\varepsilon\sum_{\ell\in\partial AB} W_\ell\right)|gs\rangle$$

such that the entanglement entropy of both states is close,

$$\left|S(|\tilde{gs}(\varepsilon)\rangle) - S(|\tilde{gs}'(\varepsilon)\rangle)\right| \leq C\varepsilon^2 n,$$

an error similar to the one already made in the approximation of $|gs(\varepsilon)\rangle$ by $|\tilde{gs}(\varepsilon)\rangle$. As we are only interested in the entropy, we now continue with the last state $|\tilde{gs}'(\varepsilon)\rangle$. It is easy to see that

$$\begin{aligned}|\tilde{gs}'(\varepsilon)\rangle &= \exp\left(i\varepsilon\sum_\ell W_\ell\right)|gs\rangle \\ &= \prod_\ell\left(\cos(\varepsilon)\mathbb{1} + i\sin(\varepsilon)W_\ell\right)|gs\rangle\,.\end{aligned}$$

The error we make by calculating the entropy of this state instead of $|gs(\varepsilon)\rangle$ is of order $n\varepsilon^2$, as was mentioned before. As all matter degrees

of freedom in $|gs\rangle$ start in a product state of $|+\rangle$ it is easy to see that the application of this last operator on $|gs\rangle$ is equal to[2].

$$\prod_{\ell\in\partial AB}(\cos(\varepsilon)\mathbb{1}+i\sin(\varepsilon)W_\ell)\,|gs\rangle=\prod_{\ell\in\partial AB}(\cos(\varepsilon)\mathbb{1}+\sin(\varepsilon)2V_\ell)\,|gs\rangle\,.$$

We will drop the factor 2 for notational convenience, it can be absorbed in ε from the start.

2.2.2 The Approximate Entropy

Let us now compute the entropy of the state $|\tilde{gs}'(\varepsilon)\rangle$. We first focus on an even sector α. After applying the gates across the boundary we find that the state in this sector is given by

$$\frac{1}{\sqrt{2^{n-1}}}\sum_{k\text{ even}}\sum_{m=1}^{\binom{n}{k}}\cos(\varepsilon)^{n-k}\sin(\varepsilon)^k\,|A_{k,m},\tilde{\vec{r}}_{k,m})\rangle\,|\vec{r}\rangle\,|B_{k,m},\tilde{\vec{r}}_{k,m}\rangle\,.$$

Here $|A_{k,m},\tilde{\vec{r}}_{k,m}\rangle$ is the state obtained from $|A,\vec{r}_{k,m}\rangle$ by acting with Z on the k vertices that neighbor edges where α differs from $\tilde{\vec{r}}_{k,m}$ and similar for the state $|B_{k,m},\tilde{\vec{r}}_{k,m}\rangle$.

2.2.2.1 The Non-Distillable Entanglement

The last expression is immediately a Schmidt decomposition of the state in the sector $\vec{r}$. The normalization of this state is then given by

$$\frac{\left((\cos^2(\varepsilon)+\sin^2(\varepsilon))^n+(\cos^2(\varepsilon)-\sin^2(\varepsilon))^n\right)}{2^n}=\frac{(1+\cos(2\varepsilon)^n)}{2^n}.$$

Similarly for odd sectors we find

$$\frac{1}{\sqrt{2^{n-1}}}\sum_{k\text{ odd}}\sum_{m=1}^{\binom{n}{k}}\cos(\varepsilon)^{n-k}\sin(\varepsilon)^k\,|A_{k,m},\tilde{\vec{r}}_{k,m})\rangle\,|\vec{r}\rangle\,|B_{k,m},\tilde{\vec{r}}_{k,m}\rangle$$

2. See footnote 1.

with normalization $\frac{1}{2^n}(1-\cos(2\varepsilon)^n)$. The sum over all p_α still sums to 1, as we applied a unitary. We can see that the non-distillable part of the entropy is now given by

$$\begin{aligned} E_{\text{non}-D}(|\tilde{gs}(\varepsilon)\rangle) &= -2^{n-1}\left(\frac{1+\cos^n(2\varepsilon)}{2^n}\right)\log\left(\frac{1+\cos^n(2\varepsilon)}{2^n}\right) \\ &\quad - 2^{n-1}\left(\frac{1-\cos^n(2\varepsilon)}{2^n}\right)\log\left(\frac{1-\cos^n(2\varepsilon)}{2^n}\right) \\ &= (n-1)\log(2) + \mathsf{h}(p_{\text{even}}, p_{\text{odd}}) \end{aligned}$$

with

$$p_{\text{even}} = \frac{1+\cos^n(2\varepsilon)}{2}, \qquad p_{\text{odd}} = \frac{1-\cos^n(2\varepsilon)}{2}.$$

2.2.2.2 The Distillable Entanglement

We now look at the distillable entanglement. Theorem 9 tells us that we can look at all sectors $\vec{r}$ independently, calculate the usual entanglement in a sector and finally average over the sectors. We start with a sector with $\vec{r}$ even. For a given sector the Schmidt values are given by the probabilities of a sequence of n Bernoulli variables B_i, with the extra restriction that the sum of all values 1 is even. The normalization constant for the probabilities is given by p_{even}. We first state a useful combinatorial identity. Taking the derivative of the equality

$$\sum_{k \text{ even}} \binom{n}{k} p^{n-k} q^k = \frac{(p+q)^n + (p-q)^n}{2}$$

to q gives

$$\sum_{k \text{ even}} \binom{n}{k} k p^{n-k} q^{k-1} = \frac{n(p+q)^{n-1} - n(p-q)^{n-1}}{2}.$$

The distillable entanglement in the even sector $\vec{r}$ is given by

$$\begin{aligned}
E_D^{\vec{r},e}(|\tilde{gs}'(\varepsilon)\rangle) &= -\sum_{k \text{ even}} \binom{n}{k} \frac{\left(\cos^2(\varepsilon)\right)^{n-k} \left(\sin^2(\varepsilon)\right)^k}{p_{\text{even}}} \\
&\qquad \times \log\left(\frac{\left(\cos^2(\varepsilon)\right)^{n-k} \left(\sin^2(\varepsilon)\right)^k}{p_{\text{even}}}\right) \\
&= -\frac{\log\left(\cos^2(\varepsilon)\right)}{p_{\text{even}}} \sum_{k \text{ even}} \binom{n}{k} (n-k) \left(\cos^2(\varepsilon)\right)^{n-k} \left(\sin^2(\varepsilon)\right)^k \\
&\quad - \frac{\log\left(\sin^2(\varepsilon)\right)}{p_{\text{even}}} \sum_{k \text{ even}} \binom{n}{k} (k) \left(\cos^2(\varepsilon)\right)^{n-k} \left(\sin^2(\varepsilon)\right)^k \\
&\quad + \log\left(p_{\text{even}}\right) \\
&= -n\cos^2(\varepsilon) \frac{\log\left(\cos^2(\varepsilon)\right)}{p_{\text{even}}} \frac{1+\cos(2\varepsilon)^{n-1}}{2} \\
&\quad - n\sin^2(\varepsilon) \frac{\log\left(\sin^2(\varepsilon)\right)}{p_{\text{even}}} \frac{1-\cos(2\varepsilon)^{n-1}}{2} + \log\left(p_{\text{even}}\right).
\end{aligned}$$

A similar calculation for $\vec{r}$ odd gives

$$\begin{aligned}
E_D^{\vec{r},o}(|\tilde{gs}'(\varepsilon)\rangle) &= -n\cos^2(\varepsilon) \frac{\log\left(\cos^2(\varepsilon)\right)}{p_{\text{odd}}} \frac{1-\cos(2\varepsilon)^{n-1}}{2} \\
&\quad - n\sin^2(\varepsilon) \frac{\log\left(\sin^2(\varepsilon)\right)}{p_{\text{odd}}} \frac{1+\cos(2\varepsilon)^{n-1}}{2} + \log\left(p_{\text{odd}}\right).
\end{aligned}$$

We conclude that the distillable entanglement is given by

$$\begin{aligned}
E_D(|\tilde{gs}'(\varepsilon)\rangle) &= p_{\text{even}} S_{\alpha,\text{even}} + p_{\text{odd}} S_{\alpha,\text{odd}} \\
&= n\mathsf{h}\left(\cos^2(\varepsilon), \sin^2(\varepsilon)\right) - \mathsf{h}\left(p_{\text{even}}, p_{\text{odd}}\right).
\end{aligned}$$

2.2.2.3 The Topological Entropy

We now discuss the constant correction to the area law. In quantum many-body physics, this is known as the topological entanglement entropy [91, 92]. It is known that the Toric Code has such a correction, equal to $-\log(2)$ and that it is stable throughout the phase. As the

Toric Code phase is stable against perturbations, we know that the full entanglement entropy still contains this correction, i.e.

$$E_{\text{non}-D} + E_D = Cn - \log(2).$$

Before we turn on the interaction $E_D = 0$, hence the correction is completely in the non-distillable part of the entropy. We will argue, although not rigorously prove, that this is a very special case and that generically the correction is part of the distillable entanglement.

First of all, for fixed ε and in the limit $n \to \infty$ we see that p_{even} and p_{odd} both go to 1/2, even for very small ε. As this is a combinatorial consequence of translation-invariance we indeed expect it to be generic. The expression for the distillable entanglement then becomes very simple in this limit,

$$\begin{aligned} E_D(|\tilde{gs}'(\varepsilon)\rangle) &\approx n\mathsf{h}(\cos^2(\varepsilon), \sin^2(\varepsilon)) - \mathsf{h}(p_{\text{even}}, p_{\text{odd}}) \\ &\approx n\mathsf{h}(\cos^2(\varepsilon), \sin^2(\varepsilon)) - \log(2) \end{aligned}$$

Clearly, as expected, the topological entropy is still $-\log(2)$ as the corrections to this term in the non-distillable and distillable parts of the entropy cancel.

We expect that a similar result holds for generic perturbations. The argument goes as follows. We know that the total entanglement entropy contains a topological $-\log(2)$ correction for small enough perturbations. We now provide some intuition as to why we expect that the non-distillable entanglement obeys an area law without a correction, which implies that the distillable entanglement indeed contains the complete $-\log(2)$ correction.

Let us start from the Hamiltonian H at zero-coupling and add a generic perturbation which can create charges. We then expect that for large enough regions A, the probability to have total charge inside even or odd is $1/2$ as calculated in the example. We suspect it holds more generally as a consequence of combinatorics, translational invariance and finite correlation length. Actually, the assumption that both probabilities are $1/2$ is already enough to conclude that the claim is true for perturbation that act as Z operators on the gauge fields and thus treat

all $\vec{r}$ equal, such as V_ℓ. Indeed, the distribution over the even and odd sectors is then uniform and the resulting entropy displays no correction to the area law.

For generic perturbations, we still expect that the classical probability distribution over the superselection sectors approximately factorizes for very large regions due to the finite correlation length ξ in the system. Suppose we have a region A with boundary length N. Denote the probability distribution for the superselection sectors on this boundary by $p^N_{\vec{r}}$. Partition this boundary in m intervals, each with length $n \gg \xi$, such that $1 \ll m, L$. Denote the probability distribution for the superselection sectors for an interval $i = 1, \ldots, m$ as $q^i_{\vec{r}}$. These are all equal due to translational invariance. We now expect that

$$p^L_{\vec{r}} \approx \prod_{i=1}^{m} q^i_{\vec{r}}$$

and thus also that

$$H\left(p^L_{\vec{r}}\right) \approx m\mathsf{h}\left(q_{\vec{r}}\right)$$

which hints at a strict area law without correction.

2.3 Outlook and Conclusion

We took an operational point of view to address the issue of defining and interpreting entanglement in lattice gauge theories. The Peter-Weyl theorem allowed us to introduce very convenient bases for the constituents of a general bipartition. In these bases the degrees of freedom that are restricted by the gauge constraints and those that are not are clearly separated. As we have shown, it is the entanglement in the multiplicity spaces of the local gauge constraints that can indeed be distilled by an LOCC protocol and thus be used in various quantum information and computation protocols.

We illustrated our results using the easiest discrete gauge theory, based on the group $\mathbb{Z}_2$. This theory is related to the Toric Code model. Using the results that were obtained throughout this dissertation we obtain

lowest order results for the entanglement in a specific perturbed, interacting gauge theory. We furthermore gave an intuition behind the presence of the topological term in the distillable entanglement.

Our work opens up several interesting questions. Interestingly, the distillable entanglement violates subadditivity as is illustrated with a basic example in Ref. [164]. More insight in the implications of the violation of this crucial property is desirable.

Second, the general results discussed in the context of discrete lattice gauge theories are still valid for relativistic gauge quantum field theories that are regulated by a spatial lattice formulation [157, 158]. Further study of this physically most relevant scenario is needed to complete our understanding.

Third, one of the main motivations to study entanglement in gauge theories was the notorious firewall paradox [165]. The crux of this paradox is the violation of the fundamental monogamy property of entanglement. As the paradox deals with gauge theories, we believe it would be worthwhile to reformulate and understand the paradox in our framework.

Chapter 3

Topological Order in PEPS

The present chapter concerns topological order and anyons and how they are represented with tensor networks. We first explain how ground states are constructed, then deal with the anyon excitations and their properties. This gives us insight in the nature of topological quantum computation. Finally, we perform a numerical study of quantum phase transition, focusing on the doubled Fibonacci model. The following papers report the core results in this chapter:

- M.B. Şahinoğlu, D.J. Williamson, N. Bultinck, M. Mariën, J. Haegeman, N. Schuch and F. Verstraete
  Characterizing Topological Order with Matrix Product Operators
  arXiv preprint arXiv:1409.2150 (2014)

- N. Bultinck, M. Mariën, D.J. Williamson, M.B. Şahinoğlu, J. Haegeman and F. Verstraete
  Anyons and Matrix Product Operator Algebras
  arXiv preprint arXiv:1511.08090 (2015)

- M. Mariën, J. Haegeman, P. Fendley and F. Verstraete
  Condensation-Driven Phase Transitions in Perturbed String-Nets
  arXiv preprint arXiv:1607.05296 (2016).

3.1 MPO-Injectivity

Quantum tensor network states and more particularly PEPS provide a natural and efficient framework for representing ground states of gapped, topologically ordered systems. We already illustrated the idea behind this framework in Section I.2.4 where we mentioned that the local virtual symmetries of the PEPS tensors give rise to all expected topological properties of the celebrated Toric Code model.

In the present section we give the correct framework to generalize this example to all know two-dimensional non-chiral topological phases. The defining feature of a topological PEPS is a set of MPOs that one can pull through the tensor network freely. Because of this, such tensor network states are referred to as MPO-injective PEPS. We now first introduce the set of MPOs that are used to construct topologically ordered ground states.

In this section we assume more properties of the tensors than strictly necessary to shorten the exposition and improve the readability. For a complete discussion, starting from a minimal set of assumptions, we refer the reader to Ref. [24].

3.1.1 Matrix Product Operator Algebras

The fundamental object that is used to construct a topological PEPS is a Projector Matrix Product Operator (PMPO). This is, as the name suggests, a matrix product operator that is also a projector. By this we mean that the operator squares to itself and is Hermitian. As we shall see, the PMPOs we write down can be seen as specific representations of abstract tensor fusion categories.

3.1.1.1 Projector Matrix Product Operators

We look at models that are translation-invariant and it is thus natural to consider PMPOs P_L that form translation-invariant Hermitian projectors

for every length L and can be represented as

$$P_L = \sum_{\{\mathbf{i},\mathbf{j}\}=1}^{D} \mathrm{tr}(\Delta B^{i_1 j_1} B^{i_2 j_2} \dots B^{i_L j_L}) \, |i_1 i_2 \dots i_L\rangle \langle j_1 j_2 \dots j_L| \, . \quad (3.1)$$

In this equation, the tensors B^{ij} are $\chi \times \chi$ matrices for fixed values of indices $i, j = 1, \dots, D$. We use this PMPO to construct a PEPS in Section 3.1.2, D then becomes the bond dimension of the resulting PEPS. Remark that both the tensors B and the dimensions D, χ are independent of N. That P_L is a projector for every length L by using the same tensors is a highly non-trivial demand. In fact, in the remainder of this section we shall see that its consequences are surprisingly strong.

In equation (3.1) we included Δ, which is a $\chi \times \chi$ matrix such that the specific position where it is inserted is irrelevant. No matter what the position of Δ results in the same PMPO P_L. We also assume that the insertion of Δ still allows for a canonical form of the MPO such that the tensors have the following block diagonal structure [4, 25],

$$B^{ij} = \bigoplus_{a=1}^{\mathcal{N}} B_a^{ij}, \qquad \Delta = \bigoplus_{a=1}^{\mathcal{N}} \Delta_a,$$

with B_a^{ij} and Δ_a $\chi_a \times \chi_a$ matrices such that $\sum_{a=1}^{\mathcal{N}} \chi_a = \chi$. P_L thus decomposes into a sum of injective MPOs

$$P_L = \sum_{a=1}^{\mathcal{N}} \sum_{\{i\},\{j\}=1}^{D} \mathrm{tr}(\Delta_a B_a^{i_1 j_1} \dots B_a^{i_L j_L}) \, |i_1 \dots i_L\rangle \langle j_1 \dots j_L| \, .$$

The resulting MPOs labeled by a in this sum are injective, this means that for each a the matrices $\{B_a^{ij} : i, j = 1, \dots, D\}$ and all their products span the entire space of $\chi_a \times \chi_a$ matrices. Injectivity of the tensors B_a then implies that Δ_a is a multiple of the identity $\Delta_a = w_a \mathbb{1}_{\chi_a}$, with w_a some complex numbers. We immediately restrict ourselves to the case were all $w_a > 0$.

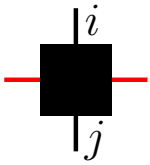

(a) The graphical notation for the full MPO tensor B^{ij} with virtual indices (red line) of dimension $\chi = \sum_a \chi_a$.

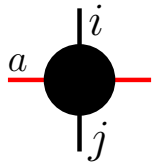

(b) The graphical notation for the injective MPO tensors B_a^{ij} with virtual indices (red line) of dimension χ_a.

Figure 3.1

3.1.1.2 Fusion Tensors

We thus arrive at the following form for P_L

$$\begin{aligned} P_L &= \sum_{a=1}^{\mathcal{N}} w_a O_a^L \\ &= \sum_{a=1}^{\mathcal{N}} w_a \sum_{\{i\},\{j\}=1}^{D} \mathrm{tr}(B_a^{i_1 j_1} \dots B_a^{i_L j_L}) \left|i_1 \dots i_L\right\rangle \left\langle j_1 \dots j_L\right| . \end{aligned}$$

Since P_L is required to be a projector, we have that

$$P_L^2 = \sum_{a,b=1}^{\mathcal{N}} w_a w_b O_a^L O_b^L = \sum_{a=1}^{\mathcal{N}} w_a O_a^L = P_L \,,$$

which has to hold for all L. The fundamental theorem for Matrix Product Vectors tells us that the same MPO tensors B_a appear in P_L and P_L^2 [4, 25]. This gives us the following relations,

$$O_a^L O_b^L = \sum_{c=1}^{\mathcal{N}} N_{ab}^c O_c^L, \tag{3.2}$$

$$\sum_{a,b=1}^{\mathcal{N}} N_{ab}^c w_a w_b = w_c, \tag{3.3}$$

where N_{ab}^c is a rank three tensor containing integer entries. We see that a PMPO immediately gives rise to a fusion ring. Indeed, the fundamental

theorem gives us that the multiplication of MPOs O_a, O_b can be written as a linear combination of MPOs O_c, which implies the MPOs form a ring. Due to the stringent demand that these coefficients are equal for all lengths L, the only allowed coefficients are integers. This gives us exactly a fusion ring.

The algebraic relations, such as the associativity and the existence of a unit can be categorified [76] to obtain a fusion tensor category. In the PMPO picture this categorification is obtained as follows. The fundamental theorem not only gives us the fusion ring structure on the MPOs. The power of this theorem is that the relation can be written locally on just the tensors B_a, B_b and B_c instead of the operators O_a, O_b and O_c. We now explain how this local condition gives us a fusion tensor category.

The fundamental theorem implies the existence of matrices

$$X^c_{ab,\mu} : \mathbb{C}^{\chi_a} \otimes \mathbb{C}^{\chi_b} \to \mathbb{C}^{\chi_c} \quad \text{for } \mu = 1, \ldots, N^c_{ab}$$

and left inverses $X^{c^+}_{ab,\mu}$ satisfying

$$X^{d^+}_{ab,\nu} X^c_{ab,\mu} = \delta_{de}\delta_{\mu\nu}\mathbb{1}_{\chi_c},$$

such that we have following identities on the level of the individual matrices that build up the injective MPOs O_a^L,

$$X^{c^+}_{ab,\mu} \left(\sum_{j=1}^{D} B^{ij}_a \otimes B^{jk}_b \right) X^c_{ab,\mu} = B^{ik}_c.$$

We represent these identities graphically as in Figure 3.2.

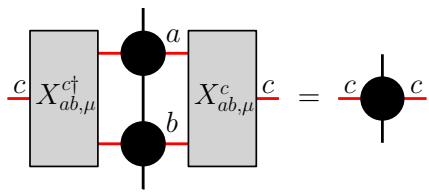

Figure 3.2: Graphical representation of the fusion rules on the level of the individual tensors.

We call the set of rank three tensors $X^c_{ab,\mu}$ the fusion tensors. These fusion tensors play an important role in constructing the anyon ansatz further on. Although not strictly necessary at this point we assume the stronger zipper condition that we graphically show in Figure 3.3,

$$\begin{aligned}\left(\sum_{j=1}^{D} B_a^{ij} \otimes B_b^{jk}\right) X^c_{ab,\mu} &= X^c_{ab,\mu} B_c^{ik} \\ X^{c\dagger}_{ab,\mu} \left(\sum_{j=1}^{D} B_a^{ij} \otimes B_b^{jk}\right) &= B_c^{ik} X^{c\dagger}_{ab,\mu}.\end{aligned} \tag{3.4}$$

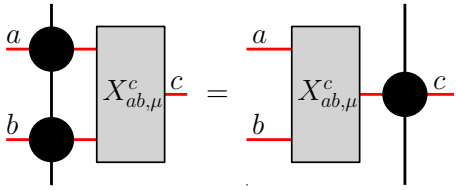

Figure 3.3: A graphical notation of the zipper condition.

From

$$\bigoplus_{\mu=1}^{N_{ab}^c} X^{c^+}_{ab,\mu} \left(\sum_{j=1}^{D} B_a^{ij} \otimes B_b^{jk}\right) X^c_{ab,\mu} = \mathbb{1}_{N_{ab}^c} \otimes B_c^{ik},$$

we see that the μ-label is arbitrary and the fusion tensors $X^c_{ab,\mu}$ are only defined up to a gauge transformation given by a set of invertible $N^c_{ab} \times N^c_{ab}$ matrices Y^c_{ab}. Moreover, the converse is also true if Eq. (3.4) holds. Two collections of fusion tensors that satisfy the zipper condition (3.4) must be related by a gauge transformation Y.

3.1.1.3 Dual Elements

Because we require P_L to be Hermitian for all L, we find that for every block a there exists a unique block a^* such that

$$\bar{w}_a = w_{a^*} \tag{3.5}$$
$$O_a^{L\dagger} = O_{a^*}^L, \tag{3.6}$$

where the bar denotes complex conjugation. The tensor N then obviously satisfies

$$N_{ab}^{c} = N_{b^* a^*}^{c^*}. \tag{3.7}$$

Even though tensors $\bar{B}_a^{ji}$ and $B_{a^*}^{ij}$, which build up $O_a^{L\dagger}$ and $O_{a^*}^{L}$, give rise to the same operator, they are in general not equal but related by a gauge transformation,

$$\bar{B}_a^{ji} = Z_a^{-1} B_{a^*}^{ij} Z_a$$

where Z_a is defined up to a multiplicative factor. By applying Hermitian conjugation twice we find

$$\begin{aligned} B_a^{ij} &= \bar{Z}_a^{-1} \bar{B}_{a^*}^{ji} \bar{Z}_a \\ &= \bar{Z}_a^{-1} Z_{a^*}^{-1} B_a^{ij} Z_{a^*} \bar{Z}_a. \end{aligned}$$

Because B_a^{ij} is injective, $Z_{a^*}\bar{Z}_a$ has to be proportional to the identity. We thus find that

$$Z_a \bar{Z}_{a^*} = \gamma_a \mathbb{1} = \bar{Z}_{a^*} Z_a$$

with $\gamma_a = \bar{\gamma}_{a^*}$ a complex number. If $a \neq a^*$, we can redefine one of the two Z matrices with an additional factor such that $\gamma_a = 1$. If, on the other hand, $a = a^*$ we can find that γ_a is real but we can at most absorb its absolute value by redefining Z_a with an extra factor $|\gamma_a|^{-1/2}$. It turns out that in this case there is an invariant, $\varkappa_a = \text{sign}(\gamma_a)$ cannot be changed by redefining Z_a. It is a discrete invariant of the algebra generated by the PMPO. This invariant has an analogous in category theory, the Frobenius-Schur indicator.

To recapitulate, Hermitian conjugation associates to every block a a unique 'dual' block a^* in such a way that $(a^*)^* = a$. In a fusion category theory there is an a priori notion of duality. Every simple object a is required to have a unique dual simple object a^* is such that the fusion product of a and a^* contains exactly once the identity object 1.

The assumption that the PMPO contains a trivial identity block, which is true for the representation of all string-net models we provide in Section 3.3, implies that this definition of a dual coincides with the categorical definition. Such PMPOs are said to have a unital structure and this additional structure implies that

$$N_{ab}^{c} = N_{bc^*}^{a^*} = N_{c^* a}^{b^*}, \tag{3.8}$$

which can further be combined with Eq. (3.7). In particular, this also shows that $N^b_{a1} = N^b_{1a} = \delta_{ab}$. A more general approach is considered in Ref [24].

3.1.1.4 Associativity and the Pentagon Equation

Associativity of the product $(O^L_a O^L_b)O^L_c = O^L_a(O^L_b O^L_c)$ implies that

$$\sum_e N^e_{ab} N^d_{ec} = \sum_f N^d_{af} N^f_{bc}.$$

In addition, there are two compatible ways to obtain the block decomposition of $B^{i,l}_{abc} = \sum_{j,k} B^{i,j}_a \otimes B^{j,k}_b \otimes B^{k,l}_c$ into diagonal blocks of type $B^{i,l}_d$. Indeed, we have

$$\begin{aligned} X^{d^+}_{ec,\nu} \left(X^{e^+}_{ab,\mu} \otimes \mathbb{1}_{\chi_c} \right) B^{i,l}_{abc} \left(X^{e}_{ab,\mu} \otimes \mathbb{1}_{\chi_c} \right) X^{d}_{ec,\nu} &= B^{i,l}_d \\ X^{d^+}_{af,\sigma} \left(\mathbb{1}_{\chi_a} \otimes X^{f^+}_{bc,\lambda} \right) B^{i,l}_{abc} \left(\mathbb{1}_{\chi_a} \otimes X^{f}_{bc,\lambda} \right) X^{d}_{af,\sigma} &= B^{i,l}_d \,, \end{aligned}$$

as illustrated in Fig. 3.4.

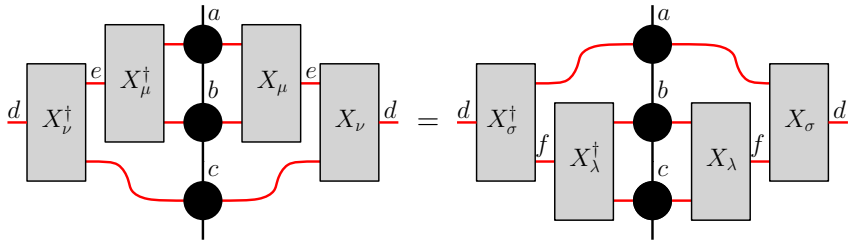

Figure 3.4: The two possible different way to reduce the product of three operators.

For PMPOs satisfying the zipper condition Eq. (3.11) we can argue that, just as two sets of fusion tensors are related by a gauge transformation Y^c_{ab}, for every a, b, c, d there must exist a transformation F such that,

$$\left(X^e_{ab,\mu} \otimes \mathbb{1}_{\chi_c} \right) X^d_{ec,\nu} = \sum_{f=1}^{\mathcal{N}} \sum_{\lambda=1}^{N^f_{bc}} \sum_{\sigma=1}^{N^d_{af}} (F^{abc}_d)^{f\lambda\sigma}_{e\mu\nu} \left(\mathbb{1}_{\chi_a} \otimes X^f_{bc,\lambda} \right) X^d_{af,\sigma}, \quad (3.9)$$

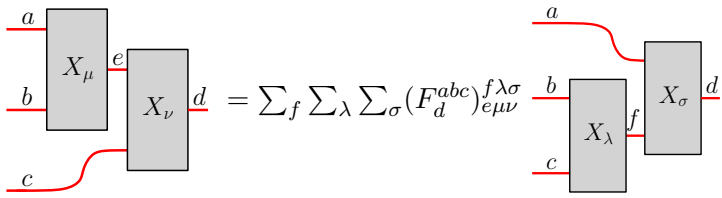

Figure 3.5: There exists a tensor F that relates the two possible reductions of the multiplication of a, b, c to d.

where F_d^{abc} are a set of invertible matrices, see Fig. 3.5.

The F-matrices have to satisfy a consistency condition called the pentagon equation, which is well-known in category theory. We obtain this equation by looking at the product of four operators and relate the two possible reductions

$$(X^f_{ab,\mu} \otimes \mathbb{1}_{\chi_c} \otimes \mathbb{1}_{\chi_d})(X^g_{fc,\nu} \otimes \mathbb{1}_{\chi_d}) X^e_{gd,\rho}$$

and

$$(\mathbb{1}_{\chi_a} \otimes \mathbb{1}_{\chi_d} \otimes X^h_{cd,\lambda})(\mathbb{1}_{\chi_a} \otimes X^i_{bh,\kappa}) X^e_{ai,\sigma}$$

in two different ways and equating the two resulting expressions. Written down explicitly, the pentagon equation reads

$$\sum_{h,\sigma\lambda\omega} (F_g^{abc})_{h\sigma\lambda}^{f\mu\nu} (F_e^{ahd})_{i\omega\kappa}^{g\lambda\rho} (F_i^{bcd})_{j\gamma\delta}^{h\sigma\omega} = \sum_\sigma (F_e^{fcd})_{j\gamma\sigma}^{g\nu\rho} (F_e^{abj})_{i\delta\kappa}^{f\mu\sigma}. \quad (3.10)$$

The two ways to obtain the same matrix leading to the pentagon equation are shown in Fig. I.2.4. Remarkably, the pentagon equation is all that is needed to ensure associativity. If it is satisfied all other possible consistency conditions originating from associativity are also automatically satisfied [78, 166].

In summary, we have associated the following set of algebraic data with a Hermitian PMPO P_L that satisfies the zipper condition Eq. (3.4),

$$(N_{ab}^c, F_d^{abc}, \varkappa_a).$$

This set of data is are very similar to the algebraic data defining a fusion category. We mentioned in Section 3.1.1.3 that under the assumption

that the PMPO has an identity block, the definition of duality as derived from Hermitian conjugation is equivalent to the categorical definition. A similar kind of reasoning also shows that our definition of $\varkappa_a$ coincides with that of the Frobenius-Schur indicator in fusion categories for a large class of PMPOs with unital structure that satisfy the zipper condition [24].

Note that (N_{ab}^c, F_d^{abc}) is (in many cases) known to be robust in the sense that every small deformation of the matrices F_d^{abc} that satisfies the pentagon equation can be absorbed in the fusion tensors via a suitable gauge transformation Y_{ab}^c. This remarkable property is called Ocneanu rigidity [78, 167] and it shows that PMPOs satisfying the zipper condition naturally fall into discrete families. In this light, it is a natural conjecture that there is a correspondence between these discrete families and quantum phases of matter.

3.1.2 MPO-Injective PEPS

In the previous section we introduced PMPOs. These are however one-dimensional objects, that can indeed be related to the boundary theory of topological states [25]. We are however interested in the full two-dimensional theory and now use the PMPOs to write down topologically ordered PEPS [21, 23, 26]. The class of states we can write down in this formalism is very general. For instance, it was shown in Ref. [23] that all string-net ground states have an exact description in terms of MPO-injective PEPS.

3.1.2.1 The Unitary and Pivotal Structure

To write down a topological PEPS starting from a PMPO, it is useful to demand the following. We require that there exists a gauge on the internal MPO indices such that the fusion tensors $X_{ab,\mu}^c$ are isometries,

$$\left(X_{ab,\mu}^c\right)^+ = \left(X_{ab,\mu}^c\right)^\dagger$$

and the gauge matrices Z_a are unitary. These extra requirements ensure that the tensor category that is represented by the MPO is a unitary fu-

sion category. They are also required for various consistency conditions throughout.

Unfortunately, we now need to complicate the notation to incorporate the difference between a label and its dual. Graphically, we use the notation in Fig. 3.6 to overcome the ambiguity between a and a^*.

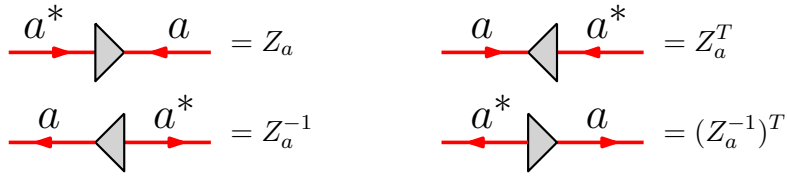

Figure 3.6: Graphical notation of the gauge matrices Z_a.

Note that absolute orientation of the symbols used to represent the matrices has no meaning, as we use those in a two-dimensional setting where the tensors can be rotated. Rotating a figure by 180° exchanges the row and column indices of the matrix and is thus equivalent to transposition, which is compatible with the graphic representation of Z_a^T. Because of unitarity, $(Z_a^{-1})^T = \bar{Z}_a$ and complex conjugation of the tensor simply amounts to reversing the arrows. The definition of the Frobenius-Schur indicator $Z_a \bar{Z}_{a^*} = \varkappa_a \mathbb{1}$ can now also be written as shown in Fig. 3.7.

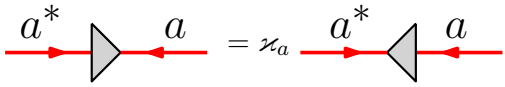

Figure 3.7: The definition of the Frobenius Schur indicator.

We also remind the reader of the essential zipper condition, illustrated here with the appropriate orientations in Fig. 3.8. From now on, we only show the label of the local Hilbert space, μ, which corresponds to degeneracies in the fusion Hilbert space. The incoming and outgoing labels are only denoted on the arrows. A normal fusion tensor $X^c_{ab,\mu}$ has two incoming arrows and one outgoing, while its left inverse has two

outgoing arrows and one incoming. In order to determine the difference between e.g. X^c_{ab} and X^c_{ba}, any fusion tensor in a graphical diagram always has to be read by rotating it back to its standard forms, one of those shown in Fig. 3.8.

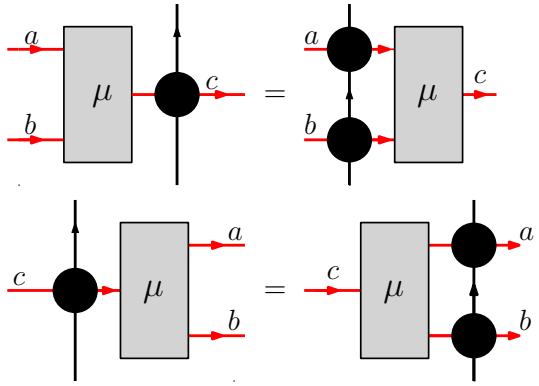

(3.11)

Figure 3.8: The graphical notation of the crucial zipper condition.

Note that one should not naively flip any of these tensors. To relate original and flipped fusion tensors, we introduce the final requirement in Fig. 3.9 and thereby introduce square matrices A^c_{ab} that satisfy

$$(A^c_{ab})^\dagger A^c_{ab} = \frac{w_c}{w_b}\mathbb{1}.$$

This requirement is closely related to the additional pivotal structure that can be imposed on a fusion category. Moreover, any unitary category admits a pivotal structure, which makes this requirement very natural from the abstract categorical point of view.

A similar property holds if we bend the lower b index on the left hand side of the Eq. 3.12, with a set of invertible matrices A'^c_{ab} satisfying $(A'^c_{ab})^\dagger A'^c_{ab} = \frac{w_c}{w_a}\mathbb{1}$.

Note that the conditions on the matrices A^c_{ab} are only possible if all the numbers w_a have the same phase. Using equation (3.5) this implies that

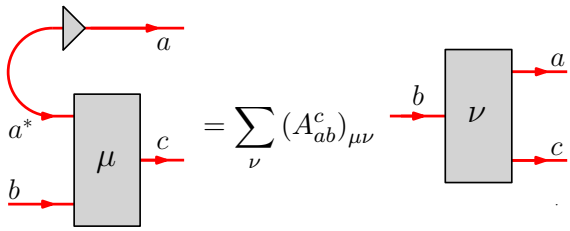

(3.12)

Figure 3.9: A graphical depiction of the pivotal poverty.

all w_a are either positive or negative real numbers. From

$$\sum_{a,b=1}^{\mathcal{N}} N_{ab}^{c} w_a w_b = w_c$$

and the fact that the tensor N consists of non-negative entries it then follows that all w_a must be positive. Furthermore, the pivotal property requires that the tensor N satisfies

$$N_{a^*b}^{c} = N_{ac}^{b}$$

which is indeed satisfied by combining Eq. (3.7) and Eq. (3.8) from Section 3.1.1.3.

We now have all the additional properties that are necessary to turn a one-dimensional PMPO into a genuine two-dimensional quantum tensor network. Note that the PMPOs that satisfy the properties discussed in this section can be thought of as classifying anomalous one-dimensional topological orders, i.e. the gapped topological orders that can be realized on the boundary of a two-dimensional bulk [25, 168].

3.1.2.2 Oriented Tensors

We now construct the PEPS tensor associated to a PMPO. We work on a square lattice but remark that the construction is more generally valid on different types of lattices. All links on the lattice are given

an orientation, similarly as in Fig. I.2.1a. On every vertex, we need a PEPS tensor. This tensor is created by combining four B tensors, one for every edge connected to the vertex. Depending on whether an edge is incoming or outgoing we use a different type of tensor. We introduce these two different types of MPO tensors in Fig. 3.10.

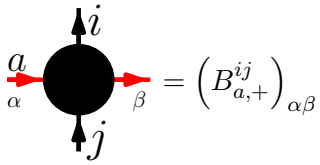

(a) Right handed tensor, constructed from the original tensors in the PMPO we started from.

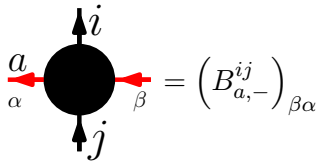

(b) Left handed tensor, obtained by complex conjugating $B_{a,+}$, which reverses arrows, and transposing i, j.

Figure 3.10

We thus have the following relation between the left and right handed tensors,

$$\left(B^{ij}_{a,-}\right)_{\beta\alpha} = \left(\bar{B}^{ji}_{a,+}\right)_{\alpha\beta} .$$

We already encountered this tensor before in Section 3.1.1.3. It is exactly the tensor that is obtained by applying Hermitian conjugation to the resulting MPO. To relate these tensors, we introduced the gauge matrices Z_a. In graphical notation, the resulting relations are shown in Fig. 3.11.

3.1.2.3 The MPO-Injective PEPS State

We can now define an MPO-injective PEPS. To do this, we assign an orientation to every edge of the lattice. This can be done arbitrarily although clearly on translation-invariant lattices, such as a square lattice, we opt for a translation-invariant definition as in Fig. I.2.1a.

We now define a PEPS tensor at every vertex. The vertices support the physical degrees of freedom and are also referred to as sites. The PEPS itself has the special structure of a small MPO loop. We assign a

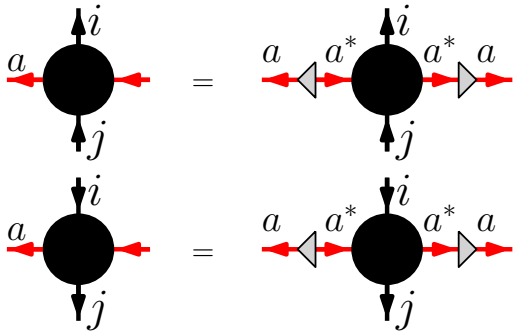

Figure 3.11: The matrices Z describe the relation between the left and right handed tensors.

counterclockwise orientation to every vertex v. We use an MPO tensor for every edge connected to the vertex. The tensor we use is the left or right oriented MPO tensor depending on the orientation of vertex and the edge. The final PEPS tensor $\tilde{P}_v$ at that site is then obtained by contracting these MPO tensors along their internal indices, where we use same weights w_a for the different blocks such that the resulting PEPS tensor $\tilde{P}_v$ is a Hermitian projector just like P_L.

Recall that we demanded unitary constraints on the gauge and fusion tensors, however the original PMPO P_L that we started from still allows for a unitary gauge freedom on the virtual indices of every MPO tensor B_a^{ij}. The Z matrices make sure that this is also a gauge freedom of the newly constructed $\tilde{P}_v$. Indeed, the transformation of the Z matrices and the $B_{a,\pm}^{ij}$ matrices cancel each other.

Note that reversing the internal orientation of a single block MPO in P_L amounts to taking the Hermitian conjugate. Because the weights in the original projector satisfy $w_a = w_{a^*}$, reversing the orientation of the internal index of $\tilde{P}_v$ is equivalent to Hermitian conjugation and this leaves $\tilde{P}_v$ invariant. So the counterclockwise global internal orientation on $\tilde{P}_v$ is completely arbitrary as it should be.

We now have a PEPS tensor $\tilde{P}_v$ at every vertex. To create the PEPS state we proceed as in the usual construction that was sketched in Section I.2.1.2. We place a maximally entangled qudit pair $\sum_{i=1}^{D} |i\rangle \otimes |i\rangle$ on

all edges of the lattice. We subsequently act at every vertex v with $\tilde{P}_v$ on the qudits closest to v. In Fig. 3.12 we show the PEPS on a 2×2 patch out of a square lattice.

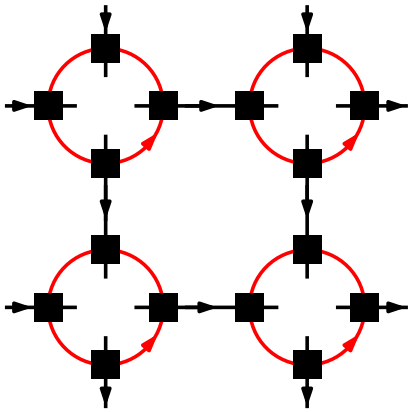

Figure 3.12: An MPO-injective PEPS constructed from the PMPO tensors on a 2×2 square lattice.

This construction gives only one PEPS, but more general PEPS are obtained by placing an additional tensor

$$A[v] = \sum_{i=1}^{d} \sum_{\{\alpha\}=1}^{D} A[v]^{i}_{\alpha_1\alpha_2\ldots\alpha_4} \left|i\right\rangle \left\langle\alpha_1\alpha_2\ldots\alpha_4\right|$$

at each vertex which maps the four indices on the inside of every MPO loop to a physical degree of freedom in $\mathbb{C}^d$. As long as $A[v]$ is injective as a linear map from $\mathbb{C}^{D^4}$ to $\mathbb{C}^d$ (which requires $d \geq D^4$) the resulting PEPS satisfies the axioms of MPO injectivity as defined in Ref. [23]. We discuss these axioms further on in this section.

For the particular case where each $A[v]$ is an isometry, the resulting network is an MPO-isometric PEPS. We remark here that MPO-isometric PEPS are in general not RG fixed points. From now on, we ignore the tensors $A[v]$ as we argue and believe that the universal properties of the quantum phase of the PEPS are completely encoded in the properties of $\tilde{P}_v$. This is exactly the idea behind and the power of the framework of MPO-injective PEPS.

We can now show that the PEPS we constructed indeed satisfies the requirements of an MPO-injective PEPS. Clearly the tensor is invariant under the action of P_L as this is a projector, $P_L^2 = P_L$. As long as the additional tensor $A[v]$ is injective, the tensor is furthermore injective, hence invertible on the subspace determined by P_L. We thus focus on the third crucial requirement, the pulling through condition. This condition is most clearly explained graphically. It allows us to move an MPO string O_a freely through the lattice on the virtual level as illustrated in Fig. 3.13. This is ensured by the local condition in Fig. 3.14.

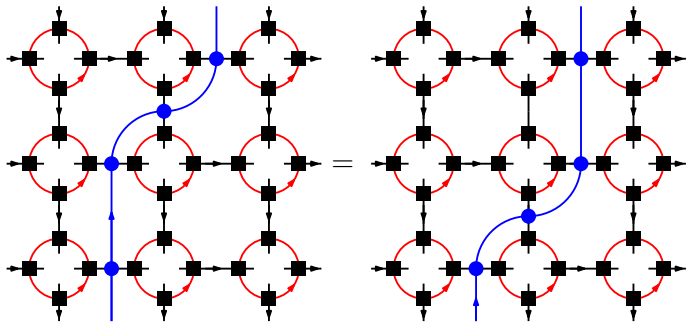

Figure 3.13: MPO strings can move freely on the virtual level in an MPO-injective PEPS.

The local pulling through condition in Fig 3.14 can be shown by using the zipper condition in Fig. (3.8) and the pivotal property in Fig. 3.9. By using the zipper condition on the left and right hand side of the equality in Fig. 3.14 we get the equality in Fig. 3.15. The pivotal property and the fact that the matrices A^c_{ab} satisfy $(A^c_{ab})^\dagger A^c_{ab} = \frac{w_c}{w_b}\mathbb{1}$ allow us to conclude that the pulling through condition is indeed fulfilled.

One could easily imagine different simple generalizations of the MPO-injectivity formalism. But as they are not necessary to understand the fundamental concepts we wish to illustrate, we keep the presentation simple and do not consider them here. However, in the string-net example later on we come across such a simple generalization and see how it leads to a slightly modified form of condition 3.12.

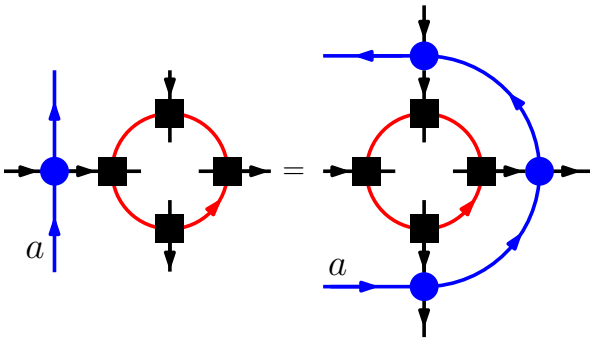

(3.13)

Figure 3.14: The local Pulling Through condition the PEPS tensors have to satisfy. Note the difference between squares that denote the superposition of the different injective MPOs $a = 1, \ldots, N$ with suitable coefficients w_a and the discs that represent a single block MPO tensor of type a. To distinguish them easier, we now use a blue color for the latter.

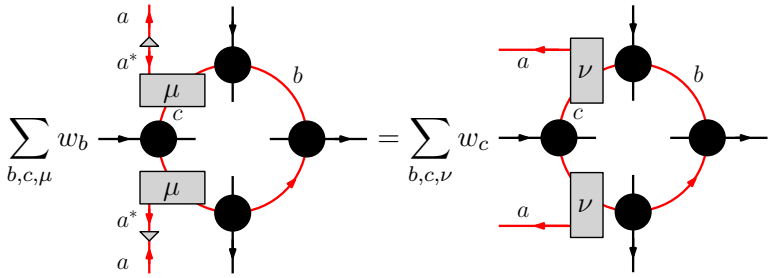

Figure 3.15: We can rewrite Eq. 3.13 with the zipper condition Eq. 3.11.

3.1.2.4 Virtual Support and Parent Hamiltonians

In this section we discuss the virtual support of the PEPS we constructed. This allows us to identify the parent Hamiltonian, its ground state subspace and the topological properties thereof. We need the invariance of the local tensors under P_L, the pulling through property and that the MPO tensors B^{ij} span the full space $\oplus_{a=1}^{N} \mathbb{C}^{\chi_a \times \chi_a}$, or equivalently that the tensors B_a are injective. In [23] a more complicated condition, referred to as a generalized inverse, was required to replace the latter

demand. We do not follow this approach here. The injectivity condition we require gives the existence of an operator that opens up the virtual index, which is all we need. This is shown in Fig. 3.16

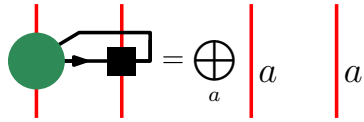

Figure 3.16: We require the existence of an operator that opens up the virtual index, it is denoted by the green disc.

We are interested in the virtual support of a patch of the PEPS network. From the pulling through condition and the local invariance it follows that the virtual support of a connected set of sites is contained in the support of the MPO P_L around the set of sites. Indeed, the MPOs of such a projector can be pulled through until they just encircle one site. We can then use the invariance of this tensor to make the projector disappear.

Conversely, we need to show that the virtual support of the patch is exactly given by P_L and not smaller. For simplicity we consider only two sites. We first use the pulling through condition as illustrated in Fig. 3.17, this gives us access to the entangled pair that connects the two sites. We can apply the operator introduced in Fig. 3.16 to this pair. The virtual indices of the operator are furthermore contracted with extra MPO operators. The effect is shown in Fig. 3.18. The final result is just the boundary projector P_L. This proves that the support of the virtual space of the two sites is at least P_L.

This method can be used for every contractible set sites and we can conclude that the support of the virtual degrees of freedom of such a region with boundary length L is indeed exactly P_L, the projector surrounding the region.

The constructed MPO-injective PEPS is an exact ground state of a local, frustration free parent Hamiltonian. This Hamiltonian can be con-

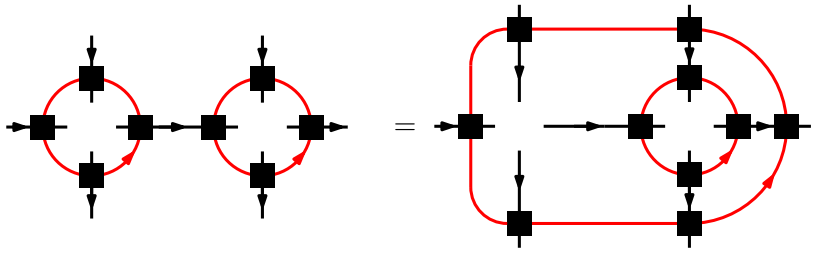

Figure 3.17: Use the pulling through on the left hand side condition to obtain the right hand side.

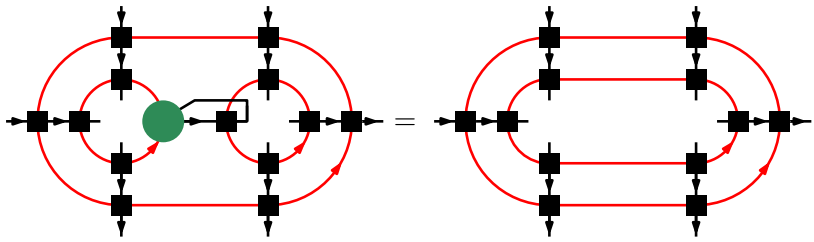

Figure 3.18: The injectivity requirement allows us to go from the left to the right hand side.

structed using standard PEPS methods [169] and is of the form

$$H = \sum_p h_p. \tag{3.14}$$

The sum runs over all 2×2 plaquettes of the square lattice and h_p is a Hermitian projector whose kernel corresponds to the image (physical support) of the PEPS map on that plaquette. On more general lattices, similar approaches can be used. In Ref. [23] the pulling through property was shown to be sufficient to prove that all the ground states of the parent Hamiltonian in Eq. (3.14) on a closed manifold are given by MPO-injective PEPS whose virtual indices along the non-contractible cycles are closed using the same MPOs connected by a so-called ground state tensor Q.

For instance on a torus, we can place MPOs O_a along the blue and

red lines in Fig. I.2.8 and their crossing point contains a Q tensor that connects them. The rest of the torus is filled with the ground state tensors. Because of the pulling through property these MPO loops can be moved freely on the virtual level of the PEPS, implying that all ground states are indistinguishable by the parent Hamiltonian.

3.1.2.5 Example: The Toric Code

In Section I.2.4.1.3 we introduced the MPO-injective PEPS based on the group $\mathbb{Z}_2$, which is in the same quantum phase as the Toric Code. The fusion algebra is given by the group multiplication and we use the MPOs O_1 and O_Z given by the tensors in Fig. I.2.11. All other requirements are trivially fulfilled, for instance the Z_a, A^c_{ab} matrices are all the identity. The zipper condition is satisfied with the following fusion tensors,

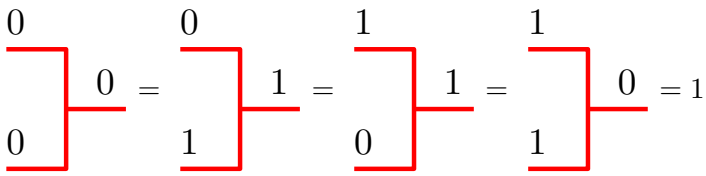

Figure 3.19: The fusion tensors for the MPOs O_1, O_Z.

This gives us indeed the PEPS tensor shown in Fig. I.2.10. The four different ground states on a torus are given by the presence of an MPO O_Z around both topologically non-trivial paths on the torus. The Q tensor is not present as the bond dimension of the MPO is one, hence they do not need to be connected with an additional tensor.

3.2 Anyons in PEPS

So far, we introduced PMPOs with some special properties that allowed us to construct MPO-injective PEPS. Moreover the PEPS we constructed are the ground states of local Hamiltonians. Using the MPOs we can construct a number of ground states that depends on the topology, a

hallmark of topological order. This is not surprising, because the framework of MPO-injective PEPS was introduced to capture all know non-chiral topologically ordered phases in two spatial dimension.

We now turn our attention to the topological sectors in these models. As argued in the previous section and shown in Ref. [23], MPO-injective PEPS give rise to degenerate ground states on non-trivial manifolds that are locally indistinguishable. This feature is typically connected with the presence of topological order and the existence of anyons. We thus expect that the low-energy eigenstates can be classified according to a finite number of topological superselection sectors. The sector of an excitations should be topological in the sense that it is not measurable by acting only locally in the region where the excitation lives, but only by acting on a larger region. Similarly, the topological sector can only be changed by acting non-locally. In this section we show that the entanglement structure of the ground state PEPS as determined by the PMPO $\tilde{P}_v$ contains all necessary information to find the anyon sectors and their topological properties.

3.2.1 Topological Charge

To find the topological sectors, or topological charges, we start by looking at a patch of the ground state PEPS on an annulus. The inside of the annulus is thought to contain an excitation. We are not interested in the microscopic properties of this anyon and only in the general topological properties. These are reflected in the virtual boundary of the annulus. It was shown in Ref. [23] that the support of the ground state tensors in the annulus is equal to the support of the tensor in Fig. 3.20. This operator is interpreted as a matrix from the indices outside the annulus to the indices inside.

The size of annulus, or the length of the MPOs is of no importance. The relevant feature is the string that exits the inside of annulus. We look at it more carefully and simplify it with the property illustrated in Fig. 3.21, which is a direct consequence of the zipper condition Eq. (3.4).

As the size and thickness of the annulus is arbitrary the only relevant part of the support is determined by just two fusion tensors, i.e. half

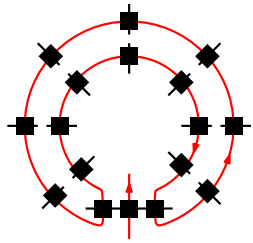

Figure 3.20: The tensor that gives the virtual support of a region in an MPO-injective PEPS that contains an excitation.

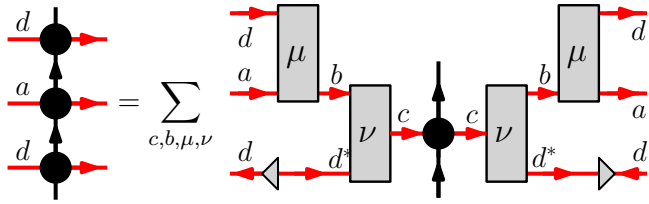

(3.15)

Figure 3.21: The property we use to simplify the annulus support in Fig. 3.20. It is a direct consequence of the zipper condition.

of the right hand side in Eq. (3.15). We show the simplified tensor in Fig. 3.22. Again, this is independent of the microscopic degrees of freedom that correspond to the tensor we use to map the virtual degrees of freedom in the annulus to physical indices.

The objects $A_{abcd,\mu\nu}$ can be seen as matrices from all the indices inside the loop to all the indices outside. A crucial observation is now that the matrices $A_{abcd,\mu\nu}$ form a C^*-algebra and that the structure of this algebra is independent of the number of MPOs in the loop, they are all isomorphic. The proof of this claim is given in Ref. [24].

It is a well known fact, commonly referred to as the Artin-Wedderburn theorem, that all finite-dimensional C^* algebras are isomorphic to a direct sum of full matrix algebras. For every summand i there is an operator $\mathcal{P}_i$ that projects onto the summand, these are called the central idempotents. The idempotents satisfy $\mathcal{P}_i\mathcal{P}_j = \delta_{ij}\mathcal{P}_i$, $\mathcal{P}_i^\dagger = \mathcal{P}_i$ and

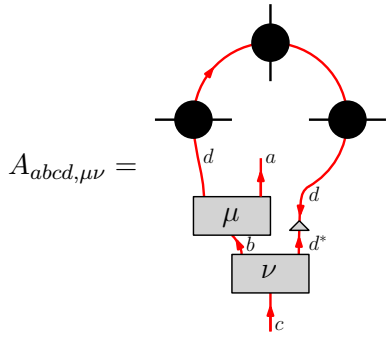

Figure 3.22: The tensor $A_{abcd,\mu\nu}$ that captures the relevant properties of the support of the tensors inside an annulus.

$A_{abcd,\mu\nu}\mathcal{P}_i = \mathcal{P}_i A_{abcd,\mu\nu}$. In general $\mathcal{P}_i$ can be written as

$$\mathcal{P}_i = \sum_{abd,\mu\nu} c^i_{abd,\mu\nu} A_{abad,\mu\nu}.$$

As mentioned before, the coefficients $c^i_{abd,\mu\nu}$ are independent of the number of MPO tensors that are used.

We now claim that the topological sectors corresponds one-to-one to the summands in the decomposition of the algebra. This means that every topological sector is determined by a unique central idempotent. The motivation of this definition follows from an operational point of view. We want to be able to measure the topological charge of excitations, hence excitations of different anyon types need to live in orthogonal subspaces. The maximal set of such orthogonal subspaces whose label cannot be changed by acting only outside or inside the region wherein the excitation lives is exactly given by the idempotents.

We note that in Ref. [170] a similar identification of anyons in string-net models with central idempotents was given. This idea dates back in the literature to the tube algebra construction of Ocneanu [171, 172]. Because of the importance of the idempotents, we use them extensively in the remainder of this work. We thus introduce a simplified graphical

notation in Fig. 3.23 that prevents the figures from becoming overly complicated.

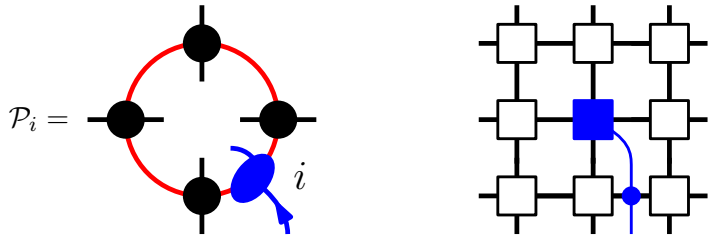

(a) The graphical representation of an idempotent. It has a similar structure to the ground state tensor, which is indeed one of the idempotents.

(b) Simplified representation of an MPO-injective PEPS with an excitation at the middle site. The PEPS tensors are shown as white squares.

Figure 3.23

3.2.2 Anyon Ansatz

We have clarified how to identify the topological sectors in an MPO-injective MPS network. Now, we turn our attention to the description of anyon excitations on top of an MPO-injective ground state. We discuss only the case of one-dimensional idempotents in the upcoming general discussion. For the interested reader, we mention that in Ref. [24] the case of higher-dimensional idempotents was also considered.

The dimension mentioned here refers to the dimension of the idempotents in the abstract algebra generated by the $A_{abcd,\mu\nu}$ not of the operator of the specific representation of $A_{abcd,\mu\nu}$ in the tensor network. By a one-dimensional idempotent we mean the following. A general central idempotent $\mathcal{P}_i$ can be decomposed as a sum of simple idempotents $P_i^{a_\alpha}$ that are not central,

$$\mathcal{P}_i = \sum_{a=1}^{D_i} \sum_{\alpha=1}^{d_{i,a}} P_i^{a_\alpha} \,, \tag{3.16}$$

where the index a refers to the D_i different MPO block labels that appear in $\mathcal{P}_i$. For a fixed label a, there can still be $d_{i,\alpha}$ different idempotents, which are labeled by α. A central idempotent that is not simple has $r_i \equiv \sum_{a=1}^{D_i} d_{i,a} > 1$ and is called a higher-dimensional central idempotent.

The simple idempotents have a diagonal block label, i.e. they can be expressed in terms of the basis elements as

$$P_i^{a_\alpha} = \sum_{bd,\mu\nu} t_{bd,\mu\nu}^{a_\alpha,i} A_{abad,\mu\nu} \,.$$

Let us now return to the MPO-injective PEPS. As explained above, every ground state tensor has virtual indices which are supported in the subspace $\tilde{P}_v$. To introduce anyonic excitations in the tensor network we need a new type of tensor I. If we want to place an anyon at vertex v, this new type of tensor has four virtual indices of dimension D, one new virtual index of dimension χ and one physical index of dimension d.

The new virtual index of dimension χ will be used to attach an MPO string to the excitation. This MPO string is responsible for a lot of the topological properties of the excitation. An graphical illustration of such a tensor I is depicted in Fig. 3.24a. The label i refers to the topological sector $\mathcal{P}_i$. A necessary condition for this tensor to describe an excitation with topological charge i is that its virtual indices are supported in the subspace determined by $\mathcal{P}_i$ as shown in Fig.3.24b.

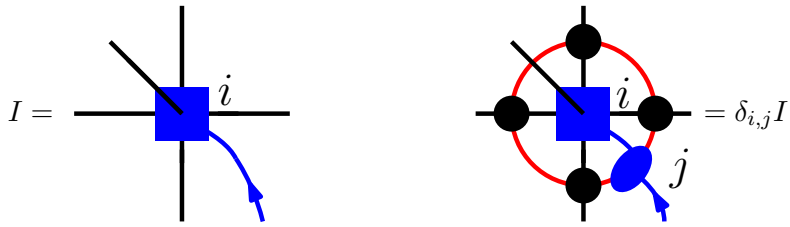

(a) An excitation tensor I of anyon type i. The d-dimensional physical index is drawn to the top left. The virtual space has an extra χ-dimensional index, drawn to the lower right.

(b) An excitation tensor of definite type i is characterized by the fact that it is invariant under the application of $\mathcal{P}_i$ to its virtual degrees of freedom and annihilated by the other idempotents.

Figure 3.24

The topological sectors are thus determined by the virtual degrees of freedom that account for the entanglement in the system. The different sectors are supported on orthogonal virtual subspaces and it is this decomposition of the entanglement degrees of freedom that contains the topological information.

As a final remark we would like to stress that we only looked at the universal properties of the anyonic excitation tensors. These tensors of course also contain a lot of degrees of freedom that one needs to optimize over using a specific Hamiltonian in order to construct eigenstates of the system. This can be done using similar methods as for non-topological PEPS [173, 174]. Because of the previous discussion, we can significantly reduce the number of variational parameters one has to keep in such computations.

3.2.3 Ground States on the Torus and the S-matrix

The projectors $\mathcal{P}_i$ automatically allow one to construct the Minimum Entropy States (MES) on a torus [85]. To do thus we put $\mathcal{P}_i$ along the non-contractible loop in the y-direction and close the 'inner' and 'outer' indices of $\mathcal{P}_i$ with an MPO along the non-contractible loop in the orthogonal x-direction. See Fig. 3.25 for a schematic representation. Both the idempotents and the MPO string can be moved freely and cannot be locally detected. We thus have constructed a ground state $|\Xi_i^x\rangle$ with an anyon flux of type i threaded through the hole in the x-direction. Equivalently, we can construct a MES $|\Xi_i^y\rangle$ with an anyon flux through the hole in the y-direction.

Since such an idempotent $\mathcal{P}_i$ effectively lowers the rank of the reduced density matrix of a segment of the torus obtained by cutting along two non-contractible loops in the y-direction it indeed implies, at least for fixed-point models, that we have minimized the entanglement entropy. In Ref. [85] the topological entanglement entropy for such a bipartition in a MES $|\Xi_i^x\rangle$ was found to be

$$\gamma_i = 2(\log D - \log d_i),$$

where D is the so-called total quantum dimension and d_i is the quantum dimension of anyon type i. The PEPS construction then shows that the topological entanglement entropy for a region in topological sector i is given by $\gamma_i' = \log D - \log d_i$.

As discussed in Section I.2.3.2.3, the identification of MES gives direct access to the S-matrix, which is defined as the unitary matrix that implements the basis transformation from one minimally entangled basis

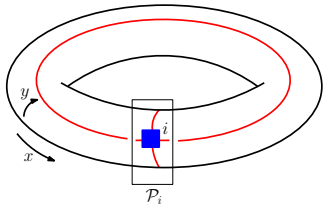

Figure 3.25: A schematic representation of the minimally entangled state $|\Xi\rangle_i^x$ with anyon flux i through the hole in the x-direction. It is obtained by placing the projector $\mathcal{P}_i$ on the virtual level of the tensor network on the torus along the non-contractible loop in the y-direction and connecting the open indices with an MPO along the x-direction.

$\{|\Xi_i^x\rangle\}$ to the other $\{|\Xi_i^y\rangle\}$. The advantage of the MPO-injectivity formalism is that we can compute readily the S-matrix on a small torus. Moreover we can also check numerically that only the central idempotents give rise to linearly dependent ground states and no further decomposition of the higher-dimensional idempotents is required to obtain a full set of ground states.

3.2.4 Topological Spin and T-matrix

Even in the absence of rotational symmetry an adiabatic rotation by 2π of the system is not physically observable. Usually, we then conclude that the 2π rotation acts as the identity times a phase, the Berry phase [72], on the total Hilbert space, $R(2\pi) = e^{i\theta}\mathbb{1}$. However, the existence of topological superselection sectors changes this conclusion [175]. Because there are no local, i.e. physical, operators that couple states in different sectors the 2π rotation could produce a different phase $e^{i2\pi h_i}$ in each sector and still be unobservable. The number h_i in a particular sector is generally called the topological spin of the corresponding anyon.

We can now consider a region of an MPO-injective PEPS network in the sector defined by $\mathcal{P}_i$. This region has an open internal MPO-index along the boundary that cannot be moved freely. We can obtain the topological spin associated to sector $\mathcal{P}_i$ by rotating the PEPS on a finite region while keeping the virtual boundary conditions fixed. After a 2π rotation the operator $\mathcal{P}_i$ is transformed as shown in Fig. 3.26a.

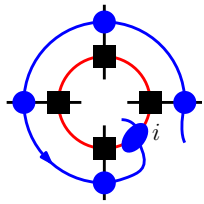

(a) The effect of a 2π rotation on the idempotent $\mathcal{P}_i$.

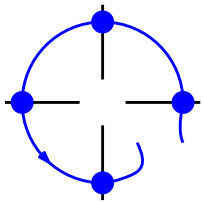

(b) The operator $\mathcal{R}_{2\pi}$ that implements the 2π and gives the topological spin.

Figure 3.26

We can see this transformation for every $\mathcal{P}_i$ as the action of the element $\mathcal{R}_{2\pi}$, shown in Fig. 3.26b, on the idempotent $\mathcal{P}_i$. A few observations are now in order. Using the zipper condition Eq. (3.4) and the pivotal property Eq. (3.12) we can see that $A_{abcd,\mu\nu}\mathcal{R}_{2\pi}$ is still an element of the algebra generated by the $A_{abcd,\mu\nu}$. From this we conclude that we can easily restrict $\mathcal{R}_{2\pi}$ to the subspace that is relevant in the network. We continue with this restriction.

Using similar methods we can see that $\mathcal{R}_{2\pi}^\dagger\mathcal{R}_{2\pi} = \mathbb{1}$, which implies that $\mathcal{R}_{2\pi}$ is unitary. Finally, again using the zipper and pivotal properties, we find that

$$\mathcal{R}_{2\pi}^\dagger A_{abcd,\mu\nu}\mathcal{R}_{2\pi} = A_{abcd,\mu\nu}.$$

Schur's lemma thus allows us to conclude that

$$\mathcal{R}_{2\pi} = \sum_i \theta_i \mathcal{P}_i,$$

with θ_i some phases because of the unitarity of $\mathcal{R}_{2\pi}$. We thus arrive at the desired result, i.e.

$$\mathcal{P}_i\mathcal{R}_{2\pi} = \theta_i\mathcal{P}_i\,,$$

where $\theta_i = e^{i2\pi h_i}$ gives the topological spin of the anyon in sector i. Finally, the collection of all these phases in a diagonal matrix gives us the T-matrix that was introduced in Section I.2.3.2.3.

3.2.5 Fusion

We can associate an algebra, called the fusion algebra, to the topological sectors. This algebra is not the same as the algebra generated by the

MPOs O_a, but corresponds to its Drinfeld center or categorical double. The new algebra describes the fusion relations of the anyons.

Consider a PEPS which is is in the ground state everywhere, by which we mean it is described by the MPO-injective PEPS tensor we have been discussing and its ground state energy density is everywhere zero, except for two spatially separated regions. In these regions we put an excitation. Using operators that surround such a region, we can measure the topological charge within the region. We prefer the terminology topological charge or sector to anyon, as in principle more excitations can be present in such a region. We then measure their combined topological charge. However, the reader can think intuitively about these processes as measuring the anyon type of an excitation.

Suppose the two measurements reveal topological charges i and j in the respective regions. Similarly, we can measure the topological charge of a big regions that contains both previously mentioned smaller regions. Even if i, j are determined, there are in general several possible outcomes of this last measurement. An anyon theory where this occurs is referred to as a non-Abelian anyon theory. The sectors that appear in this superposition for every i and j determine the integer rank three tensor $\mathcal{N}_{ij}^{k}$. This gives a commutative fusion algebra whose multiplication we denote as $i \times j = \sum_k \mathcal{N}_{ij}^{k}\, k$. The topological sector that corresponds to the ground state serves as the identity in this algebra.

One of the benefits of the MPO-injective framework is that this fusion algebra is explicitly realized in MPO-injective PEPS. In the basic example, we place two single-site idempotents $\mathcal{P}_i$ and $\mathcal{P}_j$, next to each other on neighboring lattice sites. We can then fuse together the MPO strings emanating from $\mathcal{P}_i$ and $\mathcal{P}_j$ into one string. Looking at an annular ground state region surrounding the two anyons and using similar reasoning as in Section 3.2.1 we find that the sum of all idempotents $\sum_k \mathcal{P}_k$ surrounding both anyons acts as a resolution of the identity on the relevant subspace. We can easily determine the subspaces $\mathcal{P}_k$ on which the combination of both anyons are supported. These subspaces correspond to the possible fusion products of $\mathcal{P}_i$ and $\mathcal{P}_j$. We illustrate this in Fig. 3.27.

Note that the procedure of Fig. 3.27 does not allow one to determine

fusion multiplicities, i.e. it only tells whether $\mathcal{N}_{ij}^{k}$ is non-zero. The multiplicities, the specific values of $\mathcal{N}_{ij}^{k}$, can be obtained by a generalization of the method described in Ref. [24]. However, we will not go into the details of that elaborate procedure because one can of course also just calculate the fusion multiplicities from the S-matrix using the Verlinde formula [75].

Note that a the true physical measurement of the topological charge in some region depends heavily on the details of the explicit tensors in the network. This is to be expected since the physical measurement is determined by the specific microscopic realization of the quantum phase. However, on the virtual level, these measurements are always given by the idempotents, which illustrates again the power of this approach.

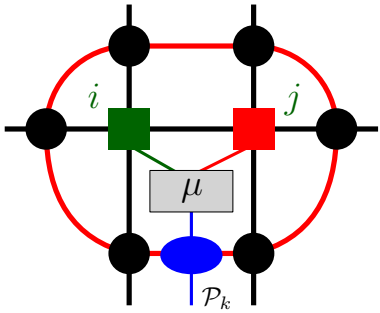

Figure 3.27: The procedure to determine the fusion product of two anyons. The anyons are given by the green and blue idempotents $\mathcal{P}_i, \mathcal{P}_j$. The combined topological charge is measured by $\mathcal{P}_k$.

3.2.6 Braiding

It is a well known, one could even say defining, feature of anyons that they detect each others presence in a topological, non-local way. The standard example of this behavior is the introduction of a Berry phase when transporting an electric charge around a magnetic flux, even when the charge is always arbitrary far away from the flux during this process. In the case of non-Abelian anyons, the action of such a process can be more complicated than just a phase and even allow for universal quantum computation [79]. Before we discuss braiding in the MPO-

injective framework, we discuss quickly which degrees of freedom are relevant in these processes.

3.2.6.1 The Braid Group

The crux is that by specifying a fixed configuration of anyons in the plane, the total quantum many-body state is not fully fixed yet. Such a configuration corresponds to a collection of quantum many-body states. A basis for this subspace is obtained by assigning an arbitrary ordering to the anyons and projecting the first two anyons in a particular fusion state. One subsequently does the same for the fusion outcome of the first two anyons and the third anyon. This can be continued until a final projection on the vacuum sector is made. So the degeneracy of an anyon configuration is given by the number of different ways an ordered array of anyons can fuse to the vacuum.

The subspace of fusion states corresponding to an anyon configuration forms a representation of the colored braid group. This means that when we exchange anyons or braid them around each other this induces a non-trivial unitary transformation. If there is only one state that we can associate to every anyon configuration then we only get one-dimensional representations. This situation is commonly referred to as Abelian statistics and the anyons are called Abelian anyons. With non-Abelian anyons we can associate multiple orthogonal states to an anyon configuration, one for each different possible fusion process to the vacuum. These states will form higher-dimensional representations of the colored braid group. It is in this Hilbert space that topological quantum computation is performed. We elaborate further on this topic in Section 3.5.

From now on, we omit the orientations and the corresponding gauge transformations Z_a to avoid cluttering the presentation. We also assume that the numbers $d_{i,a} = 1$, see Eq. (3.16) and often even that all central idempotents are simple . These issues will also not have to be taken into account for the string-net examples further on.

3.2.6.2 The Exchange Process

To specify the action of the braid group it suffices to describe the exchange and braiding of two anyons that are not in a particular fusion state, this amounts to defining the action of the generators of the braid group. We can always specify the fusion process afterwards. To obtain the effect of braiding and exchange in the tensor network, we look for a generalization of the pulling through condition in Fig. 3.14. The goal is to obtain tensors $\mathcal{R}_{\mathcal{P}_i,b}$ that describe the pulling of a MPO string of type b through a site that contains an anyon corresponding to $\mathcal{P}_i$ according to the defining equation shown in Fig. 3.28. If there is no anyon on the

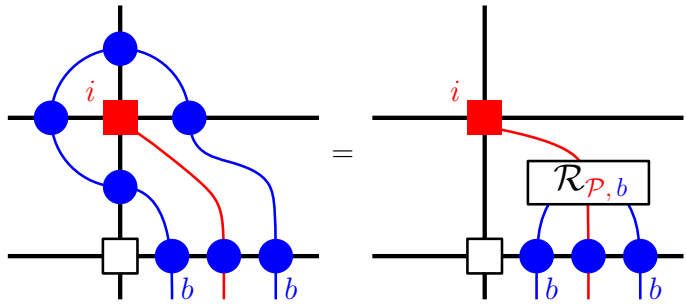

Figure 3.28: The exchange procedure is determined by the tensor $\mathcal{R}_{\mathcal{P}_i,b}$.

site we consider, i.e. the idempotent on this site is $\mathcal{P}_1$ corresponding to the trivial anyon, the operator $\mathcal{R}_{\mathcal{P}_i,b}$ is equal to the identity on the MPO indices as follows from the original pulling through property.

While in practice one could solve the equation that determines $\mathcal{R}$ numerically, we can in fact also obtain the tensors $\mathcal{R}_{\mathcal{P},b}$ analytically for a non-trivial idempotent $\mathcal{P}_i$ with $i \neq 1$. We thereto rewrite the left hand side of the equation in Fig. 3.28 by using relation (3.15) as shown in Fig. 3.29.

If by $\mathcal{P}_i.A_{abcd}$ we denote the multiplication of $\mathcal{P}_i$ and A_{abcd} in the anyon algebra, we find the equation in Fig. 3.30. With a slight abuse of notation, the gray rectangle containing $\overline{A}_{acdb,\mu\nu}$ denotes a similar tensor as

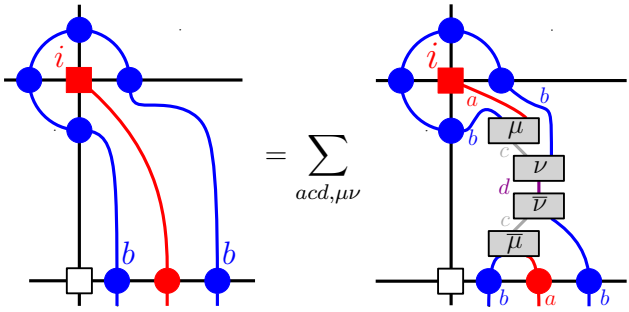

Figure 3.29

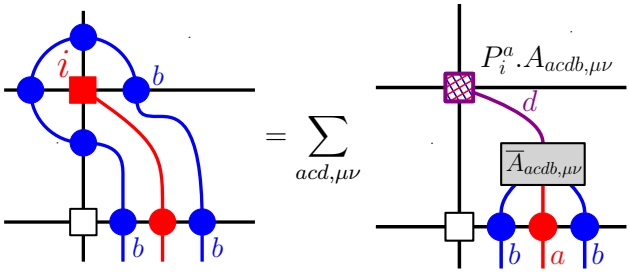

Figure 3.30

the algebra object $A_{acdb,\mu\nu}$ in Fig (3.22), but without the MPO tensors as shown in Fig. 3.31.

Recall the notation of Eq. (3.16) and assume that $d_{i,\alpha} \equiv 1$ to obtain $\mathcal{P}_i.A_{acdb,\mu\nu} = P_i^a.A_{acdb,\mu\nu}$. These tensors can easily be determined using the structure constants. Note that all tensors $\mathcal{P}_i.A_{acdb}$ are supported on the subspace determined by $\mathcal{P}_i$, hence they all correspond to the same topological sector. Indeed, braiding an anyon around another one cannot change the topological charges. Remark that after the blue MPO is pulled through the site containing the anyon, the tensor on the site and the braid tensor linking the MPOs are in general entangled, due to the summation over a, c, d, μ, ν. However, if $\mathcal{P}_i$ is a one-dimensional idempotent, the tensor $\mathcal{P}_i.A_{acdb,\mu\nu}$ is only nonzero for a unique choice

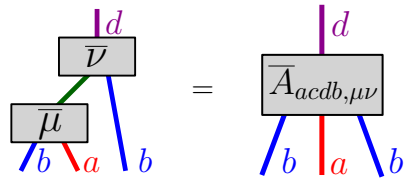

Figure 3.31: A compact notation used in Fig. 3.30

of $d = a$ and is in that case proportional to $\mathcal{P}_i$. Hence, in that case there is no entanglement between the tensor on the site and the tensor that connects the MPOs.

Once we obtain these tensors $\mathcal{R}_{\mathcal{P}_i,b}$ we know how to resolve the exchange of anyons and we can compute the R-matrix, also called braiding matrix. Suppose we have two anyons, described by idempotents $\mathcal{P}_1, \mathcal{P}_2$ and we want to compare the fusion of these anyons with and without exchanging them. Both situations correspond to Fig. 3.32a and Fig. 3.32b respectively.

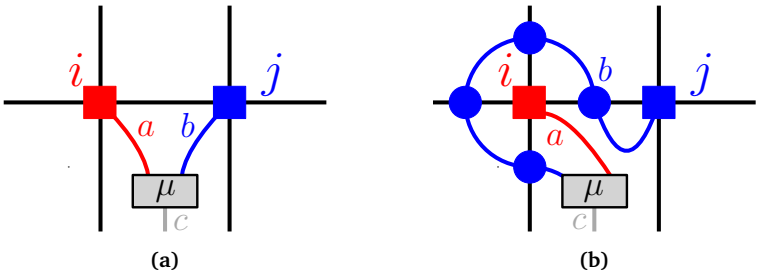

Figure 3.32: Two anyons, described by idempotents $\mathcal{P}_i, \mathcal{P}_j$, can be fused before exchanging them, as in Fig. 3.32a, or after exchanging, as in Fig. 3.32b. To compare both diagrams we first use the tensor $\mathcal{R}$ to redraw Fig. 3.32b. The result is shown in Fig. 3.33

All we need to resolve this situation is the tensor $\mathcal{R}_{\mathcal{P}_i,b}$ for all b for which $\mathcal{P}_j$ is non-zero. With this tensor we can redraw Fig. 3.32b as shown in the right hand side of Eq. (3.17). It is now clear that the $\mathcal{R}_{\mathcal{P}_i,b}$ tensors encode the R-matrices of the topological phase, i.e. the braiding information of the anyonic excitations.

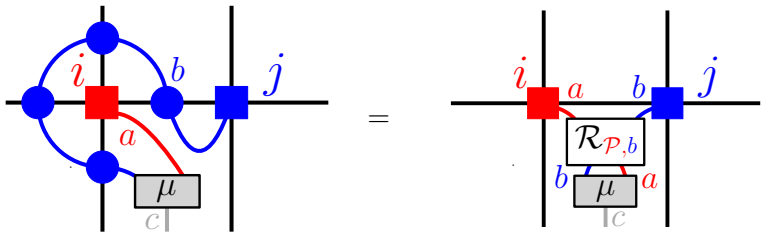

(3.17)

Figure 3.33: The tensor $\mathcal{R}_{\mathcal{P}_i,b}$ is used to resolve the situation in Fig. 3.32b.

The tensor $\mathcal{R}_{\mathcal{P}_i,b}$ in Fig. 3.33 is a unitary when interpreted as a matrix from the upper to the lower indices. Remarkably, the matrix we get by interpreting it instead as a matrix from the left to the right indices is exactly its inverse. The reason is that both matrices correspond to exchange processes in opposite directions and the sequential application of both corresponds to the identity.

3.2.6.3 The Full Braiding Process

Analogously, we now show how the full braiding, or double exchange, of one anyon around another can be determined. As before, this information is completely contained within the braid tensors $\mathcal{R}$, as shown in Fig. 3.34. We study the situation where there are two anyon pairs present and we braid one anyon of the first pair completely around an anyon of the second pair. The procedure is shown in Fig. 3.34. If we compare Fig. 3.34a and Fig. 3.34d, we note that two different changes occurred in the transition between both diagrams.

First, the use of relation (3.17) can induce a non-trivial action on the inner degrees of freedom of the idempotent. While it cannot change the support of the idempotent itself, as this determines the topological superselection sector, the degrees of freedom within a sector can change. This is important if the idempotent corresponding to the anyon is higher-dimensional. Secondly, the fusion channels of the red and blue anyon pair can change. Both pairs were originally in the vacuum sector, but

can be in a superposition of sectors after braiding, as is illustrated in Fig. 3.36.

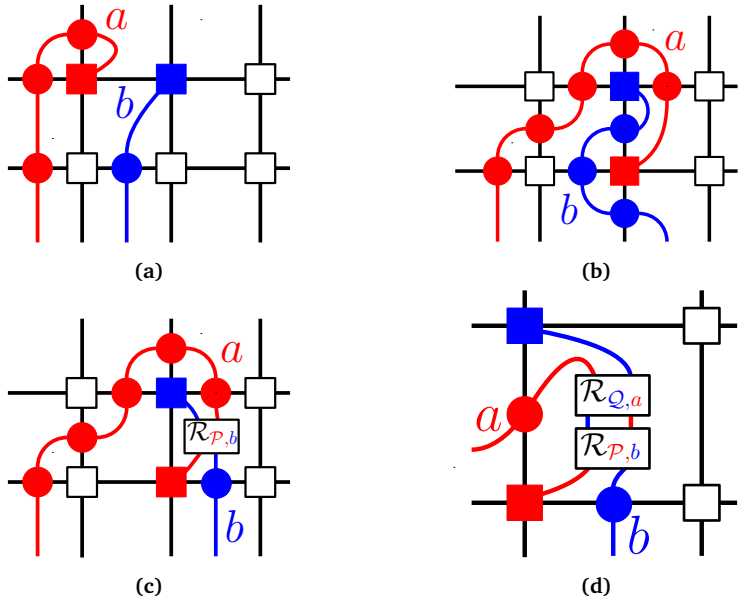

Figure 3.34: In Fig. 3.34a we show two anyons in a lattice, the lattice sites that contain the central idempotents $\mathcal{P}$, $\mathcal{Q}$ are colored red and blue respectively. In Fig. 3.34b we move the red anyon until the configuration is suited to apply equation (3.17). In Fig. 3.34c we pull the blue line though the red anyon, using the tensor $\mathcal{R}_{\mathcal{P},b}$ that depends on the red idempotent and the label of the blue line. Finally, in Fig. 3.34d we perform a similar operation, now with $\mathcal{R}_{\mathcal{Q},a}$.

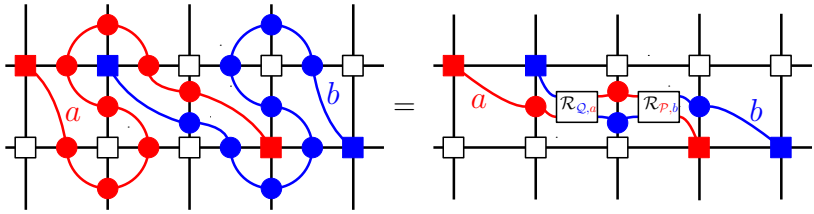

Figure 3.35: A more symmetric version of the braiding process described in figure 3.34. Completely braiding a red around a blue anyon is described by the contraction of the tensors $\mathcal{R}_{\mathcal{P},b}$ and $\mathcal{R}_{\mathcal{Q},a}$.

Finally, just as in relativistic field theories there is a spin-statistics rela-

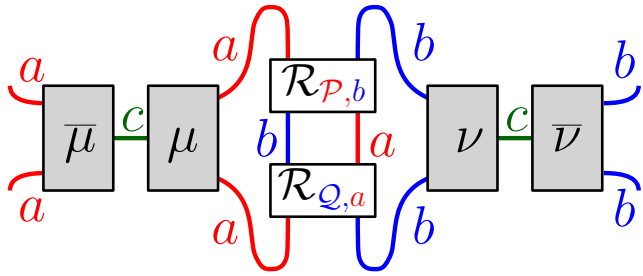

Figure 3.36: The result of braiding the red anyon around the blue, as in Fig. 3.35. The green label c correspond to the possible fusion channels of the pair of red (or blue) anyons. Before braiding, the pair of red anyons was in the trivial topological sector. After braiding, several fusion results are possible. They can be measured at the green line. A sum over the different possible fusion outcome values for these lines is implied. Due to the structure of the tensors $\mathcal{R}$, the green lines c at the left and right are equal.

tion for anyons, connecting topological spin and braiding. It is expressed by the so-called 'pair of pants' relation, which shows that braiding acts diagonally on two anyons that are in a particular fusion state, for more information see Ref. [24]. Because the topological spins can be shown to be rational numbers [83], the spin-statistics connection reveals that every anyon configuration provides a representation of the truncated colored braid group.

3.2.7 Example: The Toric Code

We no quickly discuss the topological sectors in the $\mathbb{Z}_2$-isometric PEPS. We already gave the result in Section I.2.4.2.3 but now extend the discussion and summarize the different concepts we introduced previously in this context.

There are four non-zero algebra elements A_{abcd}, shown in Fig. 3.37. We can use these algebra elements to compute the central idempotents, of which there are four, shown in Fig. 3.38.

These idempotents are easy to interpret. The idempotents $\mathcal{P}_1$ and $\mathcal{P}_e$ have only a vertical 0 index, which means they have no MPO string attached, or more correctly a string O_1. Conversely, the $\mathcal{P}_m$ and $\mathcal{P}_{em}$ idempotents have a vertical 1 index and thus an O_Z MPO attached. The idempotents with a string indicate the presence of a magnetic flux

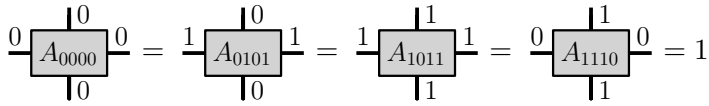

Figure 3.37: The four possible algebra elements A_{abcd} for the $\mathbb{Z}_2$-isometric PEPS.

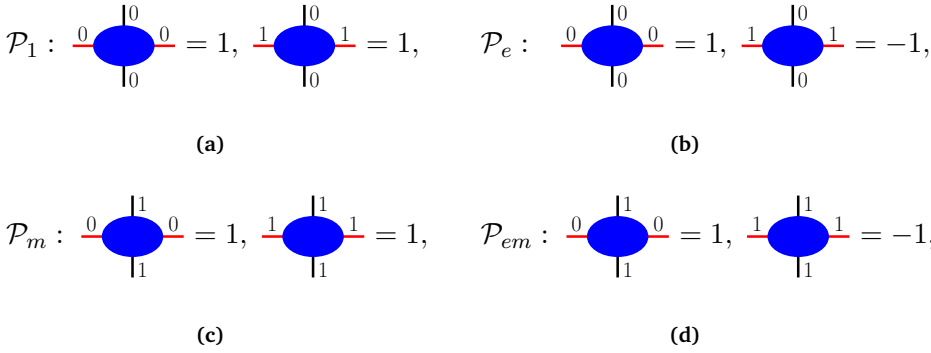

Figure 3.38: The four possible central idempotents of the $\mathbb{Z}_2$-isometric PEPS, corresponding to the anyons $1, e, m, em$.

excitation, they violate a plaquette term as shown in Fig. 2.15a. The idempotents $\mathcal{P}_1$ and $\mathcal{P}_m$ only have coefficients $+1$ which means they locally correspond to the tensor $\mathbb{1}^{\otimes 4} + Z^{\otimes 4}$. The other idempotents,$\mathcal{P}_e$ and $\mathcal{P}_{em}$ contain a -1 coefficient, thus locally they are $\mathbb{1}^{\otimes 4} - Z^{\otimes 4}$. These last ones have a charge excitation, i.e. a violation of the vertex terms as shown in Fig. 2.15b.

The braiding properties are now indeed very easy, pulling an O_Z MPO through a site that contains a $\mathcal{P}_1$ or $\mathcal{P}_m$ excitation is trivial due to the pulling through condition, hence $\mathcal{R}_{\mathcal{P}_1,Z} = 1, \mathcal{R}_{\mathcal{P}_m,Z} = 1$. On the other hand, it is clear that an extra minus sign appears when pulling an O_Z MPO through a site that contains a $\mathcal{P}_m$ or $\mathcal{P}_{em}$ excitation. Hence, $\mathcal{R}_{\mathcal{P}_e,Z} = -1, \mathcal{R}_{\mathcal{P}_{em},Z} = -1$ as it should be.

3.3 Example: String-Nets

In this section we make the rather abstract discussions of the previous sections more concrete but in a far more general setting than the Toric Code model. We show how the string-net states of Levin and Wen [176] fit naturally in the formalism. For simplicity, we restrict ourselves to models without higher-dimensional fusion spaces, i.e. all N_{ab}^c in Eq. (3.2) are either 0 or 1. Also, we only deal with models where each single block MPO is self-dual, $a = a^*$ and $N_{aa}^1 = 1$. Both restrictions can easily be lifted but avoid cluttering the clarifying examples with non-essential technicalities.

The description of string-nets in the framework presented here was introduced in Ref. [23]. The string-net models are indeed the prime example of the MPO-injectivity formalism. The PMPO is constructed from the F-symbols and the quantum dimensions of a unitary fusion category. The single block MPOs correspond one-to-one with the simple objects of the input fusion category. The fusion matrices X_{ab}^c are also easily constructed from the F-symbols and the quantum dimensions. These tensors give rise to an MPO-injective PEPS and they satisfy all the properties listed in Section 3.1.2.1, whose validity is rooted in the spherical property of unitary fusion categories. The general requirements in our formalism follow mainly from the pentagon relation (3.10) of the F-symbols.

To describe the string-nets as a tensor network, there is one extra technical subtlety we need to take into account. Every closed loop in the PEPS representation of a string-net wave function gives rise to a factor equal to the quantum dimension of the label of this loop. This is taken care of by incorporating such factors both in the tensors and by adding extra factors for every bend in an MPO. Because of this convention, the MPOs give rise to projectors P_L that are not Hermitian, except for straight loops that contain no bends.

Luckily, as all these operators are still similar to Hermitian operators via a local, positive similarity transformation, this has no implications for the general theory. The tensors we describe next are used on a square lattice, similar tensors can be used on different lattices.

First we describe the PMPO. It is convenient to introduce the G-symbols,

$$G^{abc}_{def} = \frac{1}{v_e v_f} F^{abc}_{def}. \tag{3.18}$$

We then have where the internal MPO indices are the horizontal ones

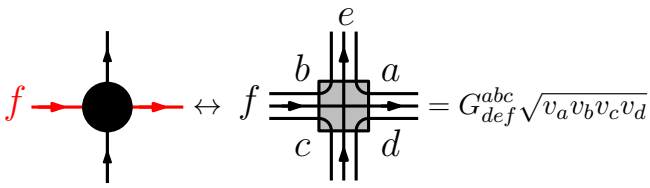

(3.19)

Figure 3.39

and all indices are N-dimensional, with N the number of labels. The injective single block MPOs are obtained by fixing the label f. The corresponding weights w_f used to construct a PMPO are given by the quantum dimensions d_f divided by $\mathcal{D}^2 = \sum_a d_a^2$, the total quantum dimension of the fusion category squared. The factors v_a in the definition of the MPO are included to take care of the closed loop factors. They are given by the square roots of the quantum dimensions, $v_a = \sqrt{d_a}$. The single block MPOs obtained by fixing f satisfy the algebraic structure of the fusion algebra of the category we used to construct the MPOs.

For the string-net MPOs we consider here the gauge transformations Z_a are all trivial, they amount to simply swapping the double line structure which is present in the virtual indices of the MPO tensor. The fusion tensors X^c_{ab} are shown in Fig. 3.40 The factor v_c is only present for the closed loop condition (and could be taken care of differently). The pivotal property for these fusion tensors is shown in Fig. 3.41 which is equivalent to Eq. (3.8) up to the diagonal matrices labeled by $\frac{1}{2}$ and $-\frac{1}{2}$ that denote the power of the quantum dimensions and are added to satisfy the closed loop condition. More specifically, these matrices are $\sum_a v_a |a\rangle \langle a|$.

With this information, the MPO and fusion tensors can now be used in our framework in order to obtain an ansatz for anyons in string-

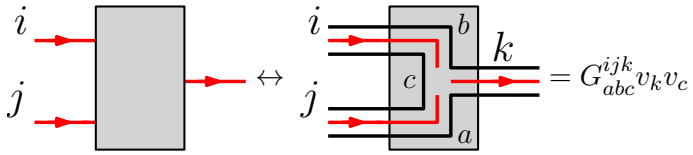

$$= G^{ijk}_{abc} v_k v_c \tag{3.20}$$

Figure 3.40

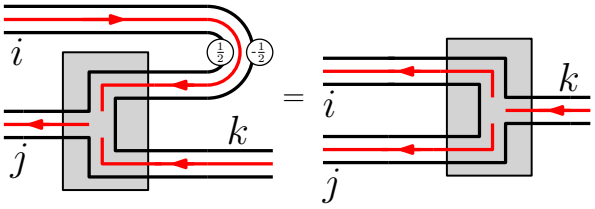

(3.21)

Figure 3.41

net models. Recall the form of the algebra elements in Fig. 3.22. The structure constants that define the multiplication of these objects can be computed analytically or numerically. The algebra that describes the anyons is similar to a construction proposed in [170], although obtained from a very different motivation. To obtain the central idempotents of this algebra we use a simple algorithm based on [177]. As expected, we obtain both one-and higher-dimensional central idempotents.

In the remainder of this section we list the central idempotents and their properties for the Fibonacci, Ising and Rep(S_3) string-nets. For each of those, we also compute the topological spin using the standard procedure described in Section 3.2.4. For string-nets, these spins can in principle be computed analytically from the central idempotents. Furthermore, we compute the fusion table describing the fusion of two anyons. Thereto, we have numerically performed the procedure explained in Section 3.3. We indeed recover the known fusion rules for the anyonic excitations of these theories. Note that there are no fusion multiplicities larger than one in the models we consider. Finally, we explicitly work

out the braid tensor $\mathcal{R}$ using the procedure of Section 3.2.6 for two τ anyons in the Fibonacci string-net model.

3.3.1 Fibonacci String-Net

The first example we discuss is the prime example of a non-Abelian string-net model. As input we use the modular tensor category of Fibonacci anyons. We expect to find central idempotents corresponding to the topological sectors of the doubled Fibonacci theory, which are believed to be realized in fractional quantum systems at filling factor $\nu = 12/5$ [178, 179].

3.3.1.1 MPO-Tensors

The categorical data of the Fibonacci theory is well known. The theory has two labels 1 and τ that satisfy the non-Abelian fusion rules

$$N_{11}^{1} = N_{\tau 1}^{\tau} = N_{1\tau}^{\tau} = N_{\tau\tau}^{1} = N_{\tau\tau}^{\tau} = 1\,,$$

the other fusion rules are zero. The quantum dimensions are given by $d_1 = 1$ and $d_\tau = \frac{1+\sqrt{5}}{2}$, this last number is the golden ratio for which we use the notation ϕ. The remaining crucial information are the F-symbols of this theory. They are given by

$$[F_d^{abc}]_e^f = F_{def}^{abc} = \delta_{abe}\delta_{cde}\delta_{adf}\delta_{bcf}F_{def}^{abc}, \tag{3.22}$$

where $\delta_{ijk} = 1$ if i, j, k can fuse to 1, i.e. $N_{ij}^{k} > 0$, and $\delta_{ijk} = 0$ otherwise. The non-trivial elements of F are given by

$$F_{\tau 11}^{\tau\tau\tau} = \frac{1}{\phi}, \quad F_{\tau\tau 1}^{\tau\tau\tau} = \frac{1}{\sqrt{\phi}}, \quad F_{\tau 1\tau}^{\tau\tau\tau} = \frac{1}{\sqrt{\phi}}, \quad F_{\tau\tau\tau}^{\tau\tau\tau} = -\frac{1}{\phi}.$$

All other non-zero components of F are one. As shown in Ref. [23], the Fibonacci string-net state can now be described by a projector MPO constructed from the tensors shown in Fig. 3.42. After removing the zero rows and columns, this MPO has bond dimension $\chi = 5$ and consists of two blocks B_1 and B_τ of dimension $\chi_1 = 2$ and $\chi_\tau = 3$ respectively. The

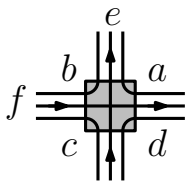

$$= G^{abc}_{def}\sqrt{v_a v_b v_c v_d} \tag{3.23}$$

Figure 3.42

blocks B_1, B_τ satisfy the Fibonacci fusion rules. The diagonal matrix Δ from equation (3.1) is given by the quantum dimensions of the block labels divided by the square of the total quantum dimension, $w_1 = \frac{1}{1+\phi^2}$ and $w_\tau = \frac{\phi}{1+\phi^2}$.

3.3.1.2 Central Idempotents

Here we give the central idempotents and their topological spins for the Fibonacci string-net. The algebra is generated by the following basis elements

$$A_{1111}, A_{\tau\tau\tau 1}, A_{1\tau 1\tau}, A_{1\tau\tau\tau}, A_{\tau 1\tau\tau}, A_{\tau\tau 1\tau}, A_{\tau\tau\tau\tau}.$$

All other possible elements are zero due to the fusion rules. We find four different idempotents, of which $\mathcal{P}_1, \mathcal{P}_2, \mathcal{P}_3$ are one-dimensional and $\mathcal{P}_4$ has dimension two,

$$\begin{aligned}
\mathcal{P}_1 &= \frac{1}{\sqrt{5}}\left(\frac{1}{\phi}A_{1111} + \sqrt{\phi}A_{1\tau 1\tau}\right)\\
\mathcal{P}_2 &= \frac{1}{\sqrt{5}}\left(\frac{1}{\phi}A_{\tau\tau\tau 1} + \frac{1}{\sqrt{\phi}}e^{-\frac{4\pi i}{5}}A_{\tau 1\tau\tau} + e^{\frac{3\pi i}{5}}A_{\tau\tau\tau\tau}\right)\\
\mathcal{P}_3 &= \frac{1}{\sqrt{5}}\left(\frac{1}{\phi}A_{\tau\tau\tau 1} + \frac{1}{\sqrt{\phi}}e^{\frac{4\pi i}{5}}A_{\tau 1\tau\tau} + e^{-\frac{3\pi i}{5}}A_{\tau\tau\tau\tau}\right)\\
\mathcal{P}_4 &= \frac{1}{\sqrt{5}}\left(\phi A_{1111} + A_{\tau\tau\tau 1} - \sqrt{\phi}A_{1\tau 1\tau} + \sqrt{\phi}A_{\tau 1\tau\tau} + \frac{1}{\phi}A_{\tau\tau\tau\tau}\right).
\end{aligned}$$

We recognize $\mathcal{P}_1$ as the vacuum particle. Indeed, when we write out this tensor, we find a diagonal tensor with weights depending on the inner MPO label. These weights correspond exactly to the weights that determine the ground state tensors in the MPO framework, denoted by Δ in equation (3.1). More generally, we see in all other examples that we always recover the vacuum particle corresponding to the ground state as it should be.

There are some other general remarks we can already see in this example. The vectors $A_{1\tau\tau\tau}$ and $A_{\tau\tau 1\tau}$ are not present in any of the idempotents. These are exactly the vectors A_{abcd} with a different incoming a and outgoing c label. We do not expect them to be present in the decomposition of a central idempotent, as they correspond exactly to off-diagonal nilpotent matrices that are not in the center of the algebra.

The decomposition of the higher-dimensional central idempotent $\mathcal{P}_4$ in irreducible, but not central, one-dimensional idempotents is very simple. The element $\mathcal{P}_4$ contains both terms with $a, c = 1$ and $a, c = \tau$. The decomposition of $\mathcal{P}_4$ in two one-dimensional idempotents is obtained by grouping all terms with $a, c = 1$ as one idempotent P_4^1 and all terms with $a, c = \tau$ as the second idempotent P_4^τ. This procedure also holds for more general models. All other, one-dimensional, idempotents only contain terms with $a, c = 1$ or $a, c = \tau$. Note that a d-dimensional idempotent projects onto a d^2-dimensional subspace, such that we indeed recover the algebra dimension as $7 = 1^2 + 1^2 + 1^2 + 2^2$. This is required for our set of central idempotents to be complete.

The topological spins we obtain are given by

$$h_1 = 0,\ h_2 = -\frac{4}{5},\ h_3 = \frac{4}{5},\ h_4 = 0.$$

Clearly, we can now make the identification with the well-known anyons from the doubled Fibonacci theory,

$$\mathcal{P}_1 = (1, 1),\ \mathcal{P}_2 = (1, \bar{\tau}),\ \mathcal{P}_3 = (\tau, 1),\ \mathcal{P}_4 = (\tau, \bar{\tau}).$$

We can compare this result with the idempotents obtained in Ref. [170] and see that both solutions have a similar structure. With a slightly different convention of the basis elements A_{abcd}, corresponding to a

normalization that depends on a, b, c, d, we obtain exactly the same multiplication table and idempotents.

3.3.1.3 Braiding in the Fibonacci String-Net

To illustrate the general braiding formalism developed in Section 3.2.6. We focus on the idempotent that describes a $(\tau, 1)$ anyon in the PEPS. We denote this idempotent by $\mathcal{P}_\tau$. If we recall the definition of the tensors A_{abcd}, we can express this idempotent as

$$\mathcal{P}_\tau = \frac{1}{\sqrt{5}} \left(\frac{1}{\phi} A_{\tau\tau\tau 1} + \frac{1}{\sqrt{\phi}} e^{\frac{4\pi i}{5}} A_{\tau 1 \tau\tau} + e^{-\frac{3\pi i}{5}} A_{\tau\tau\tau\tau} \right).$$

Suppose we have two such anyons, then we can determine their possible fusion outcomes. For this we use the fusion procedure explained in Fig. 3.27 in Section 3.2.5. Clearly, the outgoing τ strings of the two anyons can be fused to a 1 or τ string. The 1 string can give rise to a fusion product supported in the subspace corresponding to $\mathcal{P}_1$ or $\mathcal{P}_{\tau\bar{\tau}}$, while the τ string can give rise to a support in all idempotents except $\mathcal{P}_1$. Although it is not easy to determine this analytically, one can readily determine the sectors where the two $\mathcal{P}_\tau$ anyons are supported numerically. These sectors are the $\mathcal{P}_1$ and $\mathcal{P}_\tau$ sector, as we expect from the fusion rules of Fibonacci anyons.

Let us now concentrate on the exchange of two such τ anyons and determine the tensor $\mathcal{R}_{\mathcal{P}_\tau,\tau}$. We first show how one can analytically determine these tensors. This gives insight in the close relation between the idempotents and the $\mathcal{R}$ tensors. The calculation we use to determine the tensor $\mathcal{R}$ resembles the well-known teleportation protocol from quantum information theory. We follow the derivation of Section 3.2.6, which gives us the situation shown in Fig. 3.43. Since $\mathcal{P}_\tau$ is a one-dimensional idempotent, $\mathcal{P}_\tau A_{abcd} = \lambda_{abcd} \mathcal{P}_\tau$ for complex numbers λ_{abcd} that can easily be calculated from the structure constants of the algebra. We find that

$$\lambda_{\tau 1 \tau\tau} = \frac{1}{\sqrt{\phi}} e^{4\pi i/5}, \qquad \lambda_{\tau\tau 1 \tau} = 0, \qquad \lambda_{\tau\tau\tau\tau} = e^{-3\pi i/5}, \tag{3.24}$$

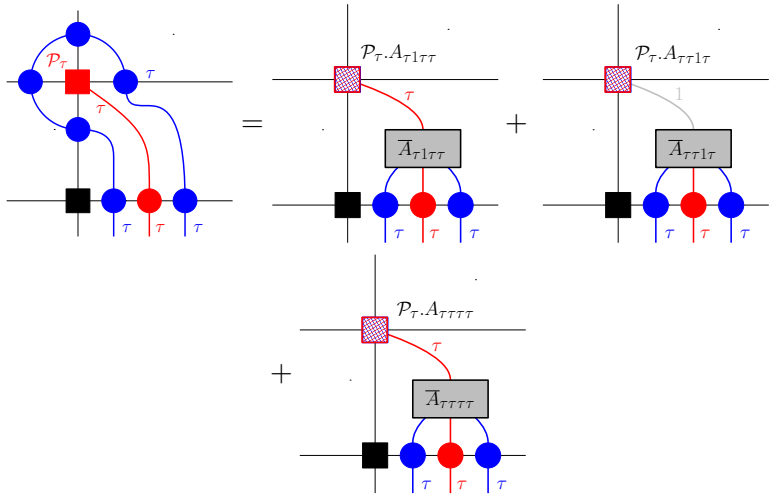

Figure 3.43

such that the equation in Fig. 3.43 is simplified to the expression in Fig. 3.44.

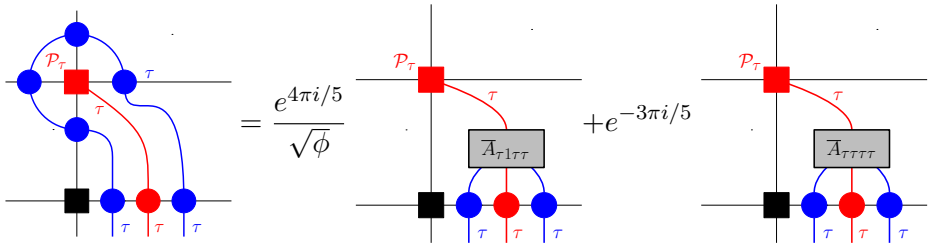

Figure 3.44

We conclude from this calculation that the tensor $\mathcal{R}_{\mathcal{P}_\tau,\tau}$ is given by

$$\mathcal{R}_{\mathcal{P}_\tau,\tau} = \frac{1}{\sqrt{\phi}} e^{4\pi i/5} \bar{A}_{\tau 1 \tau\tau} + e^{-3\pi i/5} \bar{A}_{\tau\tau\tau\tau}.$$

We can now look at the contraction of two such tensors as in Fig. 3.34c, which describes the full braiding of two anyons. This tensor then describes the monodromy matrix of two Fibonacci anyons. It is known that the elements are given by $e^{2\pi i(h_c - h_\tau - h_\tau)}$, where c is the fusion product of the two anyons, $c = 1, \tau$. As the spins of the anyons are $h_1 = 0$ and $h_\tau = 2/5$ we expect the tensor in Fig. 3.34c to contain the phases $e^{-4\pi i/5}$ and $e^{\pi i/5}$ in the respective topological sectors. One can readily check that this is indeed the case.

3.3.2 Ising String-Net

As a second example we look at the string-net obtained from the Ising fusion category. The anyons that appear in this theory are expected to be realized in a fractional quantum hall system at filling factor $\nu = 5/2$ [70, 179, 180].

3.3.2.1 MPO-Tensors

As we saw in the analysis of the Fibonacci model in the previous example, we only need the fusion rules, quantum dimensions and F-symbols to construct the relevant tensors. The Ising category has three labels $1, \sigma, \psi$ with fusion rules

$$N_{11}^{1} = 1, \quad N_{1\sigma}^{\sigma} = 1, \quad N_{1\psi}^{\psi} = 1, \quad N_{\sigma\sigma}^{\psi} = 1,$$

up to the usual allowed permutations of the labels. The only non-trivial fusion rule is $\sigma \times \sigma = 1 + \psi$. The quantum dimensions are given by $d_1 = 1, d_\sigma = \sqrt{2}, d_\psi = 1$.

The F-symbols are again only non-zero, $F_{def}^{abc} \neq 0$, if all appearing fusion processes are allowed, see equation (3.22). The non-trivial elements are given by

$$F_{\sigma 11}^{\sigma\sigma\sigma} = \frac{1}{\sqrt{2}}, \quad F_{\sigma\psi 1}^{\sigma\sigma\sigma} = \frac{1}{\sqrt{2}}, \quad F_{\sigma 1\psi}^{\sigma\sigma\sigma} = \frac{1}{\sqrt{2}},$$
$$F_{\sigma\psi\psi}^{\sigma\sigma\sigma} = -\frac{1}{\sqrt{2}}, \quad F_{\sigma\sigma\sigma}^{\psi\sigma\psi} = -1, \quad F_{\psi\sigma\sigma}^{\sigma\psi\sigma} = -1,$$

other allowed non-zero components are equal to one. Similarly as for the Fibonacci model, we can now construct the G-symbols and from these all necessary tensors, see equations (3.18), (3.19) and (3.20).

3.3.2.2 Central Idempotents

We now have all the tensors required to calculate the central idempotents of the Ising string-net. We expect to find nine anyon types that correspond to the labels of the doubled Ising theory. From the fusion rules we find that there are 12 non-zero basis elements A_{abcd}. The algebra generated by these elements contains the following nine central idempotents,

$$\begin{aligned}
\mathcal{P}_1 &= \frac{1}{4}\left(A_{1111} + 2^{3/4}A_{1\sigma1\sigma} + A_{1\psi1\psi}\right)\\
\mathcal{P}_2 &= \frac{1}{4}\left(A_{\sigma\sigma\sigma1} + 2^{1/4}e^{\frac{\pi i}{8}}A_{\sigma1\sigma\sigma} + 2^{1/4}e^{-\frac{3\pi i}{8}}A_{\sigma\psi\sigma\sigma} + e^{\frac{\pi i}{2}}A_{\sigma\sigma\sigma\psi}\right)\\
\mathcal{P}_3 &= \frac{1}{4}\left(A_{\sigma\sigma\sigma1} + 2^{1/4}e^{-\frac{\pi i}{8}}A_{\sigma1\sigma\sigma} + 2^{1/4}e^{\frac{3\pi i}{8}}A_{\sigma\psi\sigma\sigma} + e^{-\frac{\pi i}{2}}A_{\sigma\sigma\sigma\psi}\right)\\
\mathcal{P}_4 &= \frac{1}{4}\left(A_{\psi\psi\psi1} + 2^{3/4}e^{\frac{\pi i}{2}}A_{\psi\sigma\psi\sigma} - A_{\psi1\psi\psi}\right)\\
\mathcal{P}_5 &= \frac{1}{4}\left(A_{\psi\psi\psi1} + 2^{3/4}e^{\frac{-\pi i}{2}}A_{\psi\sigma\psi\sigma} - A_{\psi1\psi\psi}\right)\\
\mathcal{P}_6 &= \frac{1}{4}\left(A_{\sigma\sigma\sigma1} + 2^{1/4}e^{-\frac{7\pi i}{8}}A_{\sigma1\sigma\sigma} + 2^{1/4}e^{\frac{5\pi i}{8}}A_{\sigma\psi\sigma\sigma} + e^{\frac{\pi i}{2}}A_{\sigma\sigma\sigma\psi}\right)\\
\mathcal{P}_7 &= \frac{1}{4}\left(A_{\sigma\sigma\sigma1} + 2^{1/4}e^{\frac{7\pi i}{8}}A_{\sigma1\sigma\sigma} + 2^{1/4}e^{-\frac{5\pi i}{8}}A_{\sigma\psi\sigma\sigma} + e^{-\frac{\pi i}{2}}A_{\sigma\sigma\sigma\psi}\right)\\
\mathcal{P}_8 &= \frac{1}{4}\left(A_{1111} - 2^{3/4}A_{1\sigma1\sigma} + A_{1\psi1\psi}\right)\\
\mathcal{P}_9 &= \frac{1}{2}\left(A_{1111} + A_{\psi\psi\psi1} - A_{1\psi1\psi} + A_{\psi1\psi\psi}\right).
\end{aligned}$$

The corresponding topological spins are found to be

$$\begin{aligned}
&h_1 = 0, \quad h_2 = \frac{1}{16}, \quad h_3 = -\frac{1}{16}, \quad h_4 = \frac{1}{2}, \quad h_5 = -\frac{1}{2}\\
&h_6 = -\frac{7}{16}, \quad h_7 = \frac{7}{16}, \quad h_8 = 0, \quad h_9 = 0.
\end{aligned}$$

All central idempotents are one-dimensional, except for $\mathcal{P}_9$ which is two-dimensional, such that we indeed obtain $12 = 8 \cdot 1^2 + 2^2$. We can now identify these central idempotents with the anyons in the double Ising model as follows,

$$\begin{aligned}
&\mathcal{P}_1 = (1,1), \qquad \mathcal{P}_2 = (\sigma,1), \qquad \mathcal{P}_3 = (1,\bar{\sigma}),\\
&\mathcal{P}_4 = (\psi,1), \qquad \mathcal{P}_5 = (1,\psi), \qquad \mathcal{P}_6 = (\sigma,\bar{\psi}),\\
&\mathcal{P}_7 = (\psi,\bar{\sigma}), \qquad \mathcal{P}_8 = (\psi,\bar{\psi}), \qquad \mathcal{P}_9 = (\sigma,\bar{\sigma}).
\end{aligned}$$

3.3.3 Rep(S_3) String-Net

As a final example we consider the string-net with input fusion category the representation theory of S_3. As this last category is not modular, the anyons of the string-net are not just doubled versions of the labels of the input data.

3.3.3.1 MPO-Tensors

Again, we need to specify the categorical data of the input category and can construct the tensors of the Rep(S_3) string-net from these. The Rep(S_3) fusion category has three labels $1, 2, 3$ with the following fusion rules,

$$N_{11}^1 = 1, N_{12}^2 = 1, N_{13}^3 = 1, N_{33}^2 = 1, N_{33}^3 = 1,$$

up to the allowed permutations of the labels. The non-trivial fusion rule is $3 \times 3 = 1 + 2 + 3$. The quantum dimensions of the labels are $d_1 = 1, d_2 = 1, d_3 = 2$.

As always, the F-symbols are non-zero, $F_{def}^{abc} \neq 0$, if all appearing fusion processes are allowed as in equation (3.22). The non-trivial elements are given by

$$\begin{aligned}
&F_{333}^{323} = -1, \quad F_{333}^{332} = -1, \quad F_{333}^{233} = -1, \quad F_{233}^{333} = -1,\\
&F_{311}^{333} = \frac{1}{2}, \quad F_{312}^{333} = \frac{1}{2}, \quad F_{313}^{333} = \frac{1}{\sqrt{2}}, \quad F_{321}^{333} = \frac{1}{2}, \quad F_{322}^{333} = \frac{1}{2},\\
&F_{323}^{333} = -\frac{1}{\sqrt{2}}, \quad F_{331}^{333} = \frac{1}{\sqrt{2}}, \quad F_{332}^{333} = -\frac{1}{\sqrt{2}}, \quad F_{333}^{333} = 0\,,
\end{aligned}$$

other allowed coefficients are 1. Similarly as for the Fibonacci model, we can now construct the G-symbols and from these all necessary tensors, see equations (3.18),(3.19) and (3.20).

3.3.3.2 Central Idempotents

The algebra for the given fusion rules is 17-dimensional. We find eight different central idempotents,

$$\begin{aligned}
\mathcal{P}_1 &= \frac{1}{6}A_{3331} - \frac{1}{6}A_{3332} + \frac{1}{3\sqrt{2}}e^{-2\pi i/3}A_{3133} \\
&\quad + \frac{1}{3\sqrt{2}}e^{\pi i/3}A_{3233} + \frac{1}{3}e^{2\pi i/3}A_{3333} \\
\mathcal{P}_2 &= \frac{1}{6}A_{2221} + \frac{1}{6}A_{2122} - \frac{\sqrt{2}}{3}A_{2323} \\
\mathcal{P}_3 &= \frac{1}{2}A_{2221} + \frac{1}{4}A_{3331} - \frac{1}{2}A_{2122} \\
&\quad + \frac{1}{4}A_{3332} - \frac{1}{2\sqrt{2}}A_{3133} - \frac{1}{2\sqrt{2}}A_{3233} \\
\mathcal{P}_4 &= \frac{1}{6}A_{3331} - \frac{1}{6}A_{3332} + \frac{1}{3\sqrt{2}}e^{2\pi i/3}A_{3133} \\
&\quad + \frac{1}{3\sqrt{2}}e^{-\pi i/3}A_{3233} + \frac{1}{3}e^{-2\pi i/3}A_{3333} \\
\mathcal{P}_5 &= \frac{1}{6}A_{3331} - \frac{1}{6}A_{3332} + \frac{1}{3\sqrt{2}}A_{3133} \\
&\quad - \frac{1}{3\sqrt{2}}A_{3233} + \frac{1}{3}A_{3333} \\
\mathcal{P}_6 &= \frac{1}{3}A_{1111} + \frac{1}{3}A_{2221} + \frac{1}{3}A_{1212} \\
&= +\frac{1}{3}A_{2122} - \frac{\sqrt{2}}{3}A_{1313} + \frac{\sqrt{2}}{3}A_{2323} \\
\mathcal{P}_7 &= \frac{1}{2}A_{1111} + \frac{1}{4}A_{3331} - \frac{1}{2}A_{1212} \\
&\quad + \frac{1}{4}A_{3332} + \frac{1}{2\sqrt{2}}A_{3133} + \frac{1}{2\sqrt{2}}A_{3233} \\
\mathcal{P}_8 &= \frac{1}{6}A_{1111} + \frac{1}{6}A_{1212} + \frac{\sqrt{2}}{3}A_{1313}.
\end{aligned}$$

The idempotents $\mathcal{P}_3, \mathcal{P}_6, \mathcal{P}_7$ are two-dimensional and all other central idempotents have dimension one. We again check the consistency con-

dition $17 = 1 + 1 + 1 + 1 + 1 + 2^2 + 2^2 + 2^2$, which ensures our set of central idempotents is complete.

The only non-zero topological spins are given by

$$h_1 = -\frac{1}{3}, \qquad h_3 = \frac{1}{2}, \qquad h_4 = \frac{1}{3}.$$

As explained in Section 3.2.5 we can compute the fusion rules of the anyons corresponding to the eight central idempotents. We numerically find the following fusion table.

	$\mathcal{P}_1$	$\mathcal{P}_2$	$\mathcal{P}_3$	$\mathcal{P}_4$	$\mathcal{P}_5$	$\mathcal{P}_6$	$\mathcal{P}_7$	$\mathcal{P}_8$
$\mathcal{P}_1$	$\mathcal{P}_1, \mathcal{P}_2, \mathcal{P}_8$	$\mathcal{P}_1$	$\mathcal{P}_3, \mathcal{P}_7$	$\mathcal{P}_5, \mathcal{P}_6$	$\mathcal{P}_4, \mathcal{P}_6$	$\mathcal{P}_4, \mathcal{P}_5$	$\mathcal{P}_3, \mathcal{P}_7$	$\mathcal{P}_1$
$\mathcal{P}_2$	$\mathcal{P}_1$	$\mathcal{P}_8$	$\mathcal{P}_7$	$\mathcal{P}_4$	$\mathcal{P}_5$	$\mathcal{P}_6$	$\mathcal{P}_3$	$\mathcal{P}_2$
$\mathcal{P}_3$	$\mathcal{P}_3, \mathcal{P}_7$	$\mathcal{P}_7$	$\mathcal{P}_1, \mathcal{P}_4, \mathcal{P}_5$ $\mathcal{P}_6, \mathcal{P}_8$	$\mathcal{P}_3, \mathcal{P}_7$	$\mathcal{P}_3, \mathcal{P}_7$	$\mathcal{P}_3, \mathcal{P}_7$	$\mathcal{P}_2, \mathcal{P}_3, \mathcal{P}_4$ $\mathcal{P}_5, \mathcal{P}_6$	$\mathcal{P}_3$
$\mathcal{P}_4$	$\mathcal{P}_5, \mathcal{P}_6$	$\mathcal{P}_4$	$\mathcal{P}_3, \mathcal{P}_7$	$\mathcal{P}_2, \mathcal{P}_4, \mathcal{P}_8$	$\mathcal{P}_1, \mathcal{P}_6$	$\mathcal{P}_1, \mathcal{P}_5$	$\mathcal{P}_3, \mathcal{P}_7$	$\mathcal{P}_4$
$\mathcal{P}_5$	$\mathcal{P}_4, \mathcal{P}_6$	$\mathcal{P}_5$	$\mathcal{P}_3, \mathcal{P}_7$	$\mathcal{P}_1, \mathcal{P}_6$	$\mathcal{P}_2, \mathcal{P}_5, \mathcal{P}_8$	$\mathcal{P}_1, \mathcal{P}_4$	$\mathcal{P}_3, \mathcal{P}_7$	$\mathcal{P}_5$
$\mathcal{P}_6$	$\mathcal{P}_4, \mathcal{P}_5$	$\mathcal{P}_6$	$\mathcal{P}_3, \mathcal{P}_7$	$\mathcal{P}_1, \mathcal{P}_5$	$\mathcal{P}_1, \mathcal{P}_4$	$\mathcal{P}_2, \mathcal{P}_6, \mathcal{P}_8$	$\mathcal{P}_3, \mathcal{P}_7$	$\mathcal{P}_6$
$\mathcal{P}_7$	$\mathcal{P}_3, \mathcal{P}_7$	$\mathcal{P}_3$	$\mathcal{P}_2, \mathcal{P}_3, \mathcal{P}_4$ $\mathcal{P}_5, \mathcal{P}_6$	$\mathcal{P}_3, \mathcal{P}_7$	$\mathcal{P}_3, \mathcal{P}_7$	$\mathcal{P}_3, \mathcal{P}_7$	$\mathcal{P}_1, \mathcal{P}_4, \mathcal{P}_5$ $\mathcal{P}_6, \mathcal{P}_8$	$\mathcal{P}_7$
$\mathcal{P}_8$	$\mathcal{P}_1$	$\mathcal{P}_2$	$\mathcal{P}_3$	$\mathcal{P}_4$	$\mathcal{P}_5$	$\mathcal{P}_6$	$\mathcal{P}_7$	$\mathcal{P}_8$

The S-matrix can be calculated as explained in Section 3.2.3. We find that

$$S = \frac{1}{6}\begin{pmatrix} 1 & 3 & 2 & 1 & 2 & 3 & 2 & 2 \\ 3 & 3 & 0 & -3 & 0 & -3 & 0 & 0 \\ 2 & 0 & 4 & 2 & -2 & 0 & -2 & -2 \\ 1 & -3 & 2 & 1 & 2 & -3 & 2 & 2 \\ 2 & 0 & -2 & 2 & -2 & 0 & -2 & 4 \\ 3 & -3 & 0 & -3 & 0 & 3 & 0 & 0 \\ 2 & 0 & -2 & 2 & -2 & 0 & 4 & -2 \\ 2 & 0 & -2 & 2 & 4 & 0 & -2 & -2 \end{pmatrix}.$$

These results agree with the theoretical findings in the literature, see for instance Ref. [181]. Finally, we note that a model with the same topological properties and anyons can be constructed from the group S_3 instead of Rep(S_3). The MPO representation is of course different, as are the idempotents, but we obtain similar results for the topological properties of the eight idempotents. This was done analytically for all finite groups in Ref. [24].

3.4 An Algorithm for Central Idempotents

In this section we present a simple and constructive algorithm to calculate the decomposition of an algebra $\mathcal{A}$ over $\mathbb{C}$ in primitive central idempotents. The constructive approach to the Artin-Wedderburn theorem is well-known in the literature [177] and can be generalized to algebras over different base fields. We assume that the Jacobson radical of $\mathcal{A}$ is trivial, one can check this for instance by computing the kernel of a proper matrix, see Ref. [177] for more details.

The input of the algorithm are the structure constants d_{ij}^k of the algebra $\mathcal{A}$ with respect to a vector space basis $\{b^1, \ldots, b^r\}$. We thus have $b^i b^j = \sum_{k=1}^r d_{ij}^k b^k$. The output of the algorithm are the coefficients in this basis of the minimal central idempotents. These are the elements $p \in \mathcal{A}$ such that $p \neq 0, p \times p = p$, p commutes with every element in $\mathcal{A}$ and p cannot be written as $p = p_1 + p_2$ where p_1, p_2 also satisfy the previous requirements. Finding the minimal central idempotents is equivalent to determining the block decomposition of a matrix algebra.

We denote the column vector of coefficients of an element x with respect to the aforementioned basis as $\boldsymbol{x}$ and refer to its elements as $\boldsymbol{x}_j$. We first calculate the center $Z(\mathcal{A})$ of $\mathcal{A}$. Let $x = \sum_{j=1}^r \boldsymbol{x}_j b^j$. It holds that $x \in Z(\mathcal{A})$ if and only if $b^i x = x b^i$ for all i. It is easy to see that this is equivalent to $\sum_{j=1}^r (d_{ij}^k - d_{ji}^k)\boldsymbol{x}_j = 0$ for all k, i. We conclude that $x \in Z(\mathcal{A})$ if and only if $\boldsymbol{x} \in \mathrm{Kern}(Z)$ with $Z_{(i-1)r+k,j} = d_{ij}^k - d_{ji}^k$.

Let $\{z^1, \ldots z^c\}$ be a basis of $\mathrm{Kern}(Z)$. We can easily obtain the structure constants f_{ij}^k with respect to this basis by solving the linear system

$$\sum_k f_{ij}^k \boldsymbol{z^k} = \boldsymbol{z^i z^j}$$

for all i, j.

We now forget the algebra $\mathcal{A}$ and only work in the commutative algebra $\mathcal{C} = Z(\mathcal{A})$. From now on, we denote by $\boldsymbol{z}$ the column vector of coefficients of an element $z \in \mathcal{C}$ with respect to the basis $\{z^1, \ldots z^c\}$.

Given an element z, recall that the ideal generated by z is defined by $\langle z \rangle = \mathrm{span}\{xz \mid x \in \mathcal{C}\}$. If we take a random element $z \in \mathcal{C}$, we expect

that $\langle z \rangle = \mathcal{C}$. Let us now show how to decompose an ideal as $\langle z \rangle = \langle z_1 \rangle \oplus \langle z_2 \rangle$.

First, we find a basis of the space $\langle z \rangle$. This is easily done by computing a basis of the column space of the matrix $\left[\boldsymbol{z}\boldsymbol{z}^{\mathbf{1}} \dots \boldsymbol{z}\boldsymbol{z}^{\boldsymbol{c}}\right]$. Let $\{y^1, \dots, y^d\}$ be a basis of $\langle z \rangle$. Second, we compute the identity I_z of the ideal, this is the unique element with $I_z y^i = y^i$ for all i. After a straightforward calculation we obtain that the coefficients $\boldsymbol{I_z}$ of the identity I_z with respect to the basis $\{y^1, \dots, y^d\}$ are given by the solution of the linear system

$$\sum_{j=1}^{d} \left(\sum_{l=1}^{c} \sum_{m=1}^{c} \boldsymbol{y^j}_l \boldsymbol{y^k}_m f^p_{lm} \right) \boldsymbol{I_z}_j = \boldsymbol{y^k}_p$$

for all p.

We can now decompose the ideal $\langle z \rangle$. The minimal polynomial P with $P(z) = 0$ can be calculated as follows. Find the smallest q such that the matrix $[\boldsymbol{z^q} \dots \boldsymbol{z}\ \boldsymbol{I_z}]$ is rank deficient. Note that here, $\boldsymbol{z^q}$ denotes the q-th power of z. The zero vector of this matrix gives the coefficients of P. Let $n_1, \dots, n_q$ be the complex roots of P, hence $P(x) = \prod_{i=1}^{q}(x - n_i)$. If $q = 1$, the ideal $\langle z \rangle$ is one dimensional. This implies that $z^2 = \lambda z$, hence z/λ is an idempotent. If $q > 1$ we decompose $P(x) = P_1(x)P_2(x)$ such that P_1, P_2 have no common roots.

We claim that $R(z) = \langle P_1(z) \rangle \oplus \langle P_2(z) \rangle$ is the sought after decomposition of $\langle z \rangle$. First, we show that the equality holds in $\langle z \rangle = R(z)$. Clearly the inclusion $\supseteq$ holds. We now show the reverse inclusion. Since P_1 and P_2 are polynomials over $\mathbb{C}$ and have no common roots, they are coprime. Bézout's identity ensures the existence of two polynomials Q_1, Q_2 such that $1 = Q_1 P_1 + Q_2 P_2$. Evaluating both sides in z gives that $I_z \in R(z)$. Since $R(z)$ is an ideal, $xI_z \in R(z)$ for all x, by which we can conclude that $\langle z \rangle \subseteq R(z)$. It is worth noting that $Q_1(z)P_1(z)$ is the identity of $\langle P_1(z) \rangle$, hence the calculation of the identity only needs to be performed once at the start of the algorithm.

Second, we show that $\langle P_1(z) \rangle$ and $\langle P_1(z) \rangle$ are orthogonal spaces. Take $w_1 P_1(z) \in \langle P_1(z) \rangle$ and $w_2 P_2(z) \in \langle P_2(z) \rangle$, then the equality

$$w_1 P_1(z) w_2 P_2(z) = 0 \tag{3.25}$$

holds since $\mathcal{C}$ is commutative and $P(z) = P_1(z)P_2(z) = 0$. This implies that the sum is direct and that $\langle z\rangle = \langle P_1(z)\rangle \oplus \langle P_2(z)\rangle$. Since $\mathcal{C}$ is finite, we can apply this decomposition recursively and after a finite number of steps we find the primitive idempotents of $\mathcal{C}$, from which we can easily obtain those of $\mathcal{A}$.

3.5 Topological Quantum Computation in PEPS

The description of anyons on the virtual level of an MPO-injective PEPS gives us a possible interpretation of the phenomenon of topological quantum computation. On the virtual level, the effect of a physical topological action such as braiding translates to a standard unitary circuit. This interpretation can clarify the concepts of topological quantum computation by bringing them into the realm of standard quantum computation theory. We hope it can provide insights and lead to possible breakthroughs such as the description of physical errors in terms of which anyons are excited and threshold bounds for error correction in the computations.

3.5.1 Topological Quantum Computation

We first briefly review the topic of topological quantum computation [79, 182–184].

3.5.1.1 Topological Hilbert Space

We consider a theory with non-Abelian anyons, more specifically let us take a state with exactly n anyons of type a and let a be its own dual. For simplicity we assume that the total topological charge of all the anyons together is topologically trivial. This assumption corresponds to the physically relevant scenario where we created $\frac{n}{2}$ pairs of (a, a) particles out of the vacuum. The Hilbert space wherein the topological quantum computation takes place is rather abstract and given by the possible fusion processes of all the n anyons to the vacuum.

Take now n such anyons and arrange them along a line. We can now fuse anyons a_1 and a_2 which gives us the result b_1, which we fuse with a_3. The result of this fusion, b_2, can be fused again with a_4 and so on. The Hilbert space is than given by the direct sum over all possible fusion processes, in the case of non-Abelian anyons there are indeed several possibilities. We denote the Hilbert space as follows,

$$V^1_{a_1,\ldots,a_n} = \bigoplus_{\mathbf{b}} V^{b_1}_{a_1 a_2} \otimes V^{b_2}_{b_1 a_3} \otimes \ldots \otimes V^1_{b_{n-2} a_n}.$$

Here the V^c_{ab} spaces denote the local degrees of freedom for a given fusion process, denoted by μ in the figures. A natural basis for this Hilbert space is given by labeling the elements b_i and fusion degrees of freedom μ,

$$\{|a_1 a_2, b_1, \mu_1\rangle\, |b_1 a_3, b_2, \mu_2\rangle \ldots |b_{n-2} a_n, 1, \mu_{n-1}\rangle \mid \mathbf{b}, \boldsymbol{\mu}\}.$$

These states or graphically depicted in Fig. 3.45. Note that the ordering of the anyons and the order of fusing them is completely arbitrary and an alternative choice gives a different but equivalent description.

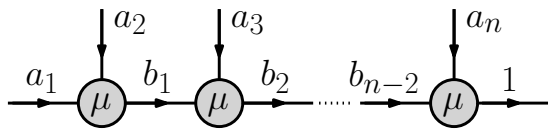

Figure 3.45: Graphical notation of the basis states of the topological Hilbert space.

3.5.1.2 Braiding in the Standard Basis

The elementary gates we can perform topologically are the exchanges of two of the particles a. We focus on the exchange of two neighboring anyons a_i, a_{i+1}. If the outcome of the fusion of these particles is known, let us call it c, this process is described by the matrix $R^c_{a_i a_{i+1}}$ introduced in Section I.2.3.2.2.

To describe the effect of such an exchange in the standard basis, shown in Fig. 3.46, is not as straightforward as the fusion outcome of such anyons a_i, a_{i+1} is not specified. We proceed as follows. By applying

first an F-move we are in the standard situation described by $R^c_{a_i a_{i+1}}$. Finally, we use an inverse F-move to bring us back to the standard basis. This process is described in Fig. 3.47.

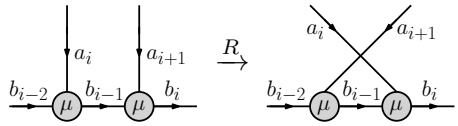

Figure 3.46: The effect of braiding two anyons a_i, a_{i+1}. The operator that implements this operation in the standard basis is denoted by B.

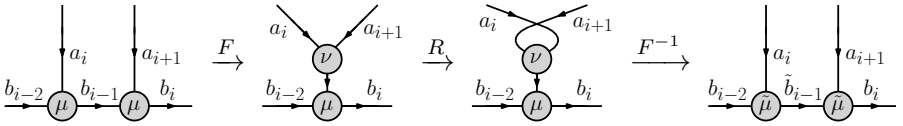

Figure 3.47: To obtain B in the standard basis, we use a combination of an F-move, R-move and the inverse F-move.

The operation shown in Fig. 3.47 is sometimes called the braid matrix. As this allows for possible confusion with the R-matrix, we refrain from the usage of this terminology and instead use the term B-matrix. As expected, the action of an exchange on the topological Hilbert space is determined by the F-matrix and the R-matrix.

3.5.1.3 Computation

Topological quantum computation is now performed as follows. We first create a bunch of particle-antiparticle pairs from the vacuum. We then guide these particles along specific trajectories. This gives us an element of the braid group that can be fully described by the exchange of neighboring anyons. Hence, in the standard basis the entire computation boils down to the application of the B-matrices. Finally, to get the result of the computation, we fuse pairs of particle-antiparticle. Importantly, we keep track of which pairs can still fuse to the vacuum as this is the

output of the computation. The information of all these fusion processes corresponds to a certain state in the topological Hilbert space.

3.5.1.4 Motivation

One can wonder why we consider such a contrived model of quantum computation. The reason is as follows. As we mentioned, the logical gates in the model are performed by braiding the anyons. Such an operation can only have a non-trivial effect on the fusion spaces. Indeed, neither the type of the anyon nor its local degrees of freedom can be affected as these can be measured locally while the braiding can be performed arbitrary far away.

Conversely, the information that we encoded in the fusion spaces is not accessible by local operations as it is a property of a pair. To change fusion properties of a pair of anyons we need to act in an extended region, for instance by braiding other anyons around an anyon of the pair. We see that the interactions with the environment cannot change the information we encode, as long as the environment couples in a local way to the system. This is the fundamental fault-tolerant property that makes topological quantum computation an attractive alternative to more standard methods that suffer from decoherence due to interactions with the environment.

This fault-tolerance is tightly connected with the stability of topologically ordered Hamiltonians [51, 56]. Indeed, we know that local, small enough perturbations do not change the topological properties of the system, which implies that decoherence is indeed avoided. However, it is also notoriously difficult to protect topologically ordered systems from thermal fluctuations [96, 97, 185, 186] and it is a problem of great interest to construct models in two or three spatial dimensions that keep their topological properties at finite temperature and are thus intrinsically protected from thermal noise [139, 187, 188].

3.5.1.5 Example: Fibonacci Anyons

We now briefly illustrate the previous concepts using Fibonacci anyons τ that obey $\tau \times \tau = 1 + \tau$. If we place n such anyons on a line, it is clear that the number of possible fusion processes scales as ϕ^n with $\phi = \frac{1+\sqrt{5}}{2}$ the golden ratio. This already shows that the topological Hilbert space cannot be described by a tensor product of local spaces.

To encode one qubit, we need a non-trivial fusion space, which two anyons do not have as they have one possible way to fuse either to 1 or to τ. It is convenient to use four τ anyons to encode one qubit of information. If we create two pairs out of the vacuum, we can bring together one τ anyon from the first pair and one from the second pair. These two anyons can be fused and have possible outcomes 1 or τ which encodes exactly one qubit of information. This situation is shown in Fig. 3.48.

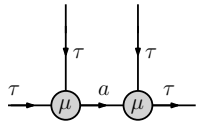

Figure 3.48: To pairs of τ anyons encode one logical qubit a. The τ anyons are labeled from left to right.

Exchanging the τ anyons gives us two different types of operations in the standard basis. If we exchange τ_1 and τ_2 or τ_3 and τ_4, who belong to the same pair, the operation is described in the standard basis by just the R-matrix. The reason is that, this operation, denoted by O_1 is diagonal in the logical basis. If we however exchange τ_2 and τ_3 we need to apply the procedure that gives the B-matrix, we denote this operation by O_2. This gives us two different operators that act on the the logical space,

$$O_1 = \begin{bmatrix} e^{4\pi i/5} & 0 \\ 0 & e^{-3\pi i/5} \end{bmatrix}, \quad O_2 = \begin{bmatrix} \phi^{-1}e^{-4\pi i/5} & -\phi^{-1/2}e^{-2\pi i/5} \\ -\phi^{-1/2}e^{-2\pi i/5} & -\phi^{-1} \end{bmatrix}.$$

It can be shown that they are dense in $\mathrm{SU}(2)$ hence we can perform any arbitrary gate up to any precision with just these two operators. We can easily measure the outcome of a computation, the logical qubit a, by fusing τ_1 and τ_2.

We can also consider the more general scenario of an arbitrary number of n anyons as shown in Fig. 3.49. There are five possible states for the anyons a, b, c, given by

$$\{|1\tau 1\rangle, |\tau\tau 1\rangle, |1\tau\tau\rangle, |\tau 1\tau\rangle, |\tau\tau\tau\rangle\}.$$

In that case, the operation we can perform is exchanging the two τ anyons, which gives the following action on the considered basis,

$$O = \begin{bmatrix} e^{4\pi i/5} & 0 & 0 & 0 & 0 \\ 0 & e^{-3\pi i/5} & 0 & 0 & 0 \\ 0 & 0 & e^{-3\pi i/5} & 0 & 0 \\ 0 & 0 & 0 & \phi^{-1}e^{-4\pi i/5} & -\phi^{-1/2}e^{-2\pi i/5} \\ 0 & 0 & 0 & -\phi^{-1/2}e^{-2\pi i/5} & -\phi^{-1} \end{bmatrix}.$$

If we take $a = c = \tau$ we obtain the last 2×2 block of this matrix which is indeed nothing but O_2. The upper diagonal part of the operator O corresponds to O_1.

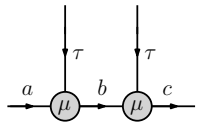

Figure 3.49: A more general scenario, the shown configuration is part of a bigger system.

Similarly, we can use eight τ anyons, this allows for operations that form a dense subset of SU(13). We can thus also easily implement two qubits and perform all operations in SU$(4) \subset$ SU(13). More generally we can encode any number of logical qubits N by using $n = 4N$ physical τ anyons. This confirms the claim that the Fibonacci model allows for universal quantum computation [189].

3.5.2 Topological Quantum Computation in PEPS

We now describe the fundamental concepts of topological quantum computation in the framework of MPO-injective PEPS. We focus on the Fibonacci model and redo the example of the previous section. Let us thus first focus on a situation where we have two pairs of τ anyons who

are pairwise in the topologically trivial sector. As mentioned before, the non-trivial operation we wish to perform is exchanging two anyons, one of each pair. The situation before exchange is shown in Fig. 3.50a and after in Fig. 3.50b. We colored the tensor $\mathcal{R}_{\mathcal{P}_\tau,\tau}$ red to make the figures more clear.

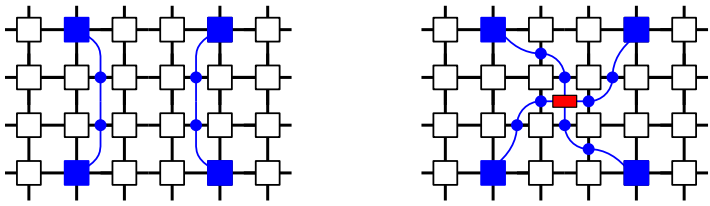

(a) Two pairs of anyons before braiding. **(b)** Two pairs of anyons after braiding.

Figure 3.50

The small middle tensor in this last figure that connects all the MPOs is $\mathcal{R}_{\mathcal{P}_\tau,\tau}$, which was calculated in Section 3.3.1.3. This is the central object to understand the exchange processes. We focus on the detailed properties of this object to relate it to the operators O, O_1 and O_2 from the previous section. A detailed close up of $\mathcal{R}_{\mathcal{P}_\tau,\tau}$ is shown in Fig. 3.51.

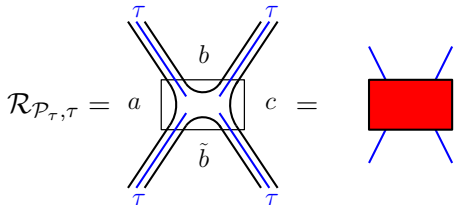

Figure 3.51: Graphical notation of the exchange operator. We use a red box in some pictures for clarification.

Recall from Section 3.3 that the tensors have a triple line structure. The middle, blue line is always fixed to the τ label in this situation as we only consider τ anyons. From the Fibonacci fusion rules, which are reflected in the non-zero elements of the tensor $\mathcal{R}_{\mathcal{P}_\tau,\tau}$, we see that there are five non-zero possibilities for $|a, b, c\rangle$ and $|a, \tilde{b}, c\rangle$. These are

$$\{|1\tau 1\rangle, |\tau\tau 1\rangle, |1\tau\tau\rangle, |\tau 1\tau\rangle, |\tau\tau\tau\rangle\}.$$

We can now consider this tensor as an operator acting from the top indices to the bottom indices. It is clearly diagonal in the a, c index. In this basis, the operator is unitary and given by

$$\mathcal{R}_{\mathcal{P}_\tau,\tau} = \begin{bmatrix} e^{4\pi i/5} & 0 & 0 & 0 & 0 \\ 0 & e^{-3\pi i/5} & 0 & 0 & 0 \\ 0 & 0 & e^{-3\pi i/5} & 0 & 0 \\ 0 & 0 & 0 & \phi^{-1}e^{-4\pi i/5} & -\phi^{-1/2}e^{-2\pi i/5} \\ 0 & 0 & 0 & -\phi^{-1/2}e^{-2\pi i/5} & -\phi^{-1} \end{bmatrix}.$$

This is exactly the same operator as the operator O we discussed in the previous section. If the fusion channel is specified, with the use of the tensor in Fig. 3.55, this operator becomes diagonal with the corresponding phases in the 1 and τ sectors.

We now describe how topological quantum computation is implemented on the virtual level of the PEPS and will see that it is remarkably similar to a standard quantum circuit description. That PEPS can be used to describe quantum computation processes was appreciated since their very introduction [190]. The virtual qubits are represented by black lines, as in Fig. 3.51 and the circuit to be read from top to bottom, such that $\mathcal{R}_{\mathcal{P}_\tau,\tau}$ is seen as a unitary gate from the upper to lower indices. For the initialization we draw the circuit horizontally instead of vertically in Fig. 3.52a for reasons of presentation.

The first part of the computation is the initialization of a state. Let us create two pairs of anyons out of the vacuum. If we just consider the tensor network as in Fig. 3.50, the information that the two left anyons and two right anyons are in the vacuum is contained in the endpoints of MPOs. This will correspond in our circuit to the end of the circuit. Clearly, the information of the initialization should be present in the beginning of the circuit. We can use the zipper condition Eq.(3.11) to redraw the network such that this is the case. This is shown in Fig. 3.52a where we denote the fusion tensors by orange triangles. Blue and gray lines denote MPOs of type O_τ and O_1 respectively. Let us denote the anyons in Fig. 3.52a from top to bottom. First, we fuse the string of the top two anyons, which gives an O_1 MPO as this pair was created from the vacuum. We then fuse in the MPO string of the third anyon,

which gives an O_τ string an finally fuse this with the string of the last anyons. As all anyons are in the vacuum, this last result is again an O_1 MPO. We can then do the inverse network and split the strings again. The rightmost part of the network will be the initialization of the virtual qubits.

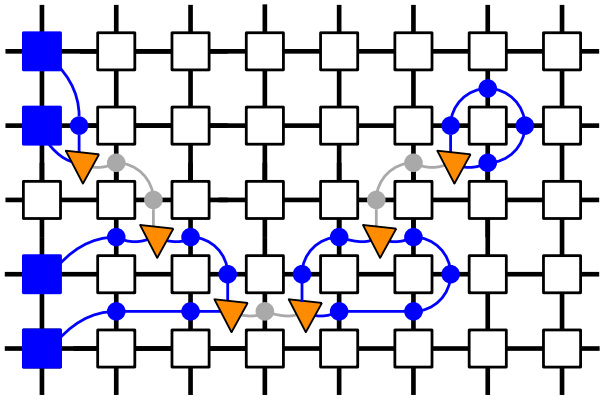

(a) Initialization of the PEPS network such that the information is present at the start of the circuit.

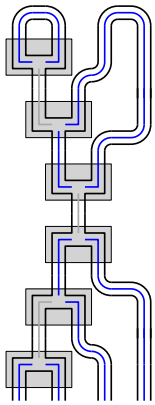

(b) The virtual qubits after the initialization.

Figure 3.52

We show the initialization of the circuit in a zoomed in, but simplified form in Fig. 3.52b. This network is rotated, its top corresponds to the right hand side of the network in Fig. 3.52a. The virtual qubits of the circuit correspond to the black lines that are open at the bottom of the network. It is clear that not all states on the virtual qubits can be created in the initialization process. First, all the virtual qubits, represented by black lines, are part of a an entangled pair with one of the neighboring qubits, and can in fact be regarded as one degree of freedom. Second all qubits need to be able to fuse to the blue τ label if there is one in between them. Thus, a general black line is in an entangled pair with one of its neighbors and constraint by fusion rules with its other neighbor. This places stringent conditions on the states that are allowed and the resulting space is clearly not a tensor product Hilbert space. The possible states form exactly the topological Hilbert space.

The next step in the computation is the application of unitary gates.

Physically, these are performed by exchanging neighboring anyons. In the virtual space, such action corresponds to the introduction of an $\mathcal{R}_{\mathcal{P}_\tau,\tau}$ gate on the virtual qubits. We now consider as an example a scenario with four different anyon pairs and several exchange operations. In the simplified graphical PEPS notation this scenario is shown in Fig. 3.53. This is now to be read as a circuit from top to bottom, but before we go into details we give a more convenient graphical representation of the same process, just as we did with the initialization. In the PEPS, the result of different braidings can all be put together on the same plaquette because of the pulling through condition. We then get a standard unitary circuit on the logical qubits, the black lines, as shown in Fig. 3.54, the blue lines are always fixed to the τ label. If we do not do this, but have the braiding tensors scattered throughout the network, this interpretation is less straightforward as the qubits are then transported by the PEPS network, which is not the identity.

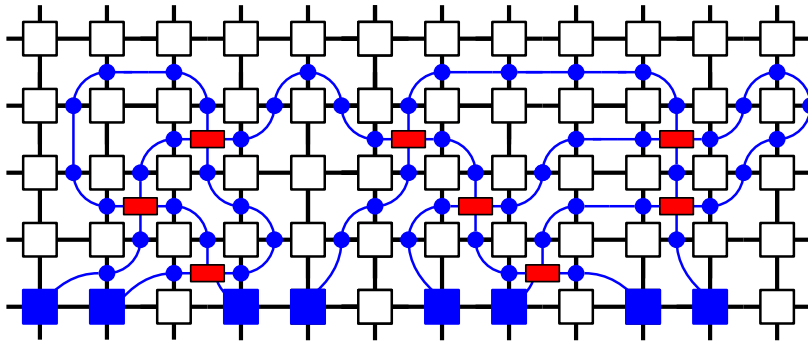

Figure 3.53: A PEPS network that contains four pairs of τ anyons, initially in the vacuum sector. Shown is the resulting state after eight exchange operations.

In Fig. 3.54 we now see the resulting circuit. Note that we did not explicitly used the initialization in Fig. 3.52b, due to space limitations. The top of the network is thus given by an entangled and constrained state on 16 qubits but represented more simply than in Fig. 3.52b. Next, we can exchange all neighboring anyon pairs an arbitrary amount of times. Every exchange gives us a unitary gate $\mathcal{R}_{\mathcal{P}_\tau,\tau}$, the ones that are performed first are higher in the circuit. Given as input a state on the qubits that satisfies all the topological constraints mentioned in

the previous discussion, the computation itself proceeds via a standard circuit of local unitary gates that commute with the constraints. Hence, all intermediate states during the application of the gates also satisfy the constraints. There is no need to impose these constraints during the computation and the quantum gates act indeed in the topological Hilbert space as they should.

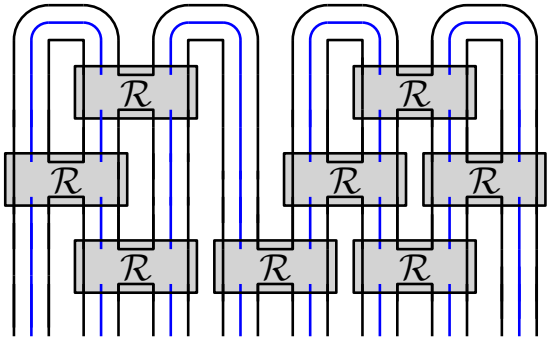

Figure 3.54: The unitary circuit on the virtual level. First, we have the initialization of four anyon pairs, we then proceed by exchanging several anyons, which gives the gates. The outcome is to be read by a measurement of the topological sectors of the pairs of excitations.

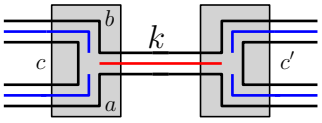

Figure 3.55: Using the fusion tensor in Eq. (3.20) we can construct the above tensor. The middle k label (red) determines whether two τ anyons fuse to 1 or τ.

Finally, the last step of the computation is a measurement to get the result. This is still to be determined by a physical measurement of the topological charge of the anyon pairs. On the virtual level, such measurement can again be performed by the fusion tensors as shown in Fig.3.55. These tensors can also be used to initialize the circuit in a different state as the one discussed. However, it is important to realize that in general both the initialization and measurement are implemented by the idempotents of the theory. These not only act on the virtual qubits, i.e. the MPO strings, but also on the endpoints, where the particles live. The reason that this is possible for the Fibonacci model, if only τ anyons

are present, is that the identification of a 1 or τ sector can be done using only the MPO label. In this case, the initialization and measurement can be performed by acting exclusively on the virtual qubits. This is no longer true in general, because the full idempotents have to be used, both for a general initialization and final measurement. Unfortunately, this makes the entire discussion less clear for general models.

3.6 Dispersion Relation of Non-Abelian Anyons

In this section we develop methods to probe the excitation spectrum of interacting topological phases of matter in two spatial dimensions. Applying these to the Fibonacci string-nets perturbed away from exact solvability, we analyze a topological phase transition driven by the condensation of non-Abelian anyons. Our numerical results illustrate how such phase transitions involve the spontaneous breaking of a topological symmetry, generalizing the traditional Landau paradigm. The topological phase transition manifests itself by symmetry breaking in the entanglement degrees of freedom of the quantum transfer matrix.

Many, or perhaps all, two-dimensional bosonic non-chiral topological phases of matter are characterized by the string-net models [176], whose Hamiltonians are constructed to be exactly diagonalizable. It has been proved that the topological order survives perturbing string-nets into models with non-trivial dispersion relations [51, 56]. However, since the interesting physics requires strong correlations, its analysis away from exactly solvable points is difficult for obvious reasons.

The goal of this section is to develop new methods to study such models, focusing on the doubled Fibonacci phase. We provide strong evidence that the simpler Hamiltonian proposed in Ref. [191] does indeed belong to this phase, going beyond the exact diagonalization results of Ref. [192] to find the anyonic excitations and their dispersion relations. Our analysis also confirms the existence of a novel quantum critical point separating this non-Abelian topological phase from a trivial one [191, 193]. Combining these results therefore corroborates the general theory of anyon-condensation-driven phase transitions via spontaneous breaking of a quantum-group symmetry [194–197].

Our method extends that of Ref. [104] for deformations of the Toric Code to the much trickier non-Abelian case. From the parametrization of the ground state as a PEPS one can construct a one-dimensional "quantum transfer matrix" [198–200], whose fixed-point subspace contains the relevant features of the entanglement structure of the ground state [104, 201, 202]. This transfer matrix is a manifestation of the holographic bulk-boundary correspondence [198, 203], and its utility does not stop at the ground state. From the other eigenvectors of the transfer matrix one can extract information about the elementary excitations as well [199]. As there are few techniques available to deal variationally with excitations in more than one dimension, but see Ref. [174] for recent progress, this insight is valuable for the understanding of the dispersion relation of two-dimensional systems.

3.6.1 PEPS Methodology

The PEPS description of general string-net wave functions has first been established in Refs. [204, 205]. We use the more recent representation discussed in this chapter, as it is especially suited to study and classify the excitations in the different possible anyon sectors. This framework was discussed extensively in Section 3.3 for the example of string-nets.

3.6.1.1 Excitations in PEPS

Given a representation of the ground state of a local Hamiltonian as a PEPS, the next question for the understanding of the low-energy physics of a system is to look at the first excited states of the Hamiltonian. One can argue that elementary excitations can be obtained by modifying a single tensor in the network and making a momentum superposition. Under fairly general assumptions, the correctness of this ansatz was shown in Ref. [206]. For topological models, these excitations additionally have an MPO string attached, one or more of the MPOs O_a that define the PEPS. This MPO is required to implement the topological character of the excitation, such as its braiding properties and its spin. Due to the pulling through condition, these strings are locally unde-

tectable, hence in the topological phase no energy penalty is associated with them.

For MPO-injective PEPS, we argued that for an excitation to be of a single well-defined anyon type, the locally modified tensor has to live exactly in the support of an idempotent, one for every anyon type. These idempotents are uniquely defined by and can be obtained from the MPOs O_a that characterize the PEPS, see Fig 3.56, which represents the same scenario as Fig. 3.23b. In this section we need explicit access to the physical labels, hence the change in the graphical notation. The physical indices are drawn upward for ket states and downward for the dual bra states.

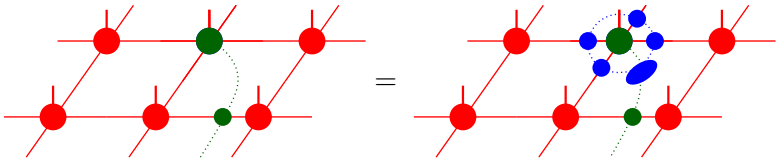

Figure 3.56: An excitation, implemented in the PEPS language by the modified green tensor, is of one definite anyon type if it lives exactly in the support of one of the elementary idempotents of the theory. These idempotents are constructed by closing an MPO loop with a fixed, specific tensor (blue oval), one for each anyon type.

3.6.1.2 The Transfer Matrix

From the local PEPS tensor of the ground state, we can construct the associated quantum transfer matrix. It is a completely positive map that acts as

$$\rho \to \sum_{\mathbf{i}} A^{\mathbf{i}} \rho (A^{\mathbf{i}})^\dagger$$

with $A^{\mathbf{i}}$ one row or column from the PEPS network and $\mathbf{i}$ the collection of physical indices on that row or column. For fixed $\mathbf{i}$, $A^{\mathbf{i}}$ is a MPO for which the local tensors have both physical and virtual dimension equal to D, the bond dimension of the PEPS. Likewise, the transfer matrix itself can be encoded as an MPO with dimensions D^2, because of the double layer (ket and bra) structure. The transfer matrix appears

naturally when we look at the norm of the PEPS $|\psi\rangle$. The norm of a PEPS is given by the value of the double layer contracted network, one column of this network can be seen as an operator and is exactly the transfer matrix, see Fig. 3.57. The normalization of the PEPS implies that the largest eigenvalue of this operator is 1.

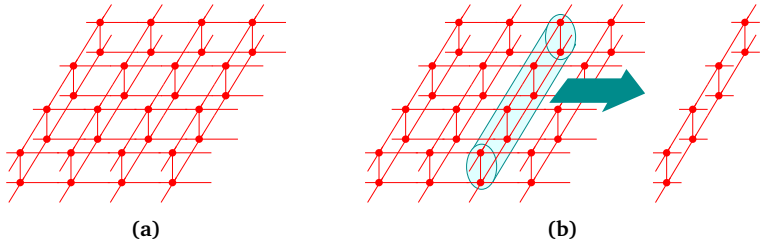

Figure 3.57: The norm $\langle\psi|\psi\rangle$ of a PEPS $|\psi\rangle$ is given by the full contraction of the double layer network as shown in Fig. 3.57a. We can take one column of the double layer and treat it as an operator from left to right, the transfer matrix as shown in Fig. 3.57b.

The topological properties of the PEPS $|\psi\rangle$ have important consequences for the structure of the transfer matrix. The pulling through condition implies that the individual operators $A^{\mathbf{i}}$ commute with the MPOs O_1 and O_τ, so that the transfer matrix commutes with the application of these MPOs on the ket or bra layer separately as shown in Fig. 3.58. We refer to this property as the symmetry of the transfer matrix, although the MPOs O_1 and O_τ are not unitary operators. In other languages, this is called topological symmetry [207], or quantum-group symmetry [196].

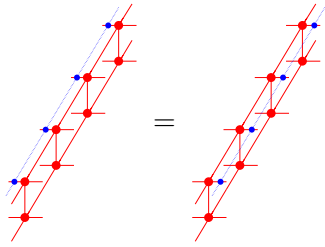

Figure 3.58: The fundamental symmetries of the transfer matrix (red) are given by MPOs (blue) that commute both on the ket and bra layer.

3.6.1.3 Fixed Point Subspace of the Transfer Matrix

We denote the, possibly degenerate, fixed points of the transfer matrix as in Fig. 3.59. Because of the pulling though property of the MPOs, given a fixed point we can construct more fixed points by applying a specific MPO in the bra or ket layer. The application of such an MPO results in a new, possibly non injective, fixed point which can be expanded as a sum of injective fixed points. We use different colors to stress that there are different fixed points, or use an extra label. In the RG fixed point, the fixed points are essentially given by the injective MPOs O_a. For string nets, they constitute a commutative fusion algebra. This implies that there is only one possible positive operator among them, which is O_1, the MPO that acts as the identity in the PEPS network. We denote the topologically trivial fixed point obtained from this MPO as ρ_1.

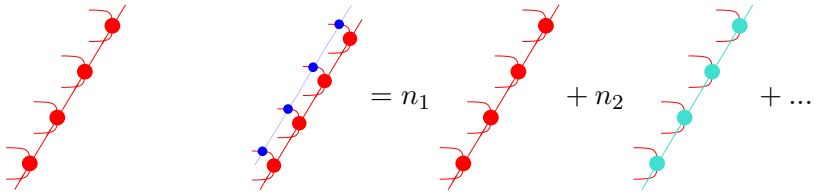

(a) A fixed point of the transfer matrix, represented as MPS.

(b) Applying an MPO to a fixed point gives us in general a non-injective MPS. It can be expanded as a combination of the injective fixed points with integer coefficients n_i.

Figure 3.59

3.6.1.4 Condensation and Confinement

Let us turn our attention again on the excitations. Let us denote the state with an extra excitation as in Fig. 3.56 as $|\psi[O]\rangle$. For the excitation to be well defined we need it to be orthogonal to the ground state and have a well-defined, non-vanishing norm. These conditions are summarized by the expressions $\langle\psi[O]|\psi[O]\rangle \neq 0$ and $\langle\psi|\psi[O]\rangle = 0$ and illustrated in Fig. 3.60. As we explain below, we can interpret a violation of these conditions in terms of particle confinement or condensation. If

$\langle\psi[O]|\psi[O]\rangle = 0$, the particle is confined, whereas if $\langle\psi|\psi[O]\rangle \neq 0$, the particle is condensed.

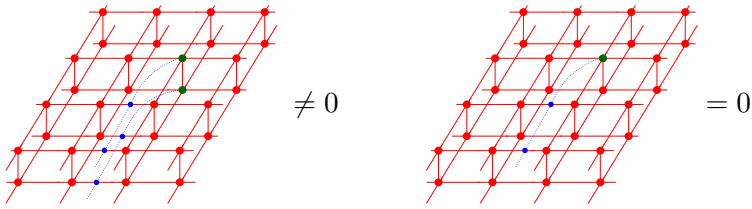

(a) **(b)**

Figure 3.60: The conditions to have a well defined, particle like, anyon excitation. Fig. 3.60a expresses that the excitation is not confined, Fig. 3.60b that it is not condensed.

To compute the norm of $|\psi[O]\rangle$ we proceed as follows. The contraction of the entire network to the left or right of the position of the excitation tensor gives us the unique positive, left and right fixed point of the transfer matrix as illustrated in Fig. 3.61. Similarly, the overlap between the ground state $|\psi\rangle$ and the excited state $|\psi[O]\rangle$ is given in Fig. 3.62.

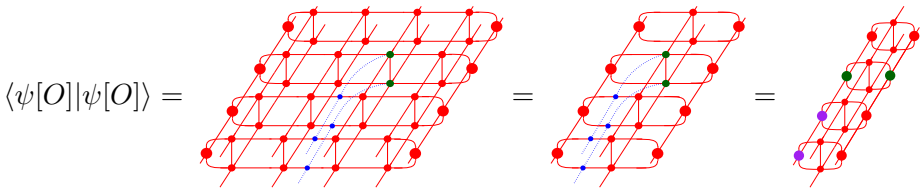

Figure 3.61: Contraction scheme to calculate the norm of an excitation. We first contract the network from left and right and obtain the trivial fixed point ρ_1 (red). Application of the MPOs in bra and ket (blue) to the left fixed point gives a new fixed point that is in general non-injective (purple).

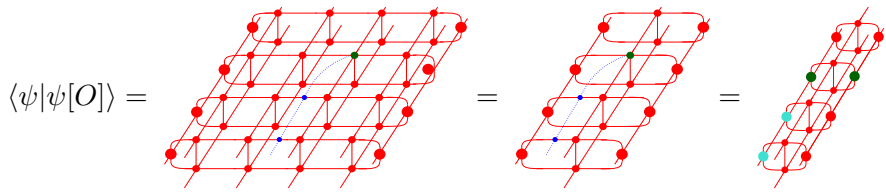

Figure 3.62: Contraction scheme to calculate the overlap of the ground state and an excited state. We first contract the network from left and right and obtain the trivial fixed point ρ_1 (red). Application of the MPOs in ket (blue) to the left fixed point gives a new fixed point that is in general non-injective (cyan).

We see that in order to have well defined excitation with an MPO string, i.e. $\langle\psi[O]|\psi[O]\rangle \neq 0$ and $\langle\psi|\psi[O]\rangle = 0$ as depicted in Fig. 3.60, it is sufficient if the conditions in Fig. 3.63 are fulfilled.

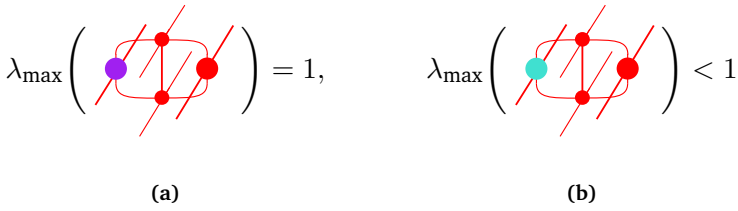

(a) **(b)**

Figure 3.63: The conditions to have a well defined, particle like, anyon excitation with blue MPO string. Fig. 3.63a ensures that the excitation is not confined, Fig. 3.63b that it is not condensed. The figures are to be interpreted as matrices from the upper to the lower indices

The first condition, Fig. 3.63a is even strictly necessary to ensure that $\langle\psi[O]|\psi[O]\rangle \neq 0$, whereas $\langle\psi|\psi[O]\rangle = 0$ could still be satisfied thanks to the local tensor at the endpoint of the string excitation even if the condition in Fig. 3.63b is not satisfied.

One can intuitively think of the strings as the flux degrees of freedom and the endpoint as the charge degrees of freedom, although the two can not always be separated in such an easy manner. The MPOs implement the symmetry action on the transfer matrix and the endpoints can be thought of as order parameters for these symmetries. This correspondence was further investigated in Ref. [104] for phases corresponding

to doubled group algebras (and in particular the Toric Code phase). In our more general setting, the idempotents living at the end point of the string are more complex, and their interpretation as virtual order parameters is beyond the current scope.

Nevertheless, it is clear that the conditions in Fig. 3.63 provide important information about the structure of the fixed point subspace. The transfer matrix commutes with the application of all MPOs, both on the bra and the ket level, as follows from the pulling through condition. Given this symmetry, the question remains what the corresponding structure of the fixed point subspace of the transfer matrix is with respect to this symmetry. The condition in Fig. 3.63a tells us that the fixed point subspace has to be symmetric under the application of the same MPO in both bra and ket layer. The condition in Fig. 3.63b on the other hand expresses the fact that the fixed point subspace is not symmetric under the application of an MPO in only the ket (or only the bra) layer.

3.6.1.5 The Transfer Matrix as a Probe for Excitations

Unfortunately, a full variational approach to perturbed string-net Hamiltonians is numerically out of reach despite recent progress [12, 13, 208]. Luckily, we can gain lots of insight by using holographic dimensional reduction, which is very natural in the language of tensor networks. One can argue that most of the information about the dispersion of a Hamiltonian is already encoded in the ground state. By looking at the transfer matrix of the ground state, we can extract this information. As the transfer matrix of a 2D ground state is itself a 1D system, we have then effectively reduced the spatial dimension of the problem and can now apply well established numerical methods. As discussed earlier, the symmetries of the fixed point subspace of the transfer matrix already contain a lot of information about the condensation or confinement of anyon excitations. We now argue that more information can be extracted.

In a translation-invariant system, excitations are naturally described as momentum eigenstates. We now explain why the transfer matrix

also contains information about the dispersion relation of such excitations [199]. The reason the transfer matrix is so relevant is that the variational dispersion relation of excitations in the PEPS picture is mainly determined by the normalization of the excited states.

Indeed, let us write the ground state of an Hamiltonian H as $|\psi_0\rangle$. As shown in Ref. [206] we can construct elementary excitations by acting with local operators on the ground state and giving them a specified momentum $k = (k_x, k_y)$. Take a local Hermitian operator O with zero ground state expectation value and denote its translates by O_{xy}, i.e. O_{xy} acts on the sites centered around (x, y). Denote the excitation with momentum k created by O with

$$|\psi[O,k]\rangle = \sum_{x,y} \exp(-i(k_x x + k_y y)) O_{xy} |\psi_0\rangle .$$

We can then write the variational expression for the energy of a state with momentum k as

$$E = \min_O \frac{\langle\psi[O,k]|H|\psi[O,k]\rangle}{\langle\psi[O,k]|\psi[O,k]\rangle}.$$

We can rewrite the numerator of this last expression as

$$\langle\psi_0| \sum_{x,y} e^{i(k_x x + k_y y)} [O_{xy}, [H, O_{x'y'}]] \sum_{x',y'} e^{-i(k_x x' + k_y y')} |\psi_0\rangle .$$

Because of the double commutator, this expression diverges at most as $\|O\|\|\text{supp}(O)|V$ in the system size V. In contrast the scaling of the denominator can, for a good choice of O and k, be significantly faster, hence the expression for E is mainly determined by the denominator. In particular, excitations with a low variational energy can be obtained by making the denominator as large as possible. For a detailed version of this reasoning, as well as other arguments that support the conclusion, we refer the reader to Ref. [199].

While the previous argument was applicable to point like excitations, it is clear that it can be extended to excitations with an MPO string attached, as the string is unobservable and does not bring along an energy cost. The denominator for such excitations is depicted in Fig. 3.64. It

represents the norm of an excited state containing one anyon, localized at the green tensor.

$$\langle\psi[O,k]|\psi[O,k]\rangle = \sum_{x,y} e^{-ik_x\Delta_x - ik_y\Delta}$$

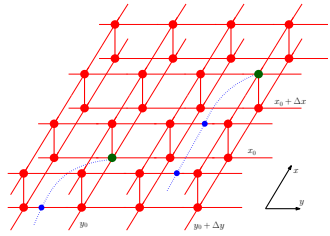

Figure 3.64: The norm of a excitation, created by acting with a local operator thereby turning a red ground state tensor in a green excited tensor. We make a momentum superposition of this state with momentum $k = (k_x, k_y)$.

We already discussed the fixed points of the transfer matrix. We now look at the other, excited, eigenstates of the transfer matrix. For this, we use the excitation ansatz for 1D systems [206]. Having obtained both fixed points, we can construct an approximation to the 'excitations' of the transfer matrix, i.e. the eigenvectors corresponding to the next eigenvalues $\mu = \mathrm{e}^{-\lambda}$ of largest magnitude (smallest real part of λ), using the ansatz discussed in [104, 173, 209]. One option is to construct excitations by locally changing a tensor of ρ_1 or ρ_τ. The second option is to construct domain-wall excitations by using both fixed points, one on each side of the locally changed tensor. We can easily make momentum eigenstates by taking the superposition of translations of such excitations with appropriate phases and hence obtain a 'dispersion relation' of the transfer matrix.

There are two alternative but equivalent ways to think about the non-trivial domain wall excitation. These excitations correspond to local tensors with an MPO string attached. The relation in Fig. 3.59 implies that this is equivalent to the usage of different fixed points to make kink excitations, one on each side of a perturbed tensor. Clearly there is an if and only if relation in this formalism between the existence of excitations with a locally invisible string and the existence of several

fixed points related via the application of an MPO. The excitations are graphically denoted as in Fig. 3.65.

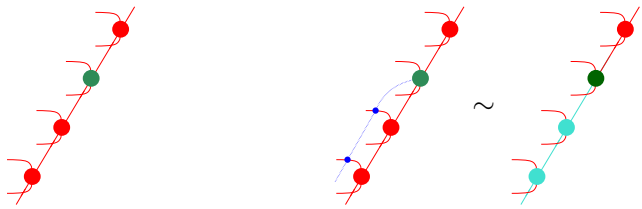

(a) **(b)**

Figure 3.65: The ansatz for the topologically trivial excitations of the transfer matrix is obtained by changing one single tensor (green) and making a momentum superposition, Fig. 3.65a. Topologically non-trivial excitation, are obtained by attaching an MPO string (blue) to the perturbed tensor. This is equivalent to a kink excitation, where we have a perturbed tensor (green) but different fixed point tensors (red and cyan) on either side of it, Fig. 3.65b.

We now return to the original question of calculating the norm of an excitation, see Fig. 3.64. The contracting steps are illustrated in Fig. 3.66. We start by contracting this network from the left and right. This gives us the trivial fixed points on the left and right, as they are the unique injective positive fixed points and the transfer matrix is a completely positive map. Physically this corresponds to the fact that at infinity the state is in the topologically trivial ground state. Once we reach the excitation in the ket from the right, we get a kink excitation, with the trivial fixed point on top (red), an excited tensor (green) and another, possibly non-injective fixed point, on the bottom (cyan). Contracting the layers between the excitation amounts to applying the transfer matrix, this does not change the fixed points tensors, although it might affect the excited tensor. Next, we reach the position of the excitation in the bra. The application of the MPO gives us a new fixed point (purple).

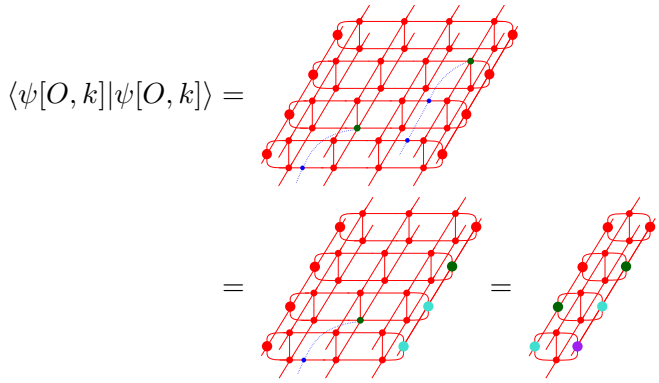

Figure 3.66: Contraction scheme to calculate the norm of an excitation, see the main text for details. The figure does not show the momentum superpositions for the sake of clarity.

Remember that we want to make this quantity as large as possible. The final outcome contains the local overlap of the red and purple fixed points. If the norm of the state is to be non-zero, the fixed points ρ_1 resulting from the application of an MPO in the bra or ket on the trivial fixed point have to contain at least once the same injective fixed point. Written differently, we see that this implies that $O_i \rho_1 O_i^\dagger = \rho_1 + \ldots$, or $N_{ii}^1 > 0$. This is indeed true at the RG fixed point and should remain so throughout the phase. We see here again that the topological properties of the bulk, the existence of anyons, is through the bulk-boundary correspondence reflected in a symmetry property of the fixed point subspace. The anyons then correspond to symmetry breaking, domain wall, excitations.

We can thus assume that both fixed points on the bottom of the diagram are the same as this is the only term that contributes to the norm. The computation then depends on what happens to the excited tensor between the location of both fixed points. Because of the momentum superposition this is the application of $(1 - e^{ip_y} T)^{-1}$ to the excited 1D state. Clearly, to maximize this, we want to choose the variational parameters in the green tensor such that the 1D state is an eigenstate of the transfer matrix with eigenvalue as close as possible to e^{-ip_y}. As the momenta are variational parameters, we see from the previous

discussion that we need to find the eigenvectors of the transfer matrix whose eigenvalues have the largest magnitude.

This calculation again reveals the importance of the symmetries of the fixed point subspace for the topological properties of a system. Because of the pulling through condition, we know that the transfer matrix commutes with the application of an MPO in its ket or bra layer. Hence, the fixed point subspace inherits this symmetry. Generically, a system with this property will have maximal symmetry breaking and (at least) N^2 different fixed points, with N the number of MPOs. However, in the PEPS picture we have just argued that $N_{ii}^1 > 0$, hence we expect less fixed points, N to be precise, if the system is topologically ordered, in the sense that it has anyonic excitations.

3.6.1.6 Classification of Excitations

We now discuss how we can classify the excitations of the transfer matrix with the appropriate anyon labels of the original two-dimensional topological theory. As discussed an excitation of the transfer matrix such as in Fig. 3.66 actually encodes the existence of an excitation with a string in the right half of the full 2D model. We can measure the anyon type of a part of the lattice using the central idempotents. To apply these to the 1D excitations we need some extra manipulations that we now explain.

In order to classify these excitations in terms of the physical anyon sectors, we need to reinterpret them in the context of the "mixed" transfer matrix. In particular, we rewrite the domain-wall excitations to replace the kink with a half-infinite extra MPO attached to the site that contains the perturbed tensor. Due to the non-Abelian character of the theory, there are several possibilities to obtain this MPO string from a kink excitation.

Let us then use the pulling through condition to rewrite the eigenvalue equation as in Fig. 3.67. It is then indeed clear that we can equivalently look for eigenvectors of the so-called mixed transfer matrix that contains an extra MPO in the ket, see Fig. 3.68.

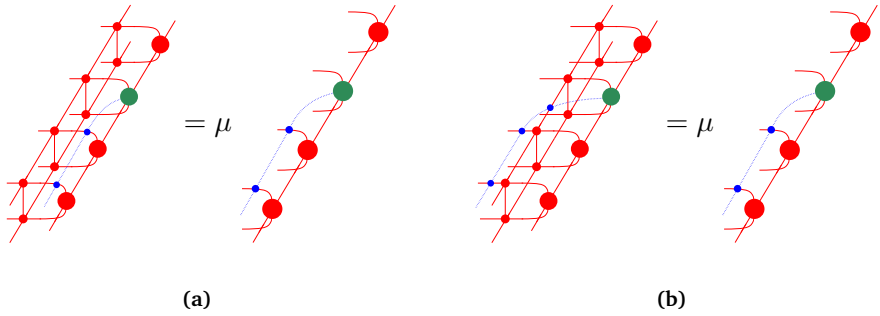

Figure 3.67: The eigenvector equation for the regular transfer matrix in Fig. 3.67a. An equivalent equation, using the pulling through property in Fig. 3.67b.

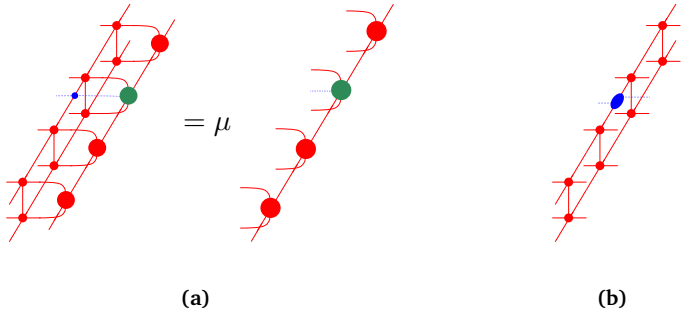

Figure 3.68: The eigenvalue equation for the mixed transfer matrix in Fig. 3.68a. This is the regular transfer matrix with a extra MPO through its ket (or bra) layer. The excitation ansatz consists now of local perturbations on the trivial fixed points, but the perturbed tensors (green) have en extra MPO index. We can naturally use the idempotents to define operators in the mixed formalism as in Fig. 3.68b.

The reason we did this is to have access to the blue MPO label, which we need to be able to apply the central idempotents. The mixed transfer matrix also reveals the extra topological structure more clearly. Indeed, all idempotents commute with the mixed transfer matrix, this gives rise to a block decomposition of the transfer matrix into the different topological sectors. It is this decomposition that makes the classification of excitations possible. This property is illustrated in Fig. 3.69. A similar property holds when we apply the idempotents in the bra instead of the

ket layer.

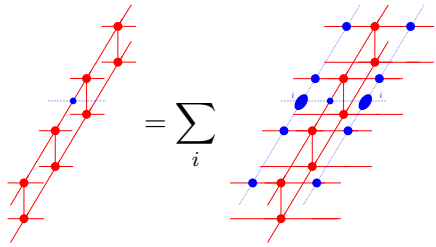

Figure 3.69: The mixed transfer matrix has a block decomposition induced by all the idempotents.

For the classification it suffices to consider only one of the cases. We only apply non-trivial idempotents in the ket, in the bra we will not place an extra idempotent, or equivalently, always place the idempotent corresponding to the topologically trivial excitations in the bra. We can now proceed as follows. We gather all excitations, both trivial and kink, of the transfer matrix that correspond to the same eigenvalue and momentum. We list all the possible ways we can explicitly obtain an MPO string from such an excitation as in Fig. 3.65. If the theory is non-Abelian, there can be several possibilities. We can now calculate the matrix elements of all the central idempotents projected onto this eigenspace using standard MPS methods and diagonalize the result as in Fig. 3.70. All the idempotents are still projectors in this subspace, due to the block structure of the transfer matrix. The central idempotents whose restrictions have non-zero rank give the anyon types of the excitations in the considered energy and momentum spaces.

3.6.2 Example: The Doubled Fibonacci Phase

We now illustrate the ideas discussed in the previous section in the context of a concrete quantum many-body wave function. We focus on the doubled Fibonacci phase as it is the prime example of a PEPS that contains non-Abelian excitations.

$$\langle\psi[O,k]|\mathcal{P}_i|\psi[O',k]\rangle =$$

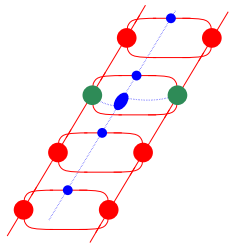

Figure 3.70: The network that gives the matrix element of a central idempotent with respect to some excitations at a given energy and momentum. As this is a 1D network it can be contracted efficiently.

3.6.2.1 General Comments

The Fibonacci phase has only one non-trivial anyon labeled τ in addition to the trivial identity particle, so the chirally symmetric doubled phase has four types, labeled $1, \tau, \overline{\tau}, \tau\overline{\tau}$. Recall that in Section 3.3.1 we indeed numerically found these four different types of anyons. We also discussed there that in the framework of MPO-injective PEPS, the doubled phase is characterized by two MPOs labeled by O_1, O_τ satisfying the Fibonacci fusion rules $O_\tau O_\tau = O_1 + O_\tau$ [23]. The projector P onto the vacuum sector defines the local PEPS tensor of the ground state at the renormalization group (RG) fixed point, the string-net model. It is

$$P = \frac{1}{1+\phi^2} O_1 + \frac{\phi}{1+\phi^2} O_\tau,$$

with ϕ the golden ratio. Acting on this tensor with a non-unitary gate on the physical level gives a perturbed PEPS no longer at the RG fixed point. Varying the gate then can drive the state through a phase transition. Below, we provide a detailed investigation of various perturbations.

For the Fibonacci model, we need exactly two fixed points to have well-defined anyons. This corresponds to the fact that the fixed point subspace is not invariant under the application of an O_τ MPO in only the ket or bra layer but is invariant under a simultaneous application in both. At the RG fixed point, we can analytically construct two fixed points and write down explicit tensor network representation for them. One is

obtained from the MPO O_1, and the other from O_τ. These correspond exactly to 'symmetry broken' states under the symmetry of the transfer matrix. It turns out that these are the only two fixed points, as is expected. Indeed, this is the generic signature of the fact that none of the anyons has condensed or is confined. After perturbing the state, the two-fold degenerate fixed point subspace persists as long as we are in the topological doubled Fibonacci phase. When passing through a phase transition, the fixed-point structure will change. The difference with the Abelian case is that under the action of an MPO, a fixed point can be mapped to a sum of several other fixed points, consistent with the Fibonacci fusion rules $\tau \times \tau = 1 + \tau$. The full rules for the result of applying MPOs to the fixed point are as expected from the notation,

$$O_\tau \rho_1 = \rho_1 O_\tau^\dagger = \rho_\tau, \qquad O_\tau \rho_1 O_\tau^\dagger = \rho_1 + \rho_\tau$$
$$O_\tau \rho_\tau = \rho_\tau O_\tau^\dagger = \rho_1 + \rho_\tau, \qquad O_\tau \rho_\tau O_\tau^\dagger = \rho_1 + 2\rho_\tau.$$

The two fixed points ρ_1 and ρ_τ furthermore have the property that they are injective as MPS, and are therefore exactly the ones that are approximated by numerical MPS algorithms.

We expect all phase transitions to be towards the topologically trivial phase because of the general arguments of Refs. [194–196]. With our approach, we find four different fixed points of the transfer matrix, which we can indeed interpret as the confinement of the τ and $\overline{\tau}$ anyons, driven by the condensation of the $\tau\overline{\tau}$ anyon. More specifically, as the fixed point $O_\tau \rho_1 O_\tau^\dagger$ is now orthogonal to the fixed point ρ_1, the presence of MPO strings is suppressed and the 'energy' associated with a pair of τ or $\overline{\tau}$ anyons increases strongly with their separation distance. More details are provided in the explicit results below.

3.6.2.2 Results for Fibonacci Model

We focus now on several perturbations of the Fibonacci string-net ground state and study the dispersion relation of the resulting states. As a full variational method to find ground states of perturbed string-net Hamiltonians is currently out of reach, we instead perturb at the level of the state by extending the filtering procedure introduced in Refs. [210, 211] using the framework of PEPS.

We stress that each of the perturbed states is still the ground state of a local Hamiltonian. Indeed, we always start from the Fibonacci string net PEPS $|\Omega\rangle$ with the corresponding positive Hamiltonian

$$H = \sum_v A_v + \sum_p B_p = \sum_j h_j$$

that consists of commuting plaquette and vertex terms [176]. All perturbed states we consider are of the form $\prod_i Q_i |\Omega\rangle$ with Q_i a local and positive operator on site i and clearly these states are ground states of the local Hamiltonian

$$\tilde{H} = \sum_j Q^{-1}(j) h_j Q^{-1}(j)$$

with $Q(j)$ the product of all Q_i with the site i in the support of h_j.

Recall that the original Fibonacci string-net model is defined by putting a two-state quantum system (a qubit) on each edge j of some lattice. Each segment of string-net corresponds to a $|1\rangle$ state on the background of the product of all $|0\rangle$ states. The original string-net ground state is a sum over configurations with no "ends" (i.e. no vertices with only one segment of string-net touching). A key fact is that the weight of each configuration in the ground state depends only on topological data [212]. Equal-time correlators in the ground state are thus the same as those in a corresponding 2D classical system in the Rokhsar-Kivelson fashion [213]. As described in detail in Ref. [191], the string-net model on the honeycomb lattice is related to the classical 2D ferromagnetic q-state Potts model with $q = 2 + \phi$ on the dual triangular lattice at infinite temperature.

The first perturbation we consider is a string tension. We act with a local $Q_j = \exp(-\beta\sigma_j^z)$ operation on every qubit. Increasing β from 0 still gives the ground state as a sum over local nets without ends, but with a local weighting that favors shorter nets. This simply corresponds to lowering the temperature in the Potts model, so the phase transition in the quantum theory therefore can be located from the classical theory. The Potts models with $q \leq 4$ have a second-order phase transition at a finite temperature, which for $q = 2 + \phi$ on the triangular lattice is

$\frac{1}{4}\log(x\sqrt{\phi+2}+1)$ with x the positive root of the polynomial [214, 215]

$$P(x) = \sqrt{\phi+2}x^3 + 3x^2 + 1 = 0.$$

The corresponding 2D conformal field theory (CFT) describing the scaling limit is the minimal rational one labeled $(9, 10)$ [216]. It is worth noting that the identical CFT describes the scaling limit of the quantum critical Fibonacci ladder [217].

The perturbed string-net exhibits a quantum phase transition at the corresponding string tension, and the quantum transfer matrix arising from PEPS shows the structure beautifully. Indeed, this transfer matrix can be mapped to that of the $2+\phi$-state Potts model. From it we can easily extract the correlation length of the state numerically. We confirm that as predicted, a critical phase transition to a trivial state occurs for $\beta \approx 0.16776$, as illustrated in Fig. 3.71(a). As a check on the methods, we obtained the same location of the phase transition using fidelity methods (not shown) [218]. Beyond the critical point, by further increasing β, the state is not topologically ordered anymore, as is indeed reflected in the fixed point structure. Beyond the phase transition, we find four different fixed points, which excludes the possibility of having anyon excitations with a non-trivial MPO string O_τ. Such strings are then suppressed and the anyons confined. Furthermore, no traces of bound states appear in the spectrum, which are expected in a generic quantum 2D phase transition out of the Fibonacci phase by perturbation theory [219].

An analogous fine-tuned transition and corresponding dimensional reduction also appears in the Toric Code model [210, 211, 220], but here the phase transition is much more intricate. Phase transition out of non-Abelian phases using fine-tuned Hamiltonian interpolations where studied previously in [221, 222] and in [223] for a perturbation corresponding to a magnetic field.

It would be interesting to recover the full CFT signature from finite-size simulations and scalings and compare these to the results for the Fibonacci ladder [217]. However, we wish to stress that the resemblance to a 1D quantum/2D classical phase transition is a mark of the specific model considered, not of the method itself. A way to consider more

generic interpolations with general PEPS that can for instance change the bond dimension of the PEPS is discussed in Chapter 4. We expect that to capture a genuine 2D quantum phase transition the bond dimension of the PEPS has to grow and eventually diverge. The topological information, however, is still contained in the MPO symmetries of the quantum transfer matrix and the tools applied here can still be used.

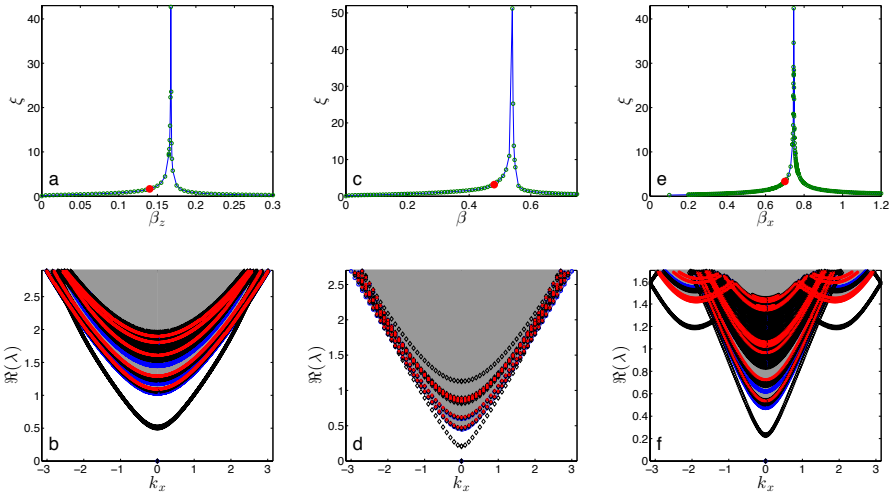

Figure 3.71: The correlation length of the $\exp(-\beta_z Z)$ interpolation (a), an interpolation to the Fendley model (c) and $\exp(-\beta_x X)$ filtering (e). The points where the dispersion relations are given are shown in red. The dispersion relation of the string-net model with $\exp(-\beta_z Z)$ filtering at $\beta_z = 0.14$ (b), the Fendley model (d) and $\exp(-\beta_x X)$ filtering at $\beta_x = 0.7$ (f).

The phase transition can be probed in more depth by plotting the dispersion relations of the excitations of the quantum transfer matrix. We consider only chirally symmetric perturbations, so the τ and $\overline{\tau}$ anyons are always exactly degenerate. Moreover, the condensation of τ or $\overline{\tau}$ individually is prohibited by general arguments [194–196], leaving $\tau\overline{\tau}$ as the only non-trivial possibility. As the fusion product of two $\tau\overline{\tau}$ anyons contains all other anyons, the two-particle continuum of these elementary excitations has support in all topological sectors. We color this continuum gray, but also continue to plot the lowest excitations found by the algorithm in every sector. The four different anyon sectors

are identified using the methods of Ref. [24], and are color coded as 1 (blue circle), $\tau, \overline{\tau}$ (red crosses and pluses) and $\tau\overline{\tau}$ (black diamond).

In Fig. 3.71(b) we plot the spectrum $\Re(\lambda) = \log|\mu|$ at $\beta_z = 0.14$. We clearly see a condensing $\tau\overline{\tau}$ anyon and no traces of a bound state. These observations are still valid and observable closer to the critical point. For instance, the same calculations where performed for $\beta_z = 0.161$ (not shown) and gave similar results.

We now consider including a weighting for trivalent vertices in the string-net, i.e. a penalty for configurations where three strings meet at a vertex. We can then check the argument that the net model with a simpler Hamiltonian described in [191, 192] is in the same topological phase as the Fibonacci string-net. We tune this weight to follow a path from the string-net ground state to the "quantum self-dual" ground state [191]. Both the correlation length in Fig. 3.71(c), and the fidelity approach (not shown) indicate a phase transition only beyond the quantum self-dual state, confirming the suggestion of Ref. [192] that the so-called Fendley loop model is in the same phase as the Fibonacci string-net. We illustrate the dispersion relation in Figure 3.71(d). Again, we see that a $\tau\overline{\tau}$ anyon condenses. Qualitatively this phase transition is similar to the first one, because the weight for trivalent vertices in the corresponding classical model is an irrelevant perturbation.

Finally, we consider a filtering with $Q_i = \exp(-\beta\sigma^x)$. This interpolation violates the closed-net condition and creates open strings in the states, which are the hallmark of anyons. We show the correlation length of the filtered state along this path in Fig. 3.71(e). The dispersion relation is shown in Fig. 3.71(f), as expected it is again the $\tau\overline{\tau}$ anyon that condenses.

3.7 Outlook and Conclusion

In this chapter we have introduced the notion of MPO-injective PEPS. These PEPS are used for the understanding of topological phases. We have seen that all expected properties are encoded in the structure and virtual symmetries of the PEPS tensor. In this way we have established a

close connection between MPO-injective PEPS and unitary fusion categories. We can see the MPO algebra as a particular convenient representation of the abstract categorical data in a quantum many-body system.

Furthermore, we discussed how we can even extract the possible types of anyons from just the properties of the ground state tensor and extract all their topological features like topological spin and braiding statistics. Similar to previous results [93, 170] we can relate topological sectors to the central idempotents of an algebra, which in our case is a C^*-algebra constructed from the PMPO that determines the injectivity subspace of the ground state tensors. The formalism is constructive and gives the correct anyon types for all the examples we worked out.

We can write down explicit PEPS wave functions that contain an arbitrary number of anyons. This gives an interpretation of topological sectors in terms of entanglement. From the PEPS wave functions containing anyons we can extract universal properties such as fusion relations and topological spins in a very natural way. For certain string-net models we also studied the effect of braiding on the PEPS.

For all the examples considered here the PEPS anyon construction is equivalent to calculating the Drinfeld center [224] of the input theory. It is known that the center construction leads to a modular tensor category, which describes a consistent anyon theory [225]. When the input theory is already a modular tensor category by itself, the center construction gives a new modular tensor category, which is isomorphic to two copies of the original anyon theory, one of which is time-reversed [225]. Such an anyon theory cannot correspond to a chiral phase. It would be worthwhile to better understand the connection between our construction and the abstract concept of a Drinfeld Center.

At this point we envision the following possibilities to have MPO-injective PEPS that describe physics beyond string-nets without having to extend the MPO-injectivity formalism. We can use PMPOs that have no canonical form, use different left handed MPO tensors to write down the PEPS tensors, or drop the zipper condition. The second option will most likely lead to a violation of unitarity, in which case the algebra $A_{abcd,\mu\nu}$ can no longer be proven to be a C^*-algebra. This will lead to non-Hermitian central idempotents, which to some extent obscures their interpretation

as topological sectors. The other options are at the moment much less clear to us, so we will not try to speculate on their implications. It would be very interesting to better understand the implications and see if there is any relation between MPO-injective PEPS and the recently constructed tensor network states for chiral phases [226, 227].

Apart from chiral phases, other open questions concerning topological order in tensor networks concern the characterization of quantum phases. We can define an equivalence relation for PMPOs, i.e. two PMPOs are said to be equivalent if the resulting central idempotents have the same topological properties. Such a relation is know in category theory as Morita equivalence but we do not fully understand it yet in the context of PEPS. There is also a very rich interplay between the topological order and global symmetries of a quantum system. Some first progress in capturing universal properties of these so-called symmetry-enriched topological phases with tensor networks was made in [228]. Another direction for future research which enforces itself upon us at the end of this chapter is the extension of the presented formalism to fermionic PEPS [229]. The concept of MPO algebras is also applicable to the understanding of topological sectors in fermionic tensor networks [230].

Besides these theoretical questions there are also a lot of new applications for MPO-injectivity A promising application of our results is the calculation of error thresholds for quantum memories based on string-net models. We hope to make progress on these matters in future work. Probably the most exciting application at this point is the study of topological phase transitions in non-Abelian anyon theories, which we initiated in this chapter.

We have shown how the dispersion relation of a perturbed 2D string-net Hamiltonian is reflected in the eigenvalues of the 1D quantum transfer matrix arising from the PEPS description of the ground state. Our results clarify how the topological properties of the ground states and the excitations are related to the symmetry properties of the PEPS transfer matrix and its fixed point spectrum, extending the findings of Ref. [104] to non-Abelian theories. This enabled us to classify the excitations into different anyonic sectors and to find their dispersion relations. We iden-

tified the anyon type of the condensing particles at a non-trivial quantum critical point, thereby confirming abstract theoretical results [196] in a concrete quantum-many-body system.

It is an interesting question how the results of our method can quantitatively match results from perturbation theory [219] by using more elaborate interpolations. We introduce a possible approach to such an interpolation in Chapter 4. A similar procedure can also be carried out for models such as the Ising string-net, which has a non-trivial condensation driven phase transition to the Toric Code phase. This transition should be reflected in the transfer matrix. Finally, we want to stress that the characterization of anyons using the idempotents can be applied, even more straightforward, to the full 2D setting. Hence, given a good PEPS representation of the ground state, the variational excitations can be calculated [174] and classified accordingly.

Chapter 4

A Variational Class of PEPS

In this chapter, we introduce a variational class of PEPS to describe phase transitions. The states we consider can be seen as a generalization of the states generated by perturbation theory. We test the method on the quantum Ising model in a transverse field and the Toric Code in a magnetic field. The results are still to be reported in an upcoming paper:

- M. Mariën, L. Vanderstraeten, J. Haegeman, J. Vidal and F. Verstraete *Bridging Different Perturbative Expansions with Tensor Networks*

4.1 Perturbation Theory in Many-Body Physics

The usual notion of perturbation theory that is taught in standard undergraduate quantum mechanics courses is not ideally suited to be applied to quantum many-body systems. Without going into too much details, we give an illustration of the core issue with the method. Let us consider a local Hamiltonian $\sum_i h_i$ with eigenvectors $|\psi_i\rangle$ and eigenvalues E_i. We now perturb it with a local operator λV. The recipe tells us that the first order correction to the ground state $|\psi_0\rangle$ is given by

$$|\psi_0^{(1)}\rangle = |\psi_0\rangle + \lambda \sum_{j\neq 0} \frac{\langle\psi_j|V|\psi_0\rangle}{E_j - E_0} |\psi_j\rangle \,. \tag{4.1}$$

Such a W-type state is very unphysical as the ground state of a quantum many-body system. Indeed, they typically correspond to excitations of the systems, not the ground state itself. What we need instead is an 'exponentiated' version of perturbation theory. There are several approaches in the literature that aim at rectifying this issue, for instance the Schrieffer-Wolff transformation [231], Magnus expansion [232], and others. We explored an alternative route ourselves in Section 2.2.1 based on the quasi-adiabatic continuation of the perturbed Toric Code model. It would be very interesting to see how useful and generally applicable this method is. In this section we focus on a different, popular approach, the method of Continuous Unitary Transformations (CUT) [233–236].

4.1.1 Continuous Unitary Transformations

Continuous Unitary Transformations are one of the methods introduced to overcome the many-body problem and, approximately, diagonalize many-body Hamiltonians. The idea behind CUT is to introduce a unitary flow that transforms the Hamiltonian in such a way that low-and high-energy subspaces start to decouple, thus enabling one to study them separately and make progress in this way. The goal is to find unitary transformations that block-diagonalize the Hamiltonian in question.

Instead of immediately giving the unitary, which amounts to diagonalizing the Hamiltonian and is virtually impossible, we write down a continuous flow with a generator. We then have a one-parameter family of Hamiltonians $H(l)$ such that

$$H(0) = H, \quad H(l) = U(l)HU(l)^\dagger$$

and we have the defining flow

$$\frac{d}{dl}H(l) = [\eta(l), H(l)], \quad \eta(l) = \left(\frac{d}{dl}U(l)\right)U(l)^\dagger.$$

The idea is to obtain an effective Hamiltonian

$$H_{\text{eff}} = \lim_{l\to\infty} H(l)$$

that is block diagonal. In practice, we assume that there is a number operator Q and that the effective Hamiltonian is block-diagonal in the particle number sectors. We can then take the generator $\eta(l) = [Q, H(l)]$ although more general choices are possible.

4.1.1.1 Perturbative Continuous Unitary Transformations

It turns out that for a restricted class of specific, but physically relevant, Hamiltonians we can solve the flow equations analytically. This method is called perturbative Continuous Unitary transformations (pCUT) [237, 238]. We now explain for which systems pCUT can be applied. We then give an illustrative example of the idea behind pCUT, but for a complete account of the method we refer to Ref. [238]. The reason is twofold. First, the author is in no way an expert in the field of pCUT. Second, the interest in pCUT comes from the fact that the obtained effective Hamiltonians up to a certain order can be treated efficiently with finite-cluster methods based on the linked-cluster theorem [239–241]. Hence, the main interest in the pCUT community is often the effective Hamiltonian, whose form is even model independent, and not the unitary that brings it into this form. In contrast, our interest is exactly the unitary itself. It can be used to define a PEPS ansatz that makes sense as a class of ground states for perturbed quantum many-body Hamiltonians unlike the state in Eq. (4.1)

4.1.1.2 Assumptions of pCUT

We assume the non-perturbed Hamiltonian H_0 has a discrete spectrum that is bounded from below. Let us denote the groundstate energy by E_0 and the other energies by E_i. Next, there must be a fundamental smallest energy gap. By this we mean there is a Δ such that all energies can be written as $E_i = n_i\Delta$. If we normalize the energies such that $E_0 = 0$ and $\Delta = 1$ we can summarize these requirements by demanding that H_0 is exactly a particle number operator. We denote $H_0 = Q$ and there is a basis of eigenstates $\{|n\rangle\}$ with $|n\rangle$ n-particle states such that $Q|n\rangle = n|n\rangle$. Note that the energy levels corresponding to a value $n \neq 0$ are usually massively degenerate and our notation is consequently a bit

sloppy. Third, we need particle creation and annihilation operators T_m such that

$$T_m |n\rangle = \begin{cases} |n+m\rangle\,, & \text{for } m+n \geq 0 \\ 0, & \text{for } m+n < 0. \end{cases}$$

These operators satisfy $T_m^\dagger = -T_{-m}$ and the fundamental relation

$$[Q, T_m] = mT_m.$$

4.1.1.3 A Recursive Approach to pCUT

Our first goal is to find anti-Hermitian operators O such that

$$H_{\text{eff}} = \exp(-\lambda O^\dagger) H \exp(-\lambda O)$$

is particle conserving up to 0-th order and $\exp(\lambda O)\,|\psi_0\rangle$ is the correct ground state, also up to 0-th order. The solution is simply $O = \mathbb{1}$. The situation gets more interesting when we get to the next order. We need to find A such that

$$\exp(-\lambda A^\dagger) H \exp(-\lambda A)$$

is particle preserving up to 1-th order. We expand this expression and get

$$(1-\lambda A^\dagger)\left(Q + \lambda T_0 + \lambda \sum_{n\neq 0} T_n\right)(1-\lambda A) = Q + \lambda T_0 + \lambda \sum_{n\neq 0} T_n - \lambda [Q, A].$$

As $Q + T_0$ is already particle preserving, we need to choose A such that

$$[Q, A] = \sum_{n\neq 0} T_n.$$

This requirement is satisfied by the choice

$$A = \sum_{n\neq 0} \frac{1}{n} T_n.$$

In our application we are mainly interested in the ground state and it is clear that the simpler operator $A = \sum_{n>0} \frac{1}{n} T_n$ has the same effect on

the original ground state. If we act with this operator, we get at order 1 that

$$\begin{aligned}|\psi^{(1)}\rangle &= \left(1 - \lambda \sum_{n>0} \frac{1}{n} T_n\right) |\psi^0\rangle \\ &= |\psi^0\rangle - \lambda \sum_{n>0} \frac{1}{N} |\psi_n\rangle \,.\end{aligned}$$

Now, with $V = \sum_n T_n$ it holds that

$$\langle \psi_m | V | \psi_0 \rangle = \langle \psi_m | \sum_n T_n | \psi_0 \rangle = \sum_n \delta_{m,n} = 1, \quad \forall m > 0,$$

from which we conclude that

$$|\psi^{(1)}\rangle = |\psi_0\rangle - \lambda \sum_{n>0} \frac{\langle \psi_n | V | \psi_0 \rangle}{E_n - E_0} |\psi_n\rangle \,,$$

as it should be to agree with standard perturbation theory. In 2-th order we expand

$$\exp(-\lambda^2 B^\dagger) \exp(-\lambda A^\dagger) \left(Q + \lambda \sum_n T_n\right) \exp(-\lambda A) \exp(-\lambda^2 B)$$

which gives

$$\begin{aligned}&\left(\mathbb{1} - \lambda A^\dagger + \frac{\lambda^2}{2} A^{\dagger 2}\right) \left(\mathbb{1} - \lambda^2 B^\dagger\right) \left(Q + \lambda \sum_n T_n\right) \\ &\qquad \times \left(\mathbb{1} - \lambda A + \frac{\lambda^2}{2} A^2\right) \left(\mathbb{1} - \lambda^2 B\right) \\ &= Q + \lambda T_0 + \lambda^2 \left(\frac{1}{2}\left(A^{\dagger 2} Q + Q A^2\right) + A^\dagger Q A \right. \\ &\qquad \left. - A^\dagger \sum_n T_n - \sum_n T_n A - B^\dagger Q - Q B\right).\end{aligned}$$

We see that we want

$$\frac{1}{2}\left(A^2 Q + Q A^2\right) + A \sum_n T_n - \sum_n T_n A - A Q A + [B, Q]$$

to be particle preserving up to 2-nd order. Before we continue, we focus on a more concrete setting to slightly lighten the notation.

4.1.1.4 pCUT for the Toric Code in a Magnetic Field

We start from the Hamiltonian $H_{\text{TC}} = Q$, which indeed behaves as a particle number operator. An additional magnetic field in the X direction can move a magnetic flux and create or destroy a pair of magnetic flux excitations. We can thus write the perturbation as $X = T_{-2} + T_0 + T_2$. From the previous discussion we see that

$$A = -A^\dagger = \frac{T_2 - T_{-2}}{2}$$

and thus

$$A^2 = \frac{1}{4}\left(T_2T_2 + T_{-2}T_{-2} - T_2T_{-2} - T_{-2}T_2\right).$$

We can calculate that

$$\begin{aligned}
\frac{1}{2}\left(A^2Q + QA^2\right) &= \frac{1}{4}(T_2T_2Q + T_{-2}T_{-2}Q + 2T_2T_2 \\
&\quad - 2T_{-2}T_{-2} - T_2T_{-2}Q - T_{-2}T_2Q) \\
A\left(T_0 + T_2 + T_{-2}\right) &= \frac{1}{2}(T_2T_2 + T_2T_{-2} + T_2T_0 \\
&\quad - T_{-2}T_{-2} - T_{-2}T_2 - T_{-2}T_0) \\
-\left(T_0 + T_2 + T_{-2}\right)A &= -\frac{1}{2}(T_0T_2 + T_2T_2 + T_{-2}T_2 \\
&\quad - T_0T_{-2} - T_2T_{-2} - T_{-2}T_{-2}) \\
-AQA &= -\frac{1}{2}(T_2T_2 + \frac{1}{2}T_2T_2Q + T_2T_{-2} - \frac{1}{2}T_2T_{-2}Q \\
&\quad - T_{-2}T_2 - \frac{1}{2}T_{-2}T_2Q - T_{-2}T_{-2} + \frac{1}{2}T_{-2}T_{-2}Q).
\end{aligned}$$

Putting everything together, we find that

$$\begin{aligned}
\frac{1}{2}\left(A^2Q + QA^2\right) + A\sum_n T_n - \sum_n T_nA - AQA &= \frac{1}{2}(T_2T_{-2} - T_{-2}T_2 \\
&\quad + [T_2, T_0] - [T_{-2}, T_0]).
\end{aligned}$$

Now the first term,

$$\frac{1}{2}\left(T_2T_{-2} - T_{-2}T_2\right)$$

is particle preserving. We thus need that the second term and the contribution of B cancel,

$$\frac{1}{2}\left([T_2, T_0] - [T_{-2}, T_0]\right) + [B, Q] = 0.$$

It holds that

$$[[T_2, T_0], Q] = -2[T_2, T_0], \quad [[T_{-2}, T_0], Q] = 2[T_{-2}, T_0],$$

from which we deduce that the choice

$$B = \frac{1}{4}[T_2 + T_{-2}, T_0]$$

satisfies the constraint. We can now apply these operators to the ground state and expand to second order

$$\begin{aligned} e^{-\lambda A} e^{-\lambda^2 B} |\psi_0\rangle &\approx \left(\mathbb{1} - \frac{\lambda^2}{4} B\right)\left(\mathbb{1} - \lambda A + \frac{\lambda^2}{2} A^2\right)|\psi_0\rangle \\ &= |\psi_0\rangle - \lambda \frac{T_2}{2}|\psi_0\rangle + \frac{\lambda^2}{8}\left(T_2 T_2 - T_{-2} T_2\right)|\psi_0\rangle \\ &\quad + \frac{\lambda^2}{4} T_0 T_2 |\psi_0\rangle \\ &= \left(\mathbb{1} - \frac{\lambda^2}{8}\right)|\psi_0\rangle - \lambda \frac{X}{2}|\psi_0\rangle + \frac{\lambda^2}{8}\sum_{(ij)} X_i X_j |\psi_0\rangle \\ &\quad + \frac{\lambda^2}{4}\sum_{\langle ij\rangle} X_i X_j |\psi_0\rangle \end{aligned} \tag{4.2}$$

where (ij) denotes that sites i, j are not part of the same plaquette and $\langle ij\rangle$ that they are. One can compare this expression to the result of standard perturbation theory and see that both are equal, as they should be.

We see that the application of the A, B operators up to a given order on the ground state $|\psi_0\rangle$ simplifies a lot. Actually, in this case we could have deduced the correct A, B operators using standard perturbation theory and some straightforward manipulations. We quickly show this for the Toric Code as a clarifying illustration.

4.1.1.5 Intuition Behind pCUT for the Toric Code

The X operator creates exact eigenstates of the Toric Code Hamiltonian, more precisely it creates a pair of flux excitations on neighboring plaquettes. Therefore it is immediately clear that $e^{-\lambda X}\left|\psi_0\right\rangle$ gives the correct state in 1-th order. Let us expand this even further,

$$\left(\mathbb{1} - \frac{\lambda}{2}\sum_i X_i + \frac{\lambda^2}{8}(\sum_i X_i)^2\right)\left|\psi_0\right\rangle$$

and recall that $X = T_0 + T_2 + T_{-2}$, to obtain

$$\left|\psi_0\right\rangle - \frac{\lambda}{2}T_2\left|\psi_0\right\rangle + \left(\frac{\lambda^2}{8}T_2T_2 + \frac{\lambda^2}{8}T_{-2}T_2 + \frac{\lambda^2}{8}T_0T_2\right)\left|\psi_0\right\rangle.$$

If we compare this with equation (4.2) we see that we need two extra terms to make them equal. First, an extra $-\frac{\lambda^2}{4}T_{-2}T_2\left|\psi_0\right\rangle$ is needed, this term is proportional to $\left|\psi_0\right\rangle$. However, as we are mainly interested in a PEPS representation of this state, we usually don't care about normalization, which is all this term does up to 2-nd order. We thus ignore this term for now.

More important is the term $\frac{\lambda^2}{8}T_0T_2$. Let us think about why this extra term is needed. The second order in the expansion of $e^{-\lambda X}$ immediately gives the correct energy to all states with two pairs of anyons. The extra factor 2 that comes from the expansion of the exponential accounts for the fact that a state with two pairs of excitations has twice the energy of a state that contains only one pair. However, if two X operators act closely together, on spins on the same plaquette, they do not create two different pairs, but rather move the excitations of one pair farther apart. Such a state only has energy two and we have to correct for the fact that the exponential treats it the same as a state where two X operators are applied farther apart. The correct energy is obtained exactly by adding the extra term $\frac{\lambda^2}{8}T_0T_2$.

We can now define a two parameter family of PEPS states as follows,

$$\left|\alpha_1,\alpha_2\right\rangle = \exp\left(-\alpha_2\sum_{\langle ij\rangle}X_iX_j\right)\exp\left(-\alpha_1\sum_i X_i\right)\left|\psi_0\right\rangle$$

with $|\psi_0\rangle$ the ground state of the unperturbed Hamiltonian. We can conclude from the previous discussion that this family of states can capture the ground states of the Hamiltonians

$$H(\lambda) = H_{TC} + \lambda \sum_i X_i$$

at least up to second order by choosing $\alpha_1 = \lambda/2$ and $\alpha_2 = \lambda^2/4$. By keeping the parameters free and optimizing over them, we can do better than this choice. Of course, for very small λ the variational optimum will return the results from perturbation theory. In the remainder of this chapter we discuss a more elaborate ansatz that can capture even more complicated states, still only containing a few free variational parameters. Although the approach we adopt is inspired by the pCUT idea, out method will differ in two ways from the above discussion.

First, the main conceptual difference in the idea is that we combine such ansatz for perturbations from both sides. For instance, we can start from the Hamiltonians H_{TC} and $\sum_i X_i$, apply the above procedure to both and finally combine them into a bigger ansatz that can hopefully capture the phase transition reasonably well from both sides. Second, the usage of PEPS allows us to make the ansatz even bigger and include some additional parameters for no extra cost in the complexity of the computations.

More details are provided in the next sections where we apply this idea both to the Quantum Ising model and the Toric Code.

4.2 Variational Results

We now introduce a general way to write down a PEPS ansatz with only a handful of parameters to capture the ground states of perturbed Hamiltonians. The method is inspired by the discussion of pCUT in Section 4.1.1.3. We then use a recently introduced conjugate gradient method for PEPS [13] to optimize for the ground state of the transverse field Ising Model and the Toric Code in a magnetic field. The motivation behind the ansatz is multifold, some of theoretical, others of numerical nature.

From the theoretical viewpoint, the usage of only a few parameters clarifies how exactly a PEPS encodes a complete many-body wave function into a local tensor. We can build a hierarchy of more complicated PEPS with the ansatz and see how the inclusion of more and more parameters leads to a more powerful and complete PEPS representation. Moreover, we can use convex sets to study the geometry of the reduced density matrices, which gives a neat explanation of the relevant physical phenomena such as phase transition and critical exponents [242]. Next, for topological phases, it is possible with this ansatz to encode the topological properties directly into the local PEPS tensor. The topological phase is then characterized by the part of parameter space where the parameters satisfy some concrete constraints, which makes the identification of phases and transitions between them almost trivial. On the contrary, this is very hard with a standard PEPS calculation as the variational optimum typically does not fulfill such constraints locally [243], hence the identification of phases and phase transitions is hard in such cases.

Numerically, the use of conjugate gradient methods was introduced only recently and the performed benchmarks have been very successful [13]. However, for more general systems than those studied up to now, this method might get stuck in local minima, as happens generally for gradient methods. One of the easiest solutions to this problem is to start from a good initial point that is close enough to the desired minimum. We can first optimize over the ansatz that only has a few parameters and should converge to the global minimum and use this as the initial point for the gradient method on a standard PEPS. Also for some applications, one only desires a quantitative picture, for which our ansatz more than suffices. This can also help for complicated systems where the full method requires too many steps to converge and our simplified ansatz can provide a fast alternative.

4.2.1 The Quantum Ising Model

In this section we study the quantum Ising model in a transverse magnetic field in two spatial dimensions. We introduce a simple variational class of PEPS states that depends on a few parameters but can still capture the interesting physics reasonably well. We study the model

on a square lattice with qubits on every vertex. The Hamiltonian H_{Ising} is defined as follows,

$$H^{\lambda}_{\text{Ising}} = -\sum_{\langle ij \rangle} Z_i Z_j + \lambda \sum_i X_i.$$

Here $\langle ij \rangle$ denotes that i, j are neighboring vertices. From various numerical studies [244] it is known that this model exhibits a phase transition from a symmetry broken to a polarized phase around $\lambda \approx 0.344$ with corresponding order parameter the magnetization, $m = \langle Z \rangle$. This model has already been studied and used as a benchmark extensively with tensor network methods [13, 208, 245, 246].

We now introduce the MPO tensors M_X and M_Z in Fig. 4.1a and Fig. 4.1b respectively.

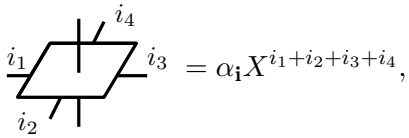

(a) The tensor M_X, for every incoming virtual 1 a physical X is applied.

(b) The tensor M_Z, for every incoming virtual 1 a physical Z is applied.

Figure 4.1

Moreover, we add local fields $L_X = \mathbb{1} - \gamma X$ and $L_Z = \mathbb{1} - \delta Z$. We use these tensors to create a PEPS ansatz as shown in Fig. 4.2.

The idea behind these tensors is the following. The operator L_X is really just a numerically more convenient reparametrization of $\exp(-\gamma X)$ which, as we have seen in Section 4.1.1.3, corresponds to an exponentiated version of the first order perturbation theory result. Next, we discussed how this operator already gets the second order result partly right. Previously, we corrected the remaining flaws by adding $\exp(-\alpha \sum_{\langle ij \rangle} X_i X_j)$ but we now use the MPO M_X that is even more general. The operators L_Z, M_Z serve a similar purpose when starting from the Hamiltonian $\sum_i X_i$ and adding the nearest-neighbor interaction as a perturbation. This is explained in Fig. 4.2.

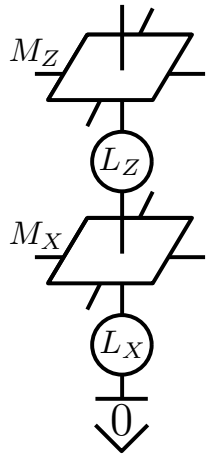

Figure 4.2: We create a PEPS $|\boldsymbol{\alpha}, \boldsymbol{\beta}, \gamma, \delta\rangle$ as follows. We start from one of two symmetry breaking states, let us take the product of all $|0\rangle$ on all spins. We then first act with the local operators L_X, next we act with the MPO M_X, this gives a PEPS with bond dimension $D = 2$. We continue by acting with L_Z and finally with the MPO M_Z. The end result is a PEPS with bond dimension $D = 4$ that depends on 34 parameters. We immediately impose rotational invariance and since furthermore the normalization is free, we end up with only ten parameters. Notice that this ansatz is at least as good as second order perturbation theory. Indeed, by choosing the parameters $\boldsymbol{\beta}$ and δ such that L_Z, M_Z act trivially, we can choose γ such that the operator $L_X = \exp(-\lambda X/8)$ covers the first order perturbation result and $\boldsymbol{\alpha}$ such that it corrects the second order. Conversely, the L_X can create the product state of all $|-\rangle$, the ground state of $\sum_i X_i$ and with aptly chosen parameters L_Z and M_Z can then capture the second order perturbation theory when adding a $\sum_{\langle ij\rangle} Z_i Z_j$ perturbation.

We use a rotation-invariant ansatz. This means we only keep the parameters γ, δ,

$$\alpha_{1000}, \alpha_{1100}, \alpha_{1010}, \alpha_{1110}, \alpha_{1111}$$

and similar for $\boldsymbol{\beta}$. We fix $\alpha_{0000} = \beta_{0000} = 1$ as we are free to normalize the state as we want at this point.

We can now use a conjugate gradient method on the energy functional

$$E(\boldsymbol{\alpha}, \boldsymbol{\beta}, \gamma, \delta) = \frac{\langle \boldsymbol{\alpha}, \boldsymbol{\beta}, \gamma, \delta | H_{\text{ising}} | \boldsymbol{\alpha}, \boldsymbol{\beta}, \gamma, \delta \rangle}{\langle \boldsymbol{\alpha}, \boldsymbol{\beta}, \gamma, \delta | \boldsymbol{\alpha}, \boldsymbol{\beta}, \gamma, \delta \rangle}.$$

We can calculate the gradient as explained in Ref. [174] and use the chain rule to find the gradient in the parameter space we consider. We then proceed in the same way as in a full PEPS gradient method calculation [13] for minimizing the energy, but with only ten parameters instead of $O(D^4 d)$. We show the resulting magnetization, $\langle Z \rangle$, in Fig. 4.3. The results are better then those obtained with a general $D = 2$ PEPS ansatz, but worse than $D = 3$. We expect to be able to obtain significantly better performance by adding additional MPOs, corresponding to even higher orders of perturbation theory.

The magnetization is determined by the parameter δ, that becomes zero at the critical point and remains so beyond the phase transition. This is to be expected because it corresponds to the only operator in the ansatz

that can break the global X symmetry. This behavior is important to identify the phase transition in topological models, where no local order parameter is present. This is illustrated in the next section.

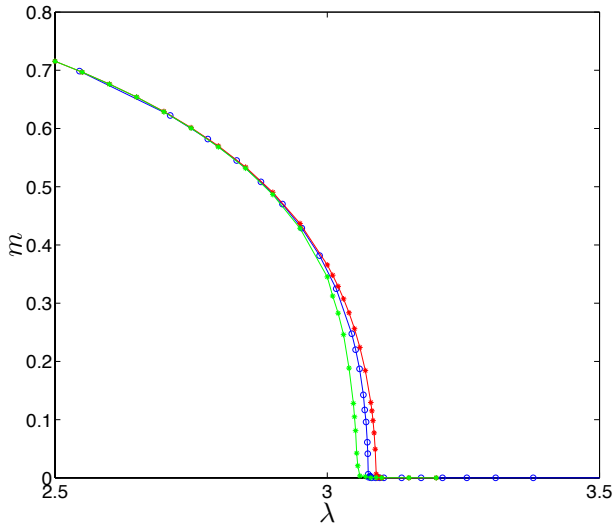

Figure 4.3: The magnetization obtained by an optimization over the discussed PEPS ansatz (blue) and general PEPS with $D = 2$ (red) and $D = 3$ green.

4.2.2 The Toric Code Model

In this section we study the Toric Code in a magnetic field. We use a similar PEPS ansatz as in the previous discussion on the quantum Ising model to describe the phase transition from the topologically ordered to the trivial phase. Recall that the Toric Code Hamiltonian in a magnetic field is given by

$$H_{\mathrm{TC}}^{\lambda} = \sum_{\text{stars } s} \left(\prod_{j \in s} \mathbb{1}_j - A_v \right) + \sum_{\text{plaquettes } p} \left(\prod_{j \in p} \mathbb{1}_j - B_p \right) + \lambda \sum_i X.$$

with the qubits living on the edges of a square lattice. For more details, see Section I.2.4. The ansatz we use is again created by applying a set of operators to a product state. We start with a generalization of the tensor introduced in Fig. 2.9, which is shown in Fig. 4.4.

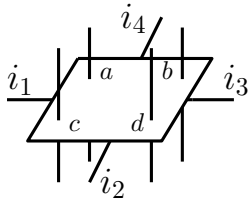

$$= \alpha_{\mathbf{i}} Z_a^{i_1+i_4} \otimes Z_b^{i_3+i_4} \otimes Z_c^{i_1+i_2} \otimes Z_d^{i_2+i_3}$$

Figure 4.4: The tensor M_Z we use to create an ansatz for the Toric Code in a magnetic field. The coefficients $\alpha_{\mathbf{i}}$ can be freely chosen, though we restrict ourselves to the rotation-invariant case.

Notice that the operator we get by contracting such tensors only contains terms that commute with the $A_v = X^{\otimes 4}$ terms in H_{TC}. Again, we choose the parameters $\alpha_{\mathbf{i}} = \alpha_{i_1 i_2 i_3 i_4}$ rotation-invariant and pick $\alpha_{0000} = 1$ which leaves five parameters. Remark that the choice $\alpha_{\mathbf{i}} = 1$ gives us an operator which, when applied to the product state of all $|+\rangle$ returns the Toric Code PEPS from Fig. 2.9.

We now turn to the generalization of the tensor M_X from Fig. 4.1a. One possibility would be the blocking of four such tensors such that it can be applied to the blocked super-sites we use in the PEPS description of the Toric Code. We opt for the alternative tensor shown in Fig. 4.5.

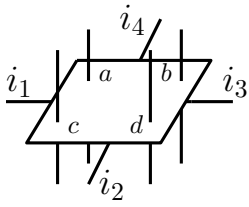

$$= \alpha_{\mathbf{i}} O_{ac}^{i_1} O_{cd}^{i_2} O_{bd}^{i_3} O_{ab}^{i_4}$$

Figure 4.5: The tensor M_X, with $O_{ab} = \mathbb{1}_a \otimes X_b + X_a \otimes \mathbb{1}_b$.

Recall that the intuition behind the operators M_Z, M_X is that they correct the state up to at least 2-nd order in perturbation theory. They achieve this typically by allowing to differentiate between a state with two pairs of excitation and a state with one pair, but where the constituting excitations are farther apart. The first order correction can typically

be achieved with only local operators.

We now turn our attention to these local operators we need to include in the ansatz. Recall that in the way we construct the Toric Code state as a PEPS by blocking four sites we made a choice such that the A_v terms are local or plaquette interactions while the B_p terms are always nearest-neighbor interactions. There is no fundamental problem with treating four-site interactions numerically with PEPS, however for simplicity we restrict ourselves to two-site interactions in our calculations. We then can only use operators that commute with the A_v terms, as we do not want to evaluate such terms. If we now start from a product state of all $|+\rangle$ states, the expectation value of the A_v terms is constant throughout the ansatz.

Given this constraint, we cannot add a non-trivial local operator that acts as a local Z. We can still include all local operators that contain only X operators. We suspect that the most relevant among these is a local $\mathbb{1} - \gamma X$ operator, which we used in the transverse quantum Ising model ansatz. We can also include

$$X_a \otimes X_b,\ X_a \otimes X_d,\ X_a \otimes X_b \otimes X_c,\ X_a \otimes X_b \otimes X_c \otimes X_d$$

and all rotations of these operators. Because they do not change the bond dimension, they also do not increase the computational complexity of the tensor contractions in the calculations.

This gives us five parameters for both M_Z, M_X and since we include five different local operators, the total number of parameters is 15, for a PEPS with bond dimension $D = 4$. This number has to be compared with the number of parameters in a general PEPS, which is 4096 in this case, although this number can also be lowered by imposing rotational invariance.

To illustrate the idea behind the ansatz, we use a simpler variant of the ansatz, given by

$$\exp\left(-\gamma \sum_{\langle ij \rangle} X_i X_j\right) \exp\left(-\beta \sum_i X\right) \prod_p \left(1 - \alpha \prod_{i \in p} Z_i\right) \prod_i |+\rangle\,. \tag{4.3}$$

We can compute the energy expectation of the terms B_p and X for all states in the ansatz, remember that A_v is constant. If we would do this with all possible quantum states, the resulting set would be convex [242]. However, this is not necessarily the case here.

We are interested in the extreme points of the set we get by computing an plotting the expectation values. For $\alpha = 1$ and β varying, the set is not convex at all, but allowing $\alpha \neq 1$ makes the set convex, at least numerically. We can look at the tangent lines at an extreme point of the set. If the derivative at a point is given by $\tan\theta$, that point corresponds to the lowest energy state in our ansatz of the Hamiltonian

$$H(\theta) = \cos\theta \sum_{\text{plaquettes } p} \left(\prod_{j \in p} \mathbb{1}_j - B_p \right) + \sin\theta \sum_i X.$$

and thus to the best approximation of the ground state of $H(\theta)$ in our ansatz.

The value $\alpha = 1$ corresponds to PEPS that are topologically ordered, whereas $\alpha \neq 1$ corresponds to PEPS in the trivial phase. We can thus determine the phase transition in our ansatz by looking at the point where the states with $\alpha = 1$ are not longer extreme points of the set. This situation is shown in Fig. 4.6. We plot the extreme points for $\alpha = 0.75$ (black), $\alpha = 0.85$ (green), $\alpha = 0.95$ (red) and $\alpha = 1$ (blue) with β the remaining free parameter, we fixed $\gamma = 0$ for now. We are interested in the lowest crossing point of the $\alpha = 1$ curve with any of the others. Remarkably, this happens not at the origin but at a finite value of $\langle X \rangle$, it is this feature that shows the stability of the topological phase to the X perturbations. We checked this for values like $\alpha = 0.99, 0.995, 0.999, \ldots$ closer to $\alpha = 1$ and this conclusion remains true. We do not plot all these curves to keep the figures as clear as possible.

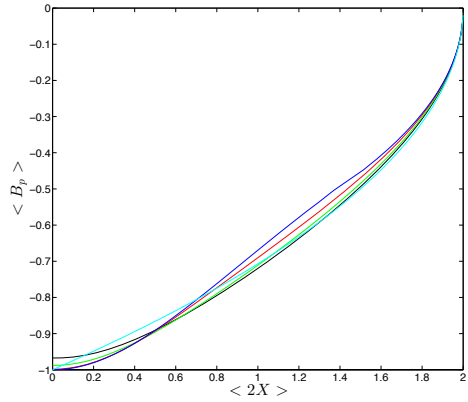

Figure 4.6: The extreme points of the variational states of the ansatz in Eq. 4.3 with $\gamma = 1$, β free and α fixed to 0.75 (black), 0.85 (green), 0.95 (red) and 1 (blue). The mean field ansatz from Ref. [247] is shown in cyan.

In Fig. 4.7 we show a zoomed in version of Fig. 4.6. Visually, the situation does not change a lot by including the parameter γ, therefor we omit this parameter from the figures.

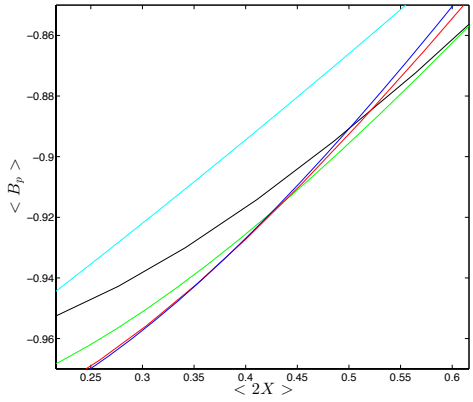

Figure 4.7: A zoomed in version of Fig. 4.6.

However, we include this parameter to compute the critical point as explained above. This gives $\lambda_c \approx 0.324$, which is to be compared with the result $\lambda_c \approx 0.328$ from Monte Carlo [99] and perturbative

calculations [101]. It is a very significant improvement on the ansatz that only includes the parameter α [247], which gives $\lambda_c = \frac{1}{4}$.

4.3 Outlook and Conclusion

In this chapter we have used insights from perturbation theory, more specifically pCUT, to motivate the usage of an ansatz for the description of ground states of perturbed Hamiltonians. The ansatz is a subset of PEPS states, but contains only a handful of parameters, as we only include operators whose present we expect from perturbation theory. The ansatz gives a good description of the ground states on both sides of the phase transition that is studied and thereby overcomes a familiar problem of PEPS methods.

A first computation results in a good approximation of the critical point of the Ising model. For the Toric Code, a full optimization over the ansatz is not yet obtained. However, we did use a simplified version of the ansatz, with only three parameters, to study the Toric Code. For such a topologically ordered model, the determination of the critical point is not straightforward with standard PEPS methods, because of the absence of a local order parameter. The topological character of the phase is however encoded in the restricted variational set of parameters we consider. This makes it straightforward to determine the critical point.

We expect that the method will be of use, both theoretically and numerically, in the future. However, at this point in time, we have not fully explored the power and usefulness of the ansatz and deeper investigations of the Toric Code as well as more complicated models are required.

Outlook and Conclusions

At the end of my dissertation, I would like to give a more personal account of my experience during the four years of my fellowship, as well as my, perhaps biased, personal opinion of the future research in and prospects of the field and my own modest contributions to it. For an academic outlook and conclusion, I refer the reader to those at the end of the individual chapters.

First of all it has been an incredibly rewarding experience to dive into the field of tensor networks and learn about its history and accomplishments. Although it started with the combination of insights from renormalization group theory, statistical physics and quantum information theory to develop methods for condensed matter systems, over the years, it has encompassed more and more branches of physics and science in general, the next one even more surprising than the previous one. At this point, black-hole physics, AdS-CFT, quantum chemistry, artificial intelligence and several others have established firm connections with tensor networks. Indeed, for a student as myself tensor networks sometimes seem like an overly holistic concept, in whose language every other field can be recast.

It is thus very clear that the field has positioned itself on a very interesting crossing point between a remarkable amount and variety of branches of science and history tells us that it are often exactly these fields that prove to be the most rewarding and successful. Although at this point, it is not clear if, or to what extent the huge expectations and promises that are attributed to tensor networks can be fulfilled, the field can already be proud of its impressive catalog of achievements.

The first accomplishments were in the numerical study of correlated quantum spin chains. Starting with work by Baxter on the corner transfer matrix, through White's immensely successful Density Matrix Renormalization Group, and now with the existence of a multitude of different methods, the application of tensor network states to 1D quantum spin chains has been nothing but a tremendous triumph. In my view, we have arrived at a point where the numerical simulation of such systems is more or less under complete control as we can compute desired quantities up to almost machine precision in a lot of cases. It is true that some problems still persist, for instance the simulation of systems for longer time frames, but there is no reason to think that they cannot be solved over time with some effort and the foreseeable increase in computational resources.

Tensor networks are nowadays also commonly used as a tool for proving theoretical results. Whereas in the beginning, mainly known results were proven in a different, insightful, way, more and more new results are obtained through their use. The most remarkable of these is perhaps the classification of symmetry protected phases in 1D spin chains. I'm confident that this area of research still has not reached its limits yet and more exciting opportunities lie waiting around the corner, ready to be discovered. However, to reach the full potential of tensor network states, we should focus our attention on higher-dimensional systems.

In this dissertation I have contributed to the study of entanglement and tensor networks in higher dimensions. I hope the entanglement rate bound will find more applications in the field of quantum information. It would be great if the result on the stability of the area law in a phase is in time superseded by a full proof of the area law, something that I reckon should be possible, at least under some additional restrictions. A lot of work is already being done throughout the communities in this direction.

The study of the entanglement of distillation in gauge theories should be generalized to more physically relevant gauge theories, not only on the lattice but eventually full-fledged quantum field theories. Hopefully this can provide insights and prove to be relevant for some of the issues, most notably the firewall paradox, that are still unresolved. I myself,

unfortunately, do not have the background to give an educated guess about how successful this approach will turn out to be.

The understanding of topological order in tensor networks has proven to be very successful and has now reproduced most known results from the literature. It has also already provided new, and from my point of view, better ways of obtaining results and opened up the way for numerical simulations. However, now that we have caught up with other communities, it is time to start making a difference and obtain truly new results and insights. Work on the understanding of fermionic phases and symmetry-enriched phases is already underway and extremely promising. I'm confident that such results will be obtained and make a difference in the very near future.

Finally, we come to the numerical aspect of tensor networks, which is the facet that excites me personally the most, although I myself only made very modest contributions to it. In the last chapter we have introduced an ansatz to do efficient calculations in 2D, and it is my conviction that this route will provide insight and useful numerics in the near future for generic phase transitions. However, I believe we can be more ambitious than this. With a more concentrated effort of the community, combined with ever increasing computational resources, new efficient algorithms for the simulation of 2D quantum spin systems can be within our grasp. Although the true understanding of the phase diagram of difficult, but extremely relevant systems, such as the Hubbard model, is probably not something that can be achieved presently, I do strongly believe that such groundbreaking accomplishments are within the reach of tensor network methods.

So it is with a mix of positive feelings that I conclude my dissertation. Grateful for the experience, proud of my achievements, excited about the possibilities and above all, hopeful for the future.

Bibliography

[1] M. Fannes, B. Nachtergaele, and R. F. Werner. “Finitely correlated states on quantum spin chains”. In: *Communications in Mathematical Physics* 144.3 (1992), pp. 443–490. ISSN: 1432-0916. DOI: 10.1007/BF02099178. URL: http://dx.doi.org/10.1007/BF02099178.

[2] F. Verstraete and J. I. Cirac. “Renormalization algorithms for quantum-many body systems in two and higher dimensions”. In: *arXiv preprint cond-mat/0407066* (2004).

[3] G. Vidal. “Class of Quantum Many-Body States That Can Be Efficiently Simulated”. In: *Phys. Rev. Lett.* 101 (Sept. 2008), p. 110501. DOI: 10.1103/PhysRevLett.101.110501. URL: http://link.aps.org/doi/10.1103/PhysRevLett.101.110501.

[4] D. Pérez-García et al. “Matrix Product State Representations”. In: *Quantum Info. Comput.* 7.5 (July 2007), pp. 401–430. ISSN: 1533-7146. URL: http://dl.acm.org/citation.cfm?id=2011832.2011833.

[5] R. Orús. “A practical introduction to tensor networks: Matrix product states and projected entangled pair states”. In: *Annals of Physics* 349 (2014), pp. 117–158.

[6] R. Orús. “Advances on tensor network theory: symmetries, fermions, entanglement, and holography”. In: *The European Physical Journal B* 87.11 (2014), pp. 1–18. ISSN: 1434-6036. DOI: 10.1140/epjb/e2014-50502-9. URL: http://dx.doi.org/10.1140/epjb/e2014-50502-9.

[7] J. C. Bridgeman and C. T. Chubb. “Hand-waving and Interpretive Dance: An Introductory Course on Tensor Networks”. In: *arXiv preprint arXiv:1603.03039* (2016).

[8] J. Eisert. “Entanglement and tensor network states”. In: *arXiv preprint arXiv:1308.3318* (2013).

[9] N. Schuch. “Condensed Matter Applications of Entanglement Theory”. In: *arXiv preprint arXiv:1306.5551* (2013).

[10] U. Schollwöck. “The density-matrix renormalization group in the age of matrix product states”. In: *Annals of Physics* 326.1 (2011), pp. 96–192.

[11] F. Verstraete, V. Murg, and J. I. Cirac. “Matrix product states, projected entangled pair states, and variational renormalization group methods for quantum spin systems”. In: *Advances in Physics* 57.2 (2008), pp. 143–224.

[12] P. Corboz. “Variational optimization with infinite projected entangled-pair states”. In: *arXiv preprint arXiv:1605.03006* (2016).

[13] L. Vanderstraeten et al. “Gradient methods for variational optimisation of projected entangled-pair states”. In: *arXiv preprint arXiv:1606.09170* (2016).

[14] S. R. White. “Density matrix formulation for quantum renormalization groups”. In: *Phys. Rev. Lett.* 69 (Nov. 1992), pp. 2863–2866. DOI: 10.1103/PhysRevLett.69.2863. URL: http://link.aps.org/doi/10.1103/PhysRevLett.69.2863.

[15] S. Östlund and S. Rommer. “Thermodynamic Limit of Density Matrix Renormalization”. In: *Phys. Rev. Lett.* 75 (Nov. 1995), pp. 3537–3540. DOI: 10.1103/PhysRevLett.75.3537. URL: http://link.aps.org/doi/10.1103/PhysRevLett.75.3537.

[16] B. Pirvu et al. “Matrix product operator representations”. In: *New Journal of Physics* 12.2 (2010), p. 025012.

[17] F. Verstraete, J. J. García-Ripoll, and J. I. Cirac. “Matrix Product Density Operators: Simulation of Finite-Temperature and Dissipative Systems”. In: *Phys. Rev. Lett.* 93 (Nov. 2004), p. 207204. DOI: 10.1103/PhysRevLett.93.207204. URL: http://link.aps.org/doi/10.1103/PhysRevLett.93.207204.

[18] M. B. Hastings. “Solving gapped Hamiltonians locally”. In: *Phys. Rev. B* 73 (Feb. 2006), p. 085115. DOI: 10.1103/PhysRevB.73.085115. URL: http://link.aps.org/doi/10.1103/PhysRevB.73.085115.

[19] M. Kliesch et al. “Locality of Temperature”. In: *Phys. Rev. X* 4 (July 2014), p. 031019. DOI: 10.1103/PhysRevX.4.031019. URL: http://link.aps.org/doi/10.1103/PhysRevX.4.031019.

[20] A. Molnar et al. “Approximating Gibbs states of local Hamiltonians efficiently with projected entangled pair states”. In: *Phys. Rev. B* 91 (Jan. 2015), p. 045138. DOI: 10.1103/PhysRevB.91.045138. URL: http://link.aps.org/doi/10.1103/PhysRevB.91.045138.

[21] N. Schuch, J. I. Cirac, and D. Pérez-García. “PEPS as ground states: Degeneracy and topology”. In: *Annals of Physics* 325.10 (2010), pp. 2153 –2192. ISSN: 0003-4916. DOI: http://dx.doi.org/10.1016/j.aop.2010.05.008. URL: http://www.sciencedirect.com/science/article/pii/S0003491610000990.

[22] D. J. Williamson et al. “Matrix product operators for symmetry-protected topological phases”. In: *arXiv preprint arXiv:1412.5604* (2014).

[23] M. Burak Şahinoğlu et al. “Characterizing Topological Order with Matrix Product Operators”. In: *arXiv preprint arXiv:1409.2150* (2014).

[24] N. Bultinck et al. “Anyons and matrix product operator algebras”. In: *arXiv preprint arXiv:1511.08090* (2015).

[25] J. I. Cirac et al. “Matrix Product Density Operators: Renormalization Fixed Points and Boundary Theories”. In: *arXiv preprint arXiv:1606.00608* (2016).

[26] O. Buerschaper. “Twisted injectivity in projected entangled pair states and the classification of quantum phases”. In: *Annals of Physics* 351 (2014), pp. 447 –476. ISSN: 0003-4916. DOI: http://dx.doi.org/10.1016/j.aop.2014.09.007. URL: http://www.sciencedirect.com/science/article/pii/S000349161400267X.

[27] N. Schuch et al. “Entropy Scaling and Simulability by Matrix Product States”. In: *Phys. Rev. Lett.* 100 (Jan. 2008), p. 030504. DOI: 10.1103/PhysRevLett.100.030504. URL: http://link.aps.org/doi/10.1103/PhysRevLett.100.030504.

[28] F. Verstraete and J. I. Cirac. “Matrix product states represent ground states faithfully”. In: *Phys. Rev. B* 73 (Mar. 2006), p. 094423. DOI: 10.1103/PhysRevB.73.094423. URL: http://link.aps.org/doi/10.1103/PhysRevB.73.094423.

[29] M. B. Hastings. “An area law for one-dimensional quantum systems”. In: *Journal of Statistical Mechanics: Theory and Experiment* 2007.08 (2007), P08024. URL: http://stacks.iop.org/1742-5468/2007/i=08/a=P08024.

[30] I. Arad et al. “An area law and sub-exponential algorithm for 1D systems”. In: *arXiv preprint arXiv:1301.1162* (2013).

[31] M. B. Hastings and T. Koma. “Spectral Gap and Exponential Decay of Correlations”. In: *Communications in Mathematical Physics* 265.3 (2006), pp. 781–804. ISSN: 1432-0916. DOI: 10.1007/s00220-006-0030-4. URL: http://dx.doi.org/10.1007/s00220-006-0030-4.

[32] B. Nachtergaele and R. Sims. “Lieb-Robinson Bounds and the Exponential Clustering Theorem”. In: *Communications in Mathematical Physics* 265.1 (2006), pp. 119–130. ISSN: 1432-0916. DOI: 10.1007/s00220-006-1556-1. URL: http://dx.doi.org/10.1007/s00220-006-1556-1.

[33] F. G.S. L. Brandão and M. Horodecki. “Exponential Decay of Correlations Implies Area Law”. In: *Communications in Mathematical Physics* 333.2 (2015), pp. 761–798. ISSN: 1432-0916. DOI: 10.1007/s00220-014-2213-8. URL: http://dx.doi.org/10.1007/s00220-014-2213-8.

[34] B. Nachtergaele. “The spectral gap for some spin chains with discrete symmetry breaking”. In: *Communications in Mathematical Physics* 175.3 (1996), pp. 565–606. ISSN: 1432-0916. DOI: 10.1007/BF02099509. URL: http://dx.doi.org/10.1007/BF02099509.

[35] I. Affleck et al. “Rigorous results on valence-bond ground states in antiferromagnets”. In: *Phys. Rev. Lett.* 59 (Aug. 1987), pp. 799–802. DOI: 10.1103/PhysRevLett.59.799. URL: http://link.aps.org/doi/10.1103/PhysRevLett.59.799.

[36] F. Verstraete et al. “Criticality, the Area Law, and the Computational Power of Projected Entangled Pair States”. In: *Phys. Rev. Lett.* 96 (June 2006), p. 220601. DOI: 10.1103/PhysRevLett.96.220601. URL: http://link.aps.org/doi/10.1103/PhysRevLett.96.220601.

[37] Y. Ge and J. Eisert. “Area laws and approximations of quantum many-body states”. In: *ArXiv e-prints-[quant-ph]* 1411 (2014).

[38] O. Bratteli and D. W. Robinson. *Operator Algebras and Quantum Statistical Mechanics Vol. 2: Equilibrium States, Models in Quantum Statistical Mechanics*. Springer-Verlag, 1981.

[39] E. H. Lieb and D. W. Robinson. “The finite group velocity of quantum spin systems”. In: *Communications in Mathematical Physics* 28.3 (1972), pp. 251–257. ISSN: 1432-0916. DOI: 10.1007/BF01645779. URL: http://dx.doi.org/10.1007/BF01645779.

[40] S. Bravyi, M. B. Hastings, and F. Verstraete. “Lieb-Robinson Bounds and the Generation of Correlations and Topological Quantum Order”. In: *Phys. Rev. Lett.* 97 (July 2006), p. 050401. DOI: 10.1103/PhysRevLett.97.050401. URL: http://link.aps.org/doi/10.1103/PhysRevLett.97.050401.

[41] B. Nachtergaele, Y. Ogata, and R. Sims. “Propagation of Correlations in Quantum Lattice Systems”. In: *Journal of Statistical Physics* 124.1 (2006), pp. 1–13. ISSN: 1572-9613. DOI: 10.1007/s10955-006-9143-6. URL: http://dx.doi.org/10.1007/s10955-006-9143-6.

[42] B. Nachtergaele et al. “On the Existence of Dynamics for Anharmonic Quantum Oscillator Systems”. In: *Reviews in Mathematical Physics* 22.02 (2010), pp. 207–231. DOI: 10.1142/S0129055X1000393X. URL: http://www.worldscientific.com/doi/abs/10.1142/S0129055X1000393X.

[43] B. Nachtergaele et al. “Lieb-Robinson Bounds for Harmonic and Anharmonic Lattice Systems”. In: *Communications in Mathematical Physics* 286.3 (2009), pp. 1073–1098. ISSN: 1432-0916. DOI: 10.1007/s00220-008-0630-2. URL: http://dx.doi.org/10.1007/s00220-008-0630-2.

[44] M. Hastings. “Quasi-adiabatic continuation for disordered systems: Applications to correlations, Lieb-Schultz-Mattis, and Hall conductance”. In: *preprint arXiv:1001.5280* (2010).

[45] M. B. Hastings and S. Michalakis. “Quantization of Hall Conductance for Interacting Electrons on a Torus”. In: *Communications in Mathematical Physics* 334.1 (2015), pp. 433–471. ISSN: 1432-0916. DOI: 10.1007/s00220-014-2167-x. URL: http://dx.doi.org/10.1007/s00220-014-2167-x.

[46] M Hastings. “Locality in quantum systems”. In: *Quantum Theory from Small to Large Scales* 95 (2010), pp. 171–212.

[47] M. B. Hastings and X.-G. Wen. “Quasiadiabatic continuation of quantum states: The stability of topological ground-state degeneracy and emergent gauge invariance”. In: *Phys. Rev. B* 72 (July 2005), p. 045141. DOI: 10.1103/PhysRevB.72.045141. URL: http://link.aps.org/doi/10.1103/PhysRevB.72.045141.

[48] M. B. Hastings. “Lieb-Schultz-Mattis in higher dimensions”. In: *Phys. Rev. B* 69 (Mar. 2004), p. 104431. DOI: 10.1103/PhysRevB.69.104431. URL: http://link.aps.org/doi/10.1103/PhysRevB.69.104431.

[49] S. Bachmann et al. “Automorphic Equivalence within Gapped Phases of Quantum Lattice Systems”. In: *Communications in Mathematical Physics* 309.3 (2012), pp. 835–871. ISSN: 1432-0916. DOI: 10.1007/s00220-011-1380-0. URL: http://dx.doi.org/10.1007/s00220-011-1380-0.

[50] M. B. Hastings. “Quasi-adiabatic continuation in gapped spin and fermion systems: Goldstone’s theorem and flux periodicity”. In: *Journal of Statistical Mechanics: Theory and Experiment* 2007.05 (2007), P05010. URL: http://stacks.iop.org/1742-5468/2007/i=05/a=P05010.

[51] S. Bravyi, M. B. Hastings, and S. Michalakis. “Topological quantum order: Stability under local perturbations”. In: *Journal of Mathematical Physics* 51.9, 093512 (2010). DOI: http://dx.doi.org/10.1063/1.3490195. URL: http://scitation.aip.org/content/aip/journal/jmp/51/9/10.1063/1.3490195.

[52] T. J. Osborne. “Simulating adiabatic evolution of gapped spin systems”. In: *Phys. Rev. A* 75 (Mar. 2007), p. 032321. DOI: 10.1103/PhysRevA.75.032321. URL: http://link.aps.org/doi/10.1103/PhysRevA.75.032321.

[53] J. E. Avron, R. Seiler, and L. G. Yaffe. “Adiabatic theorems and applications to the quantum hall effect”. In: *Communications in Mathematical Physics* 110.1 (1987), pp. 33–49. ISSN: 1432-0916. DOI: 10.1007/BF01209015. URL: http://dx.doi.org/10.1007/BF01209015.

[54] M. B. Hastings. “Topology and phases in fermionic systems”. In: *Journal of Statistical Mechanics: Theory and Experiment* 2008.01 (2008), p. L01001. URL: http://stacks.iop.org/1742-5468/2008/i=01/a=L01001.

[55] B. Nachtergaele and R. Sims. “A Multi-Dimensional Lieb-Schultz-Mattis Theorem”. In: *Communications in Mathematical Physics* 276.2 (2007), pp. 437–472. ISSN: 1432-0916. DOI: 10.1007/s00220-007-0342-z. URL: http://dx.doi.org/10.1007/s00220-007-0342-z.

[56] S. Michalakis and J. P. Zwolak. “Stability of Frustration-Free Hamiltonians”. In: *Communications in Mathematical Physics* 322.2 (2013), pp. 277–302. ISSN: 1432-0916. DOI: 10.1007/s00220-013-1762-6. URL: http://dx.doi.org/10.1007/s00220-013-1762-6.

[57] S. Bachmann and Y. Ogata. “C 1-Classification of Gapped Parent Hamiltonians of Quantum Spin Chains”. In: *Communications in Mathematical Physics* 338.3 (2015), pp. 1011–1042. ISSN: 1432-0916. DOI: 10.1007/s00220-015-2350-8. URL: http://dx.doi.org/10.1007/s00220-015-2350-8.

[58] T. J. Osborne. “Ground state of a class of noncritical one-dimensional quantum spin systems can be approximated efficiently”. In: *Phys. Rev. A* 75 (Apr. 2007), p. 042306. DOI: 10.1103/PhysRevA.75.042306. URL: http://link.aps.org/doi/10.1103/PhysRevA.75.042306.

[59] M. Mariën et al. “Entanglement Rates and the Stability of the Area Law for the Entanglement Entropy”. In: *Communications in Mathematical Physics* 346.1 (2016), pp. 35–73. ISSN: 1432-0916. DOI: 10.1007/s00220-016-2709-5. URL: http://dx.doi.org/10.1007/s00220-016-2709-5.

[60] J. D. V. S. W. Graham. “A Class of Extremal Functions for the Fourier Transform”. In: *Transactions of the American Mathematical Society* 265.1 (1981), pp. 283–302. ISSN: 00029947. URL: http://www.jstor.org/stable/1998495.

[61] J. D. Vaaler. “Some extremal functions in Fourier analysis”. In: *Bulletin of the American Mathematical Society* 12.2 (1985), pp. 183–216.

[62] A. Ingham. “A note on Fourier transforms”. In: *Journal of the London Mathematical Society* 1.1 (1934), pp. 29–32.

[63] J. Dziubanski and E. Hernández. “Band-limited wavelets with subexponential decay”. In: *Canadian Mathematical Bulletin* 41.4 (1998), pp. 398–403.

[64] L. Landau. “EM Lifshitz Statistical Physics”. In: *Course of Theoretical Physics* 5 (1958).

[65] F. J. Wegner. “Duality in Generalized Ising Models and Phase Transitions without Local Order Parameters”. In: *Journal of Mathematical Physics* 12.10 (1971), pp. 2259–2272. DOI: http://dx.doi.org/10.1063/1.1665530. URL: http://scitation.aip.org/content/aip/journal/jmp/12/10/10.1063/1.1665530.

[66] J. M. Kosterlitz and D. J. Thouless. “Ordering, metastability and phase transitions in two-dimensional systems”. In: *Journal of Physics C: Solid State Physics* 6.7 (1973), p. 1181. URL: http://stacks.iop.org/0022-3719/6/i=7/a=010.

[67] D. C. Tsui, H. L. Stormer, and A. C. Gossard. “Two-Dimensional Magnetotransport in the Extreme Quantum Limit”. In: *Phys. Rev. Lett.* 48 (May 1982), pp. 1559–1562. DOI: 10.1103/PhysRevLett.48.1559. URL: http://link.aps.org/doi/10.1103/PhysRevLett.48.1559.

[68] R. B. Laughlin. “Anomalous Quantum Hall Effect: An Incompressible Quantum Fluid with Fractionally Charged Excitations”. In: *Phys. Rev. Lett.* 50 (May 1983), pp. 1395–1398. DOI: 10.1103/PhysRevLett.50.1395. URL: http://link.aps.org/doi/10.1103/PhysRevLett.50.1395.

[69] X. G. Wen and Q. Niu. "Ground-state degeneracy of the fractional quantum Hall states in the presence of a random potential and on high-genus Riemann surfaces". In: *Phys. Rev. B* 41 (May 1990), pp. 9377–9396. DOI: 10.1103/PhysRevB.41.9377. URL: http://link.aps.org/doi/10.1103/PhysRevB.41.9377.

[70] G. Moore and N. Read. "Nonabelions in the fractional quantum hall effect". In: *Nuclear Physics B* 360.2 (1991), pp. 362 –396. ISSN: 0550-3213. DOI: http://dx.doi.org/10.1016/0550-3213(91)90407-O. URL: http://www.sciencedirect.com/science/article/pii/055032139190407O.

[71] B. Zeng et al. "Quantum Information Meets Quantum Matter–From Quantum Entanglement to Topological Phase in Many-Body Systems". In: *arXiv preprint arXiv:1508.02595* (2015).

[72] M. V. Berry. "Quantal phase factors accompanying adiabatic changes". In: *Proceedings of the Royal Society of London A: Mathematical, Physical and Engineering Sciences*. Vol. 392. The Royal Society. 1984, pp. 45–57.

[73] B. Simon. "Holonomy, the Quantum Adiabatic Theorem, and Berry's Phase". In: *Phys. Rev. Lett.* 51 (Dec. 1983), pp. 2167–2170. DOI: 10.1103/PhysRevLett.51.2167. URL: http://link.aps.org/doi/10.1103/PhysRevLett.51.2167.

[74] F. Wilczek and A. Zee. "Appearance of Gauge Structure in Simple Dynamical Systems". In: *Phys. Rev. Lett.* 52 (June 1984), pp. 2111–2114. DOI: 10.1103/PhysRevLett.52.2111. URL: http://link.aps.org/doi/10.1103/PhysRevLett.52.2111.

[75] E. Verlinde. "Fusion rules and modular transformations in 2D conformal field theory". In: *Nuclear Physics B* 300 (1988), pp. 360 –376. ISSN: 0550-3213. DOI: http://dx.doi.org/10.1016/0550-3213(88)90603-7. URL: http://www.sciencedirect.com/science/article/pii/0550321388906037.

[76] P. I. Etingof et al. *Tensor categories*. Vol. 205. American Mathematical Society, 2015.

[77] F. Wilczek. "Quantum Mechanics of Fractional-Spin Particles". In: *Phys. Rev. Lett.* 49 (Oct. 1982), pp. 957–959. DOI: 10.1103/PhysRevLett.49.957. URL: http://link.aps.org/doi/10.1103/PhysRevLett.49.957.

[78] A. Kitaev. "Anyons in an exactly solved model and beyond". In: *Annals of Physics* 321.1 (2006). January Special Issue, pp. 2 –111. ISSN: 0003-4916. DOI: http://dx.doi.org/10.1016/j.aop.2005.10.005. URL: http://www.sciencedirect.com/science/article/pii/S0003491605002381.

[79] Z. Wang. *Topological quantum computation*. Vol. 112. American Mathematical Soc., 2010.

[80] S. MacLane. "Natural associativity and commutativity". In: *Rice Institute Pamphlet-Rice University Studies* 49.4 (1963).

[81] G. Kelly. “On MacLane’s conditions for coherence of natural associativities, commutativities, etc.” In: *Journal of Algebra* 1.4 (1964), pp. 397 –402. ISSN: 0021-8693. DOI: http://dx.doi.org/10.1016/0021-8693(64)90018-3. URL: http://www.sciencedirect.com/science/article/pii/0021869364900183.

[82] G. Moore and N. Seiberg. “Polynomial equations for rational conformal field theories”. In: *Physics Letters B* 212.4 (1988), pp. 451 –460. ISSN: 0370-2693. DOI: http://dx.doi.org/10.1016/0370-2693(88)91796-0. URL: http://www.sciencedirect.com/science/article/pii/0370269388917960.

[83] C. Vafa. “Toward classification of conformal theories”. In: *Physics Letters B* 206.3 (1988), pp. 421 –426. ISSN: 0370-2693. DOI: http://dx.doi.org/10.1016/0370-2693(88)91603-6. URL: http://www.sciencedirect.com/science/article/pii/0370269388916036.

[84] R. F. Streater and A. S. Wightman. *PCT, spin and statistics, and all that*. Princeton University Press, 2000.

[85] Y. Zhang et al. “Quasiparticle statistics and braiding from ground-state entanglement”. In: *Phys. Rev. B* 85 (June 2012), p. 235151. DOI: 10.1103/PhysRevB.85.235151. URL: http://link.aps.org/doi/10.1103/PhysRevB.85.235151.

[86] X. Chen et al. “Symmetry protected topological orders and the group cohomology of their symmetry group”. In: *Phys. Rev. B* 87 (Apr. 2013), p. 155114. DOI: 10.1103/PhysRevB.87.155114. URL: http://link.aps.org/doi/10.1103/PhysRevB.87.155114.

[87] N. Schuch, D. Pérez-García, and J. I. Cirac. “Classifying quantum phases using matrix product states and projected entangled pair states”. In: *Phys. Rev. B* 84 (Oct. 2011), p. 165139. DOI: 10.1103/PhysRevB.84.165139. URL: http://link.aps.org/doi/10.1103/PhysRevB.84.165139.

[88] X. Chen, Z.-C. Gu, and X.-G. Wen. “Classification of gapped symmetric phases in one-dimensional spin systems”. In: *Phys. Rev. B* 83 (Jan. 2011), p. 035107. DOI: 10.1103/PhysRevB.83.035107. URL: http://link.aps.org/doi/10.1103/PhysRevB.83.035107.

[89] X. Chen, Z.-X. Liu, and X.-G. Wen. “Two-dimensional symmetry-protected topological orders and their protected gapless edge excitations”. In: *Phys. Rev. B* 84 (Dec. 2011), p. 235141. DOI: 10.1103/PhysRevB.84.235141. URL: http://link.aps.org/doi/10.1103/PhysRevB.84.235141.

[90] M. A. Nielsen and I. L. Chuang. *Quantum computation and quantum information*. Cambridge university press, 2010.

[91] A. Kitaev and J. Preskill. “Topological Entanglement Entropy”. In: *Phys. Rev. Lett.* 96 (Mar. 2006), p. 110404. DOI: 10.1103/PhysRevLett.96.110404. URL: http://link.aps.org/doi/10.1103/PhysRevLett.96.110404.

[92] M. Levin and X.-G. Wen. "Detecting Topological Order in a Ground State Wave Function". In: *Phys. Rev. Lett.* 96 (Mar. 2006), p. 110405. DOI: 10.1103/PhysRevLett.96.110405. URL: http://link.aps.org/doi/10.1103/PhysRevLett.96.110405.

[93] J. Haah. "An Invariant of Topologically Ordered States Under Local Unitary Transformations". In: *Communications in Mathematical Physics* 342.3 (2016), pp. 771–801. ISSN: 1432-0916. DOI: 10.1007/s00220-016-2594-y. URL: http://dx.doi.org/10.1007/s00220-016-2594-y.

[94] F. A. Bais and J. C. Romers. "The modular S-matrix as order parameter for topological phase transitions". In: *New Journal of Physics* 14.3 (2012), p. 035024. URL: http://stacks.iop.org/1367-2630/14/i=3/a=035024.

[95] A. Kitaev. "Fault-tolerant quantum computation by anyons". In: *Annals of Physics* 303.1 (2003), pp. 2 –30. ISSN: 0003-4916. DOI: http://dx.doi.org/10.1016/S0003-4916(02)00018-0. URL: http://www.sciencedirect.com/science/article/pii/S0003491602000180.

[96] E. Dennis et al. "Topological quantum memory". In: *Journal of Mathematical Physics* 43.9 (2002), pp. 4452–4505. DOI: http://dx.doi.org/10.1063/1.1499754. URL: http://scitation.aip.org/content/aip/journal/jmp/43/9/10.1063/1.1499754.

[97] R. Alicki, M. Fannes, and M. Horodecki. "On thermalization in Kitaev's 2D model". In: *Journal of Physics A: Mathematical and Theoretical* 42.6 (2009), p. 065303. URL: http://stacks.iop.org/1751-8121/42/i=6/a=065303.

[98] S. Iblisdir et al. "Scaling law for topologically ordered systems at finite temperature". In: *Phys. Rev. B* 79 (Apr. 2009), p. 134303. DOI: 10.1103/PhysRevB.79.134303. URL: http://link.aps.org/doi/10.1103/PhysRevB.79.134303.

[99] S. Trebst et al. "Breakdown of a Topological Phase: Quantum Phase Transition in a Loop Gas Model with Tension". In: *Phys. Rev. Lett.* 98 (Feb. 2007), p. 070602. DOI: 10.1103/PhysRevLett.98.070602. URL: http://link.aps.org/doi/10.1103/PhysRevLett.98.070602.

[100] I. S. Tupitsyn et al. "Topological multicritical point in the phase diagram of the toric code model and three-dimensional lattice gauge Higgs model". In: *Phys. Rev. B* 82 (Aug. 2010), p. 085114. DOI: 10.1103/PhysRevB.82.085114. URL: http://link.aps.org/doi/10.1103/PhysRevB.82.085114.

[101] J. Vidal, S. Dusuel, and K. P. Schmidt. "Low-energy effective theory of the toric code model in a parallel magnetic field". In: *Phys. Rev. B* 79 (Jan. 2009), p. 033109. DOI: 10.1103/PhysRevB.79.033109. URL: http://link.aps.org/doi/10.1103/PhysRevB.79.033109.

[102] I. Klich. "On the stability of topological phases on a lattice". In: *Annals of Physics* 325.10 (2010), pp. 2120 –2131. ISSN: 0003-4916. DOI: http://dx.doi.org/10.1016/j.aop.2010.05.002. URL: http://www.sciencedirect.com/science/article/pii/S000349161000093X.

[103] M. D. Schulz et al. “Breakdown of a perturbed Z2 topological phase”. In: *New Journal of Physics* 14.2 (2012), p. 025005. URL: http://stacks.iop.org/1367-2630/14/i=2/a=025005.

[104] J. Haegeman et al. “Shadows of anyons and the entanglement structure of topological phases”. In: *Nature communications* 6 (2015).

[105] W. Dür et al. “Entanglement Capabilities of Nonlocal Hamiltonians”. In: *Phys. Rev. Lett.* 87 (Sept. 2001), p. 137901. DOI: 10.1103/PhysRevLett.87.137901. URL: http://link.aps.org/doi/10.1103/PhysRevLett.87.137901.

[106] C. H. Bennett et al. “On the capacities of bipartite Hamiltonians and unitary gates”. In: *Information Theory, IEEE Transactions on* 49.8 (2003), pp. 1895–1911.

[107] T. S. Cubitt, F. Verstraete, and J. I. Cirac. “Entanglement flow in multipartite systems”. In: *Phys. Rev. A* 71 (May 2005), p. 052308. DOI: 10.1103/PhysRevA.71.052308. URL: http://link.aps.org/doi/10.1103/PhysRevA.71.052308.

[108] A. M. Childs, D. W. Leung, and G. Vidal. “Reversible simulation of bipartite product Hamiltonians”. In: *Information Theory, IEEE Transactions on* 50.6 (2004), pp. 1189–1197.

[109] A. M. Childs et al. “Asymptotic entanglement capacity of the Ising and anisotropic Heisenberg interactions”. In: *Quantum Information & Computation* 01.3 (2003), pp. 97–105.

[110] A. Ambainis. “Quantum lower bounds by quantum arguments”. In: *Proceedings of the thirty-second annual ACM symposium on Theory of computing*. ACM. 2000, pp. 636–643.

[111] M. Schlosshauer. “Decoherence, the measurement problem, and interpretations of quantum mechanics”. In: *Rev. Mod. Phys.* 76 (Feb. 2005), pp. 1267–1305. DOI: 10.1103/RevModPhys.76.1267. URL: http://link.aps.org/doi/10.1103/RevModPhys.76.1267.

[112] P. W. Shor. “Scheme for reducing decoherence in quantum computer memory”. In: *Phys. Rev. A* 52 (Oct. 1995), R2493–R2496. DOI: 10.1103/PhysRevA.52.R2493. URL: http://link.aps.org/doi/10.1103/PhysRevA.52.R2493.

[113] S. Bravyi. “Upper bounds on entangling rates of bipartite Hamiltonians”. In: *Phys. Rev. A* 76 (Nov. 2007), p. 052319. DOI: 10.1103/PhysRevA.76.052319. URL: http://link.aps.org/doi/10.1103/PhysRevA.76.052319.

[114] D. N. Page. “Average entropy of a subsystem”. In: *Phys. Rev. Lett.* 71 (Aug. 1993), pp. 1291–1294. DOI: 10.1103/PhysRevLett.71.1291. URL: http://link.aps.org/doi/10.1103/PhysRevLett.71.1291.

[115] S. K. Foong and S. Kanno. "Proof of Page's conjecture on the average entropy of a subsystem". In: *Phys. Rev. Lett.* 72 (Feb. 1994), pp. 1148–1151. DOI: 10.1103/PhysRevLett.72.1148. URL: http://link.aps.org/doi/10.1103/PhysRevLett.72.1148.

[116] P. Hayden, W. D. Leung, and A. Winter. "Aspects of Generic Entanglement". In: *Communications in Mathematical Physics* 265.1 (2006), pp. 95–117. ISSN: 1432-0916. DOI: 10.1007/s00220-006-1535-6. URL: http://dx.doi.org/10.1007/s00220-006-1535-6.

[117] J. Eisert, M. Cramer, and M. B. Plenio. "*Colloquium* : Area laws for the entanglement entropy". In: *Rev. Mod. Phys.* 82 (Feb. 2010), pp. 277–306. DOI: 10.1103/RevModPhys.82.277. URL: http://link.aps.org/doi/10.1103/RevModPhys.82.277.

[118] Z. Landau, U. Vazirani, and T. Vidick. "An Efficient Algorithm for Finding the Ground State of 1D Gapped Local Hamiltonians". In: *Proceedings of the 5th Conference on Innovations in Theoretical Computer Science*. ITCS '14. New York, NY, USA: ACM, 2014, pp. 301–302. ISBN: 978-1-4503-2698-8. DOI: 10.1145/2554797.2554825. URL: http://doi.acm.org/10.1145/2554797.2554825.

[119] X. Chen, Z.-C. Gu, and X.-G. Wen. "Complete classification of one-dimensional gapped quantum phases in interacting spin systems". In: *Phys. Rev. B* 84 (Dec. 2011), p. 235128. DOI: 10.1103/PhysRevB.84.235128. URL: http://link.aps.org/doi/10.1103/PhysRevB.84.235128.

[120] S. Michalakis. "Stability of the area law for the entropy of entanglement". In: *arXiv preprint arXiv:1206.6900* (2012).

[121] M. Fannes. "A continuity property of the entropy density for spin lattice systems". In: *Communications in Mathematical Physics* 31.4 (1973), pp. 291–294. ISSN: 1432-0916. DOI: 10.1007/BF01646490. URL: http://dx.doi.org/10.1007/BF01646490.

[122] K. M. R. Audenaert. "A sharp continuity estimate for the von Neumann entropy". In: *Journal of Physics A: Mathematical and Theoretical* 40.28 (2007), p. 8127. URL: http://stacks.iop.org/1751-8121/40/i=28/a=S18.

[123] K. Van Acoleyen, M. Mariën, and F. Verstraete. "Entanglement Rates and Area Laws". In: *Phys. Rev. Lett.* 111 (Oct. 2013), p. 170501. DOI: 10.1103/PhysRevLett.111.170501. URL: http://link.aps.org/doi/10.1103/PhysRevLett.111.170501.

[124] K. M. R. Audenaert. "Quantum skew divergence". In: *Journal of Mathematical Physics* 55.11, 112202 (2014). DOI: http://dx.doi.org/10.1063/1.4901039. URL: http://scitation.aip.org/content/aip/journal/jmp/55/11/10.1063/1.4901039.

[125] E. H. Lieb and A. Vershynina. "Upper Bounds on Mixing Rates". In: *Quantum Info. Comput.* 13.11-12 (Nov. 2013), pp. 986–994. ISSN: 1533-7146. URL: http://dl.acm.org/citation.cfm?id=2535639.2535644.

[126] A. Hutter and S. Wehner. "Almost All Quantum States Have Low Entropy Rates for Any Coupling to the Environment". In: *Phys. Rev. Lett.* 108 (Feb. 2012), p. 070501. DOI: 10.1103/PhysRevLett.108.070501. URL: http://link.aps.org/doi/10.1103/PhysRevLett.108.070501.

[127] X. Wang and B. C. Sanders. "Entanglement capability of a self-inverse Hamiltonian evolution". In: *Phys. Rev. A* 68 (July 2003), p. 014301. DOI: 10.1103/PhysRevA.68.014301. URL: http://link.aps.org/doi/10.1103/PhysRevA.68.014301.

[128] D. P. DiVincenzo et al. "Locking Classical Correlations in Quantum States". In: *Phys. Rev. Lett.* 92 (Feb. 2004), p. 067902. DOI: 10.1103/PhysRevLett.92.067902. URL: http://link.aps.org/doi/10.1103/PhysRevLett.92.067902.

[129] K. Audenaert and F. Kittaneh. "Problems and conjectures in matrix and operator inequalities". In: *Operator theory*. Banach Center Publications. Polish Academy of Sciences, 2012.

[130] F. Kittaneh. "Inequalities for commutators of positive operators". In: *Journal of Functional Analysis* 250.1 (2007), pp. 132 –143. ISSN: 0022-1236. DOI: http://dx.doi.org/10.1016/j.jfa.2007.05.008. URL: http://www.sciencedirect.com/science/article/pii/S0022123607001929.

[131] F. Kittaneh. "Norm Inequalities for Commutators of Self-adjoint Operators". In: *Integral Equations and Operator Theory* 62.1 (2008), pp. 129–135. ISSN: 1420-8989. DOI: 10.1007/s00020-008-1605-6. URL: http://dx.doi.org/10.1007/s00020-008-1605-6.

[132] N. Linden, S. Popescu, and J. A. Smolin. "Entanglement of Superpositions". In: *Phys. Rev. Lett.* 97 (Sept. 2006), p. 100502. DOI: 10.1103/PhysRevLett.97.100502. URL: http://link.aps.org/doi/10.1103/PhysRevLett.97.100502.

[133] P. Jordan and E. Wigner. "Über das Paulische Equivalenzverbot". In: *Z. Phys.* 47 (1928), pp. 631–651.

[134] M.-C. Bañuls, J. I. Cirac, and M. M. Wolf. "Entanglement in fermionic systems". In: *Phys. Rev. A* 76 (Aug. 2007), p. 022311. DOI: 10.1103/PhysRevA.76.022311. URL: http://link.aps.org/doi/10.1103/PhysRevA.76.022311.

[135] M. Levin. "Protected Edge Modes without Symmetry". In: *Phys. Rev. X* 3 (May 2013), p. 021009. DOI: 10.1103/PhysRevX.3.021009. URL: http://link.aps.org/doi/10.1103/PhysRevX.3.021009.

[136] A. Kitaev and L. Kong. "Models for Gapped Boundaries and Domain Walls". In: *Communications in Mathematical Physics* 313.2 (2012), pp. 351–373. ISSN: 1432-0916. DOI: 10.1007/s00220-012-1500-5. URL: http://dx.doi.org/10.1007/s00220-012-1500-5.

[137] C.-H. Lin and M. Levin. "Generalizations and limitations of string-net models". In: *Phys. Rev. B* 89 (May 2014), p. 195130. DOI: 10.1103/PhysRevB.89.195130. URL: http://link.aps.org/doi/10.1103/PhysRevB.89.195130.

[138] X.-G. Wen. "Topological orders and edge excitations in fractional quantum hall states". In: *Field Theory, Topology and Condensed Matter Physics: Proceedings of the Ninth Chris Engelbrecht Summer School in Theoretical Physics Held at Storms River Mouth, Tsitsikamma National Park, South Africa, 17–28 January 1994*. Berlin, Heidelberg: Springer Berlin Heidelberg, 1995, pp. 155–176. ISBN: 978-3-540-49455-3. DOI: 10.1007/BFb0113370. URL: http://dx.doi.org/10.1007/BFb0113370.

[139] J. Haah. "Local stabilizer codes in three dimensions without string logical operators". In: *Phys. Rev. A* 83 (Apr. 2011), p. 042330. DOI: 10.1103/PhysRevA.83.042330. URL: http://link.aps.org/doi/10.1103/PhysRevA.83.042330.

[140] R. König, B. W. Reichardt, and G. Vidal. "Exact entanglement renormalization for string-net models". In: *Phys. Rev. B* 79 (May 2009), p. 195123. DOI: 10.1103/PhysRevB.79.195123. URL: http://link.aps.org/doi/10.1103/PhysRevB.79.195123.

[141] J. Cho. "Sufficient Condition for Entanglement Area Laws in Thermodynamically Gapped Spin Systems". In: *Phys. Rev. Lett.* 113 (Nov. 2014), p. 197204. DOI: 10.1103/PhysRevLett.113.197204. URL: http://link.aps.org/doi/10.1103/PhysRevLett.113.197204.

[142] B. Swingle and J. McGreevy. "Renormalization group constructions of topological quantum liquids and beyond". In: *Phys. Rev. B* 93 (Jan. 2016), p. 045127. DOI: 10.1103/PhysRevB.93.045127. URL: http://link.aps.org/doi/10.1103/PhysRevB.93.045127.

[143] J. Haah. "Bifurcation in entanglement renormalization group flow of a gapped spin model". In: *Phys. Rev. B* 89 (Feb. 2014), p. 075119. DOI: 10.1103/PhysRevB.89.075119. URL: http://link.aps.org/doi/10.1103/PhysRevB.89.075119.

[144] G. Evenbly and G. Vidal. "Scaling of entanglement entropy in the (branching) multiscale entanglement renormalization ansatz". In: *Phys. Rev. B* 89 (June 2014), p. 235113. DOI: 10.1103/PhysRevB.89.235113. URL: http://link.aps.org/doi/10.1103/PhysRevB.89.235113.

[145] B. Zeng and X.-G. Wen. "Gapped quantum liquids and topological order, stochastic local transformations and emergence of unitarity". In: *Phys. Rev. B* 91 (Mar. 2015), p. 125121. DOI: 10.1103/PhysRevB.91.125121. URL: http://link.aps.org/doi/10.1103/PhysRevB.91.125121.

[146] A. Vershynina. "Entanglement rates for bipartite open systems". In: *Phys. Rev. A* 92 (Aug. 2015), p. 022311. DOI: 10.1103/PhysRevA.92.022311. URL: http://link.aps.org/doi/10.1103/PhysRevA.92.022311.

[147] P. Buividovich and M. Polikarpov. "Entanglement entropy in gauge theories and the holographic principle for electric strings". In: *Physics Letters B* 670.2 (2008), pp. 141 –145. ISSN: 0370-2693. DOI: http://dx.doi.org/10.1016/j.physletb.2008.10.032. URL: http://www.sciencedirect.com/science/article/pii/S0370269308012987.

[148] R. M. Soni and S. P. Trivedi. "Aspects of Entanglement Entropy for Gauge Theories". In: *arXiv preprint arXiv:1510.07455* (2015).

[149] W. Donnelly. "Decomposition of entanglement entropy in lattice gauge theory". In: *Phys. Rev. D* 85 (Apr. 2012), p. 085004. DOI: 10.1103/PhysRevD.85.085004. URL: http://link.aps.org/doi/10.1103/PhysRevD.85.085004.

[150] H. Casini, M. Huerta, and J. A. Rosabal. "Remarks on entanglement entropy for gauge fields". In: *Phys. Rev. D* 89 (Apr. 2014), p. 085012. DOI: 10.1103/PhysRevD.89.085012. URL: http://link.aps.org/doi/10.1103/PhysRevD.89.085012.

[151] S. Aoki et al. "On the definition of entanglement entropy in lattice gauge theories". In: *Journal of High Energy Physics* 2015.6 (2015), pp. 1–29. ISSN: 1029-8479. DOI: 10.1007/JHEP06(2015)187. URL: http://dx.doi.org/10.1007/JHEP06(2015)187.

[152] A. Gromov and R. A. Santos. "Entanglement Entropy in 2D non-abelian pure gauge theory". In: *Physics Letters B* 737 (2014), pp. 60 –64. ISSN: 0370-2693. DOI: http://dx.doi.org/10.1016/j.physletb.2014.08.023. URL: http://www.sciencedirect.com/science/article/pii/S0370269314005905.

[153] D. Radicevic. "Entanglement in weakly coupled lattice gauge theories". In: *Journal of High Energy Physics* 2016.4 (2016), pp. 1–31.

[154] D. Radicevic. "Notes on entanglement in abelian gauge theories". In: *arXiv preprint arXiv:1404.1391* (2014).

[155] S. Ghosh, R. M. Soni, and S. P. Trivedi. "On the entanglement entropy for gauge theories". In: *Journal of High Energy Physics* 2015.9 (2015), pp. 1–29. ISSN: 1029-8479. DOI: 10.1007/JHEP09(2015)069. URL: http://dx.doi.org/10.1007/JHEP09(2015)069.

[156] L.-Y. Hung and Y. Wan. "Revisiting entanglement entropy of lattice gauge theories". In: *Journal of High Energy Physics* 2015.4 (2015), pp. 1–14. ISSN: 1029-8479. DOI: 10.1007/JHEP04(2015)122. URL: http://dx.doi.org/10.1007/JHEP04(2015)122.

[157] J. Kogut and L. Susskind. "Hamiltonian formulation of Wilson's lattice gauge theories". In: *Phys. Rev. D* 11 (Jan. 1975), pp. 395–408. DOI: 10.1103/PhysRevD.11.395. URL: http://link.aps.org/doi/10.1103/PhysRevD.11.395.

[158] J. B. Kogut. "An introduction to lattice gauge theory and spin systems". In: *Rev. Mod. Phys.* 51 (Oct. 1979), pp. 659–713. DOI: 10.1103/RevModPhys.51.659. URL: http://link.aps.org/doi/10.1103/RevModPhys.51.659.

[159] J. C. Baez. "Spin foam models". In: *Classical and Quantum Gravity* 15.7 (1998), p. 1827.

[160] H. Barnum et al. "A Subsystem-Independent Generalization of Entanglement". In: *Phys. Rev. Lett.* 92 (Mar. 2004), p. 107902. DOI: 10.1103/PhysRevLett.92.107902. URL: http://link.aps.org/doi/10.1103/PhysRevLett.92.107902.

[161] C. H. Bennett et al. "Concentrating partial entanglement by local operations". In: *Phys. Rev. A* 53 (Apr. 1996), pp. 2046–2052. DOI: 10.1103/PhysRevA.53.2046. URL: http://link.aps.org/doi/10.1103/PhysRevA.53.2046.

[162] M. M. Wilde. *Quantum information theory*. Cambridge University Press, 2013.

[163] P. M. Hayden, M. Horodecki, and B. M. Terhal. "The asymptotic entanglement cost of preparing a quantum state". In: *Journal of Physics A: Mathematical and General* 34.35 (2001), p. 6891. URL: http://stacks.iop.org/0305-4470/34/i=35/a=314.

[164] K. Van Acoleyen et al. "The entanglement of distillation for gauge theories". In: *arXiv preprint arXiv:1511.04369* (2015).

[165] A. Almheiri et al. "Black holes: complementarity or firewalls?" In: *Journal of High Energy Physics* 2013.2 (2013), pp. 1–20. ISSN: 1029-8479. DOI: 10.1007/JHEP02(2013)062. URL: http://dx.doi.org/10.1007/JHEP02(2013)062.

[166] S. Mac Lane. *Categories for the working mathematician*. Vol. 5. Springer Science & Business Media, 2013.

[167] P. Etingof, D. Nikshych, and V. Ostrik. "On fusion categories". In: *ArXiv Mathematics e-prints* (Mar. 2002).

[168] L. Kong and X.-G. Wen. "Braided fusion categories, gravitational anomalies, and the mathematical framework for topological orders in any dimensions". In: *ArXiv e-prints* (May 2014).

[169] D. Pérez-García et al. "Peps As Unique Ground States of Local Hamiltonians". In: *Quantum Info. Comput.* 8.6 (July 2008), pp. 650–663. ISSN: 1533-7146. URL: http://dl.acm.org/citation.cfm?id=2016976.2016982.

[170] T. Lan and X.-G. Wen. "Topological quasiparticles and the holographic bulk-edge relation in $(2+1)$-dimensional string-net models". In: *Phys. Rev. B* 90 (Sept. 2014), p. 115119. DOI: 10.1103/PhysRevB.90.115119. URL: http://link.aps.org/doi/10.1103/PhysRevB.90.115119.

[171] Y. Hu, N. Geer, and Y.-S. Wu. "Full Dyon Excitation Spectrum in Generalized Levin-Wen Models". In: *ArXiv e-prints* (Feb. 2015).

[172] D. Evans and Y. Kawahigashi. "On Ocneanu's theory of asymptotic inclusions for subfactors, topological quantum field theories and quantum doubles". In: *International journal of mathematics* 6 (1995), pp. 205–228.

[173] B. Pirvu, J. Haegeman, and F. Verstraete. “Matrix product state based algorithm for determining dispersion relations of quantum spin chains with periodic boundary conditions”. In: *Phys. Rev. B* 85 (Jan. 2012), p. 035130. DOI: 10.1103/PhysRevB.85.035130. URL: http://link.aps.org/doi/10.1103/PhysRevB.85.035130.

[174] L. Vanderstraeten et al. “Excitations and the tangent space of projected entangled-pair states”. In: *Phys. Rev. B* 92 (Nov. 2015), p. 201111. DOI: 10.1103/PhysRevB.92.201111. URL: http://link.aps.org/doi/10.1103/PhysRevB.92.201111.

[175] G. C. Wick, A. S. Wightman, and E. P. Wigner. “The Intrinsic Parity of Elementary Particles”. In: *Phys. Rev.* 88 (Oct. 1952), pp. 101–105. DOI: 10.1103/PhysRev.88.101. URL: http://link.aps.org/doi/10.1103/PhysRev.88.101.

[176] M. A. Levin and X.-G. Wen. “String-net condensation: A physical mechanism for topological phases”. In: *Phys. Rev. B* 71 (Jan. 2005), p. 045110. DOI: 10.1103/PhysRevB.71.045110. URL: http://link.aps.org/doi/10.1103/PhysRevB.71.045110.

[177] K. Friedl and L. Rónyai. “Polynomial Time Solutions of Some Problems of Computational Algebra”. In: *Proceedings of the Seventeenth Annual ACM Symposium on Theory of Computing*. STOC ’85. New York, NY, USA: ACM, 1985, pp. 153–162. ISBN: 0-89791-151-2. DOI: 10.1145/22145.22162. URL: http://doi.acm.org/10.1145/22145.22162.

[178] N. Read and E. Rezayi. “Quasiholes and fermionic zero modes of paired fractional quantum Hall states: The mechanism for non-Abelian statistics”. In: *Phys. Rev. B* 54 (Dec. 1996), pp. 16864–16887. DOI: 10.1103/PhysRevB.54.16864. URL: http://link.aps.org/doi/10.1103/PhysRevB.54.16864.

[179] C. Nayak et al. “Non-Abelian anyons and topological quantum computation”. In: *Rev. Mod. Phys.* 80 (Sept. 2008), pp. 1083–1159. DOI: 10.1103/RevModPhys.80.1083. URL: http://link.aps.org/doi/10.1103/RevModPhys.80.1083.

[180] C. Nayak and F. Wilczek. “2n-quasihole states realize 2n,àí1-dimensional spinor braiding statistics in paired quantum Hall states”. In: *Nuclear Physics B* 479.3 (1996), pp. 529 –553. ISSN: 0550-3213. DOI: http://dx.doi.org/10.1016/0550-3213(96)00430-0. URL: http://www.sciencedirect.com/science/article/pii/0550321396004300.

[181] S. Beigi, P. W. Shor, and D. Whalen. “The Quantum Double Model with Boundary: Condensations and Symmetries”. In: *Communications in Mathematical Physics* 306.3 (2011), pp. 663–694. ISSN: 1432-0916. DOI: 10.1007/s00220-011-1294-x. URL: http://dx.doi.org/10.1007/s00220-011-1294-x.

[182] M. Freedman et al. “Topological quantum computation”. In: *Bulletin of the American Mathematical Society* 40.1 (2003), pp. 31–38.

[183] R. Walter Ogburn and J. Preskill. "Topological Quantum Computation". In: *Quantum Computing and Quantum Communications: First NASA International Conference, QCQC'98 Palm Springs, California, USA February 17–20, 1998 Selected Papers*. Berlin, Heidelberg: Springer Berlin Heidelberg, 1999, pp. 341–356. ISBN: 978-3-540-49208-5. DOI: 10.1007/3-540-49208-9_31. URL: http://dx.doi.org/10.1007/3-540-49208-9_31.

[184] S. D. Sarma, M. Freedman, and C. Nayak. "Topological quantum computation". In: *Physics Today* 59.7 (2006), pp. 32–38.

[185] S. Bravyi and B. Terhal. "A no-go theorem for a two-dimensional self-correcting quantum memory based on stabilizer codes". In: *New Journal of Physics* 11.4 (2009), p. 043029. URL: http://stacks.iop.org/1367-2630/11/i=4/a=043029.

[186] O. Landon-Cardinal and D. Poulin. "Local Topological Order Inhibits Thermal Stability in 2D". In: *Phys. Rev. Lett.* 110 (Feb. 2013), p. 090502. DOI: 10.1103/PhysRevLett.110.090502. URL: http://link.aps.org/doi/10.1103/PhysRevLett.110.090502.

[187] A. Hamma, C. Castelnovo, and C. Chamon. "Toric-boson model: Toward a topological quantum memory at finite temperature". In: *Phys. Rev. B* 79 (June 2009), p. 245122. DOI: 10.1103/PhysRevB.79.245122. URL: http://link.aps.org/doi/10.1103/PhysRevB.79.245122.

[188] B. J. Brown, A. Al-Shimary, and J. K. Pachos. "Entropic Barriers for Two-Dimensional Quantum Memories". In: *Phys. Rev. Lett.* 112 (Mar. 2014), p. 120503. DOI: 10.1103/PhysRevLett.112.120503. URL: http://link.aps.org/doi/10.1103/PhysRevLett.112.120503.

[189] H. M. Freedman, M. Larsen, and Z. Wang. "A Modular Functor Which is Universal for Quantum Computation". In: *Communications in Mathematical Physics* 227.3 (2002), pp. 605–622. ISSN: 1432-0916. DOI: 10.1007/s002200200645. URL: http://dx.doi.org/10.1007/s002200200645.

[190] F. Verstraete and J. I. Cirac. "Valence-bond states for quantum computation". In: *Phys. Rev. A* 70 (6 2004), p. 060302. DOI: 10.1103/PhysRevA.70.060302. URL: http://link.aps.org/doi/10.1103/PhysRevA.70.060302.

[191] P. Fendley. "Topological order from quantum loops and nets". In: *Annals of Physics* 323.12 (2008), pp. 3113 –3136. ISSN: 0003-4916. DOI: http://dx.doi.org/10.1016/j.aop.2008.04.011. URL: http://www.sciencedirect.com/science/article/pii/S0003491608000614.

[192] P. Fendley, S. V. Isakov, and M. Troyer. "Fibonacci topological order from quantum nets". In: *Phys. Rev. Lett.* 110 (June 2013), p. 260408. DOI: 10.1103/PhysRevLett.110.260408. URL: http://link.aps.org/doi/10.1103/PhysRevLett.110.260408.

[193] P. Fendley and E. Fradkin. "Realizing non-Abelian statistics". In: *Phys. Rev.* B72 (2005), p. 024412. DOI: 10.1103/PhysRevB.72.024412.

[194] F. A. Bais, B. J. Schroers, and J. K. Slingerland. "Broken Quantum Symmetry and Confinement Phases in Planar Physics". In: *Phys. Rev. Lett.* 89 (Oct. 2002), p. 181601. DOI: 10.1103/PhysRevLett.89.181601. URL: http://link.aps.org/doi/10.1103/PhysRevLett.89.181601.

[195] A. F. Bais, B. J. Schroers, and J. K. Slingerland. "Hopf symmetry breaking and confinement in (2+1)-dimensional gauge theory". In: *Journal of High Energy Physics* 2003.05 (2003), p. 068. URL: http://stacks.iop.org/1126-6708/2003/i=05/a=068.

[196] F. A. Bais and J. K. Slingerland. "Condensate-induced transitions between topologically ordered phases". In: *Phys. Rev. B* 79 (Jan. 2009), p. 045316. DOI: 10.1103/PhysRevB.79.045316. URL: http://link.aps.org/doi/10.1103/PhysRevB.79.045316.

[197] T. Neupert et al. "Boson condensation in topologically ordered quantum liquids". In: *Phys. Rev. B* 93 (Mar. 2016), p. 115103. DOI: 10.1103/PhysRevB.93.115103. URL: http://link.aps.org/doi/10.1103/PhysRevB.93.115103.

[198] J. I. Cirac et al. "Entanglement spectrum and boundary theories with projected entangled-pair states". In: *Phys. Rev. B* 83 (June 2011), p. 245134. DOI: 10.1103/PhysRevB.83.245134. URL: http://link.aps.org/doi/10.1103/PhysRevB.83.245134.

[199] V. Zauner et al. "Transfer matrices and excitations with matrix product states". In: *New Journal of Physics* 17.5 (2015), p. 053002. URL: http://stacks.iop.org/1367-2630/17/i=5/a=053002.

[200] M. Bal et al. "Matrix product state renormalization". In: *arXiv preprint arXiv:1509.01522* (2015).

[201] N. Schuch et al. "Topological Order in the Projected Entangled-Pair States Formalism: Transfer Operator and Boundary Hamiltonians". In: *Phys. Rev. Lett.* 111 (Aug. 2013), p. 090501. DOI: 10.1103/PhysRevLett.111.090501. URL: http://link.aps.org/doi/10.1103/PhysRevLett.111.090501.

[202] F. Liu and X.-G. Wen. "Environment tensor as order parameter for symmetry breaking and (symmetry-protected) topological orders". In: *arXiv preprint arXiv:1504.08365* (2015).

[203] H. Li and F. D. M. Haldane. "Entanglement Spectrum as a Generalization of Entanglement Entropy: Identification of Topological Order in Non-Abelian Fractional Quantum Hall Effect States". In: *Phys. Rev. Lett.* 101 (July 2008), p. 010504. DOI: 10.1103/PhysRevLett.101.010504. URL: http://link.aps.org/doi/10.1103/PhysRevLett.101.010504.

[204] O. Buerschaper, M. Aguado, and G. Vidal. "Explicit tensor network representation for the ground states of string-net models". In: *Phys. Rev. B* 79 (Feb. 2009), p. 085119. DOI: 10.1103/PhysRevB.79.085119. URL: http://link.aps.org/doi/10.1103/PhysRevB.79.085119.

[205] Z.-C. Gu et al. "Tensor-product representations for string-net condensed states". In: *Phys. Rev. B* 79 (Feb. 2009), p. 085118. DOI: 10.1103/PhysRevB.79.085118. URL: http://link.aps.org/doi/10.1103/PhysRevB.79.085118.

[206] J. Haegeman et al. "Elementary Excitations in Gapped Quantum Spin Systems". In: *Phys. Rev. Lett.* 111 (Aug. 2013), p. 080401. DOI: 10.1103/PhysRevLett.111.080401. URL: http://link.aps.org/doi/10.1103/PhysRevLett.111.080401.

[207] A. Feiguin et al. "Interacting anyons in topological quantum liquids: The golden chain". In: *Phys. Rev. Lett.* 98 (2007), p. 160409. DOI: 10.1103/PhysRevLett.98.160409.

[208] H. N. Phien et al. "Infinite projected entangled pair states algorithm improved: Fast full update and gauge fixing". In: *Phys. Rev. B* 92 (July 2015), p. 035142. DOI: 10.1103/PhysRevB.92.035142. URL: http://link.aps.org/doi/10.1103/PhysRevB.92.035142.

[209] J. Haegeman et al. "Variational matrix product ansatz for dispersion relations". In: *Phys. Rev. B* 85 (Mar. 2012), p. 100408. DOI: 10.1103/PhysRevB.85.100408. URL: http://link.aps.org/doi/10.1103/PhysRevB.85.100408.

[210] E. Ardonne, P. Fendley, and E. Fradkin. "Topological order and conformal quantum critical points". In: *Annals Phys.* 310 (2004), pp. 493–551. DOI: 10.1016/j.aop.2004.01.004.

[211] C. Castelnovo and C. Chamon. "Quantum topological phase transition at the microscopic level". In: *Phys. Rev. B* 77 (Feb. 2008), p. 054433. DOI: 10.1103/PhysRevB.77.054433. URL: http://link.aps.org/doi/10.1103/PhysRevB.77.054433.

[212] L. Fidkowski et al. "From string nets to nonabelions". In: *Commun. Math. Phys.* 287 (2009), pp. 805–827. DOI: 10.1007/s00220-009-0757-9.

[213] D. S. Rokhsar and S. A. Kivelson. "Superconductivity and the Quantum Hard-Core Dimer Gas". In: *Phys. Rev. Lett.* 61 (1988), pp. 2376–2379. DOI: 10.1103/PhysRevLett.61.2376.

[214] F. Y. Wu. "The Potts model". In: *Rev. Mod. Phys.* 54 (Jan. 1982), pp. 235–268. DOI: 10.1103/RevModPhys.54.235. URL: http://link.aps.org/doi/10.1103/RevModPhys.54.235.

[215] R. Baxter, H. Temperley, and S. Ashley. "Triangular Potts model at its transition temperature, and related models". In: *Proceedings of the Royal Society of London A: Mathematical, Physical and Engineering Sciences*. Vol. 358. The Royal Society. 1978, pp. 535–559.

[216] P. Francesco, P. Mathieu, and D. Sénéchal. *Conformal field theory*. Springer Science & Business Media, 2012.

[217] C. Gils et al. “Topology-driven quantum phase transitions in time-reversal-invariant anyonic quantum liquids”. In: *Nature Physics* 5.11 (2009), pp. 834–839.

[218] D. F. Abasto, A. Hamma, and P. Zanardi. “Fidelity analysis of topological quantum phase transitions”. In: *Phys. Rev. A* 78 (July 2008), p. 010301. DOI: 10.1103/PhysRevA.78.010301. URL: http://link.aps.org/doi/10.1103/PhysRevA.78.010301.

[219] M. D. Schulz, S. Dusuel, and J. Vidal. “Bound states in string nets”. In: *arXiv preprint arXiv:1606.03922* (2016).

[220] S. V. Isakov et al. “Dynamics at and near conformal quantum critical points”. In: *Phys. Rev. B* 83 (Mar. 2011), p. 125114. DOI: 10.1103/PhysRevB.83.125114. URL: http://link.aps.org/doi/10.1103/PhysRevB.83.125114.

[221] F. Burnell, S. H. Simon, and J. Slingerland. “Phase transitions in topological lattice models via topological symmetry breaking”. In: *New Journal of Physics* 14.1 (2012), p. 015004.

[222] F. J. Burnell, S. H. Simon, and J. K. Slingerland. “Condensation of achiral simple currents in topological lattice models: Hamiltonian study of topological symmetry breaking”. In: *Phys. Rev. B* 84 (Sept. 2011), p. 125434. DOI: 10.1103/PhysRevB.84.125434. URL: http://link.aps.org/doi/10.1103/PhysRevB.84.125434.

[223] M. D. Schulz et al. “Topological Phase Transitions in the Golden String-Net Model”. In: *Phys. Rev. Lett.* 110 (Apr. 2013), p. 147203. DOI: 10.1103/PhysRevLett.110.147203. URL: http://link.aps.org/doi/10.1103/PhysRevLett.110.147203.

[224] V. Drinfeld. “Quantum groups”. In: *Proceedings of the International Congress of Mathematicians* 1 (1986), pp. 798–820. URL: http://www.mathunion.org/ICM/ICM1986.1/Main/icm1986.1.0798.0820.ocr.pdf.

[225] M. Muger. “From subfactors to categories and topology II: The quantum double of tensor categories and subfactors”. In: *Journal of Pure and Applied Algebra* 180.1,Äì2 (2003), pp. 159 –219. ISSN: 0022-4049. DOI: http://dx.doi.org/10.1016/S0022-4049(02)00248-7. URL: http://www.sciencedirect.com/science/article/pii/S0022404902002487.

[226] T. B. Wahl et al. “Projected Entangled-Pair States Can Describe Chiral Topological States”. In: *Phys. Rev. Lett.* 111 (Dec. 2013), p. 236805. DOI: 10.1103/PhysRevLett.111.236805. URL: http://link.aps.org/doi/10.1103/PhysRevLett.111.236805.

[227] J. Dubail and N. Read. “Tensor network trial states for chiral topological phases in two dimensions”. In: *ArXiv e-prints* (July 2013).

[228] S. Jiang and Y. Ran. "Symmetric tensor networks and practical simulation algorithms to sharply identify classes of quantum phases distinguishable by short-range physics". In: *Phys. Rev. B* 92 (Sept. 2015), p. 104414. DOI: 10.1103/PhysRevB.92.104414. URL: http://link.aps.org/doi/10.1103/PhysRevB.92.104414.

[229] C. V. Kraus et al. "Fermionic projected entangled pair states". In: *Phys. Rev. A* 81 (May 2010), p. 052338. DOI: 10.1103/PhysRevA.81.052338. URL: http://link.aps.org/doi/10.1103/PhysRevA.81.052338.

[230] N. Bultinck et al. "To Appear". In: *To be determined* ().

[231] S. Bravyi, D. P. DiVincenzo, and D. Loss. "Schrieffer-Wolff transformation for quantum many-body systems". In: *Annals of Physics* 326.10 (2011), pp. 2793 –2826. ISSN: 0003-4916. DOI: http://dx.doi.org/10.1016/j.aop.2011.06.004. URL: http://www.sciencedirect.com/science/article/pii/S0003491611001059.

[232] J. Martin. "On the exponential representation of solutions of linear differential equations". In: *Journal of Differential Equations* 4.2 (1968), pp. 257 –279. ISSN: 0022-0396. DOI: http://dx.doi.org/10.1016/0022-0396(68)90038-7. URL: http://www.sciencedirect.com/science/article/pii/0022039668900387.

[233] F. Wegner. "Flow-equations for Hamiltonians". In: *Annalen der physik* 506.2 (1994), pp. 77–91.

[234] S. D. Glazek and K. G. Wilson. "Perturbative renormalization group for Hamiltonians". In: *Phys. Rev. D* 49 (Apr. 1994), pp. 4214–4218. DOI: 10.1103/PhysRevD.49.4214. URL: http://link.aps.org/doi/10.1103/PhysRevD.49.4214.

[235] S. D. Głazek and K. G. Wilson. "Renormalization of Hamiltonians". In: *Phys. Rev. D* 48 (Dec. 1993), pp. 5863–5872. DOI: 10.1103/PhysRevD.48.5863. URL: http://link.aps.org/doi/10.1103/PhysRevD.48.5863.

[236] S. Kehrein. *The flow equation approach to many-particle systems*. Vol. 217. Springer, 2007.

[237] Knetter, C. and Uhrig, G. S. "Perturbation theory by flow equations: dimerized and frustrated S=1/2 chain". In: *Eur. Phys. J. B* 13.2 (Jan. 2000), pp. 209–225. DOI: 10.1007/s100510050026. URL: http://dx.doi.org/10.1007/s100510050026.

[238] C. Knetter. "Perturbative continuous unitary transformations: spectral properties of low dimensional spin systems". PhD thesis. Universität zu Köln, 2003.

[239] C. Knetter, K. P. Schmidt, and G. S. Uhrig. "The structure of operators in effective particle-conserving models". In: *Journal of Physics A: Mathematical and General* 36.29 (2003), p. 7889. URL: http://stacks.iop.org/0305-4470/36/i=29/a=302.

[240] C. Knetter, K. P. Schmidt, and G. S. Uhrig. "High order perturbation theory for spectral densities of multi-particle excitations: S=1/2 two-leg Heisenberg ladder". In: *The European Physical Journal B-Condensed Matter and Complex Systems* 36.4 (2003), pp. 525–544.

[241] S. Dusuel et al. "Bound states in two-dimensional spin systems near the Ising limit: A quantum finite-lattice study". In: *Phys. Rev. B* 81 (Feb. 2010), p. 064412. DOI: 10.1103/PhysRevB.81.064412. URL: http://link.aps.org/doi/10.1103/PhysRevB.81.064412.

[242] V Zauner et al. "Symmetry breaking and the geometry of reduced density matrices". In: *arXiv preprint arXiv:1412.7642* (2014).

[243] L. Balents. "Energy density of variational states". In: *Phys. Rev. B* 90 (24 2014), p. 245116. DOI: 10.1103/PhysRevB.90.245116. URL: http://link.aps.org/doi/10.1103/PhysRevB.90.245116.

[244] H. W. J. Blöte and Y. Deng. "Cluster Monte Carlo simulation of the transverse Ising model". In: *Phys. Rev. E* 66 (Dec. 2002), p. 066110. DOI: 10.1103/PhysRevE.66.066110. URL: http://link.aps.org/doi/10.1103/PhysRevE.66.066110.

[245] J. Jordan et al. "Classical Simulation of Infinite-Size Quantum Lattice Systems in Two Spatial Dimensions". In: *Phys. Rev. Lett.* 101 (Dec. 2008), p. 250602. DOI: 10.1103/PhysRevLett.101.250602. URL: http://link.aps.org/doi/10.1103/PhysRevLett.101.250602.

[246] R. Orús and G. Vidal. "Simulation of two-dimensional quantum systems on an infinite lattice revisited: Corner transfer matrix for tensor contraction". In: *Phys. Rev. B* 80 (Sept. 2009), p. 094403. DOI: 10.1103/PhysRevB.80.094403. URL: http://link.aps.org/doi/10.1103/PhysRevB.80.094403.

[247] S. Dusuel and J. Vidal. "Mean-field ansatz for topological phases with string tension". In: *Phys. Rev. B* 92 (12 2015), p. 125150. DOI: 10.1103/PhysRevB.92.125150. URL: http://link.aps.org/doi/10.1103/PhysRevB.92.125150.